T.C.

YEDITEPE UNIVERSITY

INSTITUTE OF HEALTH SCIENCES

DEPARTMENT OF PHARMACEUTICAL CHEMISTRY

SYNTHESIS AND ACTIVITY STUDIES OF

NEW 1,3,4-OXADIAZOLE DERIVATIVES

DOCTOR OF PHILOSOPHY THESIS

TUGCE OZYAZICI, B Pharm

SUPERVISOR

Prof. Dr. Meric KOKSAL AKKOC

Istanbul-2019

THESIS APPROVAL FORM

Institute   :Yeditepe University Institute of Health Sciences

Programme   :Pharmaceutical Chemistry

Title of the Thesis   :Synthesis and Biological Activity Studies of New 1,3,4-Oxadiazole Derivatives

Owner of the Thesis   :Tuğçe ÖZYAZICI

Examination Date   :30.04.2019

This study have approved as a Doctorate Thesis in regard to content and quality by the Jury.

	Title, Name-Surname (Institution)	(Signature)
Chair of the Jury:	Prof. Dr. Hülya AKGÜN (Yeditepe University)	
Supervisor:	Prof. Dr. Meriç KÖKSAL AKKOÇ (Yeditepe University)	
Member/Examiner:	Prof. Dr. Mine YARIM YÜKSEL (Yeditepe University)	
Member/Examiner:	Prof. Dr. Mert ÜLGEN (Acibadem University)	
Member/Examiner:	Prof. Dr. Şükriye Güniz KÜÇÜKGÜZEL (Marmara University)	

APPROVAL

This thesis has been deemed by the jury in accordance with the relevant articles of Yeditepe University Graduate Education and Examinations Regulation and has been approved by Administrative Board of Institute with decision dated 03.05.2019.... and numbered 2019./07 – 12

Prof. Dr. Bayram YILMAZ

Director of Institute of Health Sciences

DECLARATION

I hereby declare that this thesis is my own work and that, to the best of my knowledge and belief, it contains no material previously published or written by another person nor material which has been accepted for the award of any other degree except where due acknowledgment has been made in the text.

<div align="right">30.04.2019</div>

<div align="right">TUĞÇE ÖZYAZICI</div>

To dedicate my dear family…

ACKNOWLEDGEMENTS

TABLE OF CONTENTS

LIST OF TABLES

LIST OF FIGURES

LIST OF SCHEMES

LIST OF SYMBOLS AND ABBREVIATIONS

λ_{max}	Maximum wavelenght
μ	Mu
α	Alpha
β	Beta
γ	Gamma
κ	Kappa
Å	Angström
M^+	Molecular ion
m/z	Mass to charge
ppm	Part per million
nm	Nanometer
COX-1	Cyclooxygenase-1
COX-1	Cyclooxygenase-2
5-LOX	5-Lipoxygenase
12-LOX	12-Lipoxygenase
NSAID	Nonsteroidal antiinflammatory drug
SAR	Structure-activity relationship
NO	Nitric oxide
inos	Inducible nitric oxide
nNOS	Neuronal nitric oxide
eNOS	Endothelial nitric oxide
PG	Prostaglandin
PGE_2	Prostaglandin E_2
TNF-α	Tumor necrosis factor- α
INF-γ	Interferon-γ
NF- κβ	Nuclear factor kappa β
PAF	Platelet activating factor
IL	Interleukin
LP	Lipid peroxidation
EP 1-4	Prostaglandin E receptor 1-4
LTB4	Leukotriene B4

5-HETE	5-hydroxyeicosatetraenoic acid
PLA_2	Phospholipase A_2
RA	Rheumatoid Arthritis
MTT	3-(4,5-Dimethylthiazol-2-yl)-2,5-diphenyltetrazolium bromide
SRB	Sulforhodamine B
DMEM	Dulbecco's modified eagle medium
HRBC	Human red blood cell
WST-1	Water soluable tetrazolium-1
HET-CAM	Hen's Egg Test–Chorioallantoic Membrane
MHS	Modified Hank's Solution
RSA	Radical scavenging activity
DPPH	α, α-diphenyl-β-picrylhydrazyl
EROD	Ethoxyresorufin-O-deethylase
FRAP	Ferric reducing antioxidant power
ABTS	2, 2'-Azino-bis-3-ethylbenzothiazoline-6-sulfonic Acid
RAP-PCR	Arbitrarily primed-Polymerase chain reaction
UV	Ultraviolet
FTIR	Fouirer transform infrared
NMR	Nuclear magnetic resonance
LC-MS	Liquid chromatography-Mass spectrometry
CDI	1,1'-Carbonyldiimidazole
THF	Tetrahydrofuran
DMF	Dimethyl formamide
TEA	Triethyl amine
CAN	Cerric ammonium nitrate
HCl	Hydrochloric acid
H_2SO_4	Sulphuric acid
$POCl_3$	Phosphoryl chloride
CH_3CN	Acetonitrile
p-TsCl	p-Toluenesulfonyl chloride
K_2CO_3	Potassium carbonate
PCl_5	Phosphorus pentachloride
KOH	Potassium hydroxide

CS_2	Carbon disulphide
DMSO	Dimethyl sulphoxide
EPP	Ethyl phenyl propiolate
Et_3N	Triethylamine
$CSCl_2$	Thiophosgene
H_2O_2	Hydrogen peroxide
TMTD	Tetramethylthiuram disulfide
BHT	Butylated hydroxy toluene

ABSTRACT

Ozyazici, T. (2019). Synthesis and Biological Activity Studies of New 1,3,4-Oxadiazole Derivatives. Yeditepe University, Institute of Health Science, Department of Pharmaceutical Chemistry PhD thesis, Istanbul.

New 1,3,4-oxadiazole-2(*3H*)-thiones and piperazine derivatives were combined to evaluate their potential antiinflammatory and antioxidant activities. In this study, synthesized compounds were divided into two groups named salicylic acid (**5a-5o**) and ibuprofen (**10a-10p**) series according to located fragments at fifth position of 1,3,4-oxadiazole-2(*3H*)-thione ring. 5-(2-Hydroxyphenyl)-1,3,4-oxadiazole-2(*3H*)-thione and 5-[1-(4-isobutylphenyl)ethyl]-1,3,4-oxadiazole-2(*3H*)-thione compounds were further derived with various piperazines via *Mannich* reaction to investigate the effect of such molecular variations on the antiinflammatory and antioxidant activities. Chemical structures elucidation were supported with IR, ^{1}HNMR, ^{13}CNMR, mass spectral methods and elementary analysis. In *vitro* cyclooxygenase-1/-2 (COX-1/-2) and nitric oxide (NO) assays were applied for all compounds while prostaglandin E_2 (PGE$_2$) assay was done just for active COX-1 inhibitor and nitrit-reducer molecule(s). Results revealed that compound **10b** (76.4%) exhibited significant COX-1 inhibition whereas **5a, 5e, 5i, 5k, 5n, 10e, 10g, 10h** and **10i** showed more than 50% inhibition on COX-1 enzyme. COX-1 responses of these compounds were also checked by "docking" studies. Additionally, nitrite level-lipophilicity association of compounds was measured by Pearson correlation coefficient (r). According to results, especially ibuprofen derivatives (r= -0.703, p<0.005**) and active nitrit-supressor compounds (r= -0.593, p<0.05*) revealed statistically significant correlations. Furthermore, PGE$_2$ inhibition response of active COX-1 inhibitor and nitrit-supressor molecules were checked and nearly all selected compounds were found able to reduce LPS induced PGE$_2$ levels. For radical scavenging features; except **10k**. Rest of compounds exhibited higher activity than ascorbic acid with in *vitro* DPPH assay. Depended on their scores, especially salicylic acid compounds displayed higher antioxidant potentials compared to ibuprofen derivatives.

Key words: Piperazine, *Mannich* reaction, 1,3,4-Oxadiazole, Antiinflammatory agents-nonsteroidal, Antioxidants

ÖZET

Ozyazici, T. (2019). Yeni 1,3,4-Oksadiazol Türevlerinin Sentezi ve Biyolojik Aktivite Çalışmaları. Yeditepe Üniversitesi, Sağlık Bilimleri Enstitüsü, Farmasötik Kimya Ana Bilim Dalı, Doktora Tezi, İstanbul.

Yeni 1,3,4-oksadiazol-2(*3H*)-tiyon ve piperazin türevleri, olası antiinflamasyon ve antioksidan aktiviteleri incelenmek üzere sentezlenmiştir. Sentez bileşiklerin bu çalışmada, 1,3,4-oksadiazol halkasının beşinci pozisyonda bulunan fragmanlarına göre salisilik asit (**5a-5o**) ve ibuprofen (**10a-10p**) serisi olmak üzere ikiye ayrılmıştır. 5-(2-hidroksifenil)-1,3,4-oksadiazol-2(*3H*)-tiyon ve 5-[1-(4-izobütilfenil)etil]-1,3,4-oksadiazol-2(*3H*)-tiyon çeşitli piperazinlerle, *Mannich* reaksiyonu ile türevlendirilerek, moleküler çeşitliliğin antiinflamatuar ve antioksidan aktiviteye etkisi araştırılmıştır. Bileşiklerin kimyasal yapısıları IR, ^{1}HNMR, ^{13}CNMR, kütle ve eleman analizi ile aydınlatılmıştır. In *vitro* siklooksijenaz-1/-2 (COX-1/-2), ve nitrik oksit (NO) testleri tüm bileşikler için uygulanırken, prostaglandin E$_2$ (PGE$_2$) inhibisyonu testi sadece aktif COX-1 inhibitör ve nitrit-süpresör aktivite gösteren bileşiklere uygulanmıştır. Sonuçlara göre; bileşik **10b** (% 76.4) önemli COX-1 inhibisyon gösterirken, bileşik **5a, 5e, 5i, 5k, 5n, 10e, 10g, 10h** ve **10i**, % 50'nin üzerinde COX-1 inhibisyon göstermiştir. Bu bileşiklerin COX-1 etkileri, "docking" çalışmasıyla da kontrol edilmiştir. Ek olarak, bileşiklerin nitrit miktarı-lipofilisite ilişkisi, Pearson korelasyon sabiti (r) ile ölçülmüştür. Sonuçlara göre, özellikle ibuprofen türevleri ve aktif nitrit-baskılayıcı bileşikler, istatistiki olarak önemli korelasyon göstermiştir. Aktif COX-1 inhibitör ve nitrit-supresör moleküller için PGE$_2$ inhibisyonu bakılmış olup, yaklaşık bütün seçilmiş bileşikler lipopolisakkarit ile indüklenen PGE$_2$ miktarını azaltmıştır. Radikal süpürücü özellik bakımından yapılan in *vitro* DPPH testinde; **10k** hariç, geri kalan tüm bileşikler askorbik asite göre daha yüksek aktivite göstermiştir. Özellikle salisilik asit türevleri, elde ettikleri skorlar bakımından ibuprofen türevi bileşiklere göre daha yüksek antioksidan potansiyel yansıtmaktadır.

Anahtar kelimeler: Piperazin, *Mannich* reaksiyonu, 1,3,4-Oksadiazol, Antiinflamatuar ajanlar-nonsteroid, Antioksidanlar

1. INTRODUCTION and PURPOSE

All living organisms have the ability to defence themselves from exogenous pathogens and repair tissue damage that results from infection. Discovering inflammatory response has led to significant advantages in the treatment of inflammatory diseases which are related to various physiological and pathological processes. Although the pathology behind inflammation is well studied, physiology of disease is not yet completely understood. However inflammation is known to be adaptive response and promoted by detrimental stimuli. Primarily, an acute inflammatory stimuli is evaluted by infection or tissue injuries that triggers distribution of blood ingredients (plasma and leukocytes) through infected or injured area. Additionally, this local event may lead to chronic inflammation and autoimmune diseases in further cases which is originated from malfunction of tissue due to homeostatic imbalance of one or several biological mechanisms [1, 2].

Unrelated to the origin of its response, 'purpose' of inflammation is to eliminate the source of the disturbance. If abnormal conditions are temporary, inflamed host is let to adapt which leads to restore functionality and homeostasis of the tissue. Therefore, these acute inflammatory responses back basal homeostatic set points. Otherwise sustained inflammatory states shift through different physiological set points, as they occur during chronic inflammation [3].

Steroidal (glucocorticoids) and non-steroidal anti-inflammatory drugs are used to relief inflammation, pain and edema through inhibition of phospholipase A_2 and cyclooxygenases (COXs) or lipoxygenases (LOXs), respectively. COX family is responsible with the biosynthesis of prostaglandin H_2 which is the precursor for some of inflammatory mediators; prostaglandins, prostacyclins and thromboxanes. Their biological missions are coordinated by two major isoforms named COX-1 and COX-2. While COX-1 is constitutively secreted and located in most tissues to maintain homeostasis, COX-2 is synthesized upon an inflammatory response and evaluated in the site of inflammation. In many cases of antiinflamatory drug therapy, due to nonselective inhibiton of the both enzymes, systemic and local gastrointestinal (GI) side effects were emerged which requires new pharmaceutical approaches to overcome these problems [4-7].

Molecular and conceptual model of inflammation have kept evolving new insights to generate novel therapeutic approaches for inflammatory diseases in recent years. Particularly, recent studies were aimed to replace the carboxylate functionality of nonsteroidal antiinflammatory drugs (NSAIDs) with many types of less acidic heterocyclic bioisosters such as 1,3,4-oxadiazole [8], 1,2,4-triazole [9, 10] and 1,3,4-thiadiazole [11] to protect the gastric mucosa from free carboxylate moiety [12]. Based on this princible, selective COX-2 inhibitors were developed in which they commonly have a heterocyclic core and their action on cytoprotective prostaglandins contribute to physiological homeostasis besides their antiinflammatory actions. However, valdecoxib (Bextra®) and rofecoxib (Vioxx®) presented severe adverse effects on cardiovascular system and have been withdrawn from the market [13-15]. A significant example for chemical modification concept to produce non-ulcerogenic and antiinflamatory drug was represented by Bhandari and co-workers in 2008. They converted carboxylic acid fragment of diclofenac into 1,3,4-oxadiazole-2(*3H*)-thione ring via a three step chemical reaction. In *vivo* carregenaan-induced paw edema test results clearly revealed that 1,3,4-oxadiazole-2(*3H*)-thione analogues increased antiinflammatory activity potential and lowered ulceration scores compared to diclofenac [16]. Also, in 2010, Manjunatha and coworkers published a similar study in which carboxylic acid of ibuprofen was converted into 1,3,4-oxadiazole-2(*3H*)-thione and statistically meaningful test results in paw edema model proved that heterocyclic ring cyclization demonstrates a better gastrointestinal profile (Scheme 1) [17].
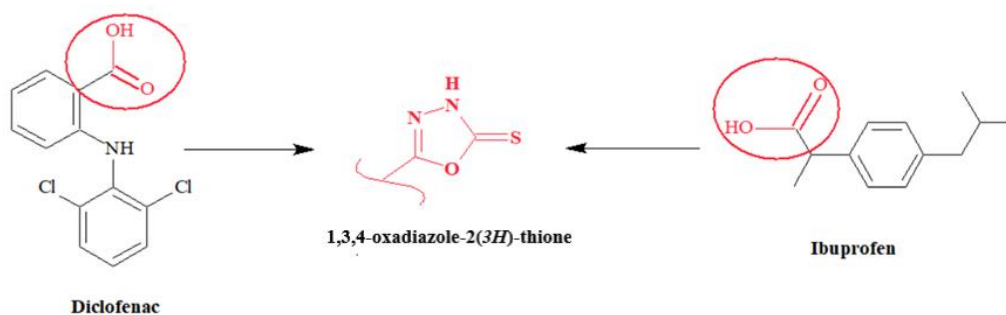
Scheme 1. Conversion of carboxylic acid functional groups of Diclofenac and Ibuprofen into 1,3,4-oxadi azole-2(*3H*)-thione

It is known that, mechanism of inflammation demonstrates a sequence of organized responses also involving cellular and vascular secretions. These pathways

include movement of defense cells and inflammatory mediators through inflamed site. A number of these mediators and other signaling molecules (histamine, prostaglandins, leukotrienes, free radicals and serotonin, etc.) are released by immune cells which participate in the event of inflammation [18, 19]. Nitric oxide (NO) is an example of cellular secretion and this chemokine has a major role in the pathogenesis of inflammation due to its signaling property. Under normal physiological conditions this molecule plays an antiinflammatory effect whereas in abnormal situations, due to being overproduced, acts as a proinflammatory mediator and promotes the induction of inflammation. Endothelial cells are able to synthesize and release NO by the activation of nitric oxide synthase (NOS) family. Particularly inducible nitric oxide synthase (iNOS) enzyme coordinates NO production at inflammation site. Therefore, NO inhibitors preserve therapeutic importance in the management of inflammatory diseases [20].

In the event of inflammation another important group of mediators secreted from vascular beds of tissues are prostanoids and particularly, prostaglandin E_2 (PGE_2). They represent important roles in the symptoms of inflammatory arthrities including rheumatoid arthritis (RA). Thereby inhibiting the biosynthesis of prostanoids, result in antipyretic, anti-inflammatory and analgesic effects. Since PGE_2 serves actions like pyrexia, pain sensation, and inflammation, it was thought that the action of NSAIDs should also be based on the inhibition of PGE_2 production [1].

The aim of this study is to design novel compounds which present stronger and safer antiinflammatory profile compared to parent compounds. Consequently, chemical part of this study has involved replacement of carboxylic acid groups in salicylic acid and ibuprofen into less acidic 1,3,4-oxadiazole ring and has derived with piperazine derivatives via *Mannich* reaction. In order to provide the desired biological properties, newly synthesized 31 compounds were studied for their antiinflammatory potentials with in *vitro* assays named COX-1/COX-2 enzyme, nitric oxide and PGE_2 inhibition. Antioxidant capacities of compounds were also checked with α, α-diphenyl-β-picryl-hydrazyl (DPPH) radical scavenging assay. Molecular docking studies were performed with crystal structures of COX-1 and COX-2 to explain structure-activity relationship of compounds.

In this study, a scheme of 3,5-disubstituted-1,3,4-oxadiazole-2(*3H*)-thiones were synthesized and summarized in Table 1:

Table 1. Newly synthesized salicylic acid (**5a-5o**) and ibuprofen (**10a-10p**) derivatives

Salicylic acid derivatives (5a-5o)		Ibuprofen derivatives (10a-10p)	
Compound	**R**	**Compound**	**R**
5a	Phenyl	**10a**	Phenyl
5b	4-fluorophenyl	**10b**	4-fluorophenyl
5c	4-trifluorophenyl	**10c**	2-fluorophenyl
5d	3-trifluorophenyl	**10d**	3-trifluorophenyl
5e	4-chlorophenyl	**10e**	4-chlorophenyl
5f	2-chlorophenyl	**10f**	2-chlorophenyl
5g	3,4-dichlorophenyl	**10g**	3,4-dichlorophenyl
5h	2,3-dichlorophenyl	**10h**	2,3-dichlorophenyl
5i	4-methylphenyl	**10i**	4-methylphenyl
5j	2,3-dimethylphenyl	**10j**	2,3-dimethylphenyl
5k	4-methoxyphenyl	**10k**	4-methoxyphenyl
5l	4-cyanophenyl	**10l**	3-methoxyphenyl
5m	2-cyanophenyl	**10m**	2-methoxyphenyl
5n	2-pyridyl	**10n**	4-cyanophenyl
5o	2-pyrimidinyl	**10o**	2-cyanophenyl
		10p	2-pyridyl

2. LITERATURE REVIEW

2.1. Chemistry

2.1.1. Oxadiazoles

Oxadiazoles are heterocyclic rings and structure has two carbons, two nitrogens and one oxygen atom on it. Oxadiazole ring isomers which were named as furo[ab]diazoles, was discovered by Tiemann and Krüger in 1884. Isosterically similar furan and oxadazole rings can be comparible but instead of two methine groups (−CH=) replaced two sp^2 nitrogens (−N=) was consequensed as four oxadiazole isomers [21-23].

1,2,3-oxadiazole   1,2,4-oxadiazole   1,2,5-oxadiazole   1,3,4-oxadiazole
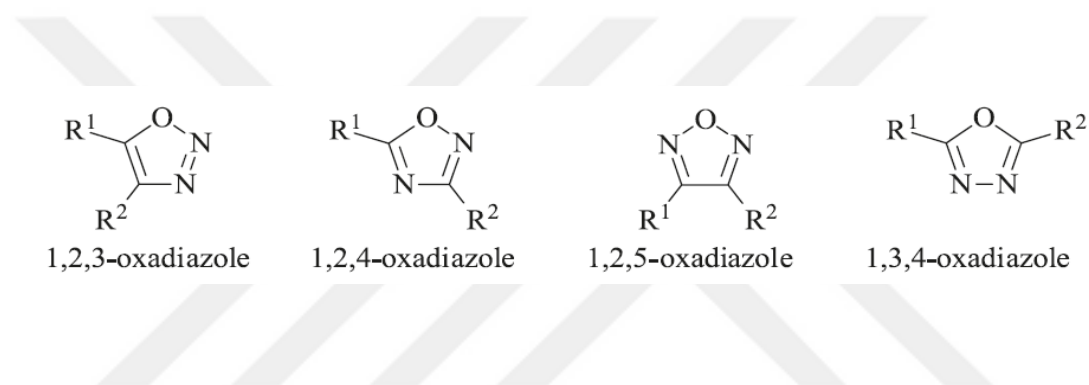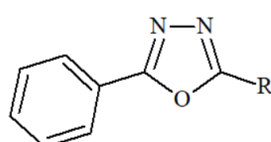
In pharmaceutical sciences, oxadiazole ring is known as bioisoster of esters, amides, carbamates and hydroxamic esters. In biologial media, these carbonyl-containing groups are well-known with their stability problems in which it is an important obstacle for being a drug candidate. Therefore, oxadiazole isomers are able to use synthetic alternatives for these groups and depended on their similar spatial geometries, bioisosteric properties of oxadiazoles may also represent desired pharmacological responses [24, 25].

2.1.2. 1,3,4-Oxadiazoles

2.1.2.1. Chemical properties

In 1964, Moussebois and Oth confirmed experimentally the idea that 1,3,4-oxadiazoles are chemically aromatic structures. To obtain an accurate data via UV spectroscopy, mono phenyl substituted 1,3,4-oxadiazole was compared with diphenyl substituted ring. According to the concept of UV study, if a heterocyclic structure has an

aromaticity, insertion of second phenyl ring would lead a bathochromic shift for λ_{max} value which means low level of energy is used for the $\pi \rightarrow \pi^*$ transition due to an elevated level of conjugation in whole molecule. UV data consequences clearly showed the presence of two phenyl rings considerably increased λ_{max} value which refers aromatic feature of 1,3,4-oxadiazole ring (Figure 1) [26-28].

R	λ_{max}
H	245
-C_6H_5	276

Figure 1. Chemical structure and λ_{max} values of substituted 1,3,4-oxadiazoles

Due to aromaticity of 1,3,4-oxadiazole-containing compounds show specific cation-π binding model for biological targets. Particularly in physiological pH, this noncovalent interaction occurs frequently between aromatic pi face of molecule and cationic part of receptor. Conjugation (6π electron) in aromatic fragment of 1,3,4-oxadiazole center and its two nitrogen atoms (each one is electron pair) fully present to bind with a receptor (Figure 2) [29, 30].

Figure 2. 1,3,4-oxadiazole moiety and His279 interaction via cation-π bonding.

2.1.2.2. Chemical synthesis
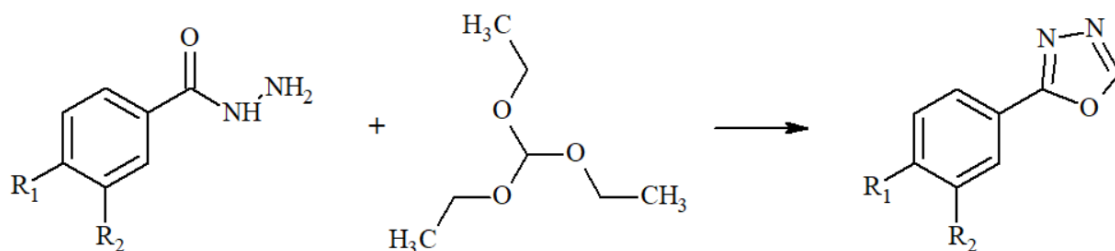
Dabiri and co-workers reported a synthesis pathway of 5-monosubstituted-1,3,4-oxadiazole. Reaction procedure included sulphuric acid impragnated silica gel catalyzer of hydrazide and triethyl orthoester to obtain desired compounds. Chemical process and yield of products were seemed profitable. Researchers also noticed that instead of triethyl orthoester, potassium aluminium sulphate and p-tolenesulfonic acid were also able to catalyze the reaction [31, 32].

Another synthesis method of monosubstituted-1,3,4-oxadiazole was reported by Polshettiwar in 2008. Aromatic hydrazides and triethyl orthoester were reacted on the surface of Nafion NR-50 (P_4S_{10}/Al_2O_3) under microwave irradiation. Particularly methoxy and flouro substitutions on fourth position of aromatic ring increased reaction yields [33].
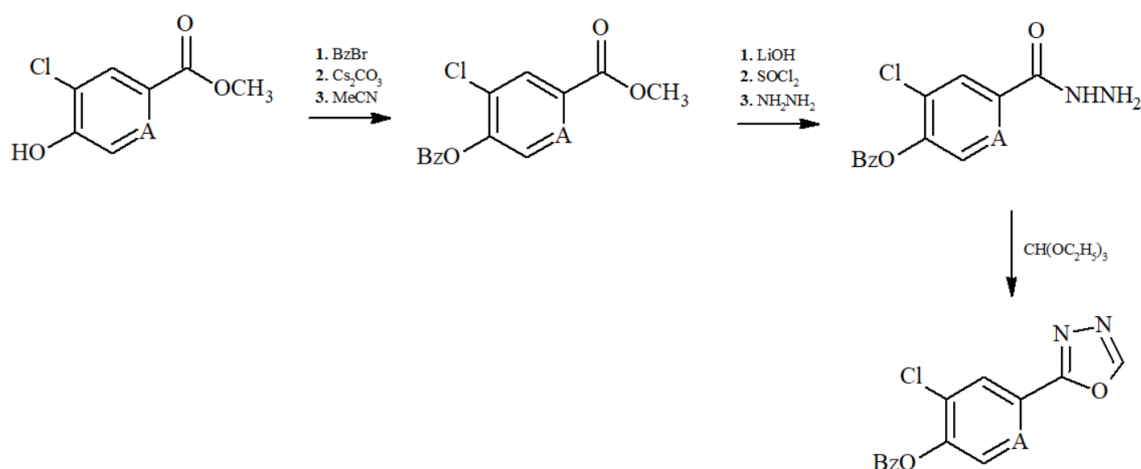
Inhibitors of pathogenic bacteria biosynthesis were derived by Montgomery and friends. Initial step of chemical reaction was necessary for protecting of hydroxyl group on aromatic esters with benzyl bromide. Next step, compounds containing ester group were converted to hydrazide and final products were obtained in hot media with trimethyl orthester reagent [34].
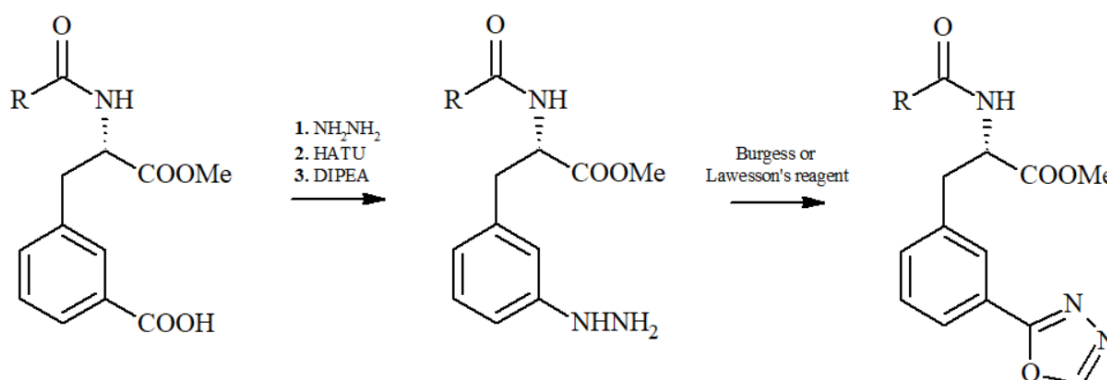
Regioselective synthesis of hydrazides were obtained from carboxylic acids with spesified catalyzers and 1,3,4-oxadiazole cyclization was evaluated with 1-methoxy-N-trimethylammoniosulfonyl-methanimidate (Burgess reagent) under microwave irradiation. Instead of Burgess reagent, 2,4-bis(methoxyphenyl)-1,3,2,4-dithiaphospheta-ne-2,4-disulfide in tetrahydrofuran (THF) solution (Lawesson's reagent) was used to cyclized hidrazid group into 1,3,4-oxadiazole by Bethel and friends in 2009 [35].
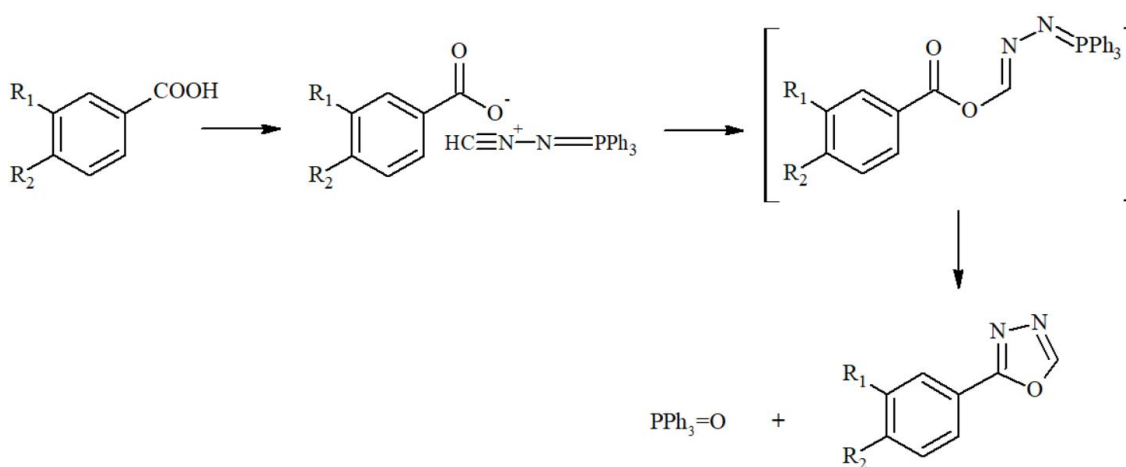
Ramazani and co-workers developed another synthesis method for monosubstituted-1,3,4-oxadiazole with (N-isocyananimino)triphenylphosphine reagent with different substituted benzoic acids at room temperature. Synthesized compounds were obtained via high percentage of yields and values were seemed independent from the position or chemical nature of substitutent on aromatic ring [36-39].
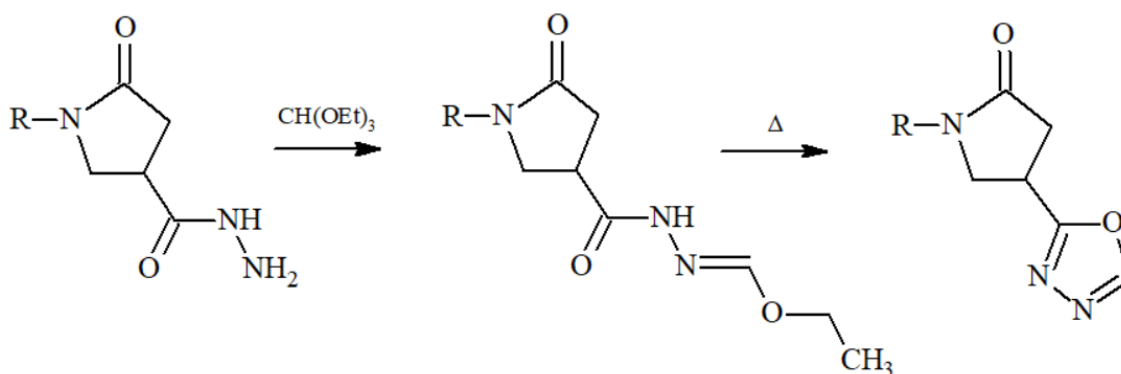
Mickevicius and friends used approximately same pathway with Dabiri and friends while synthesizing monosubtituted-1,3,4-oxadiazole by hydrazide and triethyl orthoformate with the ratios of 1:8. After reflux process, the reaction was cooled and the crystals were taken off to obtain final compounds [40].
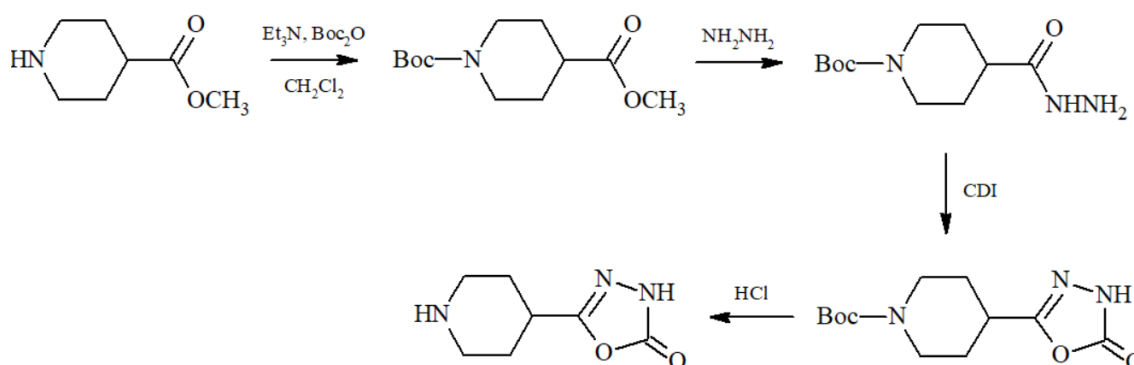
5-(Piperidin-4-yl)-1,3,4-oxadiazole-2-one synthesis pathway included a protection step for secondary amine moiety of piperidine ring. For the next step, hydrazine hydrate in alcoholic solution produced hydrazide from methyl ester in compound **2**. Carbonyldiimidazole (CDI), tetrahydrofuran (THF) and dimethylformamide (DMF) were

used with hydrazide in cold media to get 1,3,4-oxadiazole-2-one ring. However, IR and NMR spectra indicated that they exist predominantly in their amide-form; Theoretically, oxadiazol-2-ones may exist in two tautomers named as amide and imino-alcohol. At the end of the process desired compounds were deprotected with alcoholic hydrochloric acid (HCl) [41].
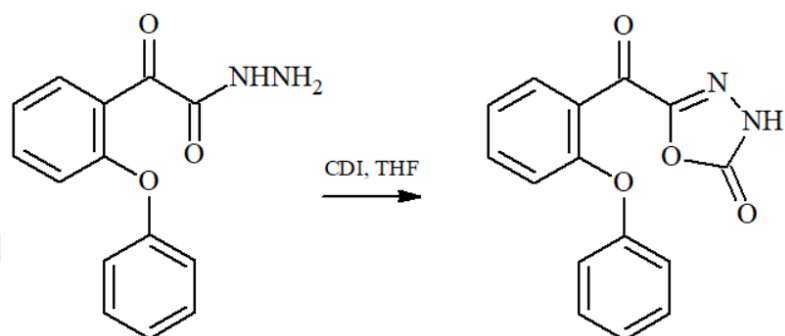
Tabatabai and co-workers in 2013 studied on the synthesis of 1,3,4-oxadiazole-2-one structure. Chemical pathway of desired product was proceed in the presence of 1,1'-carbonyldiimidazole (CDI) and dry tetrahydrofuran coctail at 0°C in which then continued at room temperature for 5 hours.
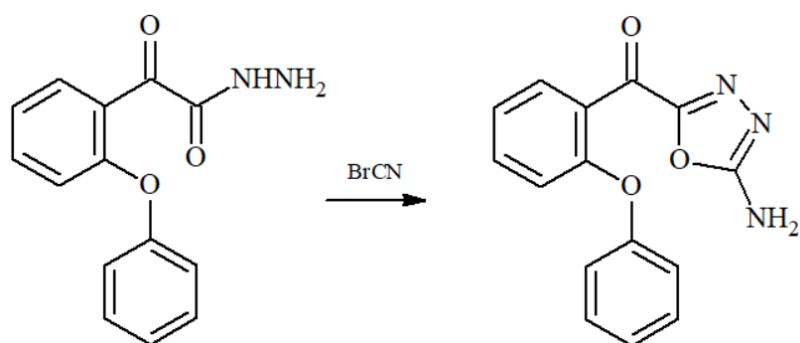
Instead of ketone group at second position of 1,3,4-oxadiazole; primary amine was substituted by Tabatabai and coworkers *via* cyanogen bromide in methanol with a hidrazid-containing compound [42].

Ar$_{1,2}$ = Aryl halide
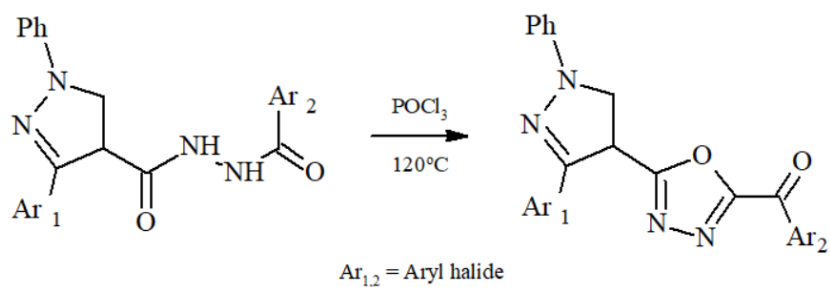
Other synthesis pathway of 2,5-disubstituted-1,3,4-oxadiazole derivatives was studied by Ningaiah and co-workers. *N'*-aroyl-5-methyl-1,3-disubstituted-1*H*-pyrazole-4-carbohydrazide compounds were heated with phosphorusoxychloride via 120°C to produce title derivatives of 1,3,4-oxadiazole in moderate yields [43].
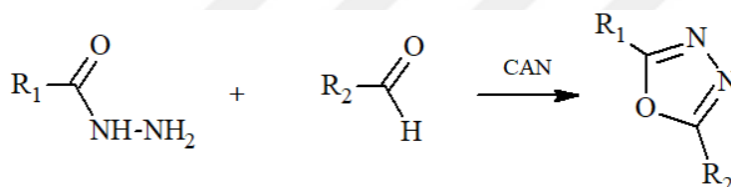
Dabiri and co-workers synthesized many nonsymmetrical 2,5-disubstituted-1,3,4-oxadiazole from monoacyl hydrazines by the use of cerric ammonium nitrate (CAN) as a catalyzer for condensation and oxidative cyclization of 1,3,4-oxadiazole ring. According to procedure, aromatic aldehytes in ethanol with presence of CAN under solvent-free conditions produced 2,5-disubstituted series of 1,3,4-oxadiazole [44].
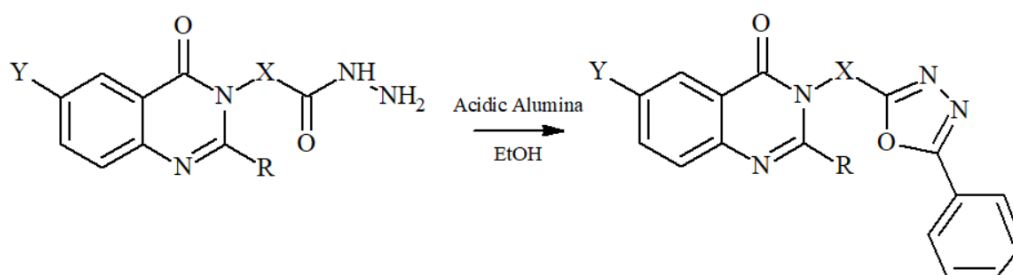
Desai *et al.* reported the synthesis of 1,3,4-oxadiazole in the presence of acidic alumina by treating the hydrazide with benzoic acid in ethanolic solution through microwave irradiation [45].
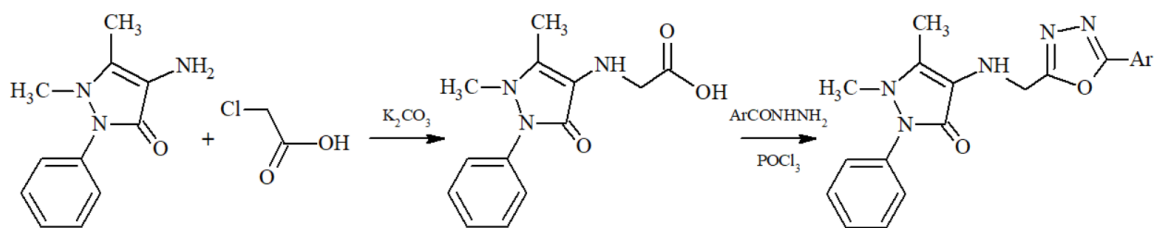
Ahsan and co-workers studied on oxadiazole ring cyclization in two step reaction. Initially, primary amine group of starting material was treated with 2-chloroacetic acid in dry acetone and potassium carbonate were refluxed and the reaction was continued with electrophilic substitution mechanism. In the last step obtained carboxylic acid-containing compound was reacted with aroylhydrazine in presence of phosphorus oxychloride which resulted with title compounds [46].
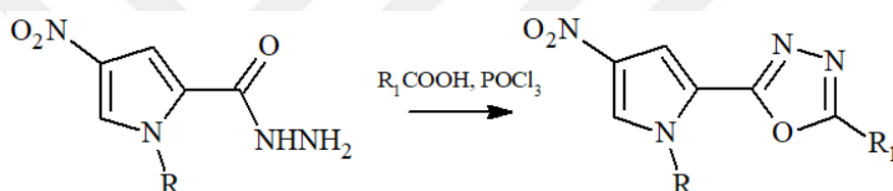
Rane and researchers realised that hidrazide condensation with equimolar quantities of different aromatic and heteroaromatic acids via phosphorus oxychloride in hot media resulted the formation of 2,5-disubtituted-1,3,4-oxadiazoles [47].
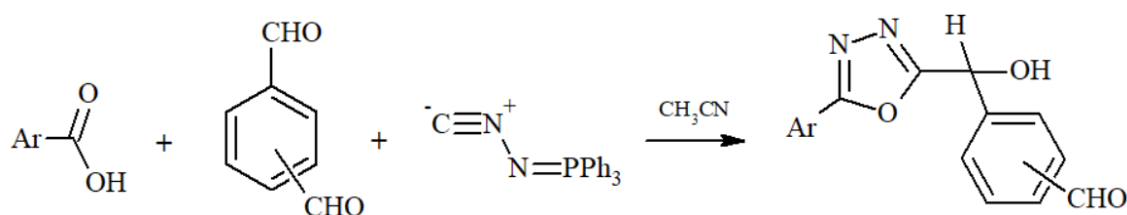
A convenient reaction was studied by Ramazani and researchers in which (N-isocyanimino)triphenylphosphorane, bis-aldehydes (isophthalaldehyde and terphthal aldehyde) and aromatic (or heteroaromatic) carboxylic acids were put in a flask under neutral condition and at the end of reaction, theoritically significant yield values were found [48].
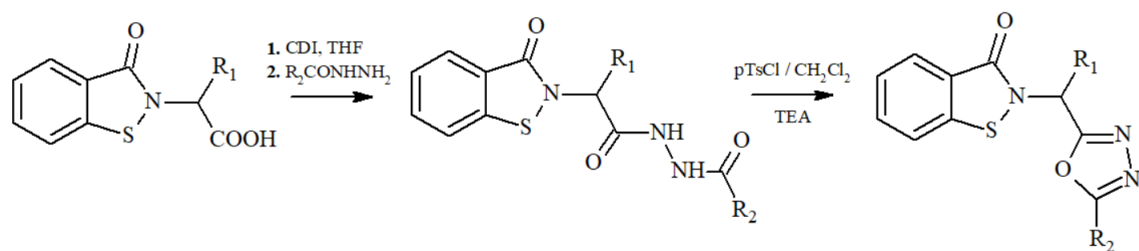
Carbonyldiimidazole (CDI) and tetrahydrofuran (THF) were used to produce hydrazide group from carboxylic acid moiety of benzisothiazol-3(2H)-one series. Corresponding products yielded desired 2,5-disubstituted-1,3,4-oxadiazole compounds with p-toluenesulfonylchloride-mediated cyclodehydration mechanism by Lai and researchers in 2013 [49] .

R^1= H, Cl, OCH$_3$
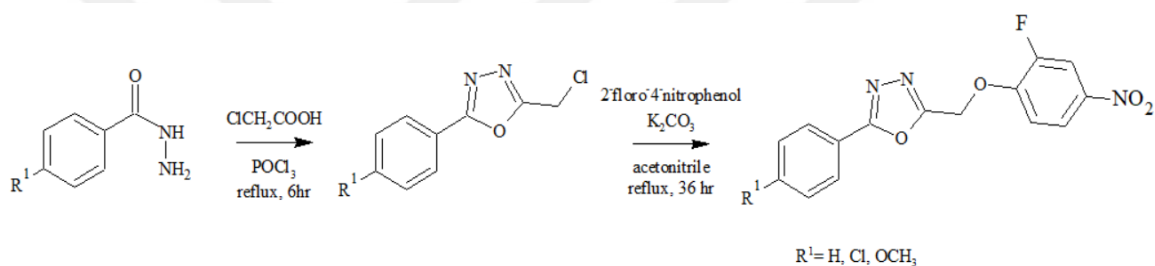
Cyclization of 5-aryl-2-(chloromethyl)-1,3,4-oxadiazole analogs were evaluated through chemical reaction of hydrazide with chloroacetic acid in phosphorus oxychloride. Nucleophilic substitution of chloroethyl group on second position of 1,3,4-oxadiazole attacked to hydroxyl group on 2-fluoro-4-nitrophenol and ether-containing final products were obtained [50, 51].

R= substituted phenyl
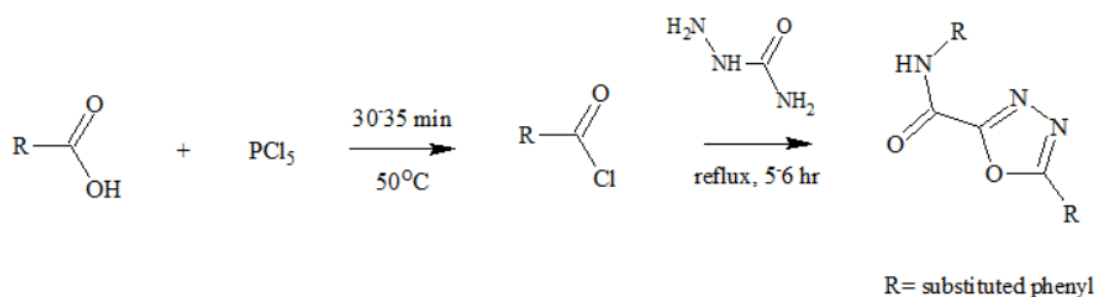
By Singh and co-workers, different substituted phenyl derivatives of 1,3,4-oxadiazole compounds were evaluated with two step reaction. Acyl chlorides were

obtained from carboxylic acids in the presence of phosphorus pentachloride. After hidrazid addition, desired 2,5-disubstituted-1,3,4-oxadiazole analogues were produced [52].

2.1.2.3. Spectral Properties

2.1.2.3.A. Infrared (IR) Spectroscopy
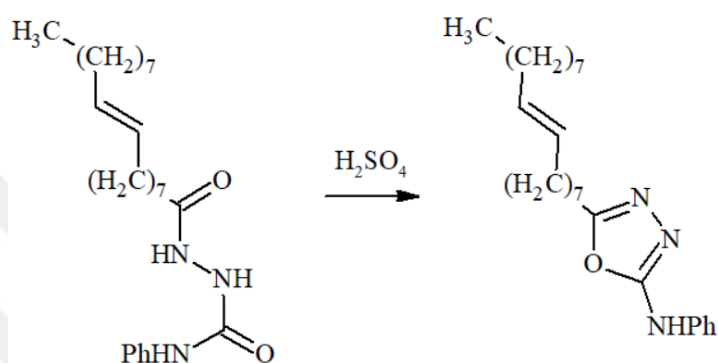
Asghar and researchers studied infrared spectrums of different compounds and 1,3,4-oxadiazole derivatives were evaluated according to signal variations of semicarbazide group. Disappearance of signals at 3342 and 1708 cm^{-1}, suggesting the conversion of N–H and C=O group in semicarbazide, respectively into C=N and C–O–C group signals in 1,3,4-oxadiazole at 1660 and 1193 cm^{-1} [53].
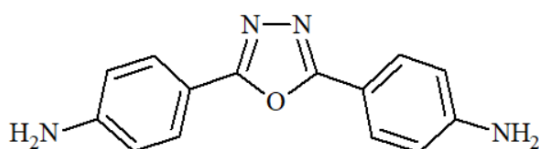
The FT-IR spectrum of 2,5-bis-(4-aminophenyl)-1,3,4-oxadiazole showed strong signals in the range of 3460-3363 cm^{-1} which could be related to asymmetric and symmetric stretching vibration of the NH$_2$. Other stretching bands related to C=N and C-O-C groups at 1596 and 1172 cm^{-1} were important indicators of 1,3,4-oxadiazole production according to Zobaydi and researchers [54].
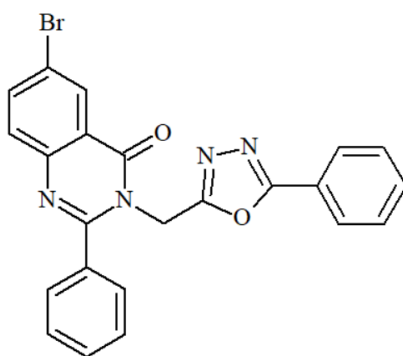
The structure of 6-bromo-2-phenyl-3-[4-(5-phenyl-1,3,4-oxadizole-2-yl)phenyl]-quinazoline-4(*3H*)-one compounds were confirmed with different spectral and analytical results by Desai in 2005. IR spectra of compounds obviously showed spectral bands at 1600 cm^{-1} (C=N) for formation of quinazolone and 1590 cm^{-1} (C=N) and 1339 cm^{-1} (C-O-C) for formation of 1,3,4-oxadiazole [55].

2.1.2.3.B. Ultraviolet-Visible (UV-Vis) Spectroscopy

1,3,4-Oxadiazole ring indicates no absorption itself above 200 nm whereas 2-substituted and 2,5-disubstituted derivatives displays absorption peaks slightly above 200 nm [55] Electronic transitions through the oxadiazole ring have been shown efficiently and hence, their infrared spectra responses have been deeply worked and reported in many researches.
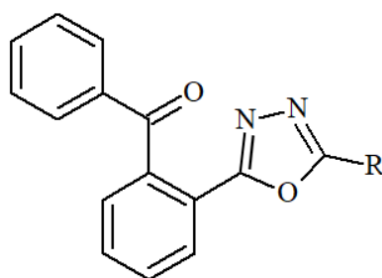
According to Bala and coworkers, novel 2,5-disubstituted-1,3,4-oxadiazole derivatives were characterized by some spectroscopic analysis in which one of them was UV-visible spectroscopy. λ_{max} values of compounds were calculated by using double

beam UV-Visible spectrophotometer and based on substituent effect, scores were found in range of 245-285 nm [56].
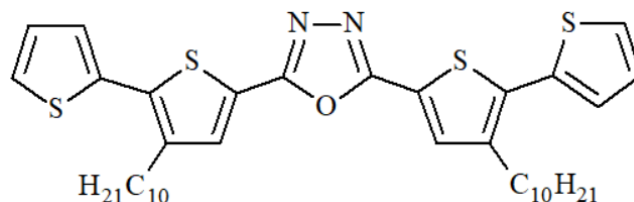
2,5-Disubstituted-1,3,4-oxadiazole compounds revealed an intense absorption band at the visible range where π–π* transitions are occurred. The maximum wavelength of this band obviously shifts with the azole unit, as well as with the oxadiazole moiety showed an absorbance peak at 376 nm [57].

2.1.2.3.C. [1]H Nuclear Magnetic Resonance (^{1}H NMR) Spectroscopy

In ^{1}H NMR spectrum, the disappearance of N-H peak in hydrazide function while it converts 1,3,4-oxadiazole structure is well-descriptor point for ring cyclization. 1,3,4-Oxadiazole does not have hydrogen atom itself which corresponds no ^{1}H NMR response [58].

2.1.2.3.D. [13]C Nuclear Magnetic Resonance (^{13}C NMR) Spectroscopy
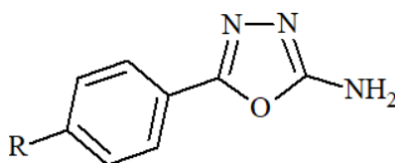
In ^{13}C NMR spectra, second and fifth carbons of the 1,3,4-oxadiazole nucleus were seen around 171 and 168 ppm, respectively [59].

2.1.2.3.E. Mass Spectrometry
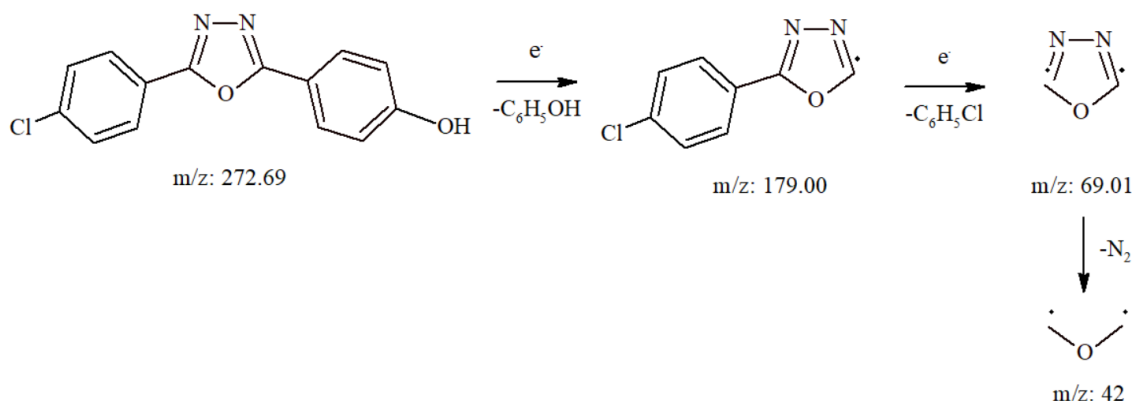
Scheme 2. Mass fragmentation of 2,5-disubstituted-1,3,4-oxadiazole

2,5-Disubstitutedphenyl-1,3,4-oxadiazole molecular structure was recorded with mass spectra by Singh and researchers in 2012. The general mass fragmentation pattern of 1,3,4-oxadiaozle ring was shown in Scheme 2 and molecular ion peak at 272.69 of compound was found in conformity with the molecular formula [60].

2.1.3. 1,3,4-Oxadiazole-2(*3H*)-thione

2.1.3.1. Chemical Properties

Recently, intra- or intermolecular proton transfer on a molecule has been an interesting point for many chemical and biological processes [61-64]. As an example mercapto-azoles tautomeric forms exhibit variety of chemical reactivities like substitution reactions [65]. In this respect, there is a growing interest in chemists for investigation of thione-thiol tautomers of 1,3,4-oxadiazole and their electronic natures [66-69].

Scheme 3. Thiol-thione tautomerism of 1,3,4-oxadiazole

In 2014, Arslan and coworkers studied on tautomerization energies of 1,3,4-oxadiazole-2-thiol/thione structures (Scheme 3). Experimental data revealed that C_1-N_1

bond length was found 1.323 Å and this value was good to be in range of reference C-N (1.47 Å) and C=N (1.28 Å) bond lenghts. Besides C_1-N_1 bond longer than C_2-N_2 (1.281 Å) data ; multiple nature of this bond could also be explained with C_1-S_1 bond length (1.649 Å). Consequently, the N_1-C_1 and C_1-S_1 bonds lenghts were seemed to be remarkable indicator to decide the exact tautomer type. For thione tautomer; C_1-S_1 bond has a double bond character while this bond exhibits single bond character in the thiol tautomer. On the contrary, the N_1-C_1 bond is a single bond in the thione tautomer whereas it is a double bond in the thiol tautomer [70].

2.1.3.2. Chemical Synthesis
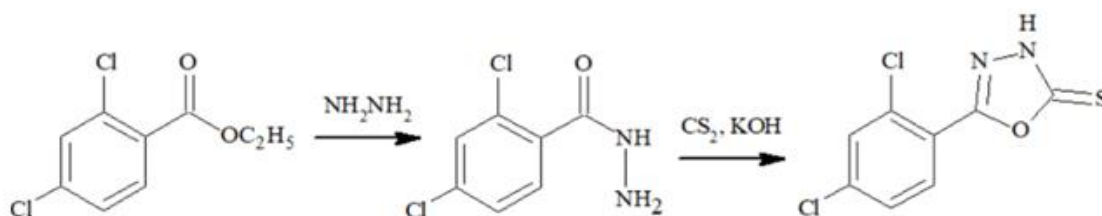
Young and Wood in 1955, found the synthesis pathway of 1,3,4-oxadiazole-2(*3H*)-thione ring in 1982. Alkyl esters of different benzoic acids were converted into hidrazid group by hydrazine hydrate. Yield products were reacted with carbondisulphide and potassium hydroxide to provide the cyclization of 1,3,4-oxadiazole-2(*3H*)-thione ring. As a result of the study, product yields were found in range of moderate to good scores [71].
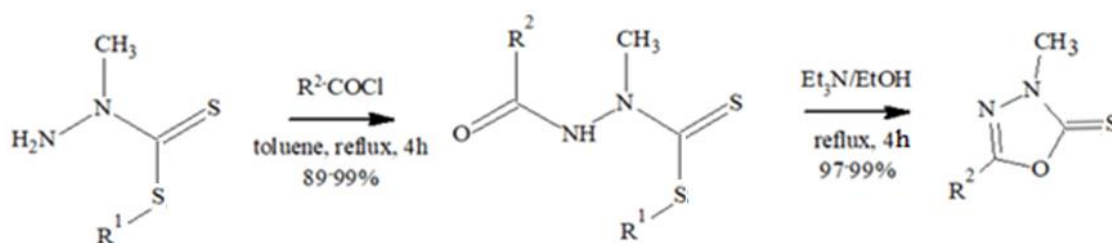
In 1988 Molina and friends presented a new method for 1,3,4-oxadiazole-2(*3H*)-thione ring closure. Alkyl 2-methyldithiocarbazates were converted alkyl 3-acyl-2-

methyldithiocarbazate derivatives via presence of acyl chloride derivatives in dry toluene with significant reaction yields [72].
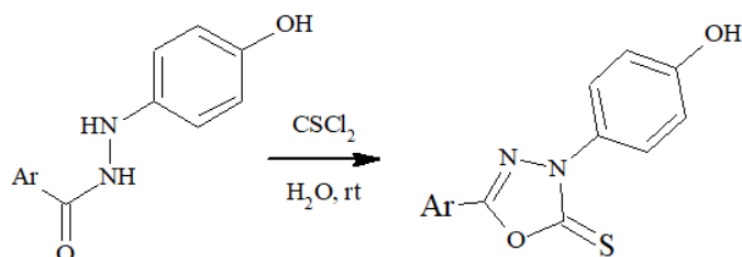
Loetchutinat and co-workers dealt with synthesis concept of 3,5-disubstituted,3,4-oxadiazole-2(*3H*)-thiones by cyclocondensation of aroylhydrazides with thiophosgene [73].
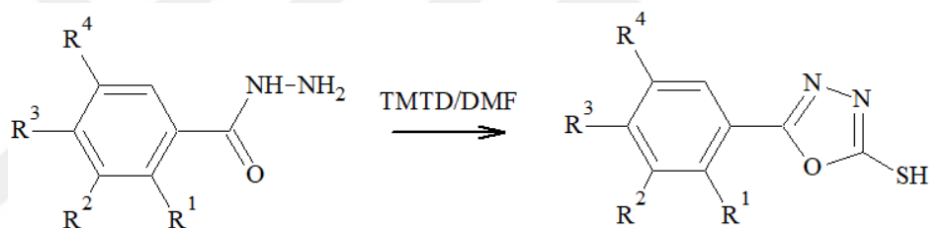
Macaev and researchers reported other pathway of 2,5-disubstituted-1,3,4-oxadiazole synthesis from hydrazine derivatives using tetramethylthiuram disulfide (TMTD) in DMF. According to the procedure, 1,3,4-oxadiazole nucleus was produced with cyclization of acyl hydrazones [74].

2.1.3.3. Spectral Properties

2.1.3.3.A. Infrared (IR) Spectroscopy

IR data of 1,3,4-oxadiazole-2(*3H*)-thione can indicate thiol or thione tautomer of the ring. Presence of a sharp band in range of 1467-1200 cm^{-1} without an absorption at 2600-2550 cm^{-1} (S-H) refers thione (C=S) form of the ring. Also broad band 3192 cm^{-1} represents N-H moiety in 1,3,4-oxadiazole fragment which supports the state of thione tautomer [75].

2.1.3.3.B. Ultraviolet-Visible (UV-Vis) Spectroscopy

The λ_{max} values of 1,3,4-oxadiazole-2(*3H*)-thione structure in UV spectrum, represent as strong absorptions at 260 and 208 nm [76].

2.1.3.3.C. [1]H Nuclear Magnetic Resonance (^{1}H NMR) Spectroscopy

Besides IR data, ^{1}H NMR responses are also used for a cross-check to determine exact tautomer type of 1,3,4-oxadiazole-2-thione/thiol ring. The presence of S-H peak in range of 1-3 ppm reveals thiol form whereas broad peak in between 7-10 ppm represents thione tautomer of the ring [69, 77].

2.1.3.3.D. [13]C Nuclear Magnetic Resonance (^{13}C NMR) Spectroscopy

Signals at 157.1 and 155.3 ppm for second and fifth carbons present in the 1,3,4-oxadiazole-2(3H)-thione in ^{13}C NMR spectra, confirms the formation of ring [78].

2.1.3.3.E. Mass Spectrometry

Molecular ion (M[+]) peaks of different 5-substituted-1,3,4-oxadiazole-2-(*3H*)-thiones were compatible with molecular weights of compounds [79, 80].

2.1.4. *Mannich* Bases of 1,3,4-Oxadiazole-2(*3H*)-thiones

2.1.4.1. Chemical Properties

The NH proton at third position of 1,3,4-oxadiazole-2-(*3H*)-thione is adequately acidic to obtain the *Mannich* base compounds. Particularly, *N-Mannich* bases like piperazine derived compounds represent higher reaction yields and lipophilic properties [81, 82].

2.1.4.2. Chemical Synthesis
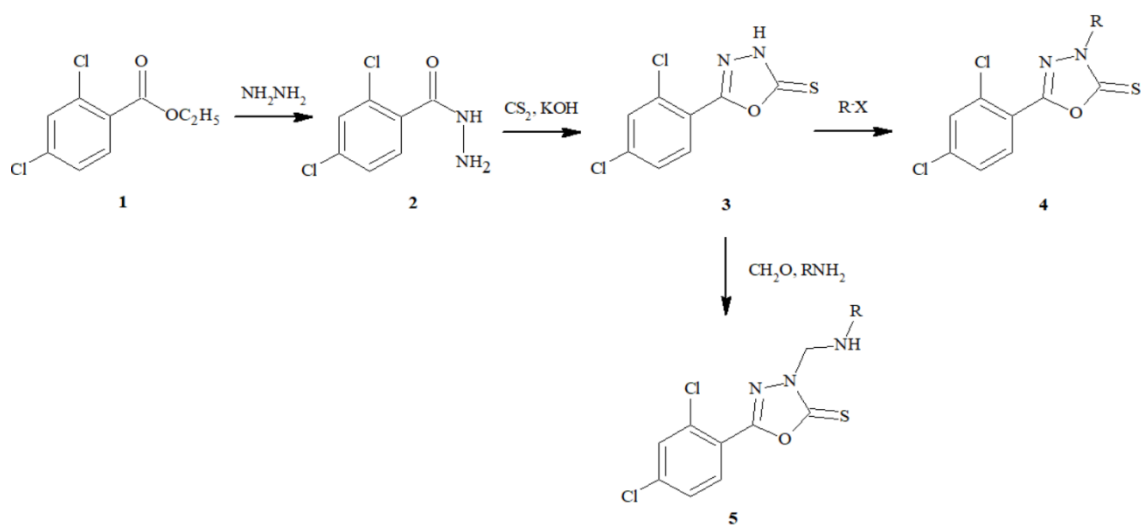
Following the method of Young and Wood in 1955, Soni and co-workers continued the chemical process with substitution on third position of 1,3,4-oxadiazole ring in 1982. According to their synthesis pathway, presence of formaldehyde and primary amine groups, compound **5** was substituted with different amines via a methylene bridge. As a result of the study, yield percentages of obtained products were in range moderate to good values [71, 83].

Chemical reactions of N-*Mannich* derivatived 1,3,4-oxadiazole-2(*3H*)-thiones are resulted with high yield products in researches. Equimolar doses of primary or secondary amines which contains active hydrogen and formaldehyde composes this three-step reaction with desired results [17, 84]. Some N-*Mannich* bases of 1,3,4-oxadiazole-2(*3H*)-thione compounds that were mentioned as to have significant level of reaction yields in previous researches are depicted in Scheme 4 [17, 84-88].
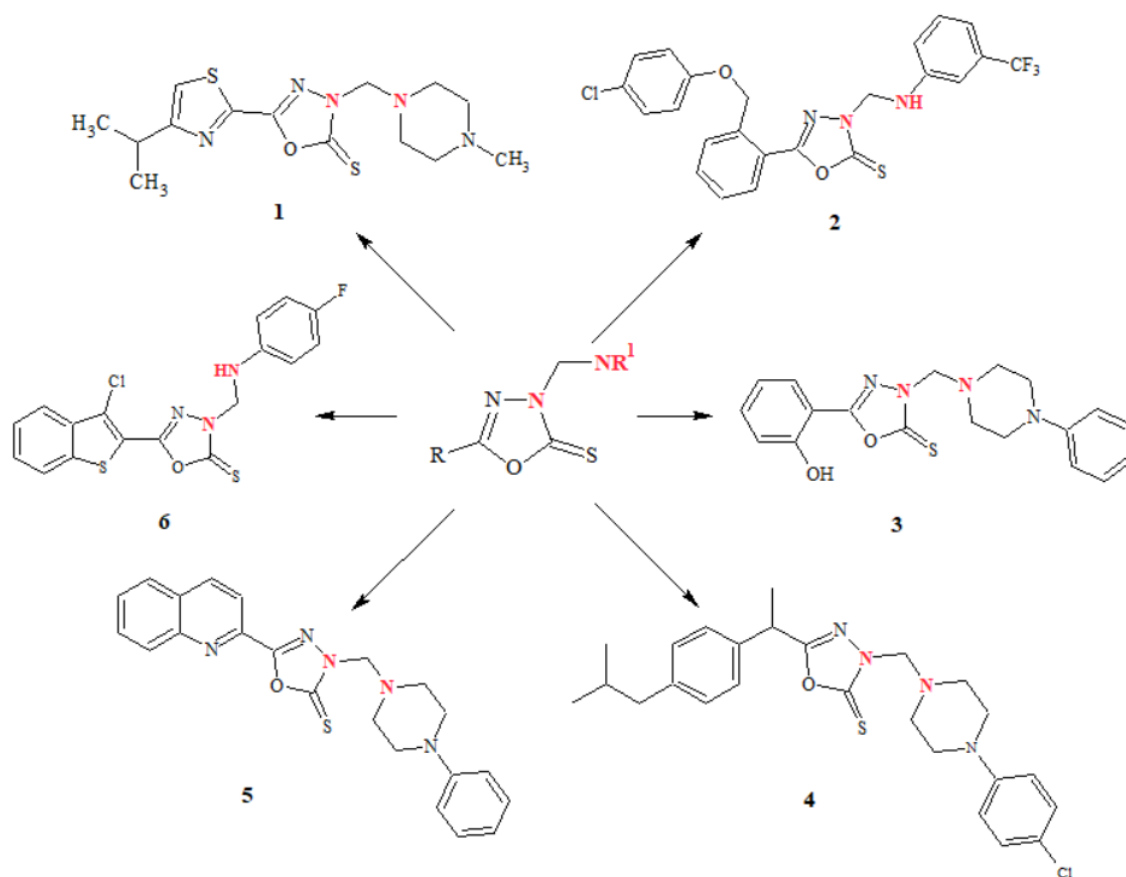
Scheme 4. Different N-*Mannich* bases of 1,3,4-oxadiazole-2(*3H*)-thione ring: Compound **1** [85], **2** [86], **3** [84], **4** [17], **5** [87], **6** [88]

2.1.4.3. Spectral Properties

2.1.4.3.A. Infrared (IR) Spectroscopy

Disappearance of N-H band nearly 3300 cm^{-1} and continuation of spesific C=S signals in 1,3,4-oxadiazole-2(*3H*)-thione structure in 1300-1100 cm^{-1} confirms the IR spectra to assign the structures of *Mannich* bases [17].

2.1.4.3.B. Ultraviolet-Visible (UV-Vis) Spectroscopy

λ$_{max}$ values of N-*Mannich* bases may be variable based on their molecular contents. Particularly, aromatic structure containing derivatives reveal bathochromic shifts depend on $\pi \rightarrow \pi *$ transitions [81].

2.1.4.3.C. ^{1}H Nuclear Magnetic Resonance (^{1}H NMR) Spectroscopy

The absence of signal due to N-H in ^{1}H NMR spectra and the presence of a new singlet for N-CH$_2$-N in the range of 4.79-5.13 confirms that 1,3,4-oxadiazol-2(*3H*)-thiones (3) are converted into corresponding *Mannich* bases [17].

2.1.4.3.D. ^{13}C Nuclear Magnetic Resonance (^{13}C NMR) Spectroscopy

In the ^{13}C NMR spectra; thione C=S and imine C=N carbons appear at around 179 and 155 ppm, respectively. Additionally, other characteristic signals for N-CH$_2$-N carbon presents in range of 60-70 ppm [17].

2.1.4.3.E. Mass Spectrometry
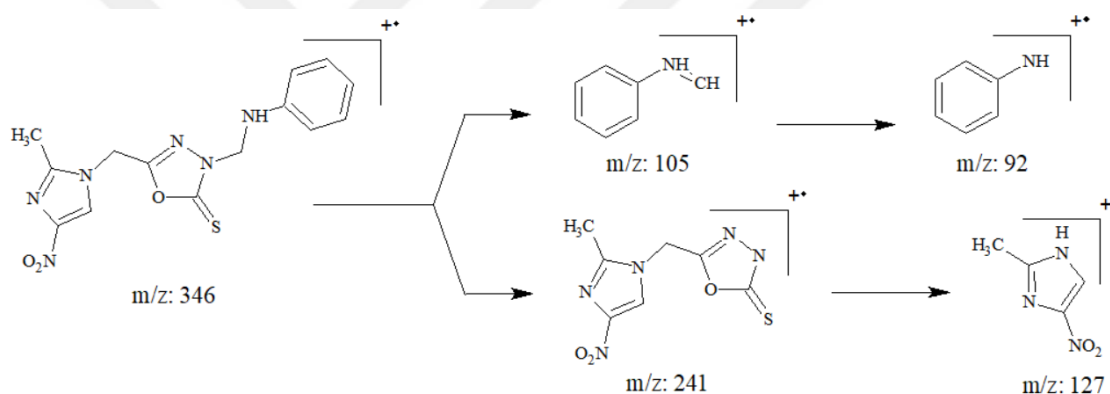
Scheme 5. Mass fragmentation of N-*Mannich* base

Frank and researchers synthesized secondary amine derived 1,3,4-oxadiazole-2(*3H*)-thione compounds by *Mannich* reaction procedure. Mass fragmentations of target molecules were found compatible with molecular masses of compounds. As depicted in Scheme 5, fragmentation was occured primarily from methylene bridge that combine primary amine and third position of 1,3,4-oxadiazole ring [89].

2.2. Biology

2.2.1. Biologic Properties of 1,3,4-Oxadiazole

2.2.1.1. Antiinflammatory Property
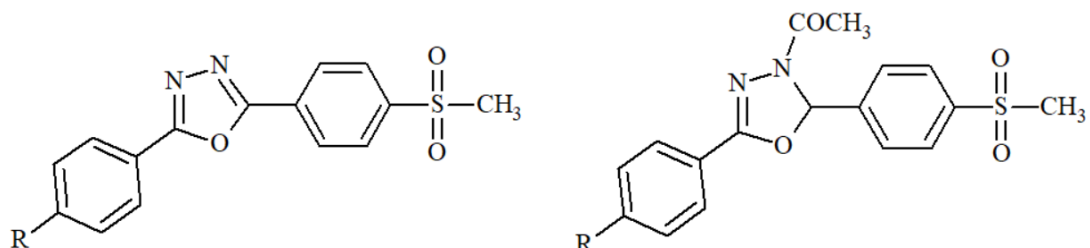
Grover and researchers dealed with a new series of 2,5-biaryl-1,3,4-oxadiazole synthesis and test molecules were investigated for their selective COX-2 inhibition. In *vivo* carregenan-induced paw edema assay method, structure-activity relationship indicated that methylsulfonyl moieties of synthesized compounds increased COX-2 inhibitor potential which were also supported by molecular docking studies [90].
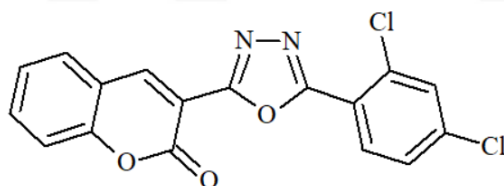
A series of 3-[5-(phenyl/phenylamino)-1,3,4-oxadiazole-2-yl]-chromen-2-one derivatives were synthesized and screened for antiinflammatory activity by Akhter and coworkers. According to in *vivo* carrageenan-induced inflammation test results, percentage of edema inhibition was in range of 35-89%. Particularly 2,4-dichlorophenyl containing was evaluated as the most active compound (89% inhibition of oedema) than reference ibuprofen [91].
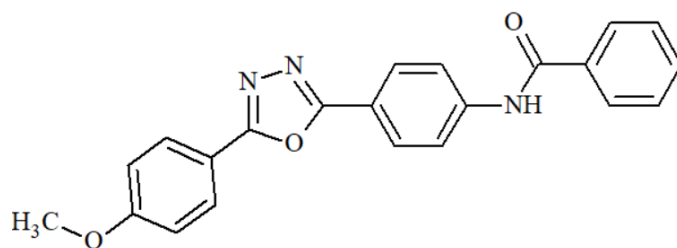
In 2008, Nagalakshmi dealed with the synthesis of 2,5-disubstituted-1,3,4-oxadiazole and screened them for antiinflammatory potential via in *vivo* carregenan-induced paw edema test model. 4-methoxyphenyl derivative was found to have 50% inhibitor potential whereas reference drug phenylbutazone exhibited 53.57% [92].
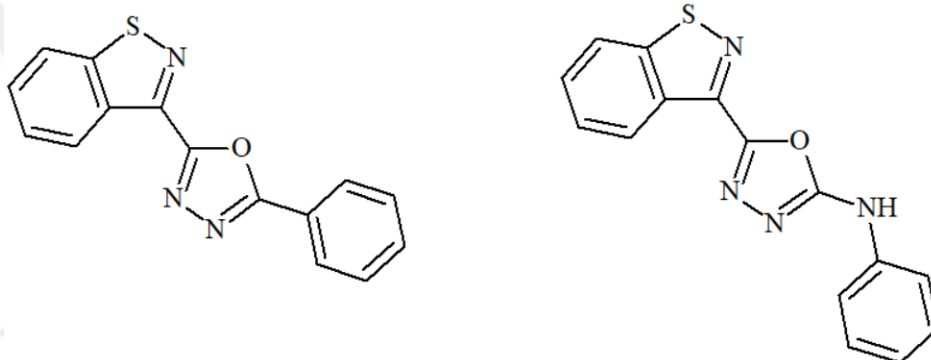
A number of compounds that have 2,5-disubstituted-1,3,4-oxadiazole ring which were bonded to third position of 1,2-benzisothiazole nucleus; screened for their antiinflammatory properties. Research procedure was applicated by in *vivo* carrageenan-induced rat paw edema model and results revealed that second positioned phenyl/anilino derivatives were found to have good inhibitor values [93].

R^1= H, OCOCH$_3$
R^2= H, OCOCH$_3$
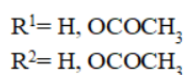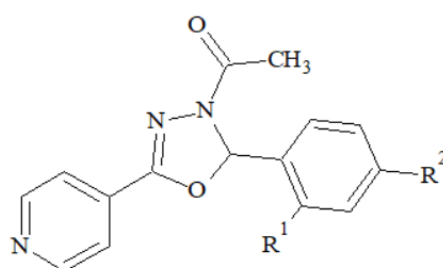
According to Durgashivaprasad and researchers in 2014, 2,5-disubstituted-1,3,4-oxadiazoles showed antiinflammatory activity in both of acute and chronic inflammation models. Structures of OSD and OPD (related to positions of o-acetyl group on benzen rings) revealed that the former compound had an o-acetyl substitution in the benzene moiety attached to second position of oxadiazole moiety like molecular structure of aspirin. OSD (second positioned o-acetyl group on benzene ring) reduced carrageen-induced paw edema by 60% while OPD (para-positioned o-acetyl group on benzen ring) produced 32.5% reduction. The significant point was the mechanism of antiinflammatory effect of OSD may be through inhibition of cyclooxygenase pathway [94].
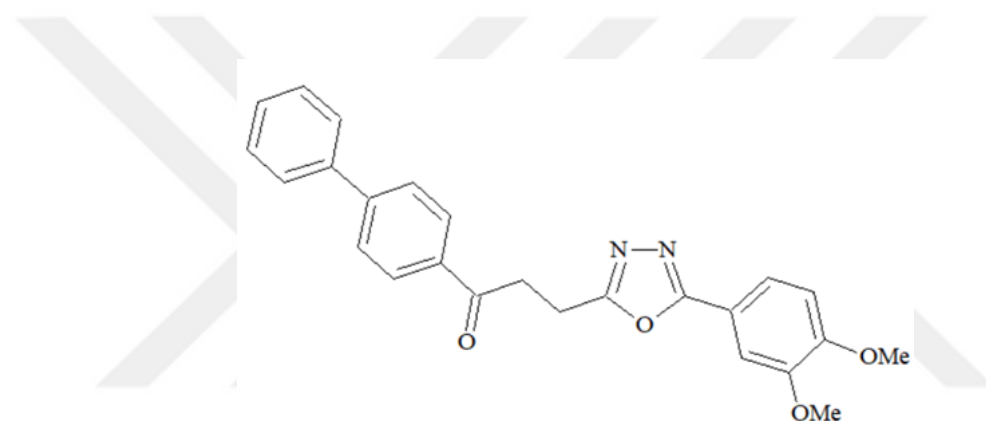
Husain and researchers derived a series of 3-[5-(substitutedaryl)-1,3,4-oxadiazol-2-yl]-1-(biphenyl-4-yl)propan-1-ones and screened for their in *vivo* antiinflammatory activity by carrageenan-induced paw edema method. Test scores of compounds were in range of 43.75% to 62.50% which meaned equipotent to reference compound fenbufen Particularly, 2-naphtyloxymethyl, 4-methoxyphenyl or 3,4-dimethoxy phenyl substitutions were seemed to develop antiinflammatory activity of these fenbufen derivatives [95].

2.2.1.2. Antioxidant Property

R= 2,4-diF, 4-F
R¹= 4-Cl, 4-F, 4-H
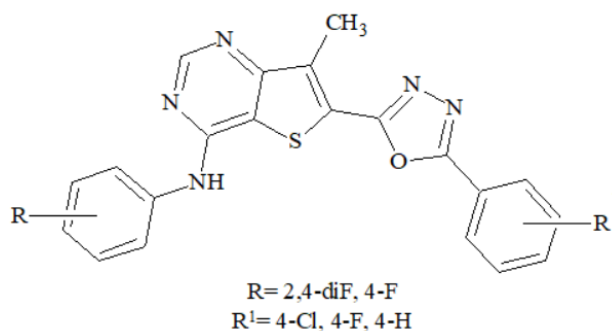
A new class of 1,3,4-oxadiazole tagged thieno[2,3-d]pyrimidines derivatives were prepared and studied for their antioxidant activity by Kotaiah and coworkers in 2012. Compounds were tested for with variety of in *vitro* antioxidant assays. As a common critic for all assays (DPPH, nitric oxide (NO) and hydrogen peroxide (H_2O_2) inhibition), compounds containing mild electron-withdrawing groups like fluoro, chloro or both of them located on benzene rings revealed good radical scavenging activity than reference ascorbic acid [96].
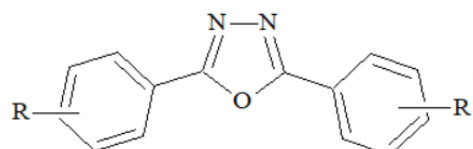
Eight 1,3,4-oxadiazole derivatives containing phenolic acid moieties and eight of their diacylhydrazine precursors were synthesized and examined by scavenging of DPPH radicals by Mihailovic and research team. According to test results, phenolic 1,3,4-oxadiazoles were found as the most active antioxidant compounds when they compared with their corresponding diacylhydrazine precursors. These biologic activity data could be explained *via* substitution types and positions on both aromatic rings and their contribution about resonance stabilization on the molecule with 1,3,4-oxadiazole ring [97].
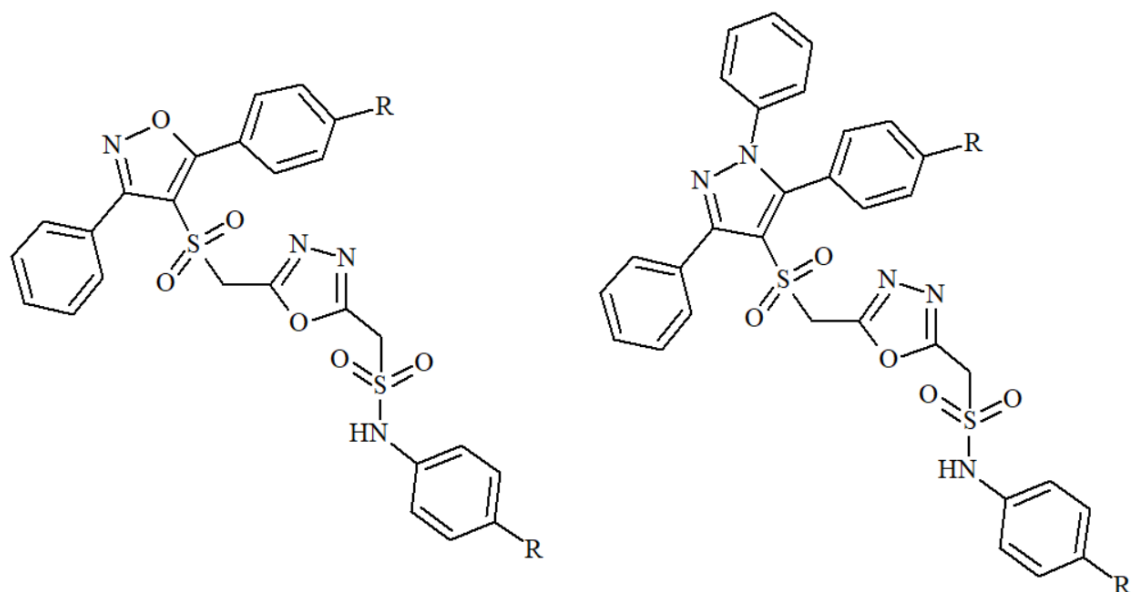
Reddy and researchers were studied on new class of 2-{[(substitutedanilino) sulfonyl]methyl}-5-{[(substitutedpyrazolyl/isoxazolyl)sulfonyl]methyl}-1,3,4-oxadiazo les synthesis and controlled for their antioxidant activity with in *vitro* DPPH, nitric oxide (NO), hydrogen peroxide (H$_2$O$_2$) inhibiton methods. Biological studies were done with different sample doses and according to the reference ascorbic acid, 100 μM was found statistically the most active dosage. As a comparison about antioxidant potencies of compounds, isoxazolyl derivatives preserved better activity profile [98].
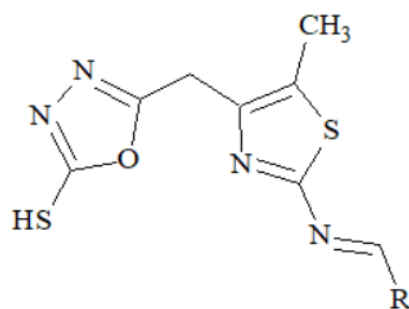
Mohana and coworkers designed a series of 5-substituted-1,3,4-oxadiazole-2-thiols that synthesized by different aldehydes. The antioxidant activity of synthesized compounds were evaluated with DPPH, hydroxyl, superoxide radical scavenging and nitric oxide inhibiton assay methods. Compounds that showed significant radical scavenging potential contained electron donating substituents on aldehydes groups of their molecular structures [99].

2.2.1.3. Analgesic Property
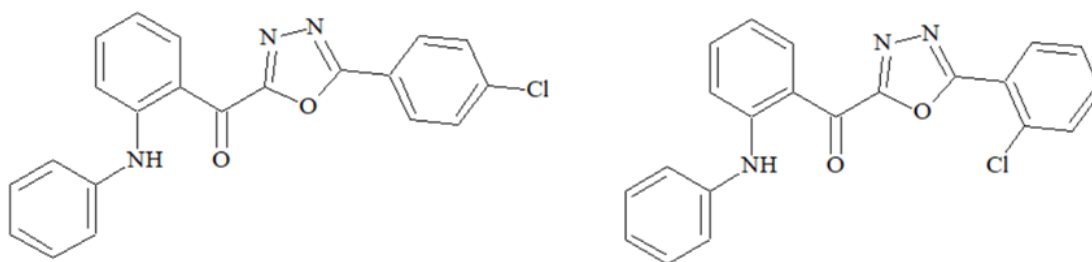
1,3,4-Oxadiazole compounds were screened for their analgesic activity by in *vitro* tail immersion method by Bala and coworkers in 2013. Among all the compounds, 4-chloro and 2-chloro substituted molecules showed maximum analgesic property at 100 mg/kg. Actual reason for that observable activity potential difference were originated due to electron-withdrawing nature of halogens, which ultimately enhanced the lipophilicity to contribute the entrance of compounds through biological membranes [8].
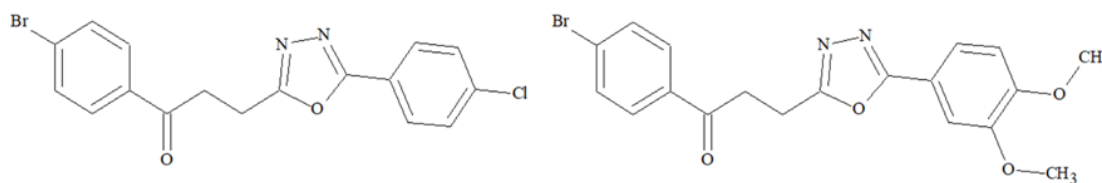
Analgesic potency of 1,3,4-oxadiazole ring was also studied with Husain and Ajmal in 2009. Compounds that revealed antiinflammatory activity higher than 45 % were checked for their analgesic activity. In *vitro* acetic acid induced writhing method was used for analgesic activity and compound scores were in between 44.1 to 70.6 %, whereas the reference drug acetylsalicylic acid showed 63.2 % with same molar dosages (25 mg/kg). As a consequence, compounds having 3,4-dimethoxyphenyl or 4-chlorophenyl substitutions of heterocyclic ring enhanced analgesic activity with theoritically significant level [100].
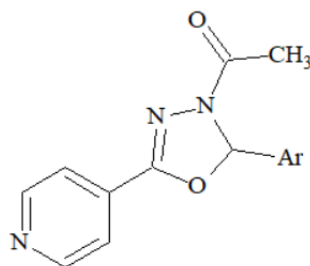
Bhardwaj and coworkers evaluated that second and fifth positions of 1,3,4-oxadiazole ring are extremely important sites for molecular modification. Synthesized compounds exhibited good antiinflammatory activity (44.45–83.34%) against carragenean induced paw edema, whereas the standard drug diclofenac showed 83% inhibition under similar conditions. Among tested compounds, pyridine on second and acetyl on fourth position of 1,3,4-oxadiazole containing compound represented the highest (83.34%) antiinflammatory activity. The presence of methoxy group at second position and pyridine revealed the best analgesic activity of 1,3,4-oxadiazole derivative [101].
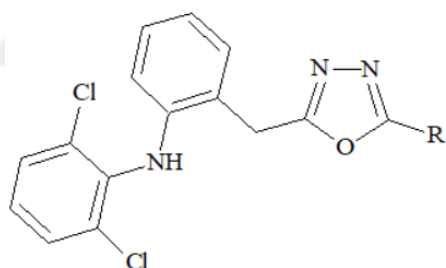
In 2004 Amir and coworkers synthesized a compound serie which included a heterocyclization step of carboxylic acid moiety of diclofenac and then derivatized with different chemical substituents. Biologic activities of tested compounds reflected that 1,3,4-oxadiazole derivatives showed analgesic activity in range of 78.57-81.86% and they were better than the reference drug diclofenac (70.32%). According to test results, electron-withdrawing groups elevated the analgesic activity of the compounds [102].

2.2.2.4. Antimicrobial Property
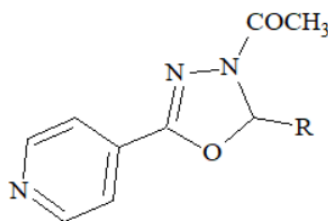
Panda and friends prepared some novel pyridine derived 1,3,4-oxadiazole compounds and studied on their antibacterial potentials. All the synthesized compounds were found effective against both gram positive and gram negative microorganisms. Especially, amine-containing molecule showed most inhibitor score against *E. coli, S. epidermidis* and *P. vulgaris* [103].

Also Ahsan and coworkers studied on similar core structure and all the synthesized compounds were tested against two gram-positive bacterial strains which were *S.aureus, B. subtilis* and two gram-negative bacterial strains *E. coli, P. Aeruginosa.* Obtained scores were compared with standard drug ciprofloxacin. According to results, particularly, halogen-containing molecules were active on all four bacterial strains and chlorine-containing molecule was found most active against *E.coli* and *P. aeruginosa.* Hydroxy-contaning molecules was active on *B.subtitis* and *S.aureus* [104].

In a further study in which presented by Kumar and coworkers, series of 2,5-disubstituted-1,3,4-oxadiazole were tested for their antibacterial properties against *S. aureus* and *K. pneumoniae* with reference streptomycin. Compounds antifungal activity capacities against *P. salmonicolor* and *M. phaseolina* was also checked with standart griseofulvin. The antimicrobial activity of the compounds were differentiated according to the type and position of the substituents at 5-substituted-2-amino-1,3,4-oxadiazole moiety. Antimicrobial test results clearly revealed that, aryl halide fragments located on 1,3,4-oxadiazoles were seemed to induce desired activity [105].
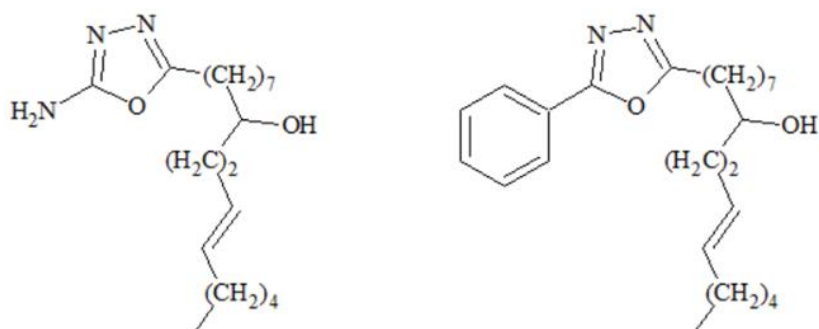
Banday and coworkers evaluated 2,5-disubstituted-1,3,4-oxadiazoles and screened their antimicrobial activity profiles. Consequences showed that nature of substituent at 2 and 5 position of oxadiazole ring may have significant effect in particular $-NH_2$ group on oxadiazole ring and the –OH group on fatty acid chain were seemed as to enhance desired responce [106].

2.2.1.5. Anticancer Property
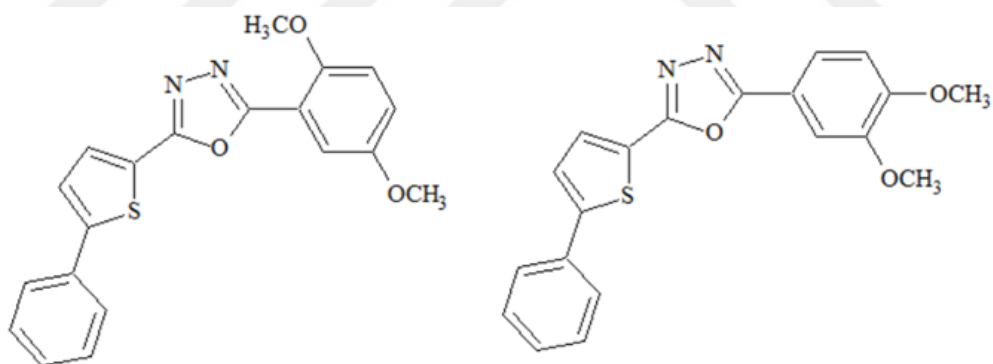
A series of regioisomeric 2-(disubstituted)phenyl-5-(5-phenyl-thien-2-yl)-1,3,4-oxadiazole analogues were synthesized and screened for in *vitro* anticancer studies by using MTT colorimetric assay. Particularly, 2,5-dimethoxyphenyl substituted derivative demonstrated superior activity against breast (MDA-231) cancer cells. Also this compound displayed excellent activity against prostate cancer (DU-145), colon cancer (HCT-15) and 3,4-dimethoxyphenyl substituted derivative revealed strong potency against breast cancer (MDA-231) cells [107].
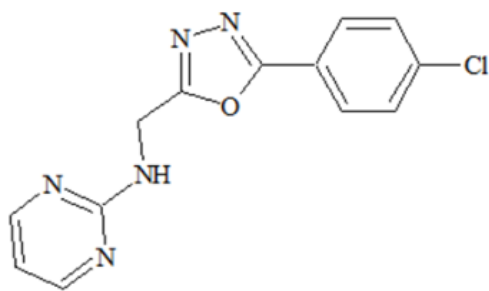
A novel series of 2,5-disubstituted-1,3,4-oxadiazole analogs were screened for in vitro anticancer activity on leukemia, melanoma, colon, central nervous system, ovarian, renal, prostate and breast cancer cell lines. Among synthesized compounds, 4-chloro-containing candidate showed maximum activity with percentages of growth inhibition (GI); 61 % for prostate (UO-31) and 76 % for breast (MCF) cancer cells [104].

(NSC-776965)

(NSC-776971)
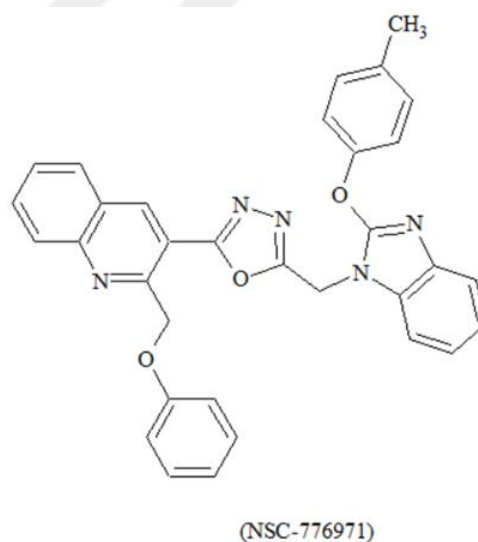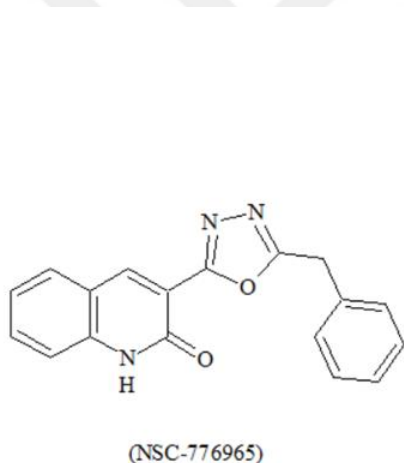
Salahuddin and researchers synthesized new 2,5-disubstituted-1,3,4-oxadiazoles to detect their potential therapeutic effects for cancer. Among all tested molecules, two of them were able to generate desired mean growth percentage of 66.23 and 46.61 [108].

2.2.2. Biologic Properties of 1,3,4-Oxadiazole-2(*3H*)-thione

2.2.2.1. Antiinflammatory Property
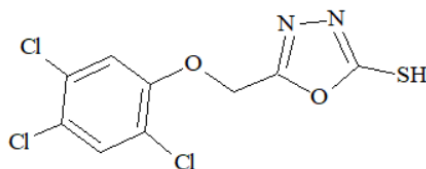
Amir and coworkers synthesized some novel 2,5-disubstituted-1,3,4-oxadiazole derivatives and screened for their antiinflammatory property by in *vivo* carregenaan-induced rat paw edema test. Compounds that have chloro atoms on phenyl moiety showed good antiinflamatory property in which they also tested for their ulcerogenic and lipid peroxidation activities for the next step [109].
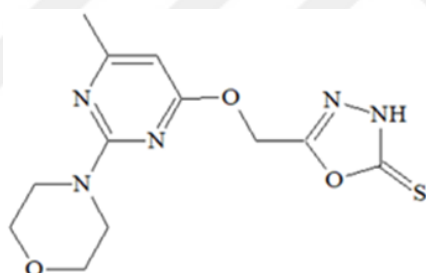
Some 1,3,4-oxadiazole-2-thiones were designed by Jakubkiene and coworkers and their antiinflammatory activities were decribed by both of in *vivo* carregenan/bentonite-induced paw edema assays. Most of the tested compounds were showed better antiinflammatory activity than reference compound acetylsalicylic acid. Especially, morpholino-possessed 1,3,4-oxadiazole-2(*3H*)-thione was one of the most active compound in which its carragenan induced edema score 29.7% and bentonite-induced edema score 26.4% whereas acetylsalicylic acid was found as 19.8 and 21.6%, respectively [110].
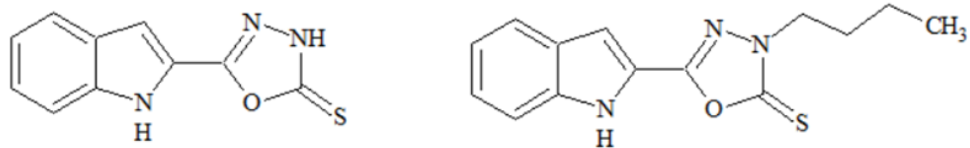
El Sayed and coworkers modelled a series of indol bonded 1,3,4-oxadiazole-2(*3H*)-thione derivatives. Compounds were screened for their antiinflammatory with in *vitro* proinflammatory and immunomodulator cytokine inhibition potentials. None of compounds seemed to be able to supress immunomodulator cytokines like interleukine-2 (IL-2) and interleukine-4 (IL-4). However 5-indol and 3-alkyl-5-indol derived analogues revealed excellent nitric oxide (proinflammatory cytokine) inhibitor effect, compared to reference ibuprofen [111].
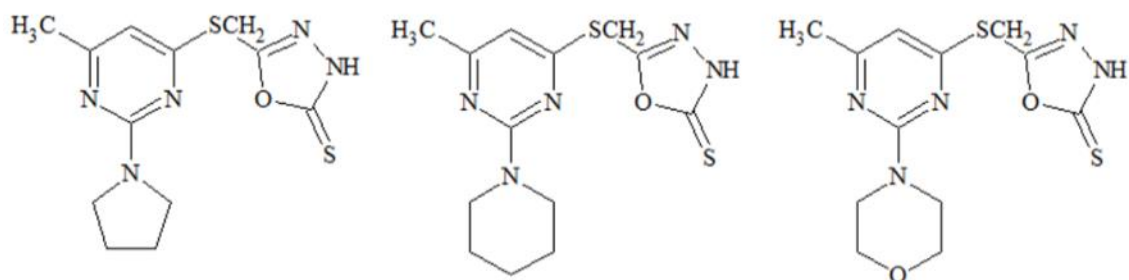
Antiinflammatory activity of 1,3,4-oxadiazole-2(*3H*)-thione derivatives were studied by Burbuliene and researchers with in *vitro* carrageenin and bentonite-induced paw oedema in rats. As reference compounds in experiments; acetylsalicylic acid and ibuprofen were used. The results of in *vitro* inflammation tests showed that title 1,3,4-oxadiazole-2(*3H*)-thiones represented antiinflammatory activity and compounds that involve pyrrole, piperidine and morpholine moieties represented better potential than acetylsalicylic acid in carrageenin and bentonite-induced test their activity. Particularly morpholine-containing compound was found as the most potent molecule [112].
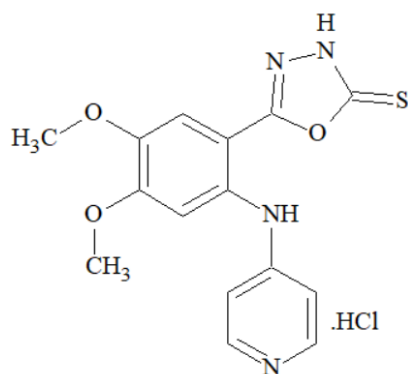
Concerning the pyridyl derived 1,3,4-oxadiazole-2(*3H*)-thiones; 3,5-dimethoxy phenyl containing molecule served the highest PGE_2 inhibitor effect which was about 68% while indomethacin as reference drug exhibited just 60% inhibitor potential [113].
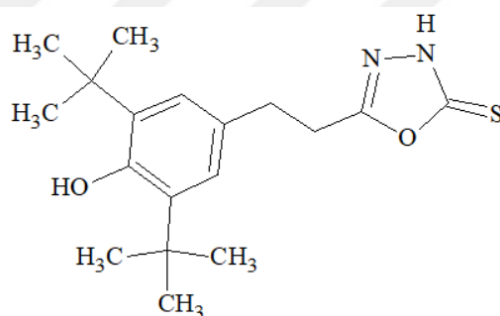
5-(3,5-Di-tert-butyl-4-hydroxyphenyl)-1,3,4-oxadiazole-2-one/thiones were designed and synthesized to be potent dual inhibitors of 5-LOX/COX by Mullican and coworkers [114].
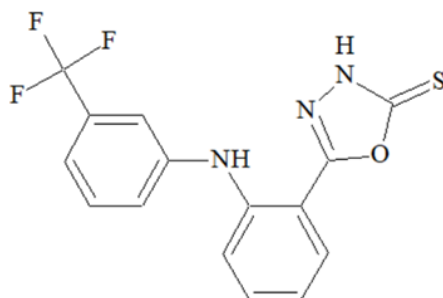
Based on many research studies, different substituted 1,3,4-oxadiazole-2(*3H*)-thione compounds were known as to have severe antiinflammatory potential via several biologic pathway without gastric side effects. In this manner to support one of the effector mechanisms; 1,3,4-oxadiazole-2-thione derivatives were reported as dual 5-LOX/COX inhibitors by Boschelli and researchers. Lipoxygenases (LOXs) are other enzyme family that originated from arachidonic acid like COXs. Their subgroups are mainly 5-LOX and 12-LOX in which 5-LOX is mainly responsed by allergic reactions and inflammation. According the chemical modifications and their biological results; replacement of thione group in 1,3,4-oxadiazole core by carbonyl showed lower suppressor effect on this inflammatory 5-LOX enzyme group [115].
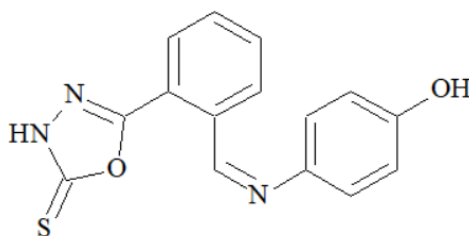
The docking results showed that Schiff base series of 1,3,4-oxadiazole-2(*3H*)-thione analogues were screened to act as selective inhibitors of COX-2 in comparison to the reference indomethacin. Antiinflammatory screening data represented that biological activity is directly associated with molecular structures of compounds. Among the tested 1,3,4-oxadiazole-2-thione derivatives, para-positioned hydroxy group containing compounds showed significant antiinflammatory activity [116].

2.2.2.2. Antioxidant Property
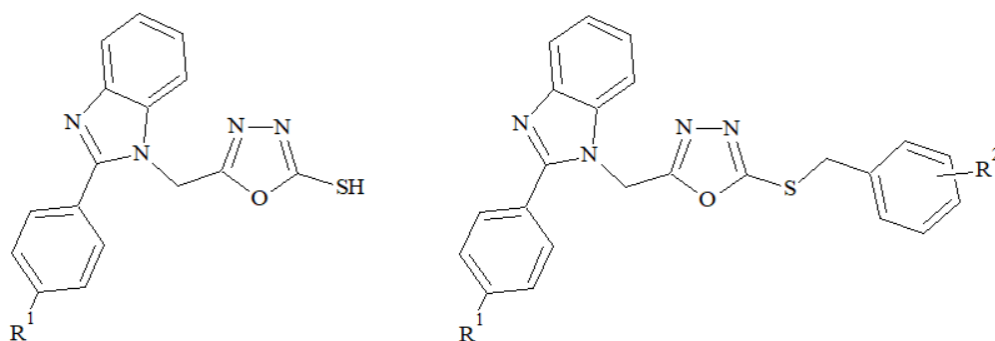
Alp and researchers modelled and synthesized novel 2,5-disubstituted-1,3,4-oxadiazoles and their in *vitro* antioxidant capacities were examined by lipid peroxidation (LP) test and microsomal EROD activity. *S*-substituted-1,3,4-oxadiazole-5-thiols represented moderate inhibitory activity on LP levels in the range of 46%-61% in which they were seemed to highly responsed for EROD activity. Besides LP and EROD methods, free radical scavenging potentials of the compounds were also checked and paralelly resulted with in *vitro* DPPH method [117].
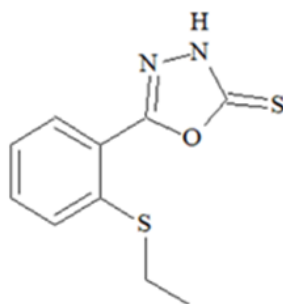
Nazarbahjat concerned with new derivatives of 1,3,4-oxadiazole synthesis and studied for their antioxidant activities. In *vitro* DPPH and ferric reducing antioxidant power (FRAP) assay tests were used to determine free radical scavenging capacity of compounds. Five positive controls (quercetin, BHT, trolox, rutin, and ascorbic acid) were screened compare the antioxidant capacity of test compounds. DPPH results obviously showed that ortho substituted ethylmercapto moiety was seemed to significantly increase radical scavenging activity according to other test molecules [118].

2.2.2.3. Analgesic Property

X= S, SO, SO$_2$
R= H, Cl
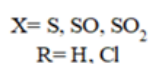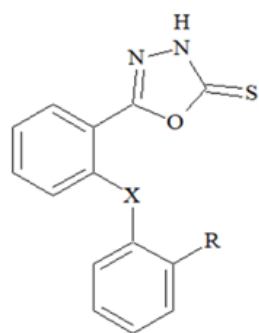
A series of new 1,3,4-oxadiazoles were synthesized in order to have potent analgesic activity by Almasirad and coworkers. Compounds were searched for their analgesic activities by formalin-induced nociception test. All sulphone and thione containing compounds showed analgesic activity in the late phase of formalin test in comparison to control mefenamic acid [119].

R^1= H, CH$_3$, Cl
R^2= H, CH$_3$
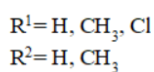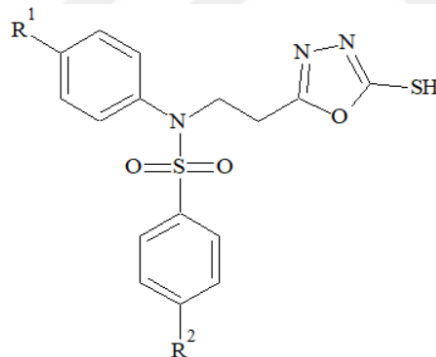
Desai and co-workers were studied on various benzene sulphonyl derived 1,3,4-oxadiazole-2-thiols. Analgesic activities of synthesized compounds were done with in *vivo* radiant heat induced rat tail flick method using aspirin as a standard. Most of the compounds demonstrated significant analgesic activity (64.20-120.72%) compared to reference aspirin (49.39%) [120].
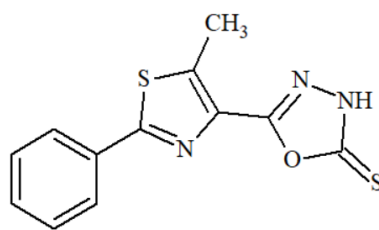
5-Substituted-1,3,4-oxadiazole-2(*3H*)-thione derivatives were evaluated for their analgesic activity by the use of acetic acid induced writhing method at equimolar doses equivalent to 25 mg/kg (diclofenac sodium) body weight using wistar albino mice. Active compounds possessed significant analgesic activity in the range of 56.30–62.70% whereas standard diclofenac sodium, represented activity 57.96% [121].

2.2.2.4. Antimicrobial Property
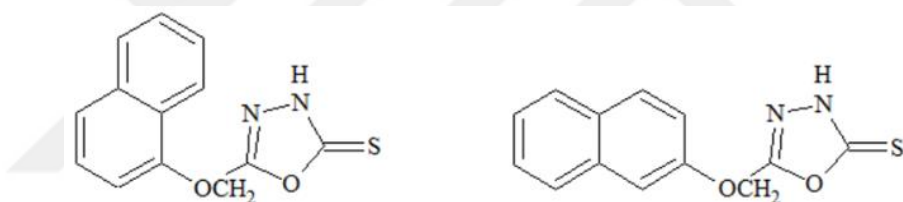
Different 1,3,4-oxadiazole-2-thiones that contain 1- or 2-napthyloxymethyl containing compounds were synthesized by Sahin and research team. Compounds were were investigated against *S. aureus*, *E. coli and P. aeruginosa, C. albicans, C. krusei* and *C. parapsilosis* by the use of microbroth dilution method in which test results showed napthyl fragments were seemed moderately active particularly against *C. Krusei* [122].
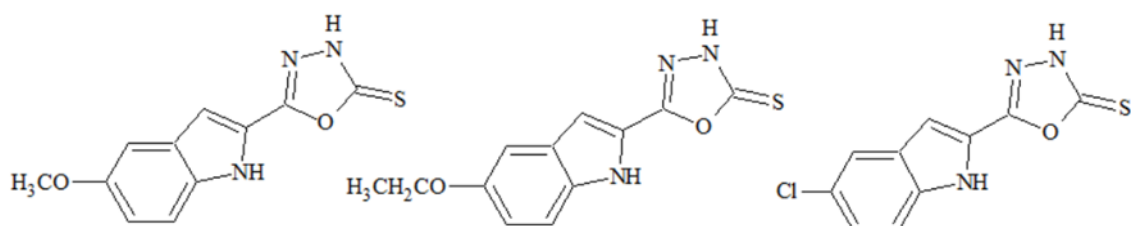
2-(5-Thioxo-1,3,4-oxadiazol-2-yl)indoles analogues were synthesized with the reaction of indole-2-carboxy hydrazides with CS_2 and KOH. Antimicrobial screening demonstrated that these compounds showed moderate activity against *S. aureus, E. Coli. P. vulgaris* and *B. Subtilis* [123].
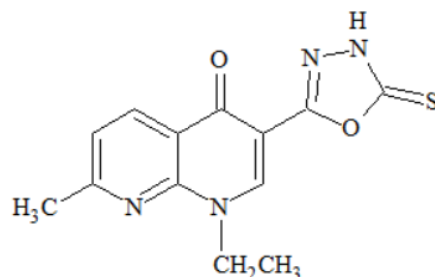
Evaluation of in *vitro* antimicrobial activity of synthesized nalidixic acid derived 1,3,4-oxadiazole-2(*3H*)-thiones were studied by Grover and research team. Test samples were resulted mild to moderate antimicrobial activity against *E. coli, K. aerogenes* and good inhibitor activity against enteric pathogen *A. hydrophilia* [124].

2.2.2.5. Anticancer Property
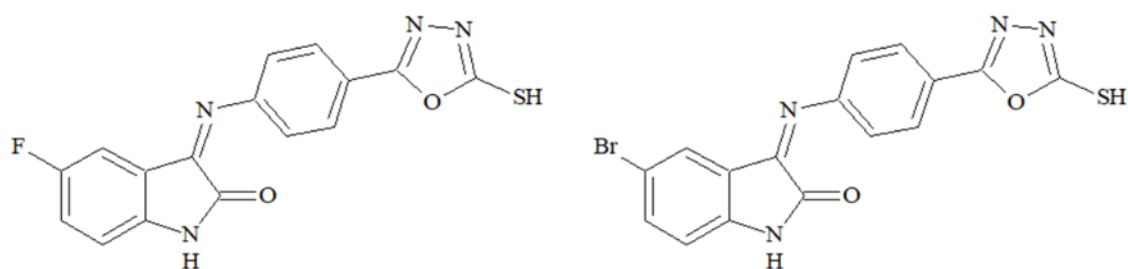
A series of 5-substituted-indol-2-one derivatives were screened against HeLa cancer cell lines using MTT assay. Halogen-containing derivatives (fluoro, bromo) at fifth position showed the most potent activities [125].
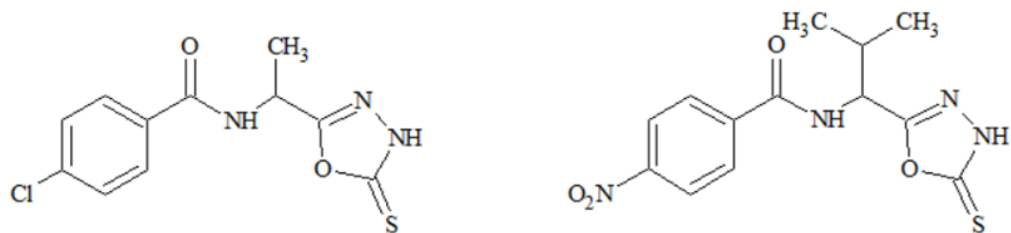
Feng and researchers designed and synthesized a series of 1,3,4-oxadiazole-2(*3H*)-thione derivatives and studied for their anticancer activity. In silico compounds were docked into the ATPase domain of TP-II and according to docking scores, 4-chloro and 4-nitro substitutions provided excellent anticancer prototype human leukemia cancer cell line (K-562) [126].

2.2.3. Biologic Properties of *Mannich* Bases of 1,3,4-Oxadiazole-2(*3H*)-thione

2.2.3.1. Antiinflammatory Property
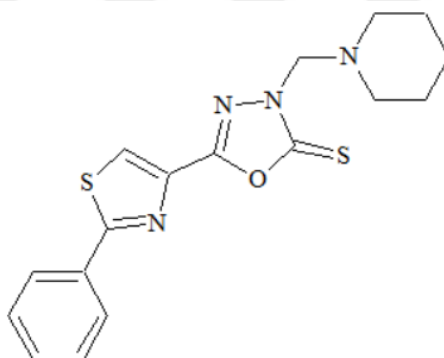
N-*Mannich* base in which contan piperidine moiety had strong antiinflammatory activity comparable to reference drug indomethacin in carrageenan-induced rat paw edema test [127].
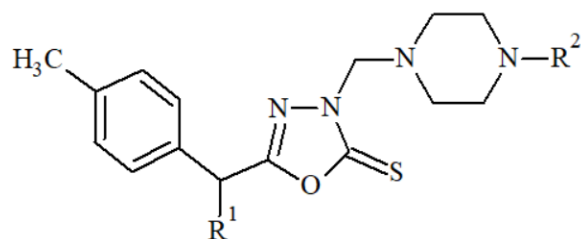
Manjunatha studied on the antiinflammatory activity of novel N-*Mannich* bases of 2,3-dihydro-1,3,4-oxadiazole-2-thiones. Ibuprofen derived several *Mannich* bases were found as active as diclofenac to reduce rat paw edema [17].

2.2.3.2. Antioxidant Property
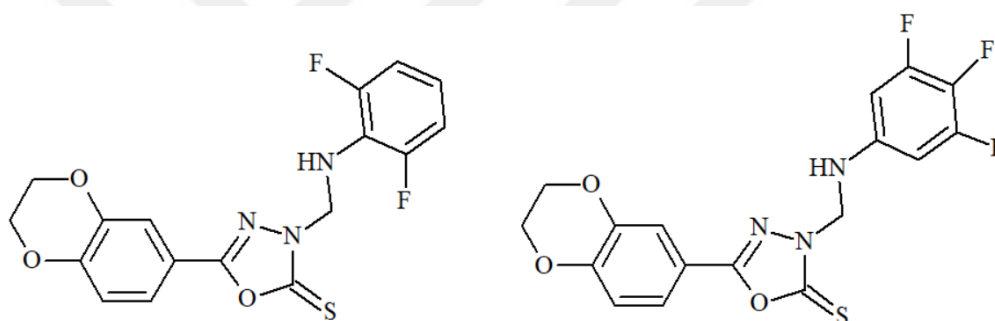
N-*Mannich* bases of 1,3,4-oxadiazole-2-thione were designed for their antioxidant properties by Ma and coworkers. Compounds antioxidant potencies were evaluated by different iv vitro assay methods like DPPH, FRAP and ABTS radical assays. N-*Mannich* bases that contain halogen groups (particularly flourine atom) were only the compounds that generated high potency in all three assays with higher scores than reference Trolox [128].
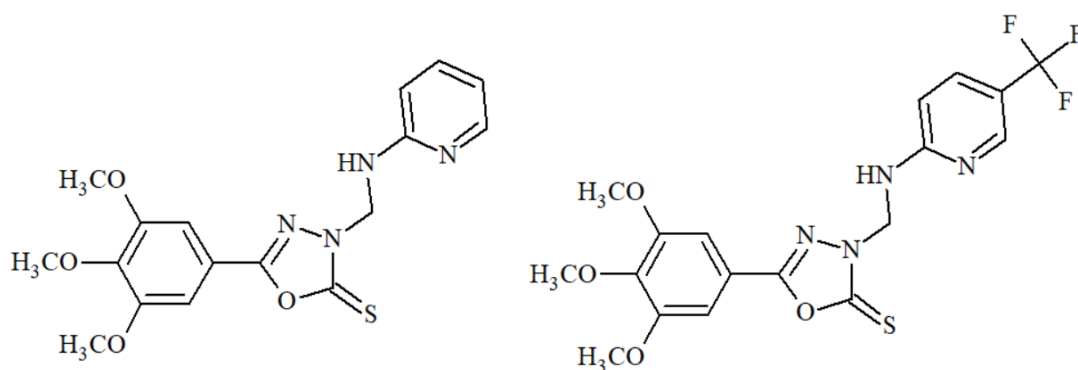
The antioxidant properties of the most effective compounds were found to have 3,4,5-trimethoxy-substituted benzene attacched to 1,3,4-oxadiazole ring. Also compounds including substituted pyridine ring and trifluoromethyl pyridine next to amino methyl group in parent 1,3,4-oxadiazole-2(*3H*)-thione core were seemed to facilitate their antioxidant activities when compared with reference propyl gallate [129].
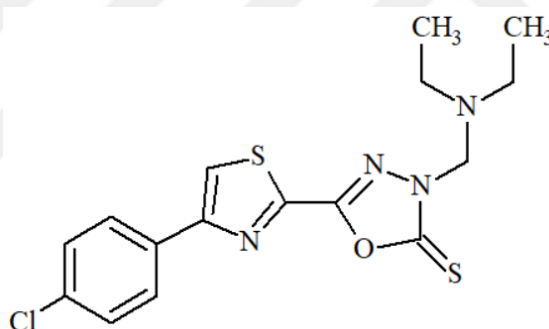
In *vitro* antioxidant activity studies of 3,5-disubstituted-1,3,4-oxadiazole-2-thiones were tested by DPPH, nitric oxide inhibition and hydrogen peroxide scavenging assays. Consequences obviously revealed that electron donating group that incorporate on aromatic ring, can act as free radical scavenging agents. Chloro moiety at fourth position of phenyl ring and two diethyl groups on amine served maximum antioxidant activity in common for all test methods. This may be due to electron-donating properties of both chloro and diethyl group that leads to induction of radical scavenging [130].

2.2.3.3. Analgesic Property
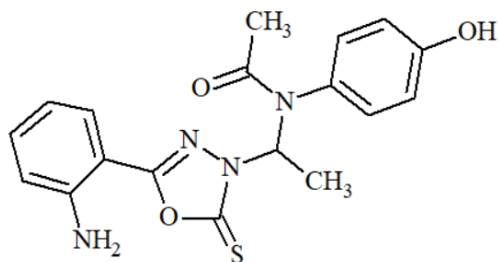
Mannich bases of 1,3,4-oxadiazole-2(*3H*)-thione investigated for their analgesic properties by the use of hot plate and tail flick methods. Compounds showed highly significant analgesic activity according to reference pentazocine [131].
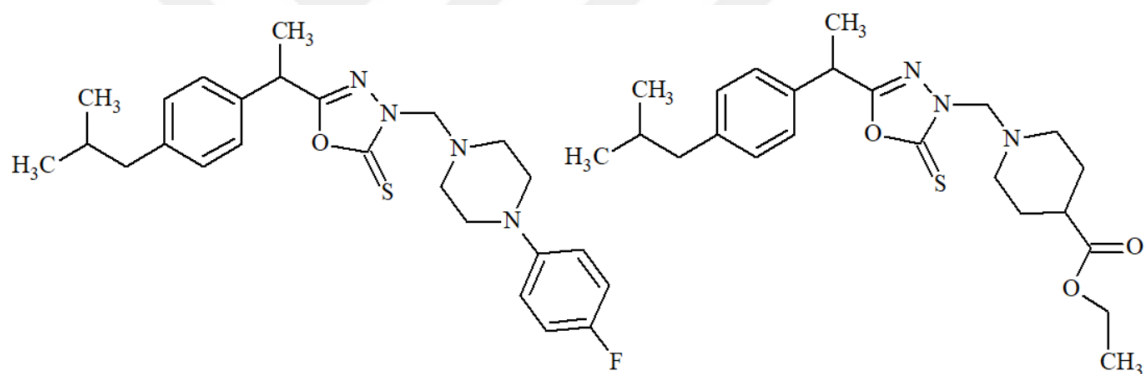
Two candidates that synthesized from ibuprofen were converted to 2,3-dihydro-1,3,4-oxadiazole-2(*3H*)-thiones. By the use of either 4-(4-fluorophenyl)piperazine or ethyl piperidine-4-carboxylate with 1,3,4-oxadiazoles, some *Mannich* bases were produced with a special reaction mechanism. Obtained compounds were seemed to be more efficient analgesics than reference drug diclofenac in hot plate test [17].
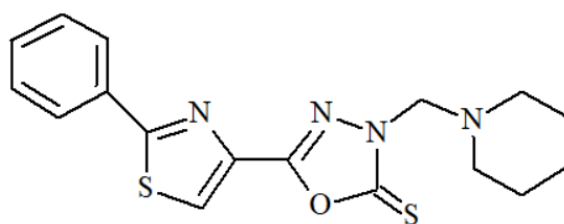
N-*Mannich* base that possessing thiazole ring was equipotent to reference drug diclofenac in acetic acid-induced writhing test [127].

2.2.3.4. Antimicrobial Property

4,4'-diaminophenyl sulphone
(Dapson)
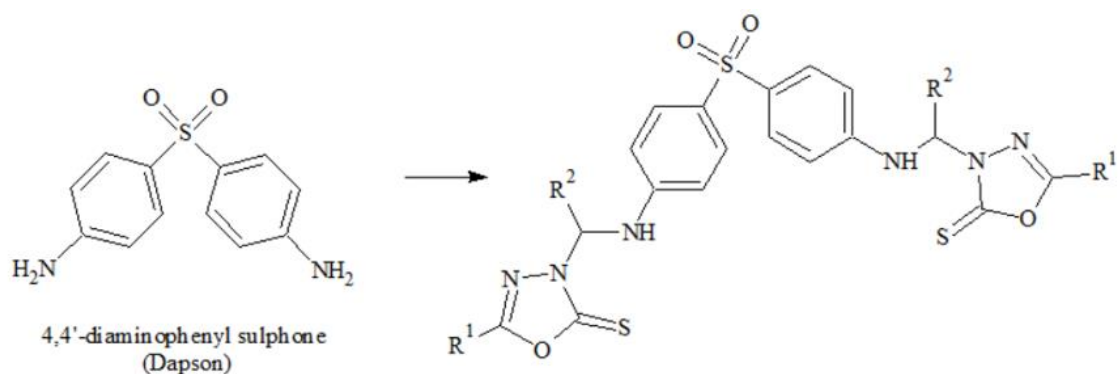
Bis-*Mannich* bases derived from dapsone as amine reagent, aldehytes and variously 5-substituted-1,3,4-oxadiazole-2(*3H*)-thiones were found to have excellent antimicrobial activities against both isoniazid-sensitive and isoniazid-resistant strains of *M. tuberculosis* and synthesized compounds were evaluated as 5-fold more than isoniazid-sensitive, 10-fold more than isoniazid-resistant strain [132].
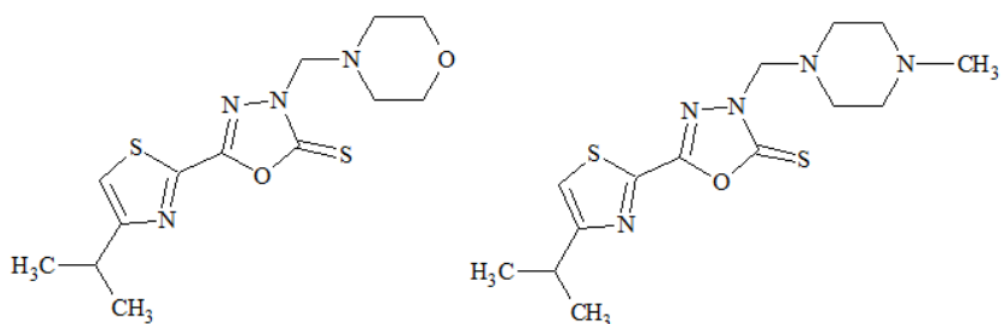
Another study about antimicrobial capacities was done for *Mannich* bases of 2,3-dihydro-1,3,4-oxadiazole-2(*3H*)-thiones and reference drug isoniazid. Morpholino and 4-methyl piperazine derived compounds responsed to have moderate activity potentials compared to reference drug [85].
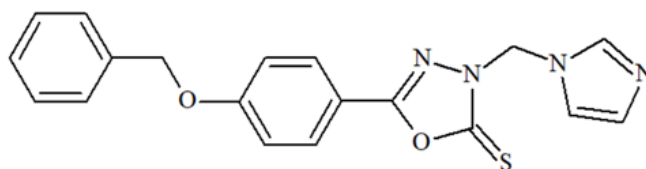
Nimbalkar and coworkers produced a novel series of 5-(4-(benzyloxy)substituted phenyl)-3-((phenylamino)methyl)-1,3,4-oxadiazole-2(*3H*)-thione *Mannich* bases, in good yields. The antifungal activity of the new molecules was evaluated against seven human pathogenic fungal strains and among synthesized imidazole-condaining derivative generated good antifungal activity against all the tested fungal pathogens [133].
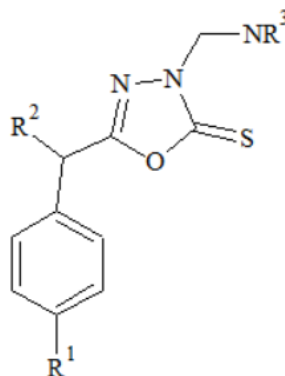
R^1= i-C$_3$H$_7$, SCH$_3$
R^2= H, CH$_3$
NR^3= secondary aliphatic amines

Antifungal activity of *Mannich* bases has been reported in many researches up to this time. Several *Mannich* bases were seemed to have equipotent activity with reference drug cyclopiroxolamine against *A. fumigatus, T. mentogrophytes, A. flavus* and but not against *P. marneffei* [17].
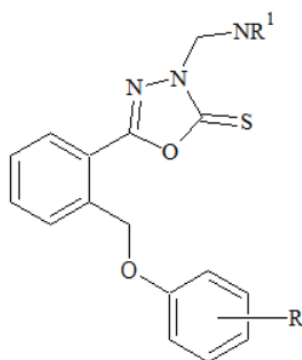
R= 2-CH₃, 3-CH₃, 4-CH₃, 4-Cl
NR¹= morpholine, primary arylamines

Morpholine or 3-trifluoromethylaniline derived *Mannich* bases showed high activity against *A. fumigatus, T. mentogrophytes, A. flavus* and *P. Marneffei* compared to reference drug cyclopiroxolamine [86].
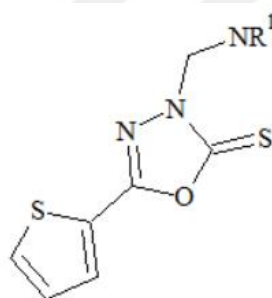
NR¹= piperazines, primary and secondary arylamines

Mannich base set of 1,3,4-oxadiazole-2(*3H*)-thione demonstrated moderate antifungal potenties on *Candida spp.* [134].
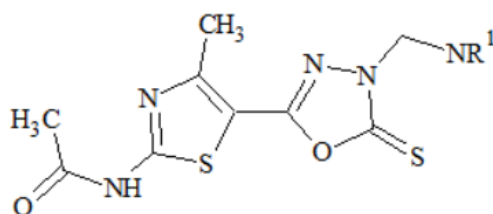
NR¹= substituted arylamines

Most *Mannich* bases 5-[2-acetylamino-5-methyl-1,3-thiazole-4-yl]-1,3,4-oxadiazole-2(*3H*)-thione group had weak antifungal activity against *A. niger, C. albicans* and *A. clavatus*, but one candidate that contain 4-methoxy phenyl was 2-fold more active than reference drug ketoconazole against *A. niger* and *C. albicans* [135].

2.2.3.5. Anticancer Property
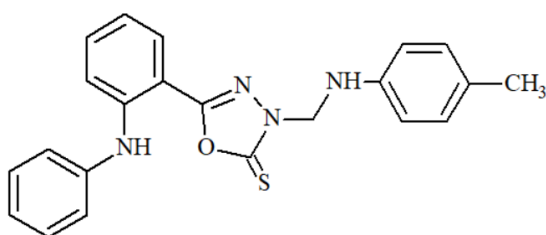
Rahman and coworkers studied on anticancer potentials of 1,3,4-oxadiazole-2(*3H*)-thione *Mannich* bases; 2-chlorophenyl or 4-chlorophenyl containing ones were found to serve higher cytotoxicity than reference drugs 5-fluorouracil (5-FU) or cyclophosphamide against NCI-H460 (lung), SF-268 (glioblastoma) and MCF-7 (breast) cancer cell lines using SRB assay [136].
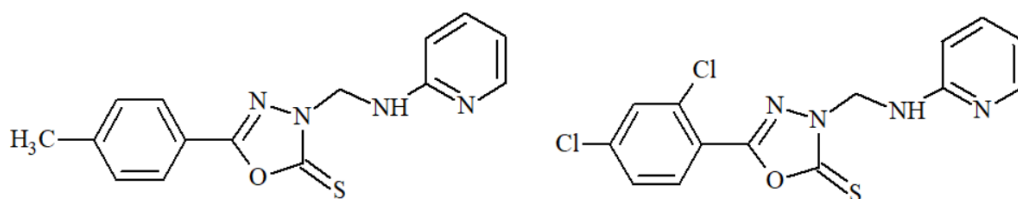
Several *Mannich* bases of 1,3,4-oxadiazole-2(*3H*)-thione core was investigated for their ability to block the growth of tumors with an in *vivo* method by Dash and researchers. Especially compounds that having methyl, hydroxyl, nitro or chloro substituents on the phenyl ring at fifth position of 1,3,4-oxadiazole-2(*3H*)-thione ring, were evaluated as the most potent ones on Ehrlich ascites carcinoma cells. These compounds reduced the growth of tumor volume in range of 52-74% whereas 5-FU inhibited tumor formation by 93%. [137].

$R^1 = H$, m-NO_2, p-$N(CH_3)_2$

$R^2 =$ —NH—, —NH—, —NH—, —NH—, —N, —N—O
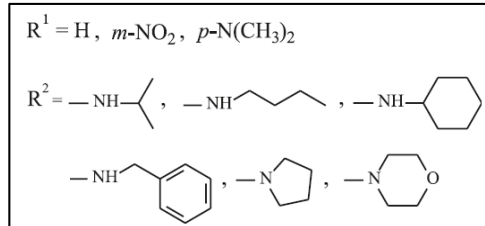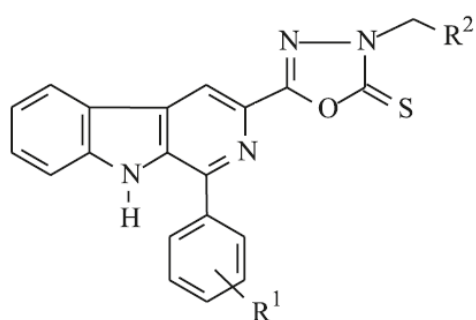
Cytotoxicity studies of different Mannich bases were evaluated against a panel involving many cancer cell lines using SRB assay and several candidates exhibited cytotoxic activities against these cancer cell lines [138].

-NR_1R_2: -NMe2, NEt2, piperidin-1-yl, morpholin-4-yl, 4-methylpiperazin-1-yl, anilino, 4-methoxyanilino, 2-methoxyanilino, 4-methylanilino, 4-chloroanilino
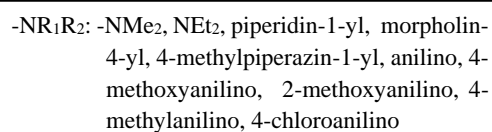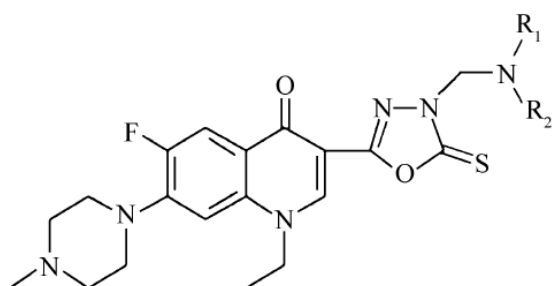
Furthermore, *Mannich* bases of a fluoroquinolone derived 1,3,4-oxadiazole-2(*3H*)-thione hybrids were screened for their cytotoxicity against Hep3B cancer cells using MTT assay. Results demonstrated that synthesized compounds were more potent than standart compound. Especially, dimethyl amino substituted molecule was more potent that reference drug bisantrene [139].
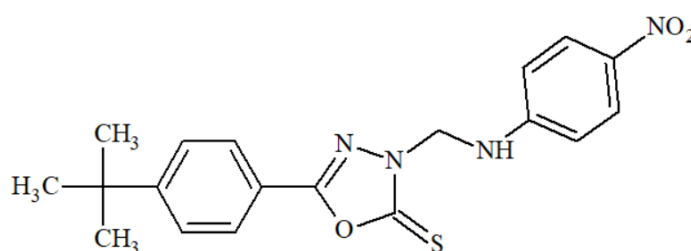
In the work of Yadav and research team, new 5-(4-(tert-butyl)phenyl)-1,3,4-oxadiazole-2(*3H*)-thiones have been synthesized and searched for their in *vitro* anticancer activity using various assays. Among synthesized molecules, p-nitro substituted derivative represented best apoptotic activity on HeLa cervical cancer cells which was greater than those of previous studies about oxadiazole derivatives on the same cancer cell line [140].
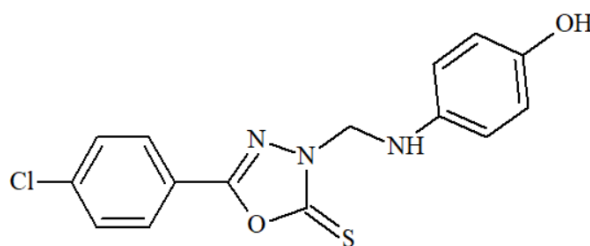
Recently published study by Bajaj in 2018, about structure activity relationships (SARs) of substitutions on aromatic rings at third and fifth positions, also thione group at second position of 1,3,4-oxadiazole moiety were important for MCF-7 cell inhibitory activity. Compound with 4-hydroxyaniline and 4-chlorophenyl and at third and fifth positions of 1,3,4-oxadiazole-2-thione ring showed potent cytotoxicity against MCF-7 cells when compared with reference drug adriamycin [141].
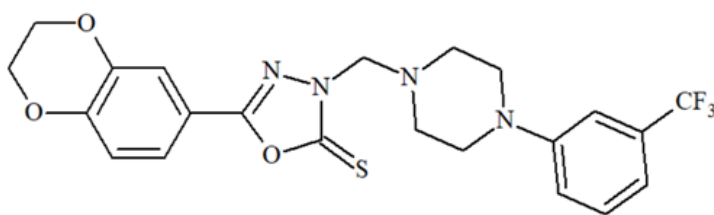
Sun and coworkers represented a series of novel 1,3,4-oxadiazole-2(*3H*)-thione derivatives containing phenylpiperazine groups. Compounds were evaluated against different cancer cells. According to consequences, trifluorophenyl substituted candidate revealed significant antitumor activity compared with the 5-FU [142].
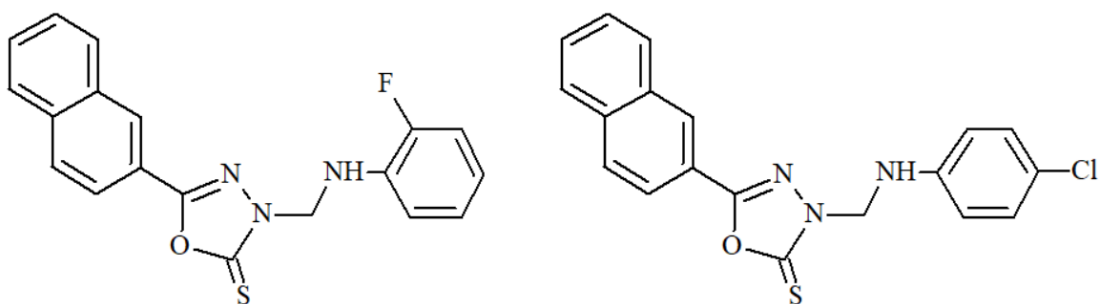
A series of quinoline derivatives bearing 1,3,4-oxadiazole ring were synthesized by Juan and coworkers. For broad-spectrum cancer screening, telomerase inhibitor and antitumor activity potential of compounds were evaluated with RAP-PCR-ELISA assay and three cancer cell lines (HepG2, SGC-7901 and MCF-7) respectively. According to test results, compounds contain 2-fluoro and 4-chloro showed the most potent anticancer activities, which were comparable to the reference drug [143].

2.3. Biologic Activity

Inflammation is an immune system response and caused by damaged cells, toxic compounds or irradiation [144]. In acute inflammation, biologic signals are rapidly generated in order to release inflammatory mediators in which removal of these harmful stimuli is corresponded to initiate the healing process [145]. Thereby, inflammation could named also as a defense mechanism [146] that during acute inflammatory processes, cellular and molecular interaction sequences tend to decrease the severity of injury or infection *via* restoration of tissue homeostasis. However, if acute inflammation become uncontrolled, it may turned into chronic inflammatory diseases [147]. In this condition, local vascular, immune and inflammatory cell responses are responsed to the symptoms of swelling, heat, pain and loss of tissue function [148]. As a consequence of vascular response; increased vascular permeability corresponds leukocyte accumulation and inflammatory mediator secretion through damaged cell region [145, 149]. Depended on these immunologic responses, organism initiates a chemical signaling cascade which aims to heal the affected tissues. For example, leukocyte chemotaxis is occurred from the general circulation to sites of damage and stimulate the formation of cytokines to moderate inflammatory facts [150]. At this time, resident tissue cells are hosted these biologic stimuli for the coordination of inflammatory mediator levels at associated site of injury [151]. Inflammation is a common pathogenesis of various chronic diseases,

including diabetes, arthritis, cardiovascular problems, bowel diseases and cancer [152]. Even though inflammatory response processes depend on the feature of the initial stimulus and its location in the body, they all share a common biologic cascade which could be sequenced as:

1. Cell surface pattern receptors recognize harmful signals

2. Inflammatory mechanisms are activated

3. Inflammatory markers are secreted

4. Inflammatory cells are augmented

These inflammatory mediators which are organized by intracellular signaling pathways might be exemplified with histamine, prostaglandins and nitric oxide function to dilate vascular smooth muscle in order to increase blood flow for bring in circulating leukocytes. Also acting on endothelial cells to increase vascular permeability is resulted as plasma protein and leukocyte transportation from the systemic circulation. In particular, tumor necrosis factor (TNF) and interleukin-1 (IL-1) that named as cytokines, promote leukocyte extravasation (Figure 3). In this condition, molecules generated from plasma proteins and cells are corresponded to tissue destruction or pathogens coordinate inflammation by changing vascular responces, leukocyte transportation and inflammatory system initiation (Granulocytes include neutrophils, basophils, and eosinophils) [153].
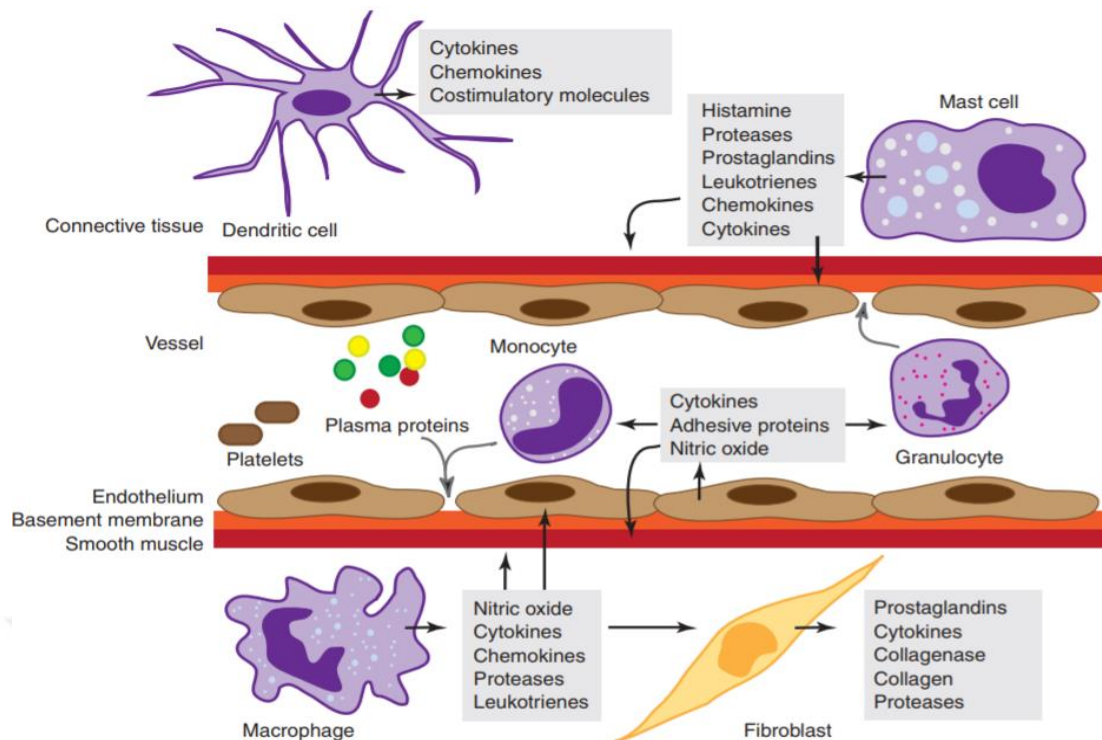
Figure 3. Activation pathways of responced cell types and their secreted mediators in an inflammatory condition [153]

To deep insight for biochemical mediators that are secreted during inflammation, responsed to propagate the inflammatory phenomenons. These mediators are soluble and diffusible molecules that able to act locally or systemically in which functioned as to induce vascular permeability, smooth muscle contraction, leukocyte activation and increase mast-cell degranulation. As inflammatory mediators like **bradykinin**, which is purposed to dilate vessels and increased vascular permeability to activate phospholipase A_2 (PLA$_2$) to actuate arachidonic acid (AA). Bradykinin is also a major mediator responsed in the pain stimuli. Other mediators are produced in injured tissue cells or leukocytes augmented to the site of inflammation. For example, histamine and serotonin which are a type of vasoactive amines released by mast cells, platelets, and basophils. **Histamine** causes arteriolar dilation so capillary permeability, contraction of nonvascular smooth muscle and associated with pain. Also histamine-induced vascular effects are mediated by H_2 receptors in which they also have special function for gastric secretion. Similar to histamine, **serotonin** (5-hydroxytryptamine) is located at platelets and mast cells in the gastrointestinal tract (GI) and central nervous system (CNS). Serotonin also induces vascular permeability and contracts nonvascular smooth muscle. Additionally, **interleukins 1–10 (IL 1-10)**, **tumor necrosis factor α (TNF-α)**, **interferon γ (INF-γ)**

are named as cytokines, majorily produced by macrophages and lymphocytes and functionalized as inflammatory molecules like histamin and seratonin. Particularly, **interleukin-1 (IL-1)** and **TNF-α** mobilize and stimulate leukocyte activation, induce proliferation of **B** and **T** cells and **natural killer cell** cytotoxicity takes place in inflammatory processes. **IL-1, IL-6**, and **TNF-α** organize the acute responses and pyrexia that may provoke infection and can cause systemic clinical signs, possessing anorexia and sleepy mood. In the acute phase, interleukins effect the liver to synthesize acute-phase proteins, including **complement components, coagulation factors, protease inhibitors, and metal-binding proteins** (Scheme 6). In chronic inflammation, cytokines like; **IL-1, IL-6**, and **TNF-α** provide the activation of osteoblasts and fibroblasts and the secretion of enzymes such as stromelysin and collagenase that can cause cartilage and bone resorption. Several studies also claims that cytokines mediate synovial cells and chondrocytes to secrete pain-inducing mediators [154].
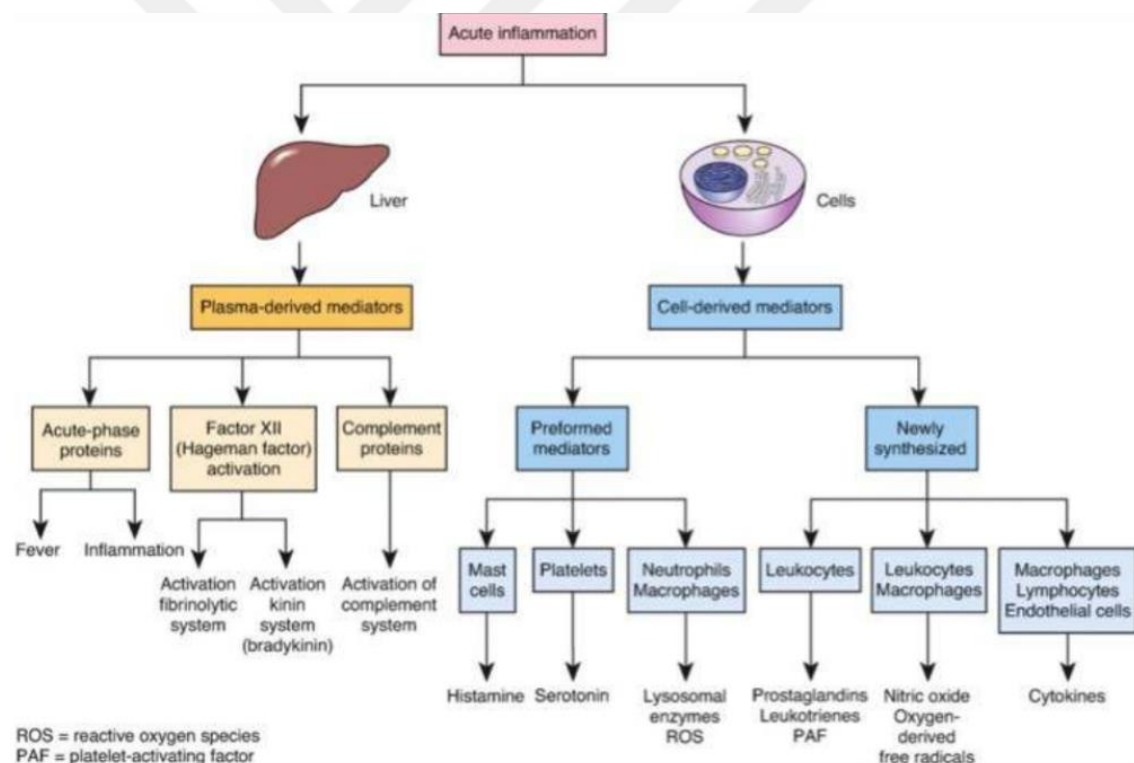
Scheme 6. Inflammatory mediators and their cellular sources [155]

Besides immun responced cytokines like; interleukins and TNF-α, lipid-derived autocoids also play important roles in the inflammatory responses and they are recent focus point for design of new anti-inflammatory drugs. These autocoids are named as eicosanoids and involving **prostaglandins, prostacyclin, thromboxane A, leukotrienes**

and the modified phospholipids such as **platelet activating factor (PAF)**. Eicosanoids are synthesized by activated leukocytes, mast cells, and platelets, therefore, widely distributed in organisms. Hormones and other inflammatory mediators (TNF-α, bradykinin) stimulate eicosanoid production either by direct activation of phospholipase A_2 (PLA_2) or indirectly by increasing intracellular calcium (Ca^{2+}) concentrations (Figure 4). Cell membrane damage can also cause an increase in intracellular Ca^{2+}. Activated PLA_2 directly hydrolyzes arachidonic acid (AA) which is rapidly metabolized via one of two enzyme pathway as, cyclooxygenase (COX) pathway leading to the formation of prostaglandin and thromboxanes or the 5-lipoxygenase (5-LOX) pathway that produces the leukotrienes [154].
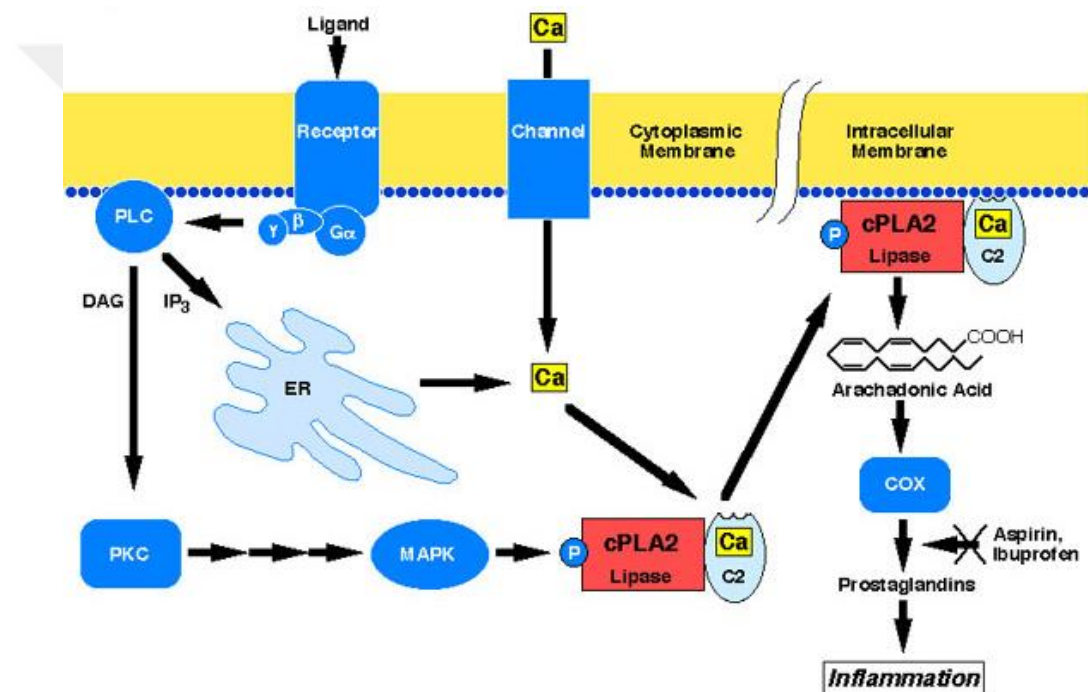
Figure 4. Inflammatory response of cPLA2 by the entrance of calcium into the cell [156].

Cyclooxygenase catalyzes the oxygenation of arachidonic acid to form the cyclic endoperoxide prostaglandin **G_2 (PGG$_2$),** which is converted to **prostaglandin H$_2$ (PGH$_2$)**. Both **PGG$_2$** and **PGH$_2$** are unstable and rapidly converted to various prostaglandins, **prostacyclin (PGI$_1$)** and **thromboxane A$_2$ (TXA$_2$)**. In the vascular beds, **prostaglandin E$_1$ (PGE$_1$), prostaglandin E$_2$ (PGE$_2$)** and **prostaglandin I$_1$ (PGI$_1$)** are potent arteriolar dilators and enhance vascular permeability whereas **prostaglandin F-2α (PGF2α)** and **thromboxane (TXA)** result smooth muscle contraction and vasoconstriction [136]. On the other hand, cyclooxygenases (COXs) are exerted in two

isoforms (Figure 5) in which first subtype cyclooxygenase-1 (COX-1) emerges constitutively in most of the mammalian cells and platelets. Main target organs of this enzyme are stomach, forebrain, kidney, uterine and vascular endothelium. As afore mentioned, their physiological role is to support the production of prostoglandins (PGs) which are necessary for homeostatic functions and gastric cytoprotection whereas second subtype named cyclooxygenase-2 (COX-2) enzyme exhibits in PG formation during inflammation and tumorigenesis [155-158].
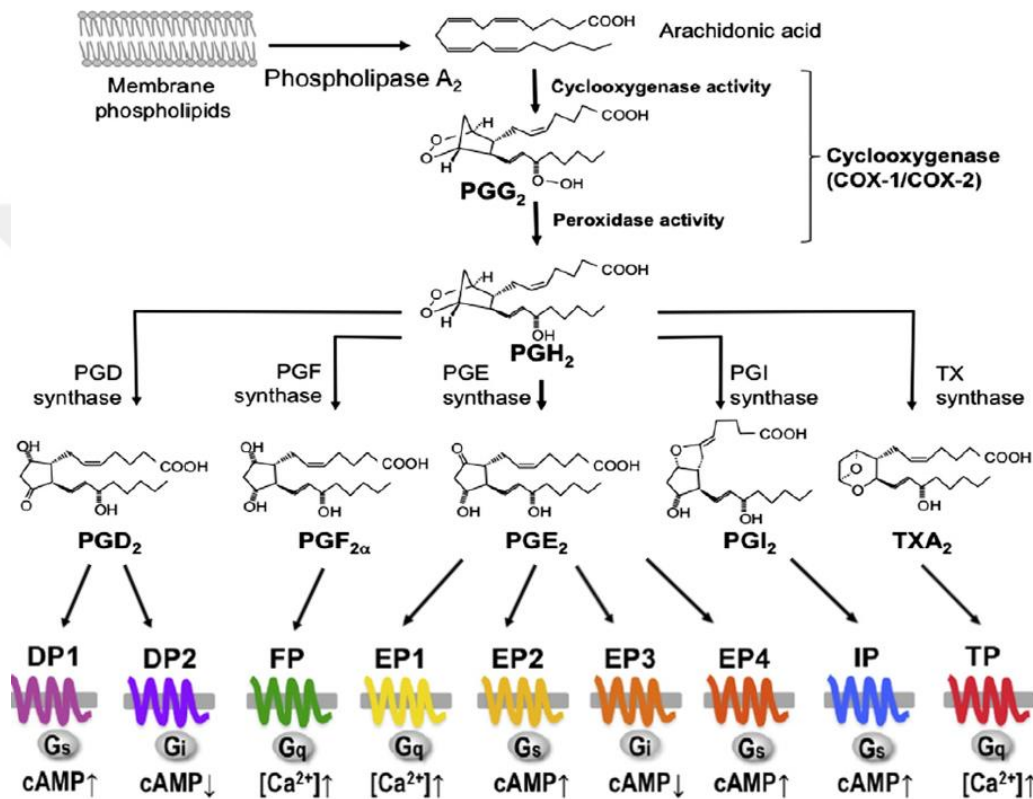
Figure 5. General prostanoids and their effector subtypes in arachidonic acid cascade [159]

During inflammatory processes, especially prostaglandin E_2 (PGE_2) is able to elicit a wide range of biological effects. During the initial phase of the inflammatory response, PGE_2 and related prostanoids such as PGI_2, act as vasodilators to promote the tissue entrance of macrophages, neutrophils and mast cells from the bloodstream lead to edema at inflamed area [160]. Additionally PGE_2 has four kinds of receptor subtypes (EP1–EP4) which corresponds variety of actions including pyrexia, pain sensation and particularly inflammation. In recent years, the molecular mechanisms refering the PGE_2 activity mediated-EP subtypes have been set up by studies using mice deficient in each EP subtypes. Many compounds that selective to each EP subtype contributed different

responses in which it was well to discuss how PGE_2 initiates and triggers inflammation at the molecular level showed in Figure 5 [159]. According to clinical reveals, particularly COX-1 induced PGE_2 is responsed to facilitate homeostatic phenomenons (vasodilation, smooth muscle relaxation and protecting GI barrier) based on bonding different EP-subtypes, COX-2 induced PGE_2 is formed during inflammatory situations and forms associated physiological symptoms (heat, redness, swelling, pain, etc.) [161]. Other biologic function of prostaglandins is to stimulate nociceptors for facilitating the formation of pain-inducer mediators like bradykinin and histamine and in high concentrations, can directly effect sensory nerve endings. Last COX-induced eicosanoid named TXA_2, is a potent platelet-aggregating agent involved in thrombocyte activation and found majorily in leukocytes, platelets and the lungs. Besides COX, another main enzyme family is **5-lipooxygenase (5-LOX)** and catalyzes the production of unstable hydroxyperoxides from arachidonic acid. These hydroxyperoxides are subsequently converted to peptide leukotrienes. **Leukotriene B4 (LTB4)** and **5-hydroxyeicosatet ranoate (5-HETE)** are strong chemoattractants stimulating polymorphonuclear leukocyte movement. **LTB4** also stimulates the production of cytokines in neutrophils, monocytes and eosinophils. Other leukotrienes contribute the secretion of histamine and other autocoids from mast cells and stimulate bronchiolar constriction and mucous secretion. In some species, **leukotrienes C4** and **D4** are more potent than histamine in contracting bronchial smooth muscle (Figure 6). Leukotriene group autocoids are predominantly involved in allergic reactions [154].
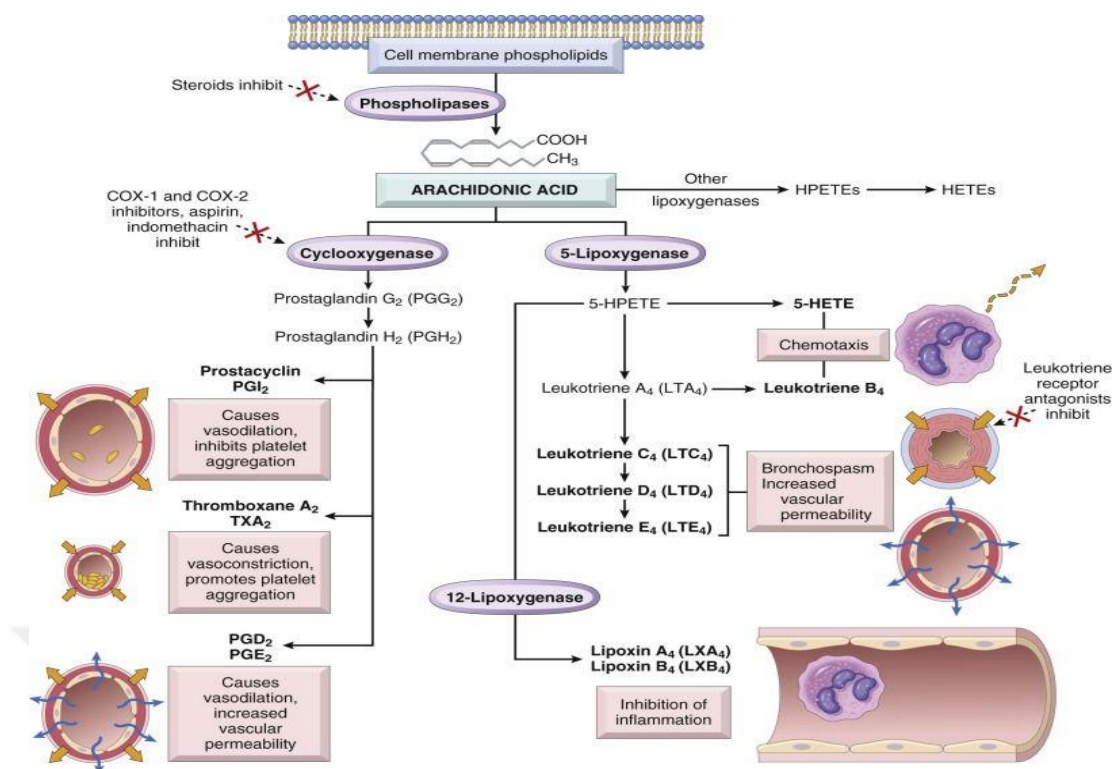
Figure 6. Many prostaglandins and eicosanaoids derived from COX and LOX families in inflammatory processes [157]

Platelet activating factor (PAF) is composed from cell membrane phospholipids by the action of PLA_2. PAF is synthesized by mast cells, platelets, neutrophils, eosinophils and increases platelet aggregation and promotes platelets to release vasoactive amines and synthesize thromboxanes. PAF also induces vascular permeability and causes neutrophils to aggregate and degranulate [154]. PAF plays a significant role in pathology of many inflammatory diseases. In recent years, some of natural PAF antagonists (andrographolide, α-bulnesene, cinchonine) have been used as therapeutic agents for the humans against many inflammatory diseases in which these problems either originated from immunological or non-immunological types. (Figure 7) [162].
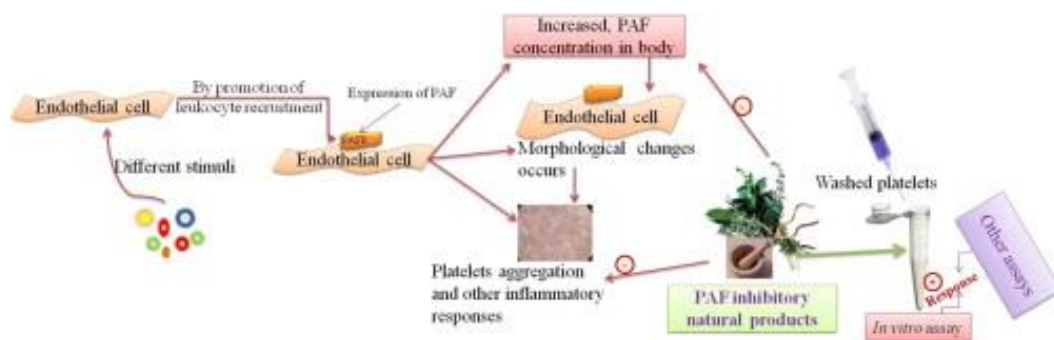
Figure 7. PAF antagonism mechanism in inflammatory processes [162]

Another chemical mediator named nitric oxide (NO), is an important cell-signaling messenger in a wide range of physiologic and pathophysiologic processes. Small amounts of NO play a role in maintaining resting vascular tone, vasodilation, and antiaggregation of platelets. By physiological effect of certain cytokines (TNF-α, IL-1) and different responsed mediators, large quantities of NO are stimulated in this inflammatory conditions. Vasodilator effect of NO, facilitates macrophage-induced cytotoxicity and may facilitate to joint destruction in some types of arthritis [154]. This important chemokine is considered as a proinflammatory mediator and induces inflammation due to overproduction in abnormal situations. The process is controlled by an enzyme system which is called as nitric oxide synthases (NOSs). These are responsible from stimulation of NO production and its augmentation into the damaged location of endothelial cells . There are three isoforms of NOS named according to their target which are neuronal NOS (nNOS), constitutive endothelial NOS (eNOS) and inducible NOS (iNOS) in Figure 8. They are also numbered as NOS1, NOS2, NOS3 associated with nNOS, iNOS and eNOS, respectively [163]. Particularly for inflammatory reactions, proinflammatory cytokines correspond to induction of the iNOS in monocyte-macrophages, neutrophil granulocytes and many other cells; in the case of bacterial infection or another strong inducer of expression. As a results, amounts of NO are produced, exceeding the physiological NO level by up to nearly 1000-fold [164-166].
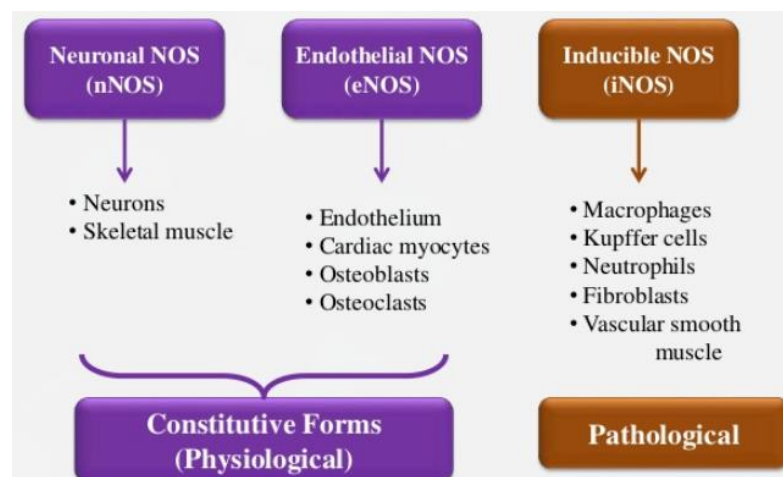
Figure 8. Schematic representation of nitric oxide syntheases (NOSs) [163]

As a traditional drug regimen, steroidal (corticosteroids), non-steroidal antiinflammatory drugs (NSAIDs) and disease-modifying antirheumatic drugs are used

to relief inflammatory symptoms for many years. However clinically used compounds like prednisolone, naproxen, ibuprofen, diclofenac, etc. have been caused severe gastrointestinal and renal side effects. Depended on phosholipase A2 (for prednisolone) and non-selective COX inhibition, many patients have been suffering from these pathologic situations [167]. Thereby, routine therapy models are tried to developed by pharmaceutical industries to reduce severe side effects which is primarily gastric ulceration. As a consequence, selective COX-2 inhibitors were seemed to overcome these problems but in this case, cardiotoxicity was emerged as another significant side effect [168]. To lower the risk of inflammatory drug therapy, researchers need new strategies to evaluate desired effects within the safe responses [169]. In these regards, new molecular modulations have been settled, depended on bioisosteric replacement of specific molecular functional groups that cause ulcerogenesis, to be able to suppress especially gastric side effects [17]. Besides new molecular modulation approach, designed compounds are also evaluated for their inhibitor potentials on different inflammatory mediators like prostaglandins, leukotrienes, interleukins, tumor necrosis factors, nitric oxide, etc.

2.4. In *vitro* Antiinflammatory Assay Models

Depended on different inflammatory mediators in which they originate either from plasma (e.g. complement proteins [kinins]) or from cells (e.g. prostaglandins, cytokines, histamines). Large amount of experimental issues and detailed data subject inflammatory mediators and particularly, the most common mediators that are studied for inflammation are histamine, prostaglandins (PGs), leukotrienes (LTB4), nitric oxide (NO), platelet-activation factor (PAF), bradykinin, serotonin and cytokines [170, 171]. Majorily in *vitro* antiinflammatory assay models were summarized as:

2.4.1. Conjugated Diene Assay

Conjugated dienes are major products of lipid peroxidation in inflammatory process. Inserting more double bond enhances the rate of lipid peroxidation by 30 to 100 fold which corresponds chain to conjugate after peroxidation [172, 173].

2.4.2. Anti-proteolytic Activity Assay

In order to investigate antiinflammatory activity, the presence of a powerful antiprotease activity is evaluated and exact information concerning the activity of antiprotease percentages reflect the growth of pathogenic bacteria which corresponds bacteria-associated inflammation [174].

2.4.3. β-Glucuronidase Inhibition Assay

Casein hydroxylate consumers have been patients of neonatal jaundice. In order to block enterohepatic circulation of bilirubin, patients who are tended to this inflamed lived illness, have to inhibit β-glucuronidase activity that is found in casein hydroxylate formula [175].

2.4.4. WST-1 Antiinflammatory Assay

The WST-1 assay protocol is depended on the cleavage of WST-1 to formazan by mitochondrial dehydrogenases. It is also used to assess human neutrophil dysfunction and to compare antiinflammatory activity [176, 177].

2.4.5. HET-CAM Antiinflammatory Assay

Choriallantoric membrane of incubated hen's eggs as in *vitro* model (HET-CAM) are studied compared to the in *vivo* croton oil test by possessing indomethacin, phenyl butazone and aspirin etc. These bioassays are able to reflect the antiinflammatory property of the constituents tested [178].

2.4.6. MHS Antiinflammatory Assay

The anti-inflammatory assay was determined as, the total volume of 250 ml MHS solution with pH 7.4 containing neutrophils/ml, WST-1 and various concentration of the drug samples. IC_{50} values are calculated by the comparison of DMSO, as blank and demonstrated as percent inhibition of superoxide generation [179, 180].

2.4.7. LPS-induced Nitric Oxide (NO) Inhibition Assay

Sodium nitroprusside (SNP) is a natural source of nitric oxide and induced by bacterial lipopolysaccharide (LPS). For the evaluation of antiinflammatory properties of tested samples; inflammatory nitric oxide in terms of nitrite secretion by cells (RAW 264.7 cells) are measured colometrically using Griess reagent [181].

2.4.8. LPS-induced Prostaglandin E2 (PGE$_2$) Inhibition Assay

Prostaglandin E2 (PGE$_2$) is measured by a colorimetric assay by the use of a PGE$_2$ assay kit (R&D Systems, Minneapolis, MN, USA), according to the kit manufacturer's instructions [181].

2.4.9. Tumor Nectosis Factor-α (TNF-α) Inhibition Assay

TNF-α is measured by ELISA using a mouse-specific TNF-α ELISA Kit (Komabiotech, Seoul, Republic of Korea) based on the manufacturer's instructions [181].

2.4.10. Interleukin-1β (IL-1β) and Interleukin-6 (IL-6) Inhibition Assay

IL-1β and IL-6 are determined by colorimetric assays using mouse-specific immunoassay kits (R&D Systems) according to the manufacturer's instructions [181].

2.4.11. Necrosis Factor-$\kappa\beta$ (NF-$\kappa\beta$) Inhibition Assay

Free radicals and reactive oxygen metabolites provoke inflammation by the induction of some inflammatory genes, possessing NF-$\kappa\beta$ [21, 22]. Activation of NF-$\kappa\beta$ corresponds to elevation of the inflammatory stimuli by generation of several proinflammatory cytokines and enzymes. In order to evaluate the antiinflammatory potencies of test samples based on NF-$\kappa\beta$ inhibition mechanism, a NF-$\kappa\beta$ (p65) Transcription Factor Assay Kit (Cayman Chemical Company, Ann Arbor, MI, USA) according to the manufacturer's protocol [181].

2.5. In *vivo* Antiinflammatory Assay Models

Inflammation is an orchestrated defense mechanism by the organism to eject the injurious stimuli and to start up the recovery process. Without inflammation, infectional conditions would never recover and organized destruction of the tissue would prevent survival of the organism [182]. In *vivo* antiinflammatory assay models are given below in which they are studied as time-dependent acute and chronic inflammatory applications.

2.5.1. Acetic Acid-induced Vascular Permeability

The antiinflammatory activity of tested compound may be depended on inhibition of proinflammatory cytokine production, neutrophil-mediated myeloperoxidase activity, inhibition of IL-1β and TNF-α and inhibition of leukocyte augmentation. Test results suggest a compound may have therapeutic effect for different immune-related cutaneous diseases [183].

2.5.2. Carrageenan–induced Edema

The inhibition activity of test compound is correlated with inflammatory mediators such as histamine, serotonin and prostaglandin by using this assay model.. After the application of test sample, the percentage inhibition of paw volume in drug treated group is compared with the reference group [184].

2.5.3. Carrageenan-induced Air Pouch Model

The anti–inflammatory activity is evaluated by inhibiting either release of lysosomal enzymes or by stabilizing the lysosomal membrane, which is one of the major events responsible for the inflamatory process [185].

2.5.4. Carrageenan-induced Pleurisy in Rats

After the intrapleural injection of carrageenan on the right side of the thorax to detect the antiinflammatory effect of compounds, they are applicated on test animals. Results are showed an inhibitory effect on leukocyte migration and a reduction on the pleural exudates [186].

2.5.5. Carrageenin- and Arachidonic Acid-induced Paw Edema

Inflammatory mediators such as kinin, serotonin, and PGs are released by ethyl phenylpropiolate (EPP) and phenylbutazone (COX inhibitor) represented a marked decresion of the ear edema. It has a good indicator value to evaluate antiinflammatory compounds [187].

2.5.6. Cotton Pellet-induced Granuloma

Cotton pellets weighing are autoclaved and implanted subcutaneously into both sides of the groin region of each rat. Antiinflammatory activity of sample may be generated by inhibition of histamine, serotonin and prostaglandin mediators [187].

2.5.7. Croton Oil-induced Mouse Ear Edema

Croton oil and test sample are induced to inner part of right ear of animal. In the concept of this model, The inflammatory process is originated from the secretion mediators from tissues and migrated cells with their released molecules like prostaglandins (PGs), leucotrienes (LTs), histamine, bradykinin, platelet-activating factor (PAF) and interleukin-1 [188].

2.5.8. Egg White-induced Hind Paw Edema

Animals were divided into groups and samples are administered orally into those group of animals. In this model, desired response is measured by the release of active pain, substance such as histamine, serotonin, polypeptides or prostaglandins [189].

2.5.9. Human Red Blood Cell (HRBC) Membrane Stabilization

HRBC membrane have similar properties with lysosomal membrane composition, the prevention of hypotonicity induced HRBC membrane destruction is used as a parameter of antiinflammatory activity of tested samples [190].

2.5.10. Formalin-induced Edema in Rat Paw

Rats were divided into groups and inflammation is emerged by subponeurotic injection of formaldehyde in the right hind paw. Depended on formalin exposure process, before antiinflamatory drug application demonstrates the acute and/or chronic anti-inflammatory activity responces of compounds [191].

2.5.11. Hyaluronidase Inhibitory Assay

Hyaluronidase is an enzyme that decomposes hyaluronic acid in which it is an important part of extracellular matrix in connective tissue. By degrading the components of connective tissue, hyaluronidase contributes the distribution of inflammatory mediators throughout these tissues, therefore facilitating to the pathogenesis of inflammatory diseases like allergic reactions, transportation of cancer cells, inflammation and the induction in permeability of vascular system [192].

2.5.12. Kaolin-induced Paw Edema

Tested compounds are evaluated to act as inhibitors of cyclooxygenase and 5-lipooxygenase. They are also deteched for their agonistic effect of histamine and down regulation of cyclooxygenase activity. It also blocks the secretion of prostaglandin synthesis by the use of kaolin-induced paw oedema test method [193].

3. MATERIAL and METHODS

3.1. Chemistry

3.1.1. Materials

In this work, salicylic acid, ibuprofen, sulphuric acid, hydrazine hydrate, carbondisulphide, 1-phenylpiperazine, 1-(4-fluorophenyl)piperazine, 1-(2-fluorophenyl)-piperazine, 1-(4-trifluoromethylphenyl)piperazine, 1-(3-trifluoromethylphenyl)piperazine, 1-(4-chlorophenyl)piperazine, 1-(2-chlorophenyl)piperazine monohydrochloride, 1-(3,4-dichlorophenyl)piperazine, 1-(2,3-dichlorophenyl)piperazine hydrochloride, 1-(4-methylphenyl)piperazine, 1-(2,3-xyxyl)piperazine, 1-(4-methoxyphenyl)piperazine, 1-(3-methoxyphenyl)piperazine, 1-(2-methoxyphenyl)piperazine, 4-piperazinobenzonitrile, 1-(2-cyanophenyl)piperazine, 1-(2-pyridyl)piperazine, N-(2-pyrimidinyl)piperazine, ethanol, methanol, n-hexane were purchased from Sigma–Aldrich (Germany).

3.1.2. Methods of Synthesis

3.1.2.1. General procedure for the preparation of methyl esters

A solution of 1g salicylic acid (0.007 mol) or ibuprofen (0.005 mol), 10 ml methanol and 0.75 ml concentrated sulphuric acid was prepared. Mixture was gently refluxed at 85°C about 75 minutes by mixing. At the end of reaction, solution mixture was cooled and extracted with hexane. Organic layer was taken and evaporated. Isolated ester compounds were checked by thin layer chromatography with benzene:methanol (90:10) mobile phase system [194].

3.1.2.2. General procedure for the preparation of aroylhydrazides

The mixture of 0.1 mol methyl esters of salicylic acid or ibuprofen and 0.2 mol of hydrazine hydrate was refluxed in 20 ml absolute alcohol about 10-20 hours. The excess solvent was evaporated under reduced pressure and the concentrated solution was quenched into ice cold water. The precipitated white solid was filtered, rewashed with water and dried about 2 days. The crude product was purified by recrystallization from water to produce pure hydrazide compounds. Isolated hidrazide compounds were checked by thin layer chromatography with benzene:methanol (40:60) mobile phase system [17].

3.1.2.3. General procedure for the preparation of 5-substituted-1,3,4-oxadiazole-2-(*3H*)-thione

Approciate aroyl hidrazide (0.1 mol), KOH (0.1 mol) in absolute alcohol (50 mL) and CS_2 (0.2 mol) was taken in a round bottom flask and refluxed for about 20-25 hours untill evolution of hydrogen sulfide was ceased. The reaction mixture was cooled to room temperature and diluted with water. The product precipitated out on acidification with 10% hydrocloric acid was filtered, thoroughly crystallized with hexane. Isolated 5-substituted-1,3,4-oxadiazole-2(*3H*)-thione compounds were checked by thin layer chromatography with benzene:methanol (90:10) mobile phase system [17].

3.1.2.4. General procedure for the preparation of *Mannich* bases

A mixture of 5-substituted-1,3,4-oxadiazole-2(*3H*)-thione (0.01 mol), formaldehyde (0.015 mol) and piperazine derivative (0.01 mol) in 15 ml ethanol or methanol was continously reacted at room temperature through overnight. The precipitated solids in reaction media were filtered and recrystallized from ethanol or methanol to obtained desired *Mannich* bases [17]. Acetic acid was added preferently, depended on reaction yields.

3.1.3. Analytical Methods

3.1.3.1. Melting point determination

Melting points (ºC) determination of compounds were determined by using a Mettler Toledo FP62 capillary melting point apparatus and are uncorrected.

3.1.3.2. Controls by Thin Layer Chromatography

Material:

Plates: Silicagel F-254 (Merck) plaques (20x20 cm)

Solvents: Three different solvents systems were prepared to be used as mobile phases chromatographic controls of compounds

S1: Benzene:Methanol (90:10) T:25ºC

S2: Benzene:Methanol (40:60) T:25°C

S3: Toluene: Acetone: Acetic acid (75:25:10) T:25°C

Method:

Dragging condition: Solvent systems were poured to chamnbers and kept for 1 hour for saturation.

Reactions were monitored with TLC after dissolving the synthesized compounds and starting materials with suitable solvents and application of them with Pasteur pipettes onto silica gel plates. The plates were dragged for 10 cm at room temperature. R_f values of compounds were calculated.

Stain determination: Stains of synthesized compounds and their starting materials were determined by UV light (254/365 nm).

3.1.4. Spectral Analysis

3.1.4.1. Ultraviolet Spectra

Ultraviolet spectra were recorded on Agilent 8453 UV-Spectroscopy. Compound were dissolved in acetonitrile in which UV cut-off value is 190 nm.

3.1.4.2. Infrared Spectra

Infrared spectra or synthesized compounuds were recorded on Perkin-Elmer Specrum One series FT-IR apparatus (Version 5.0.1.), using potassium bromide pellets, the frequencies were demonstrated in cm^{-1}.

3.1.4.3. ^{1}H-NMR Spectra

^{1}H-NMR spectra were recorded with a Varian Mercury-400 FT-NMR spectrometer (Varian Inc., Palo Alto, CA, USA), using tetramethylsilane (TMS) as the internal reference, with dimethyl sulphoxide (DMSO-d_6) as solvent, the chemical shifts were recorded in parts of milllion (ppm).

3.1.4.4. ¹³C-NMR Spectra

^{13}C-NMR spectra were recorded with a Varian Mercury-400 FT-NMR spectrometer (Varian Inc., Palo Alto, CA, USA), using tetramethylsilane (TMS) as the internal reference, with dimethyl sulphoxide (DMSO-d$_6$) as solvent, the chemical shifts were recorded in parts of milllion (ppm).

3.1.4.5. Mass Spectra

The Mass spectra of compound **5c** and **10a** were recorded with LC/MS Agilent Single Quad AGT-G61258A.

3.1.4.6. Elemental analysis

Elemental Analysis were performed on LECO 392 CHNS (Leco-932, St. Joseph, MI, USA) instrument.

3.2. Biological Studies

3.2.1. Cell Viability

The murine macrophage RAW264.7 cell line (ATCC, USA) were maintained in DMEM High Glucose supplemented with 10% FBS and 1% penicillin (10,000 units/mL) and streptomycin (10,000 μg/mL) at 37°C in a 5% CO2 atmosphere. Cell viability was measured by using MTT colorimetric assay which depends on the mitochondrial dependent reduction of MTT formazan. Plated RAW264.7 cells were treated with various concentrations of compounds (50-100 μM). After 24 hours, cell medium was discarded and MTT solution (0.5 mg/mL) was added to wells for additional 2 hours at 37°C. After incubation, cell culture medium was removed and 100 μl of isopropanol was used to dissolve the formazan. The absorbance was determined at 570 nm wavelengths by a microplate reader (Thermo Multiskan Spectrum, Finland). The absorbance of control group was considered as 100%. The percentage of cell viability was calculated as follows:

$$\%\text{Viability} = \frac{(\text{Absorbance of treatment group} - \text{Absorbance of background})}{(\text{Absorbance of the control group} - \text{Absorbance of background})} \times 100\%.$$

3.2.2. Antiinflamatory Activity

3.2.2.1. COX-1/COX-2 Enzyme Inhibition Assay

Synthesized compounds were evaluated for their selective cyclooxygenase (COX) inhibition with COX Assay Kit (Cayman No: 700100) to analyze the inhibitory potential of the test compounds on COX-1 and COX-2 enzymes provides a fluorescent assay method in which ADHP (10-acetyl-3,7-dihydroxyphenoxazine) is used to serve as substrate to peroxidase component of the enzyme and the enzymecatalyzed formation of resorufin, a highly fluorescent compound, is measured with an excitation wavelength of 530 nm and an emission wavelength of 585 nm. Each test compound was analyzed in dublicate applications. The enzyme-free and inhibitor-free assay systems were used as control experiments. The percentage of enzyme inhibition was calculated as follows:

$$\% \text{ inhibition} = \frac{(\text{Initial activity} - \text{Sample activity})}{(\text{Initial activity})} \times 100\%$$

3.2.2.2. Nitric oxide (NO) Inhibition Assay

Anti-inflammatory activity of compounds were evaluated by measuring the stable nitric oxide (NO) metabolite, nitrite, levels in cell culture media, with Griess reagent (Kiemer and Vollmar, 1997). RAW264.7 cells were plated at density of 1x106/ml in a 48 well-plate and incubated for 24 hours at 37°C in 5% CO2. After cell culture media was aspirated, cells were pre-treated with various concentrations of compounds (50-100 μM) for 2 hours and then stimulated with 1 μg/mL of LPS (lipopolysaccharide from E.coli 0111:B4, Sigma, USA) for additional 22 hours. The collected culture supernatant was mixed with equal volume of Griess reagent [1% sulfanilamide and 0.1% N-(1-naphthyl) ethylenediamine dihydrochloride in 5 % phosphoric acid] in a 96 well-plate and incubated at room temperature for 10 min in the dark. The absorbance was determined using a microplate reader (Multiskan Ascent, Finland) at 540 nm wavelength. The concentration

of nitrite in samples was calculated by using sodium nitrite standard curve. Indomethacin (100 μM) was used as a positive control [195, 196].

3.2.2.3. Prostaglandin E₂ (PGE₂) Inhibition Assay

PGE₂ concentrations in cell culture supernatants of the molecules which have shown to reduce inflammation in NO assay were measured by using a commercially available quantitative enzyme-linked immunosorbent assay (ELISA) kit (Abcam PGE₂ ELISA Kit, UK) according to manufacturer's instructions.

3.2.3. Antioxidant Activity

3.2.3.1. DPPH Scavenging Assay

The capacity of compounds to scavenge free radicals was measured by using DPPH (2,2'-diphenyl-1-picrylhydrazyl) assay (Blois, 1958). The reaction mixture 0.1 mM DPPH was prepared in methanol. The absorbance of samples was measured at 517 nm at room temperature after 30 minutes under dark conditions. Ascorbic acid (100 μM) was used as a reference compound. The radical scavenging activity (RSA) of compunds were calculated as the percentage of radical scavenging as follows [197]:

$$\text{DPPH RSA \%} = \frac{(\text{Absorbance of control} - \text{Absorbance of sample})}{(\text{Absorbance of the control})} \times 100\%$$

3.2.4. Statistical Analysis

All repeated experiments were conducted in triplicate. Statistical analysis was performed by using GraphPad Prism 6 (Version 6.01; GraphPad software, Inc., San Diego, CA). Differences between groups were analyzed by using one-way ANOVA following the post-hoc tests by Tukey. Statististical correlation was measured by Pearson coefficient. Group differences were considered to be significant at $p < 0.05$.

3.3. Docking Studies

Docking studies were carried out by GLIDE [198], as a standard docking program for the targets of COX-1 (PDB ID: 5U6X [199]) and COX-2 (PDB ID: 5IKT [200]) enzymes. To test whether the docking program can correctly reproduce the binding mode and to evaluate docking program, redocking experiments were performed using the co-crystallized inhibitors and the crystal structures. Glide was tested and Glidescore (SP) was chosen as fitness function. The proper pose was evaluated according to the root mean square deviation (RMSD) of predicted conformations versus the corresponding native one; based on the principle of docking poses with RMSD of less than 2.0 Å are in agreement with the X-ray structure. Therefore, this docking program and setup were used in further studies. Then, a dataset of totally 16 samples was generated. For this dataset, 25 conformers for each molecule were produced using ConfGen [201]. The aim of conformer generation is to generate a set of low energy 3D structures which includes the so-called bioactive conformation of a molecule that is the conformation in which it binds to the target [202].

4. RESULTS

4.1. Chemical Data

5-(2-Hydroxyphenyl)-3-[(4-phenylpiperazin-1-yl)methyl]-1,3,4-oxadiazole-2(*3H*)-thione (**Compound 5a**) **[84]**
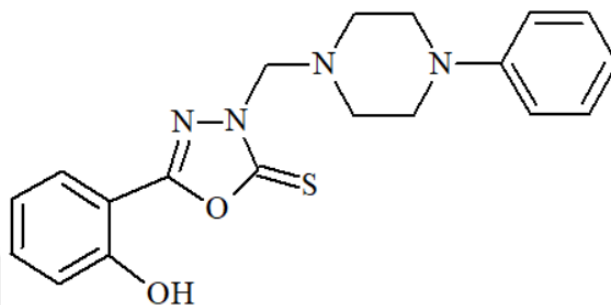
5-(2-Hydroxyphenyl)-1,3,4-oxadiazole-2(*3H*)-thione (0.01 mol, 1.94 g), 1-phenyl-piperazine (0.01 mol, 1.62 g), formaldehyde (0.015 mol, 0.55 ml) in 15 ml ethanol were reacted according to general synthesis method at 3.1.2.4.

Yield (%)	:	84
Retention factor (R$_f$)	:	0.61 [Toluene: Acetone: Acetic acid (75:25:10)]
Physical appearance	:	White powder
Melting point (ºC)	:	170
Solubility	:	Highly soluble with acetone and DMSO. Practically insoluble in water

Spectral Analysis

Infrared (IR) spectrum

ν_{max} **(cm^{-1}) :** 3332 (O-H stretching); 2886 (aromatic C-H stretchings); 1626 (C=N stretching); 1598, 1573, 1502, 1489 (aromatic C=C stretchings); 1441 (O-H bending); 1326 (C-O stretching); 1223 (C=S stretching) ; 766 (phenyl C-H bendings); 746 (2-hydroxyphenyl C-H bendings) (Figure 9).
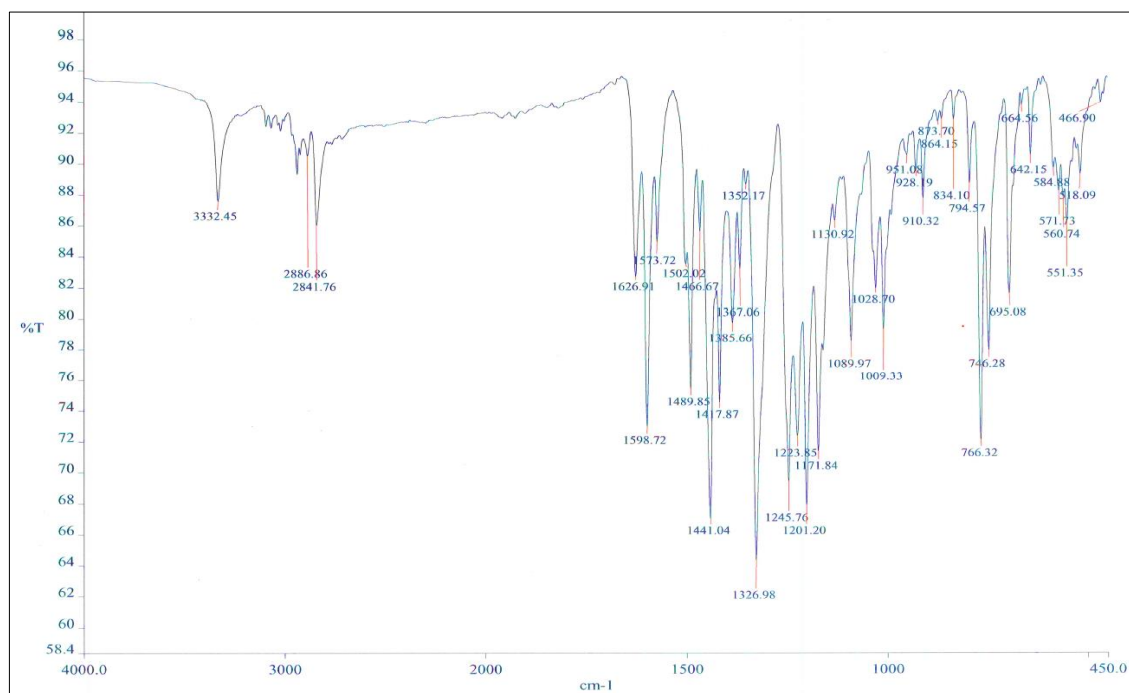
Figure 9. IR spectrum of Compound **5a**

^{1}H NMR spectrum

δ **ppm (400 MHz/DMSO-d_6):** 2.90 (4H, t, J=4.8 Hz, piperazin H_2+H_6); 3.13 (4H, t, J=4.8 Hz, piperazin H_3+H_5); 5.1 (2H, s, -N-CH$_2$-N-); 6.76 (1H, t, J=7.2 Hz, phenyl H_4'); 6.90 (2H, bd, J=8 Hz, phenyl H_2'+ H_6'); 6.95-6.99 (1H, m, phenyl H_5); 7.05 (1H, bd, J=8.4 Hz, phenyl H_6); 7.18 (2H, t, J=7.8 Hz, phenyl H_3'+H_5'); 7.42-7.46 (1H, m, phenyl H_4); 7.66 (1H, dd, J=8 J'=1.6 Hz, phenyl H_3); 10.51 (1H, bs, -OH) (Figure 10).

Figure 10. ^{1}H NMR spectrum of Compound **5a**

5-(2-Hydroxyphenyl)-3-{[4-(4-fluorophenyl)piperazin-1-yl]methyl}-1,3,4-oxadiazole-2(*3H*)-thione (Compound 5b)
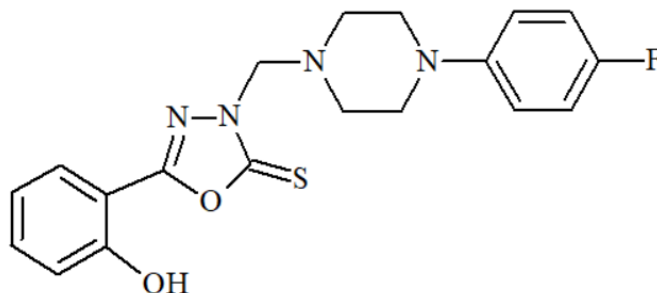
5-(2-Hydroxyphenyl)-1,3,4-oxadiazole-2(*3H*)-thione (0.01 mol, 1.94 g), 1-(4-fluoro-phenyl)piperazine (0.01 mol, 1.80 g), formaldehyde (0.015 mol, 0.55 ml) in 15 ml ethanol were reacted according to general synthesis method at 3.1.2.4.

Yield (%)	: 76
Retention factor (R$_f$)	: 0.63 [Toluene: Acetone: Acetic acid (75:25:10)]
Physical appearance	: White powder
Melting point (ºC)	: 160
Solubility	: Highly soluble with acetone and DMSO. Practically insoluble in water
Elemental analysis	
Molecular formula	: C$_{19}$H$_{19}$FN$_4$O$_2$S
Molecular weight (g/mol)	: 386.44

	C	H	N	S
Calculated (%)	59.05	4.96	14.50	8.30
Found (%)	58.56	4.99	14.52	8.52

Spectral Analysis

Infrared (IR) spectrum

ν_{max} **(cm^{-1}) :** 3425 (O-H stretching); 2956 (aromatic C-H stretchings); 1613 (C=N stretching); 1598, 1499, 1490 (aromatic C=C stretchings); 1454 (O-H bending); 1404 (C-O stretching); 1259 (C=S stretching); 809 (4-fluorophenyl C-H bending); 746 (2-hydroxyphenyl C-H bending) (Figure 11).

Figure 11. IR spectrum of Compound **5b**

^{1}H NMR spectrum

δ ppm (400 MHz/DMSO-d_6): 2.86 (4H, t, *J*=5 Hz, piperazin H$_2$+H$_6$); 3.06 (4H, t, *J*=5 Hz, piperazin H$_3$+H$_5$); 5.09 (2H, s, -N-C$\underline{H}_2$-N-); 6.9 (1H, d, *J*=4.8 Hz, phenyl H$_6$'); 6.92 (1H, d, *J*=4.8 Hz, phenyl H$_2$'); 6.94-6.98 (1H, phenyl H$_5$); 7.00 (1H, d, *J*=8.8 Hz, phenyl H$_5$'); 7.02 (1H, d, *J*=8.8 Hz, phenyl H$_3$'); 7.03 (1H, d, *J*=8.4 Hz, phenyl H$_6$); 7.40-7.44 (1H, m, phenyl H$_4$); 7.64 (1H, dd, *J*=7.6 *J'*=1.6 Hz, phenyl H$_3$); 10.51 (1H, bs, -O$\underline{H}$) (Figure 12).
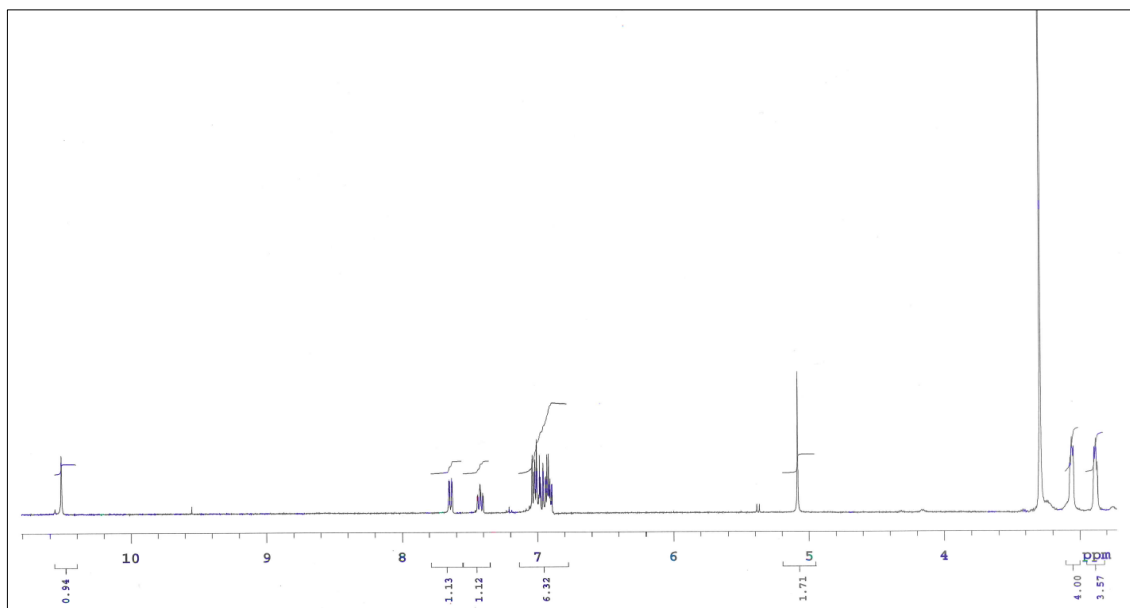
Figure 12. ^{1}H NMR spectrum of Compound **5b**

^{13}C NMR spectrum

δ ppm (400 MHz/DMSO-d_6): 49.08 (piperazine C_2+C_6); 49.57 (piperazine C_3+C_5); 69.53 (-N–$\underline{C}H_2$-N-); 109.00 (phenyl C_1); 115.09+115.31 (phenyl C_2'+ C_6'); 117.04 (phenyl C_3); 117.39+117.47 (phenyl C_3'+C_5'); 119.46 (phenyl C_5); 129.09 (phenyl C_6); 133.63 (phenyl C_4); 147.87+147.89 (phenyl C_1'); 154.90 (phenyl C_2); 156.40 ($\underline{C}$=N); 157.25+158.02 (phenyl $\underline{C}_4$'-F); 177.11 ($\underline{C}$=S) (Figure 13).

Figure 13. ^{13}C NMR spectrum of Compound **5b**

5-(2-Hydroxyphenyl)-3-{{4-[4-(trifluoromethyl)phenyl]piperazin-1-yl}methyl}-1,3,4-oxadiazole-2(3H)-thione (Compound 5c)
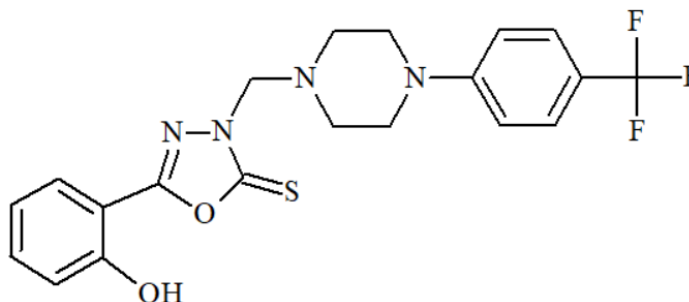
5-(2-Hydroxyphenyl)-1,3,4-oxadiazole-2(3H)-thione (0.01 mol, 1.94 g), 1-(4-trifluoro-methylphenyl)piperazine (0.01 mol, 2.30 g), formaldehyde (0.015 mol, 0.55 ml) in 15 ml ethanol were reacted according to general synthesis method at 3.1.2.4.

Yield (%)	:	60
Retention factor (R$_f$)	:	0.67 [Toluene: Acetone: Acetic acid (75:25:10)]
Physical appearance	:	White powder
Melting point (ºC)	:	161
Solubility	:	Highly soluble with acetone and DMSO. Practically insoluble in water

Elemental analysis

Molecular formula	:	C$_{20}$H$_{19}$F$_3$N$_4$O$_2$S
Molecular weight (g/mol)	:	436.45

	C	H	N	S
Calculated (%)	55.04	4.39	12.84	7.35
Found (%)	54.86	4.47	12.90	7.46

Spectral Analysis

Infrared (IR) spectrum

ν_{max} **(cm^{-1}) :** 3336 (O-H stretching); 2837 (aromatic C-H stretchings); 1618 (C=N stretching); 1598, 1577, 1522, 1490 (aromatic C=C stretchings); 1445 (O-H bending); 1334 (C-O stretching); 1256 (C=S stretching); 823 (4-(trifluoromethyl)phenyl C-H bendings); 746 (2-hydroxyphenyl C-H bendings) (Figure 14).

Figure 14. IR spectrum of Compound **5c**

^{1}H NMR spectrum

δ ppm (400 MHz/DMSO-d_6): 2.88 (4H, t, J=4.8 Hz, piperazine H$_2$+H$_6$); 3.28 (4H, t, J=4.8 Hz, piperazine H$_3$+H$_5$); 5.09 (2H, s, -N-C$\underline{H}_2$-N-); 6.93-6.97 (1H, m, phenyl H$_5$); 7.03 (3H, bd, J=8.8 Hz, phenyl H$_3$'+H$_5$'+H$_6$); 7.40-7.44 (1H, phenyl H$_4$); 7.46 (2H, bd, J=8.8 Hz, phenyl H$_2$'+H$_6$'); 7.64 (1H, dd, J=7.6 J'=1.6 Hz, phenyl H$_3$); 10.51 (1H, bs, -O$\underline{H}$) (Figure 15).
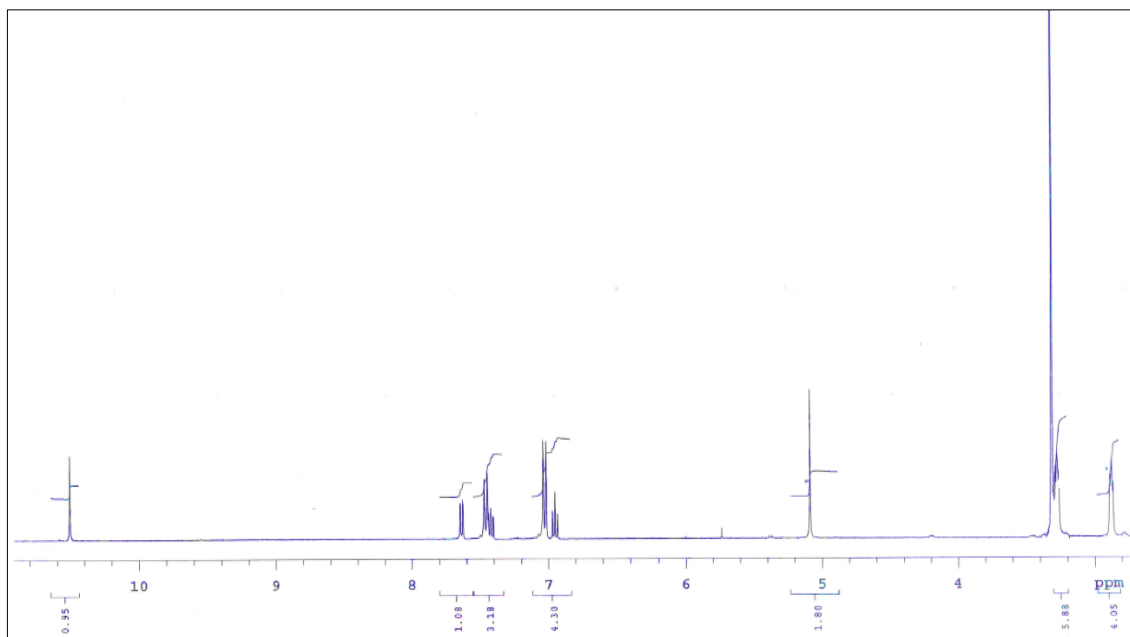
Figure 15. ^{1}H NMR spectrum of Compound **5c**

^{13}C NMR spectrum

δ ppm (400 MHz'DMSO-d_6): 46.98 (piperazine C_2+C_6); 49.31 (piperazine C_3+C_5); 69.49 (-N–$\underline{C}H_2$-N-); 108.99 (phenyl C_1); 114.32 (phenyl C_2'+ C_6'); 117.04 (phenyl C_3); 117.43+117.76+118.07+118.39 (phenyl C_4'-$\underline{C}F_3$); 119.44 (phenyl C_3'+ C_5'); 123.57 (phenyl C_6); 126.08+126.11 (phenyl $\underline{C_4}$'-CF_3); 129.12 (phenyl C_5); 133.65 (phenyl C_4); 153.16 (phenyl C_1'); 156.40 (phenyl C_2); 158.03 ($\underline{C}$=N); 177.09 ($\underline{C}$=S) (Figure 16).

Figure 16. ^{13}C NMR spectrum of Compound **5c**

82

5-(2-Hydroxyphenyl)-3-{{4-[3-(trifluoromethyl)phenyl]piperazin-1-yl}methyl}-1,3,4-oxadiazole-2(*3H*)-thione (Compound 5d)
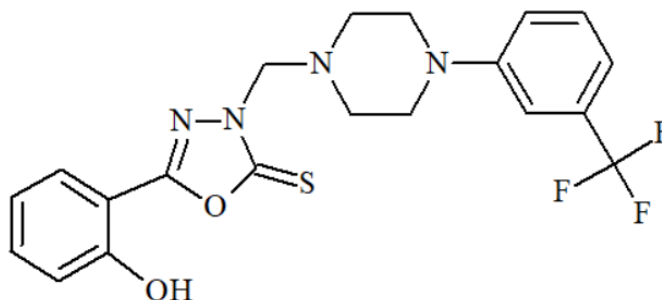
5-(2-Hydroxyphenyl)-1,3,4-oxadiazole-2(*3H*)-thione (0.01 mol, 1.94 g), 1-(3-trifluoro-methylphenyl)piperazine (0.01 mol, 2.30 g), formaldehyde (0.015 mol, 0.55 ml) in 15 ml ethanol were reacted according to general synthesis method at 3.1.2.4.

Yield (%)	: 30
Retention factor (R$_f$)	: 0.63 [Toluene: Acetone: Acetic acid (75:25:10)]
Physical appearance	: White powder
Melting point (ºC)	: 172
Solubility	: Highly soluble with acetone and DMSO. Practically insoluble in water

Elemental analysis

Molecular formula	: C$_{20}$H$_{19}$F$_3$N$_4$O$_2$S
Molecular weight (g/mol)	: 436.45

	C	H	N	S
Calculated (%)	55.04	4.39	12.84	7.35
Found (%)	54.91	4.29	12.79	7.42

Spectral Analysis

Infrared (IR) spectrum

ν_{max} **(cm^{-1}) :** 3348 (O-H stretching); 2961 (aromatic C-H stretchings); 1627 (C=N stretching); 1598, 1571, 1491 (aromatic C=C stretchings); 1450 (O-H bending); 1331 (C-O stretching); 1250 (C=S stretching); 849 (3-(trifluoromethyl)phenyl C-H bendings); 743 (2-hydroxyphenyl C-H bendings) (Figure 17).

Figure 17. IR spectrum of Compound **5d**

^{1}H NMR spectrum

δ ppm (400 MHz/DMSO-d_6): 2.89 (4H, t, J=4.8 Hz, piperazine H$_2$+H$_6$); 3.22 (4H, t, J=4.8 Hz, piperazine H$_3$+H$_5$); 5.09 (2H, s, -N-C$\underline{H}_2$-N-); 6.95 (1H, t, J=7.8 Hz, phenyl H$_5$'); 7.03 (2H, bd, J=8.4 Hz, phenyl H$_4$'+H$_6$'); 7.14 (1H, bs, phenyl H$_2$'); 7.18-7.23 (1H, m, phenyl H$_5$); 7.36 (1H, bd, J=8 Hz, phenyl H$_6$); 7.40-7.45 (1H, m, phenyl H$_4$); 7.64 (1H, dd, J=7.6 J'=1.6 Hz, phenyl H$_3$); 10.53 (1H, bs, -O$\underline{H}$) (Figure 18).
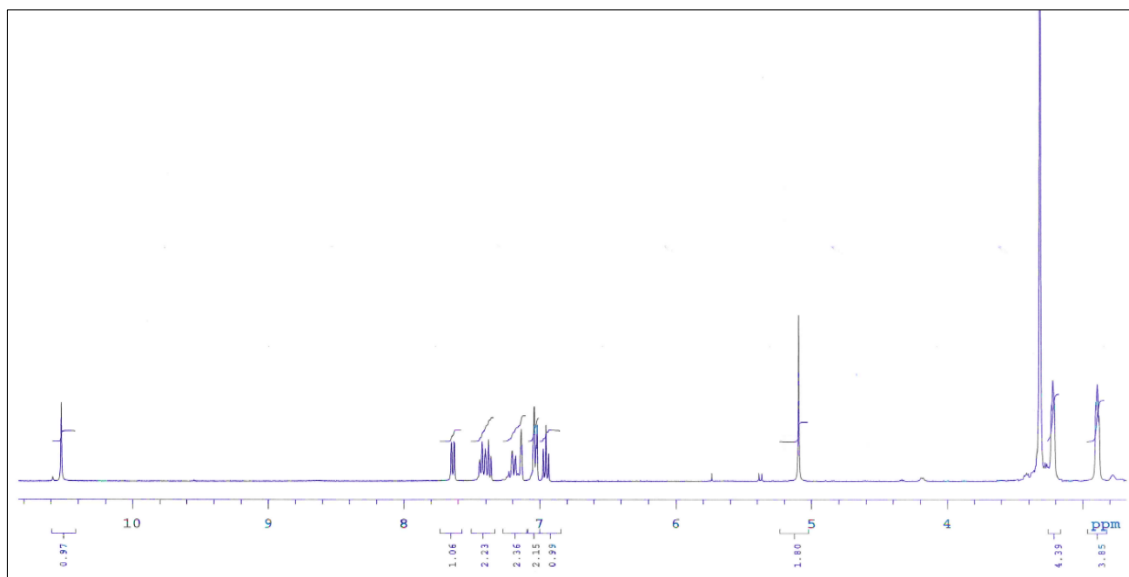
Figure 18. ^{1}H NMR spectrum of Compound **5d**

^{13}C NMR spectrum

δ ppm (400 MHz/DMSO-d_6): 47.60 (piperazine C_2+C_6); 49.36 (piperazine C_3+C_5); 69.44 (-N–$\underline{C}H_2$-N-); 108.93 (phenyl C_5); 111.03+111.07 (phenyl C_2'); 114.65+114.69 (phenyl C_4'); 117 (phenyl C_4); 118.91 (phenyl C_6'); 119.39 (phenyl C_6); 122.97+125.68 (phenyl C_3'-$\underline{C}F_3$); 129.11 (phenyl C_3); 129.84 (phenyl C_5'); 129.31+129.61+129.92 +130.22 (phenyl $\underline{C}_3$'-CF_3); 133.64 (phenyl C_1); 151.13 (phenyl C_1'); 156.37 (phenyl C_2); 157.92 ($\underline{C}$=N); 177.02 ($\underline{C}$=S) (Figure 19).
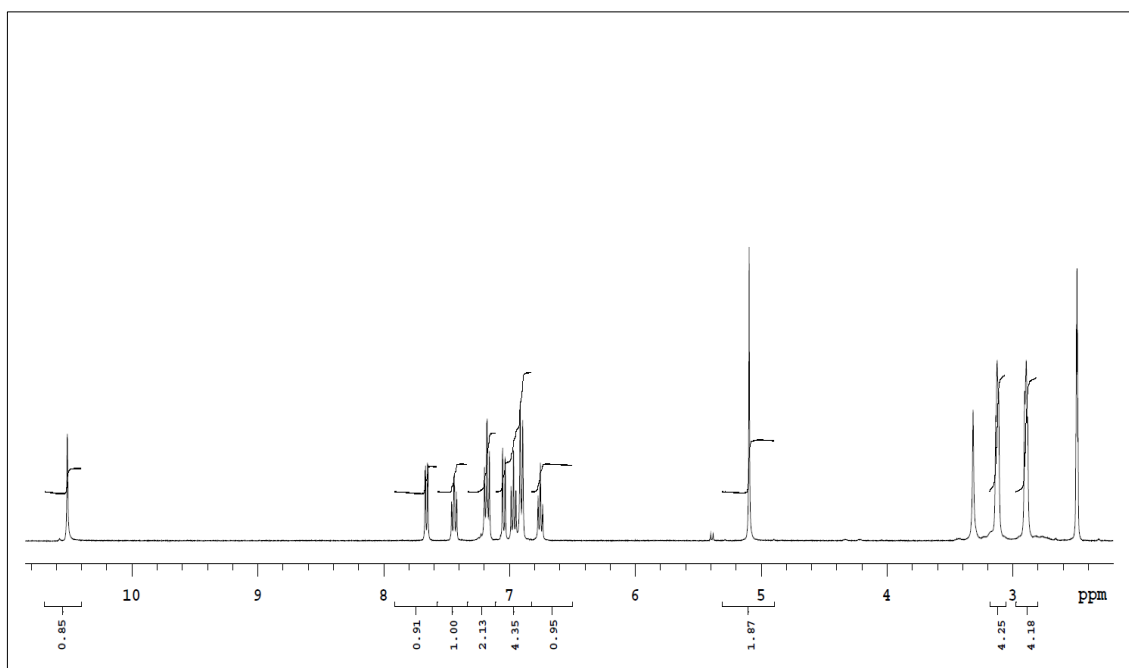

Figure 19. ^{13}C NMR spectrum of Compound **5d**

5-(2-Hydroxyphenyl)-3-{[4-(4-chlorophenyl)piperazin-1-yl]methyl}-1,3,4-oxadiazole-2(3H)-thione (Compound 5e)
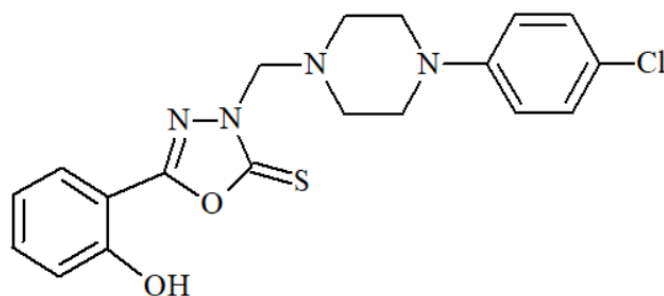
5-(2-Hydroxyphenyl)-1,3,4-oxadiazole-2(3H)-thione (0.01 mol, 1.94 g), 1-(4-chloro-phenyl)piperazine (0.01 mol, 1.96 g), formaldehyde (0.015 mol, 0.55 ml) in 15 ml ethanol were reacted according to general synthesis method at 3.1.2.4.

Yield (%)	: 56
Retention factor (R$_f$)	: 0.68 [Toluene: Acetone: Acetic acid (75:25:10)]
Physical appearance	: White powder
Melting point (ºC)	: 150
Solubility	: Highly soluble with acetone and DMSO. Practically insoluble in water

Elemental analysis

Molecular formula	: C$_{19}$H$_{19}$ClN$_4$O$_2$S
Molecular weight (g/mol)	: 402.89

	C	H	N	S
Calculated (%)	56.64	4.75	13.91	7.96
Found (%)	56.49	4.88	13.84	7.98

Spectral Analysis

Infrared (IR) spectrum

ν_{max} **(cm^{-1}) :** 3348 (O-H stretching); 2948 (aromatic C-H stretchings); 1622 (C=N stretching); 1596, 1569, 1496, 1489 (aromatic C=C stretchings); 1430 (O-H bending); 1323 (C-O stretching); 1235 (C=S stretching); 815 (4-chlorophenyl C-H bendings); 742 (2-hydroxyphenyl C-H bendings) (Figure 20).
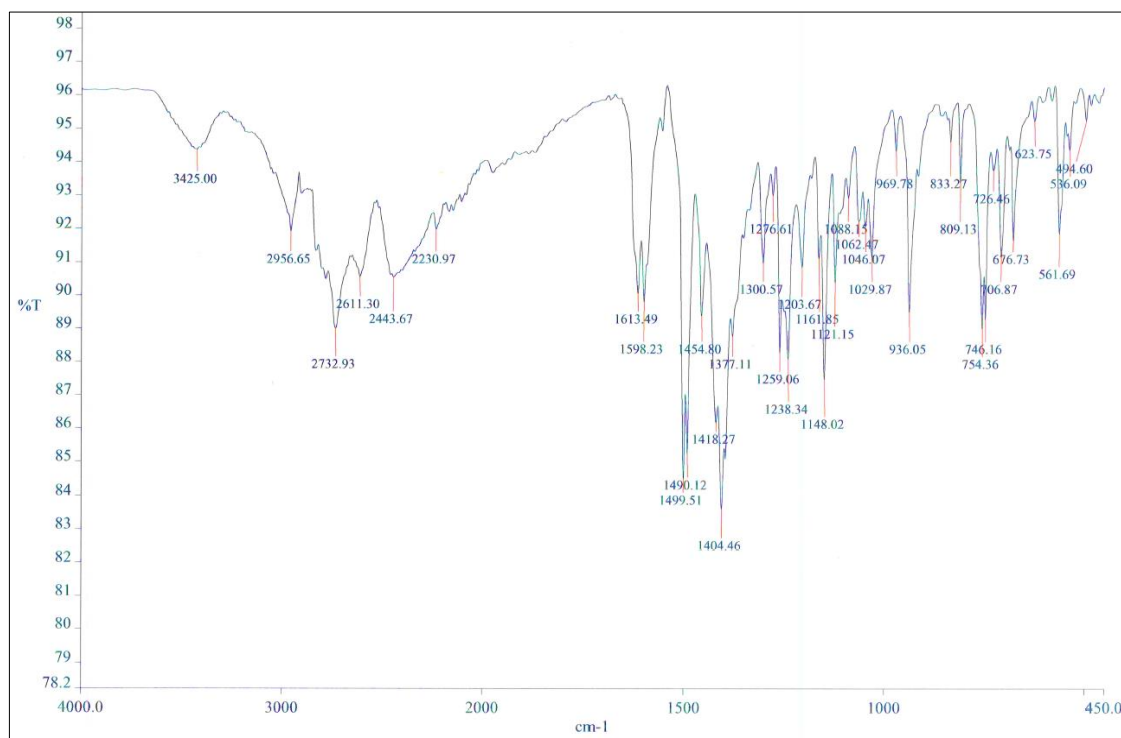

Figure 20. IR spectrum of Compound **5e**

^{1}H NMR spectrum

δ ppm (400 MHz/DMSO-d_6): 2.87 (4H, t, J=4.8 Hz, piperazine H_2+H_6); 3.12 (4H, t, J=4.8 Hz, piperazine H_3+H_5); 5.08 (2H, s, -N-C$\underline{H}_2$-N-); 6.91 (2H, bd, J=9 Hz, phenyl H_2'+H_6'); 6.94-6.98 (1H, m, phenyl H_5); 7.03 (1H, bd, J=8 Hz, phenyl H_6); 7.19 (2H, bd, J=9 Hz, phenyl H_3'+H_5'); 7.41-7.45 (1H, m, phenyl H_4); 7.64 (1H, dd, J=7.6 J'=1.6 Hz, phenyl H_3); 10.52 (1H, s, -O$\underline{H}$) (Figure 21).
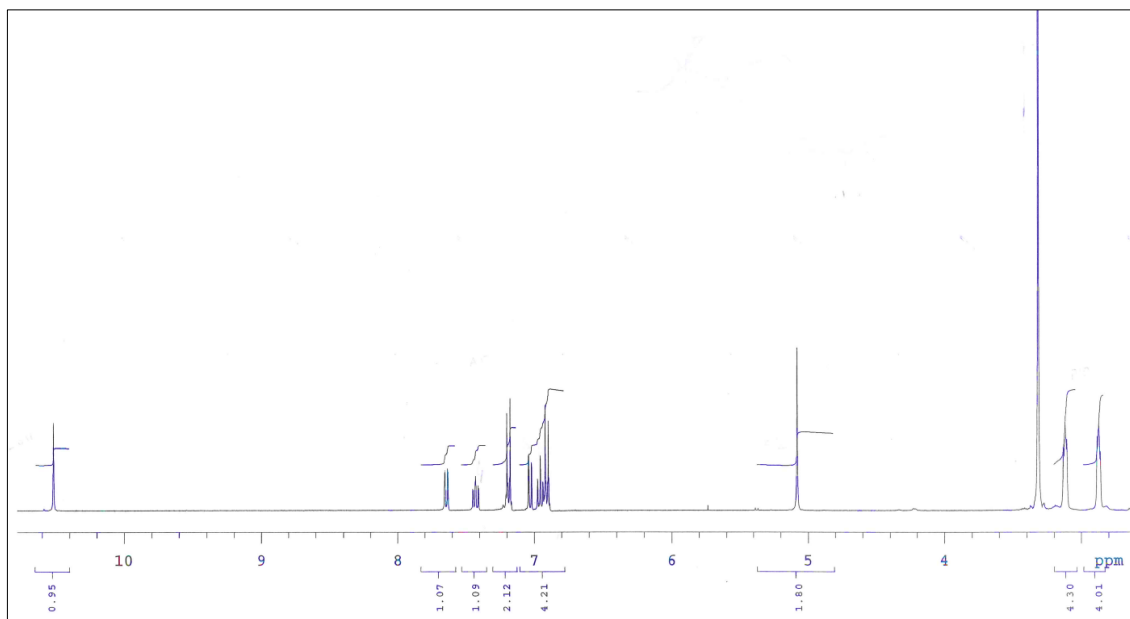
Figure 21. ^{1}H NMR spectrum of Compound **5e**

^{13}C NMR spectrum

δ ppm (400 MHz/DMSO-d_6): 48.06 (piperazine C_2+C_6); 49.42 (piperazine C_3+C_5); 69.51 (-N–$\underline{C}H_2$-N-); 108.99 (phenyl C_5); 117.52 (phenyl C_2'+C_6'+C_4); 119.44 (phenyl C_6); 122.47 (phenyl C_4'); 128.55 (phenyl C_3'+C_5'); 129.15 (phenyl C_3); 129.15 (phenyl C_3); 133.67 (phenyl C_1); 149.75 (phenyl C_1'); 156.41 (phenyl C_2); 157.97 ($\underline{C}$=N); 177.07 ($\underline{C}$=S) (Figure 22).
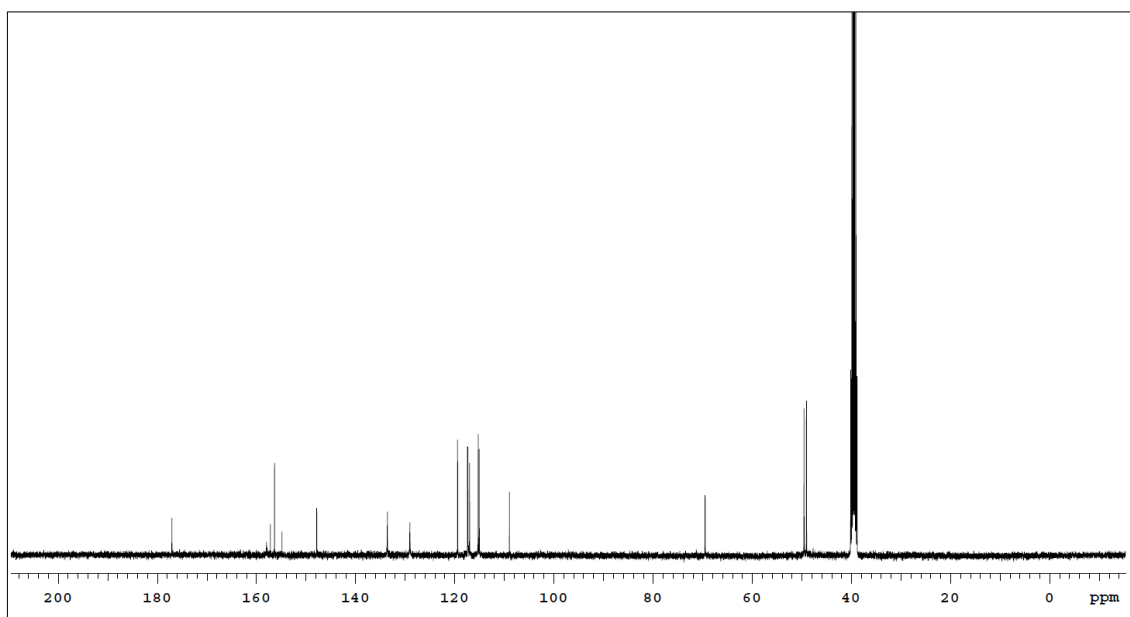

Figure 22. ^{13}C NMR spectrum of Compound **5e**

5-(2-Hydroxyphenyl)-3-{[4-(2-chlorophenyl)piperazin-1-yl]methyl}-1,3,4-oxadiazole-2(*3H*)-thione (Compound 5f)
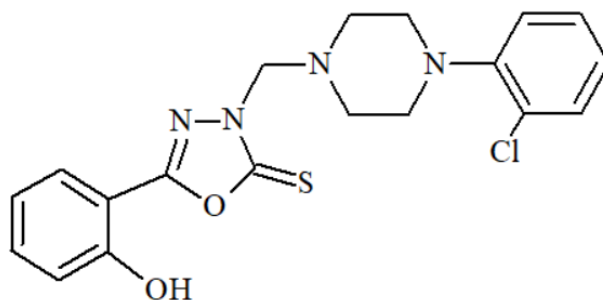
5-(2-Hydroxyphenyl)-1,3,4-oxadiazole-2(*3H*)-thione (0.01 mol, 1.94 g), 1-(2-chloro-phenyl)piperazine monohydrochloride (0.01 mol, 2.33 g), formaldehyde (0.015 mol, 0.55 ml) in 15 ml ethanol were reacted according to general synthesis method at 3.1.2.4.

Yield (%)	: 32
Retention factor (R$_f$)	: 0.67 [Toluene: Acetone: Acetic acid (75:25:10)]
Physical appearance	: White powder
Melting point (ºC)	: 180
Solubility	: Highly soluble with acetone and DMSO. Practically insoluble in water

Elemental analysis

Molecular formula	: C$_{19}$H$_{19}$ClN$_4$O$_2$S
Molecular weight (g/mol)	: 402.89

	C	H	N	S
Calculated (%)	56.64	4.75	13.91	7.96
Found (%)	56.71	4.88	13.88	8.05

Spectral Analysis

Infrared (IR) spectrum

v_{max} (cm^{-1}) : 3435 (O-H stretching); 3012 (aromatic C-H stretchings); 1615 (C=N stretching); 1603, 1560, 1484 (aromatic C=C stretchings); 1435 (O-H bending); 1311 (C-O stretching); 1264 (C=S stretching); 772 (2-chlorophenyl C-H bendings); 743 (2-hydroxyphenyl C-H bendings) (Figure 23).
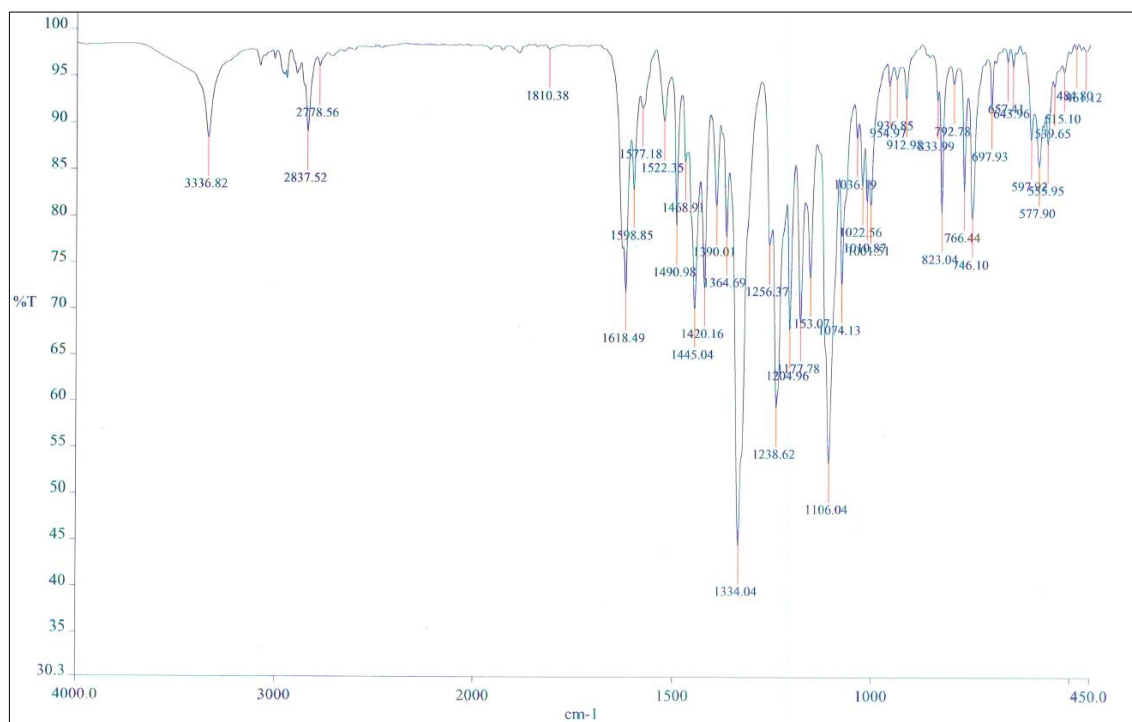

Figure 23. IR spectrum of Compound **5f**

^{1}H NMR spectrum

δ ppm (400 MHz/DMSO-d_6): 2.93 (4H, d, J=4.8 Hz, piperazine H$_2$+H$_6$); 2.97 (4H, d, J=4.8 Hz, piperazine H$_3$+H$_5$); 5.1 (2H, s, -N-C$\underline{H}_2$-N-); 6.98 (1H, t, J=7.6 Hz, phenyl H$_5$'); 7.00-7.04 (1H, m, phenyl H$_5$); 7.05 (1H, bd, J=8 Hz, phenyl H$_6$'); 7.14 (1H, dd, J=7.8 J'=1.4 Hz, phenyl H$_6$); 7.25-7.30 (1H, m, phenyl H$_4$'); 7.37 (1H, dd, J=8 J'=1.2 Hz, phenyl H$_3$'); 7.43-7.47 (1H, m, phenyl H$_4$); 7.68 (1H, dd, J=7.6 J'=1.6 Hz, phenyl H$_3$); 10.54 (1H, bs, -O$\underline{H}$) (Figure 24).
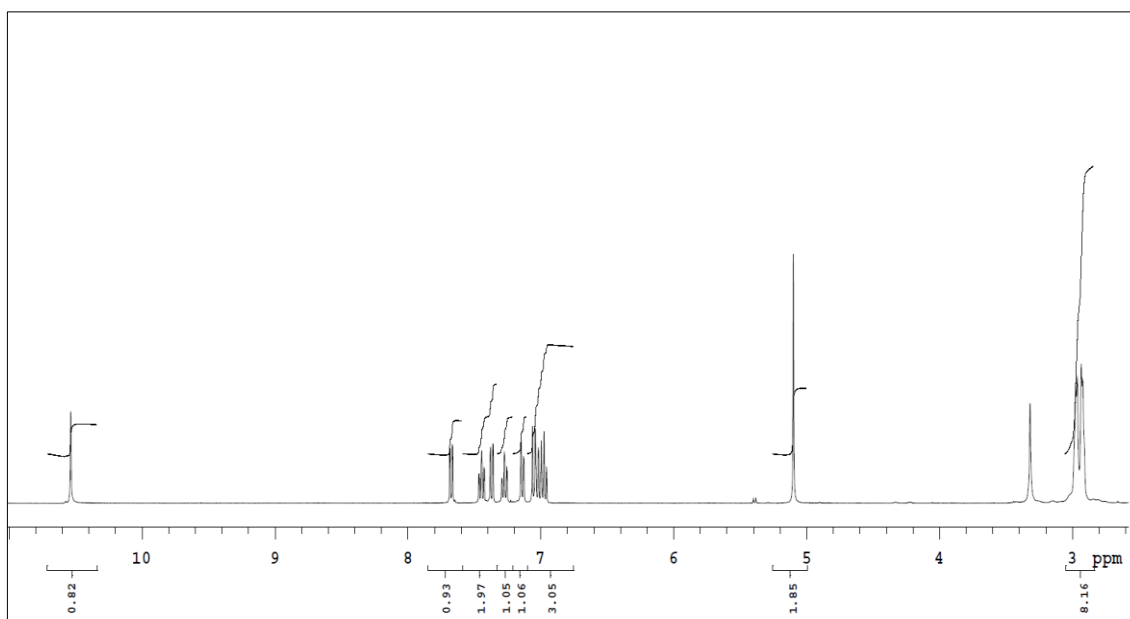
Figure 24. ^{1}H NMR spectrum of Compound **5f**

^{13}C NMR spectrum

δ ppm (400 MHz/DMSO-d_6): 49.82 (piperazine C_2+C_6); 50.78 (piperazine C_3+C_5); 69.69 (-N–$\underline{C}H_2$-N-); 108.98 (phenyl C_5); 117.07 (phenyl C_4); 119.48 (phenyl C_6); 120.90 (phenyl $C_6^{'}$); 123.95 (phenyl C_4'); 127.61 (phenyl C_2'); 128.01 (phenyl $C_5^{'}$); 129.11 (phenyl C_3); 130.27 (phenyl C_3'); 133.67 (phenyl C_1); 148.86 (phenyl $C_1^{'}$); 156.42 (phenyl C_2); 157.99 ($\underline{C}$=N); 177.09 ($\underline{C}$=S) (Figure 25).
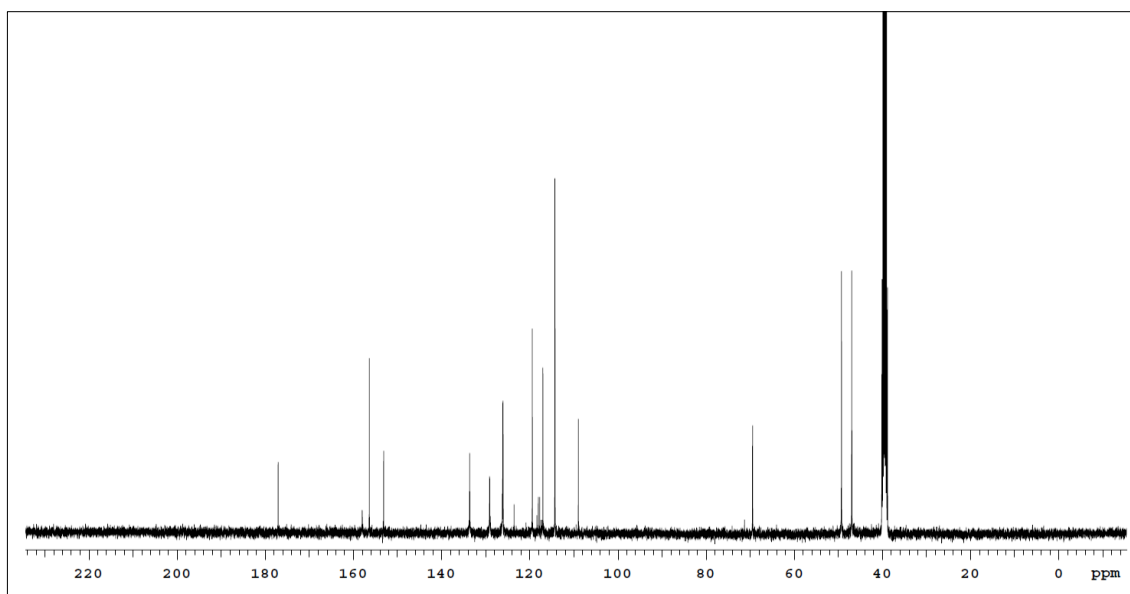

Figure 25. ^{13}C NMR spectrum of Compound **5f**

5-(2-Hydroxyphenyl)-3-{[4-(3,4-dichlorophenyl)piperazin-1-yl]methyl}-1,3,4-oxadi-azole-2(*3H*)-thione (Compound 5g)
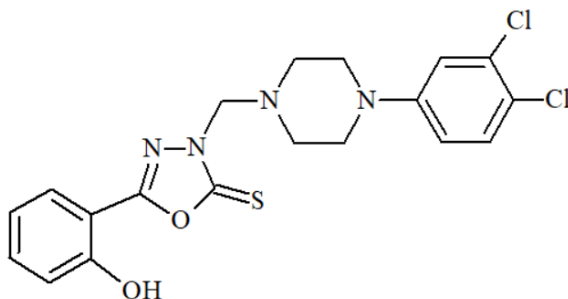
5-(2-Hydroxyphenyl)-1,3,4-oxadiazole-2(*3H*)-thione (0.01 mol, 1.94 g), 1-(3,4-dichloro-phenyl)piperazine (0.01 mol, 2.31 g), formaldehyde (0.015 mol, 0.55 ml) in 15 ml ethanol were reacted according to general synthesis method at 3.1.2.4.

Yield (%)	: 75
Retention factor (R$_f$)	: 0.65 [Toluene: Acetone: Acetic acid (75:25:10)]
Physical appearance	: White powder
Melting point (°C)	: 172
Solubility	: Highly soluble with acetone and DMSO. Practically insoluble in water

Elemental analysis

Molecular formula	: C$_{19}$H$_{18}$Cl$_2$N$_4$O$_2$S
Molecular weight (g/mol)	: 437.34

	C	H	N	S
Calculated (%)	52.18	4.15	12.81	7.33
Found (%)	51.98	4.02	12.83	7.39

Spectral Analysis

Infrared (IR) spectrum

v_{max} **(cm^{-1}) :** 3336 (O-H stretching); 2837 (aromatic C-H stretchings); 1618 (C=N stretching); 1598, 1577, 1522, 1490 (aromatic C=C stretchings); 1445 (O-H bending); 1334 (C-N stretching); 1256 (C=S stretching); 823 (3,4-dichlorophenyl C-H bendings); 746 (2-hydroxyphenyl C-H bendings) (Figure 26).
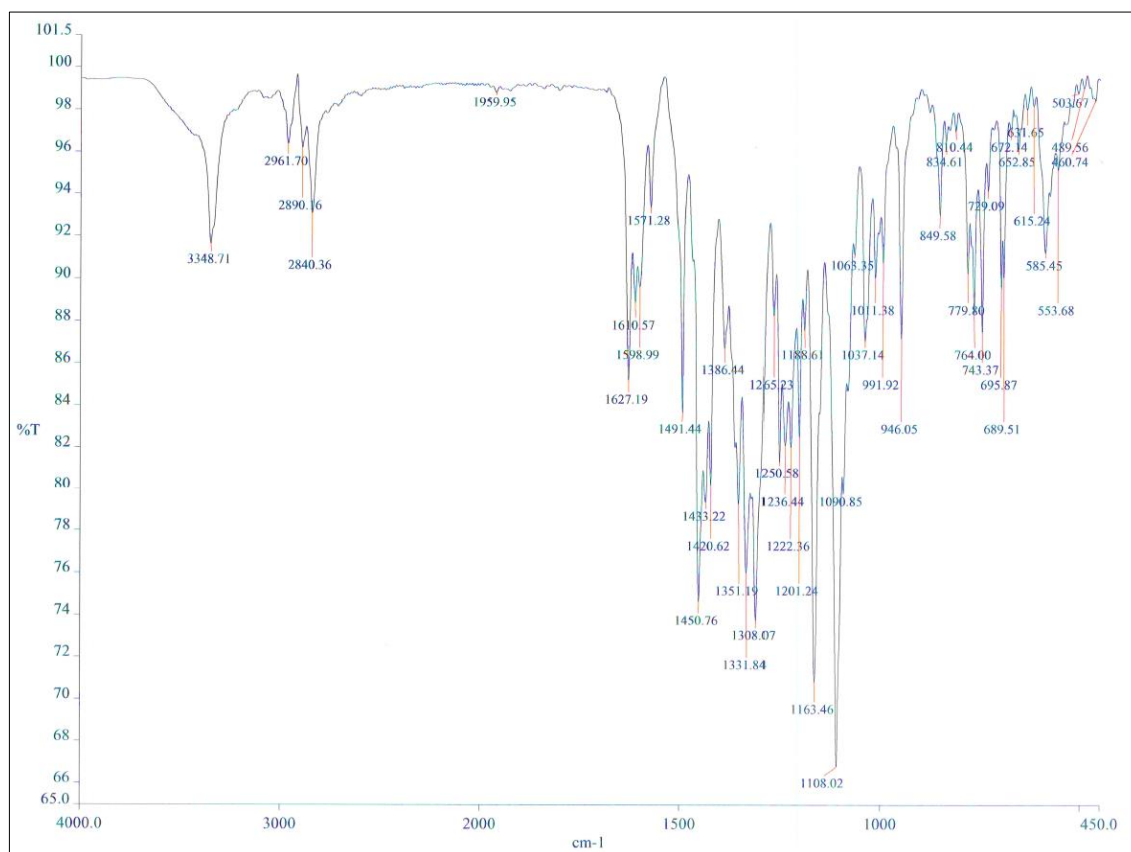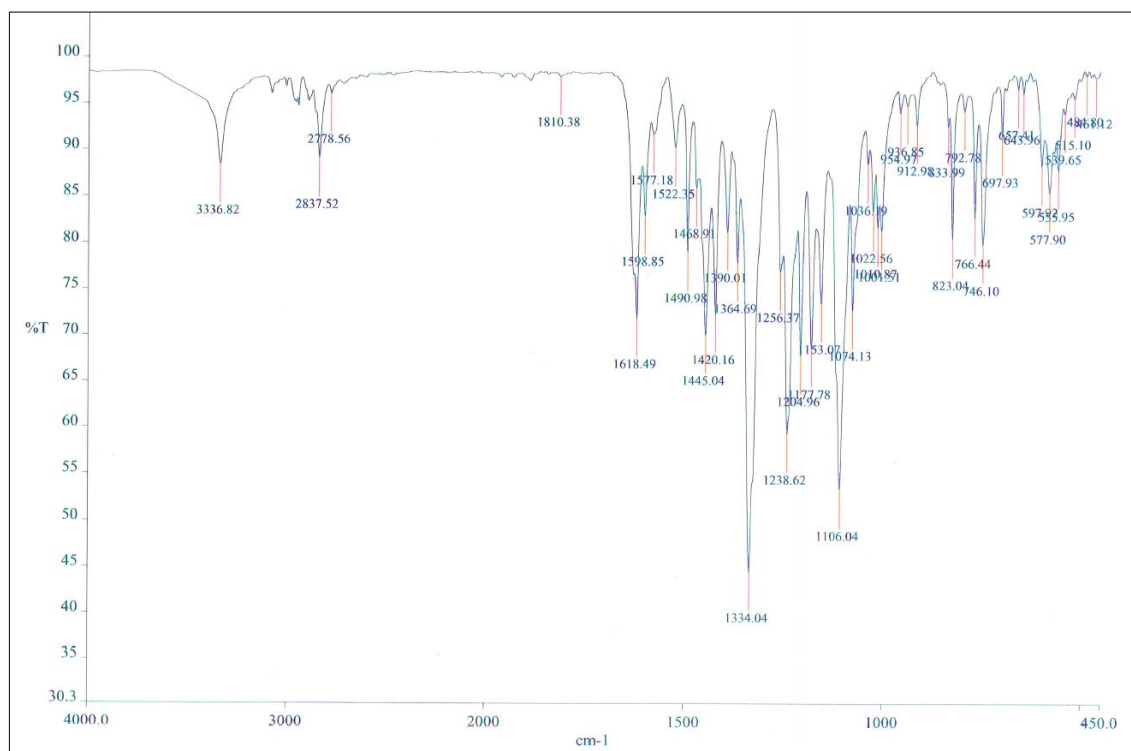

Figure 26. IR spectrum of Compound **5g**

^{1}H NMR spectrum

δ ppm (400 MHz/DMSO-d_6): 2.88 (4H, t, J=5 Hz, piperazine H$_2$+H$_6$); 3.39 (4H, t, J=5 Hz, piperazine H$_3$+H$_5$); 5.1 (2H, s, -N-C$\underline{H}_2$-N-); 6.92 (1H, dd, J=9 J'=3 Hz, phenyl H$_6$'); 6.95-6.99 (2H, m, phenyl H$_4$+H$_5$); 7.03 (1H, bd, J=8 Hz, phenyl H$_5$'); 7.13 (1H, d, J=2.4 Hz, phenyl H$_2$'); 7.37 (1H, d, J=8.8 Hz, phenyl H$_6$); 7.46 (1H, d, J=9.2 Hz, phenyl H$_3$); 10.61 (1H, bs, -O$\underline{H}$) (Figure 27).
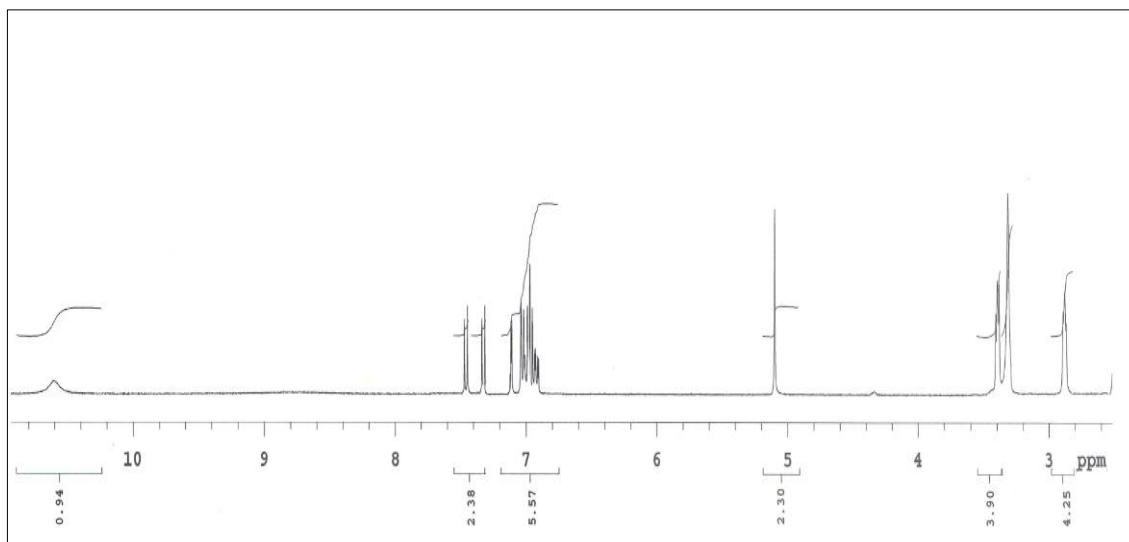
Figure 27. ^{1}H NMR spectrum of Compound **5g**

^{13}C NMR spectrum

δ ppm (400 MHz/DMSO-d_6): 42.43 (piperazine C_2+C_6); 44.85 (piperazine C_3+C_5); 69.40 (-N–$\underline{C}H_2$-N-); 109.31 (phenyl C_5); 115.45 (phenyl C_4); 115.84 (phenyl C_6); 116.33 (phenyl $C_6^{'}$); 116.62 (phenyl C_5'); 116.98 (phenyl C_2'); 119.49 (phenyl C_3); 120.78 (phenyl $C_4^{'}$); 130.34 (phenyl C_3'); 130.56 (phenyl C_1); 131.57 (phenyl $C_1^{'}$); 149.61 (phenyl C_2); 150.61 ($\underline{C}$=N); 155.91 ($\underline{C}$=S) (Figure 28).
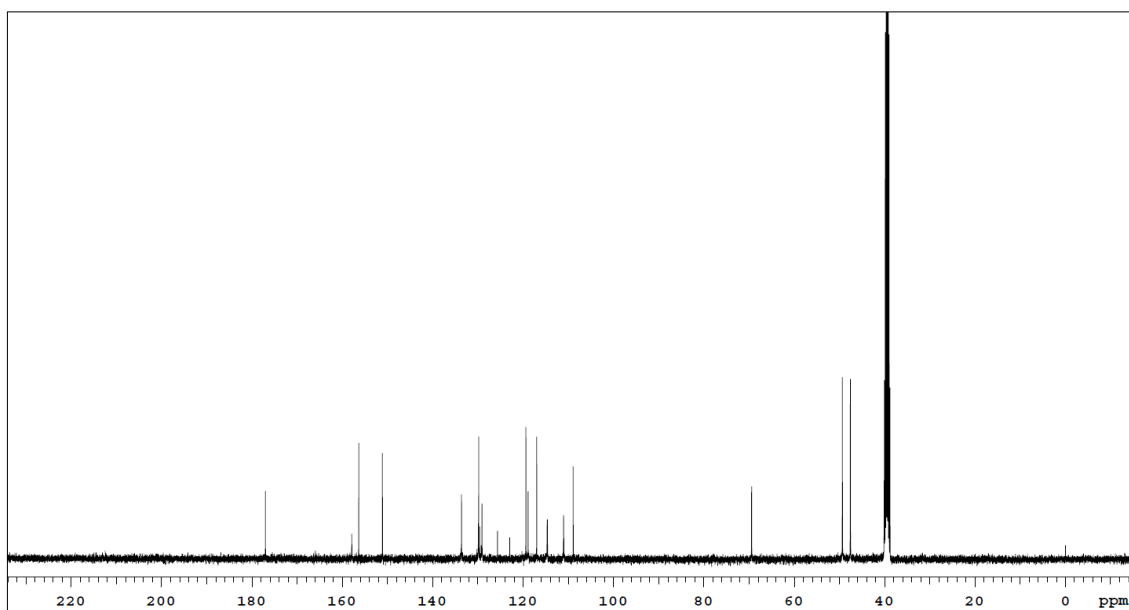

Figure 28. ^{13}C NMR spectrum of Compound **5g**

5-(2-Hydroxyphenyl)-3-{[4-(2,3-dichlorophenyl)piperazin-1-yl]methyl}-1,3,4-oxadiazole-2(*3H*)-thione (Compound 5h)
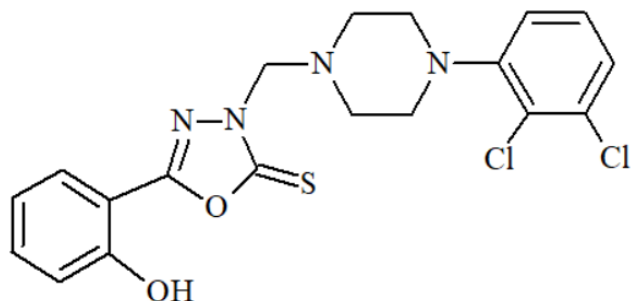
5-(2-Hydroxyphenyl)-1,3,4-oxadiazole-2(*3H*)-thione (0.01 mol, 1.94 g), 1-(2,3-dichlorophenyl)piperazine hydrochloride (0.01 mol, 2.67 g), formaldehyde (0.015 mol, 0.55 ml) in 15 ml ethanol were reacted according to general synthesis method at 3.1.2.4.

Yield (%)	:	40
Retention factor (R$_f$)	:	0.63 [Toluene: Acetone: Acetic acid (75:25:10)]
Physical appearance	:	White powder
Melting point (°C)	:	165
Solubility	:	Highly soluble with acetone and DMSO. Practically insoluble in water

Elemental analysis

Molecular formula	:	C$_{19}$H$_{18}$Cl$_2$N$_4$O$_2$S
Molecular weight (g/mol)	:	437.34

	C	H	N	S
Calculated (%)	52.18	4.15	12.81	7.33
Found (%)	51.75	4.17	13.52	7.07

Spectral Analysis

Infrared (IR) spectrum

ν_{max} **(cm^{-1}) :** 3348 (O-H stretching); 2961 (aromatic C-H stretchings); 1627 (C=N stretching); 1610, 1598, 1571, 1491 (aromatic C=C stretchings); 1450 (O-H bending); 1308 (C-O stretching); 1265 (C=S stretching); 849 (2,3-dichlorophenyl C-H bendings); 743 (2-hydroxyphenyl C-H bendings) (Figure 29).
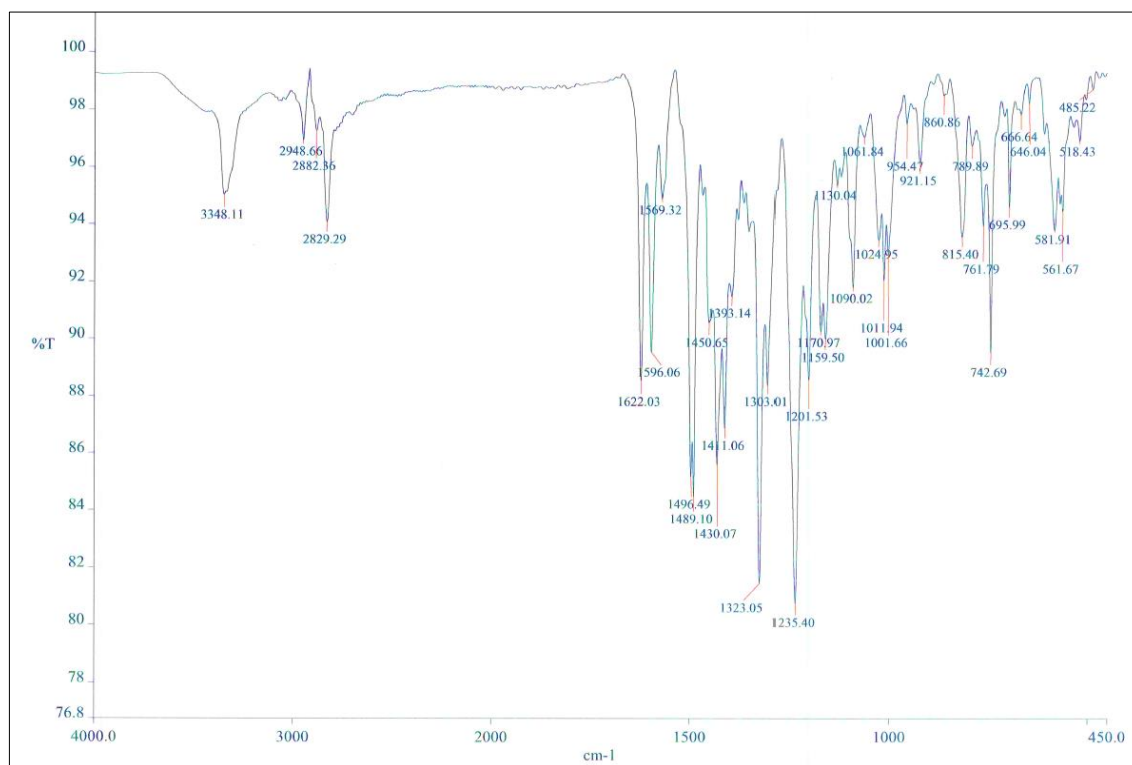

Figure 29. IR spectrum of Compound **5h**

^{1}H NMR spectrum

δ ppm (400 MHz/DMSO-d_6): 2.93-2.99 (8H, m, piperazine H$_2$+H$_3$+H$_5$+H$_6$); 5.1 (2H, s, -N-C$\underline{H}_2$-N-); 6.98 (1H, t, J=7.4 Hz, phenyl H$_5$'); 7.05 (1H, bd, J=8 Hz, phenyl H$_4$'); 7.12-7.16 (1H, m, phenyl H$_5$); 7.27-7.32 (2H, m, phenyl H$_6$+H$_6$'); 7.43-7.47 (1H, m, phenyl H$_4$); 7.67 (1H, dd, J=7.6 J'=1.6 Hz, phenyl H$_3$); 10.54 (1H, bs, -O$\underline{H}$) (Figure 30).
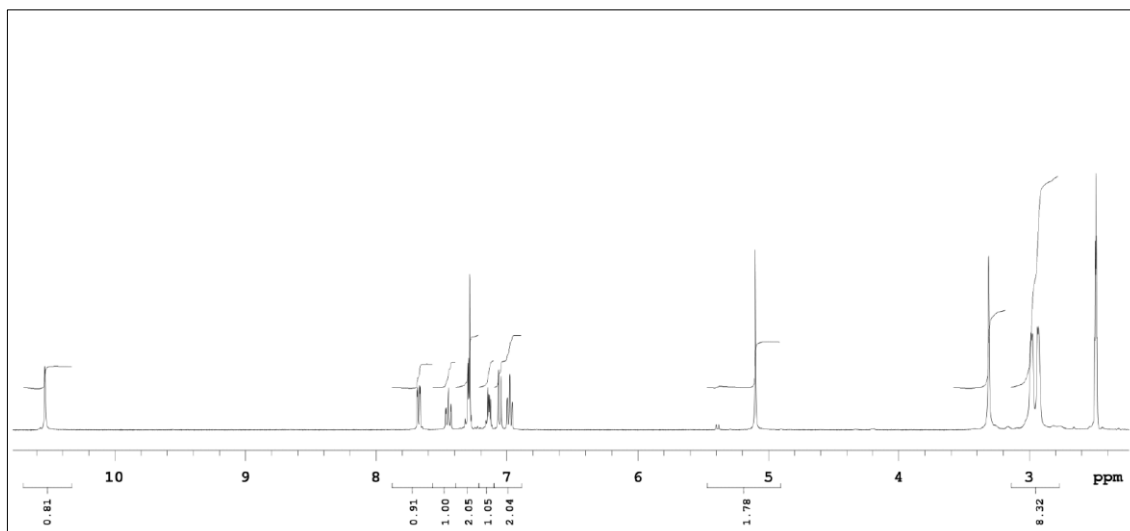
Figure 30. ^{1}H NMR spectrum of Compound **5h**

^{13}C NMR spectrum

δ ppm (400 MHz/DMSO-d_6): 49.77 (piperazine C_2+C_6); 50.87 (piperazine C_3+C_5); 69.65 (-N–$\underline{C}H_2$-N-); 108.99 (phenyl C_1); 117.07 (phenyl C_3); 119.49 (phenyl C_5); 119.67 (phenyl $C_2^{'}$); 124.49 (phenyl C_6'); 126.06 (phenyl C_6); 128.40 (phenyl $C_4^{'}$); 129.09 (phenyl C_5'); 132.56 (phenyl C_4); 133.65 (phenyl C_3'); 151.03 (phenyl C_1'); 156.41 (phenyl C_2); 158.06 ($\underline{C}$=N); 177.11 ($\underline{C}$=S) (Figure 31).

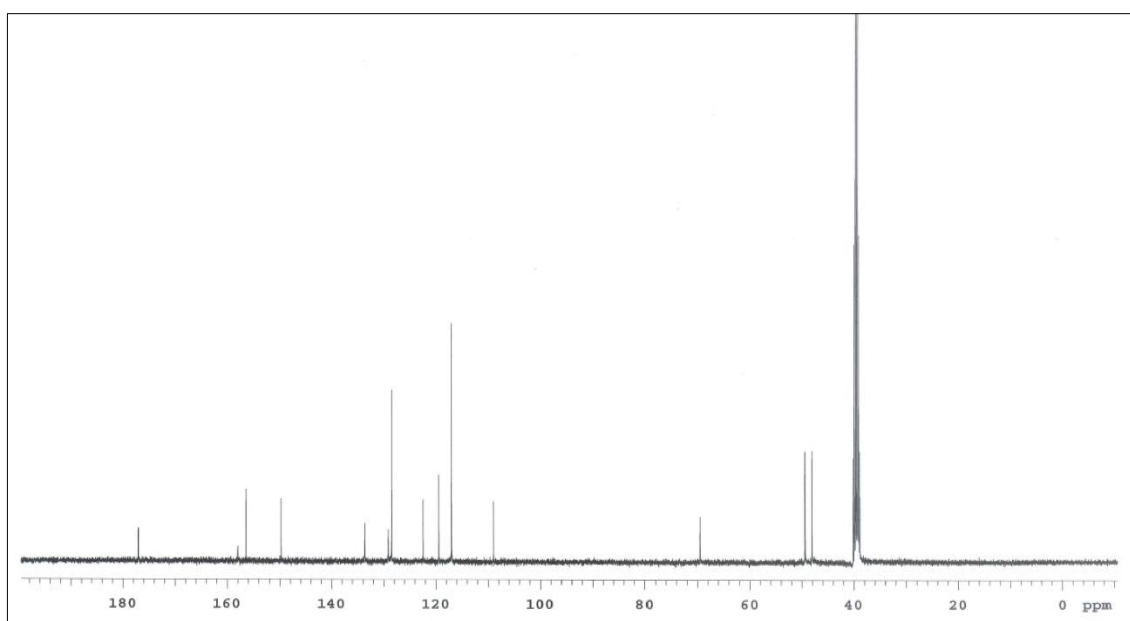**Figure 31.** ^{13}C NMR spectrum of Compound **5h**

5-(2-Hydroxyphenyl)-3-[4-(4-methylphenyl)piperazin-1-yl]methyl-1,3,4-oxadiazole-2(_3H_)-thione (Compound 5i)
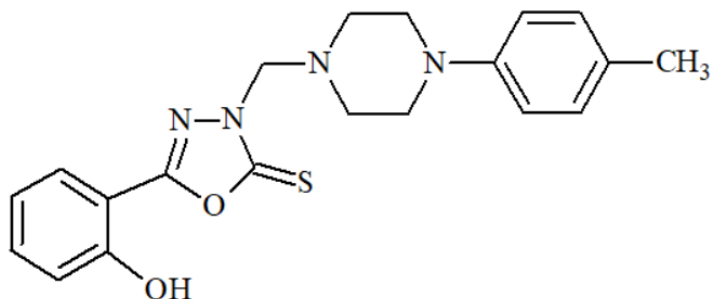
5-(2-Hydroxyphenyl)-1,3,4-oxadiazole-2(_3H_)-thione (0.01 mol, 1.94 g), 1-(4-methyl-phenyl)piperazine (0.01 mol, 1.76 g), formaldehyde (0.015 mol, 0.55 ml) in 15 ml ethanol were reacted according to general synthesis method at 3.1.2.4.

Yield (%)	:	51
Retention factor (R$_f$)	:	0.62 [Toluene: Acetone: Acetic acid (75:25:10)]
Physical appearance	:	White powder
Melting point (ºC)	:	155
Solubility	:	Highly soluble with acetone and DMSO. Practically insoluble in water

Elemental analysis

Molecular formula	:	C$_{20}$H$_{22}$N$_4$O$_2$S
Molecular weight (g/mol)	:	382.48

	C	H	N	S
Calculated (%)	62.80	5.80	14.65	8.38
Found (%)	62.87	5.96	14.56	8.41

Spectral Analysis

Infrared (IR) spectrum

ν_{max} **(cm^{-1}) :** 3342 (O-H stretching); 3028 (aromatic C-H stretchings); 1624 (C=N stretching); 1597, 1514, 1498 (aromatic C=C stretchings); 1445 (O-H bending); 1324 (C-O stretching); 1260 (C=S stretching); 767 (4-methylphenyl C-H bendings); 745 (2-hydroxyphenyl C-H bendings) (Figure 32).
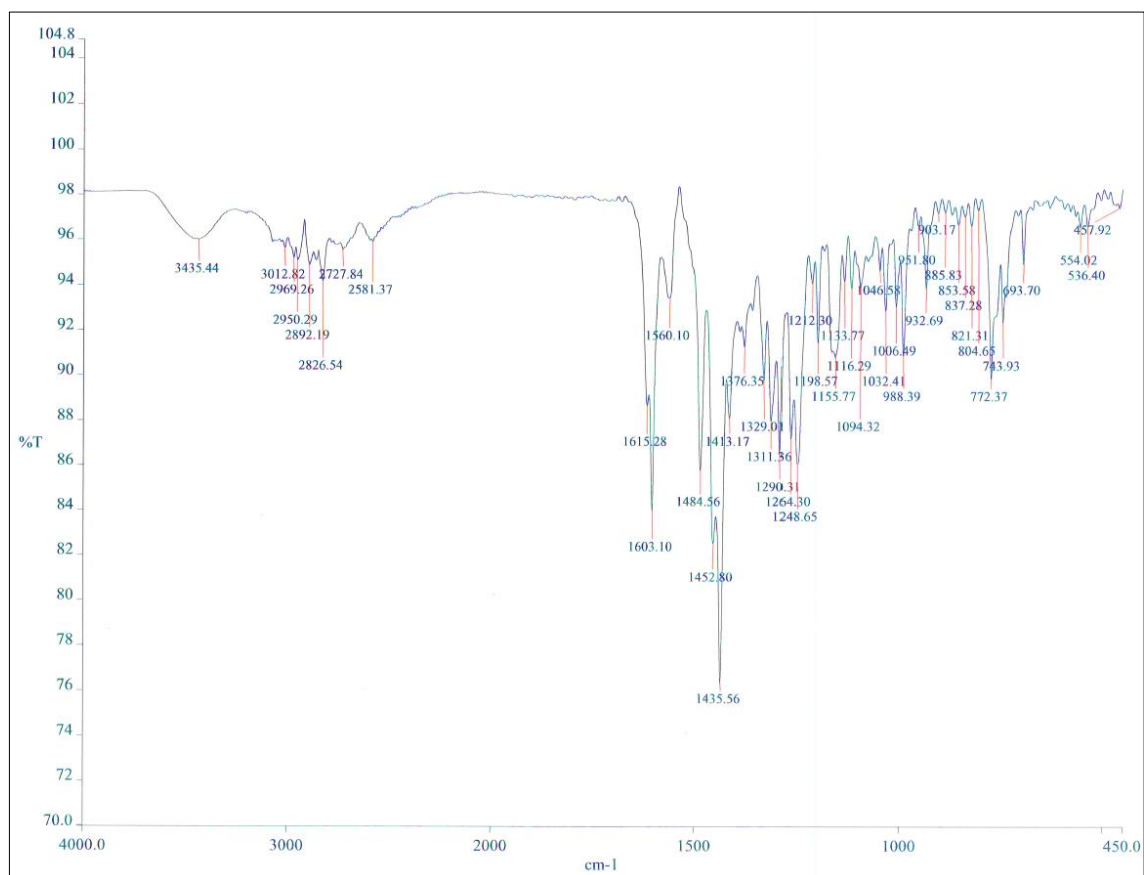

Figure 32. IR spectrum of Compound **5i**

^{1}H NMR spectrum

δ ppm (400 MHz/DMSO-d_6): 2.16 (phenyl -C$\underline{H}_3$); 2.87 (4H, d, J=4.8 Hz, piperazine H$_2$+H$_6$); 3.05 (4H, d, J=4.8 Hz, piperazine H$_3$+H$_5$); 5.08 (2H, s, -N-C$\underline{H}_2$-N-); 6.79 (2H, d, J=8.6 Hz, phenyl H$_3$'+H$_5$'); 6.94-6.97 (1H, m, phenyl H$_5$); 6.98 (1H, bd, J=8 Hz, phenyl H$_6$); 7.03 (2H, d, J=8.6 Hz, phenyl H$_2$'+H$_6$'); 7.39-7.44 (1H, m, phenyl H$_4$); 7.34 (1H, dd, J=7.6 J'=1.6 Hz, phenyl H$_3$); 10.53 (1H, bs, -O$\underline{H}$) (Figure 33).
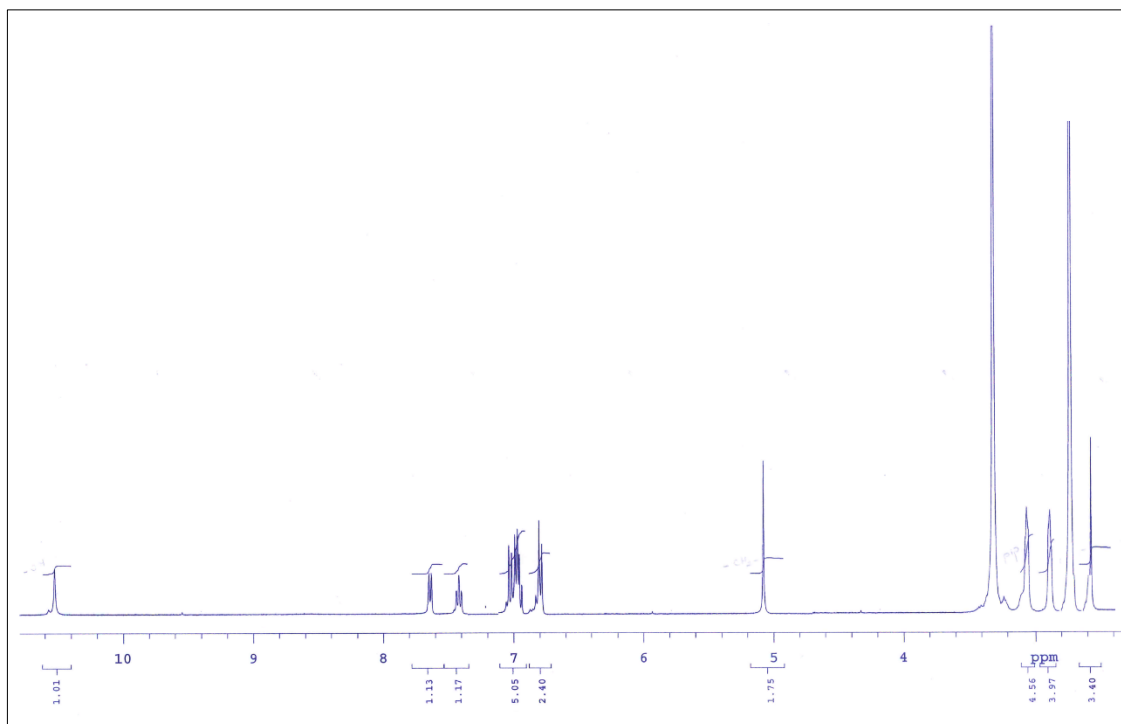
Figure 33. ^{1}H NMR spectrum of Compound **5i**

^{13}C NMR spectrum

δ ppm (400 MHz/DMSO-d_6): 19.94 (phenyl -$\underline{C}$H$_3$); 48.71 (piperazine C$_2$+C$_6$); 49.53 (piperazine C$_3$+C$_5$); 69.52 (-N–$\underline{C}$H$_2$-N-); 108.93 (phenyl C$_5$); 115.85 (phenyl C$_2$'+ C$_6$'); 116.99 (phenyl C$_4$); 119.39 (phenyl C$_6$); 127.75 (phenyl C$_4$'); 129.08 (phenyl C$_3$); 129.23 (phenyl C$_3$'+ C$_5$'); 133.60 (phenyl C$_1$); 148.84 (phenyl C$_1$'); 156.35 (phenyl C$_2$); 157.89 ($\underline{C}$=N); 177.01 ($\underline{C}$=S) (Figure 34).
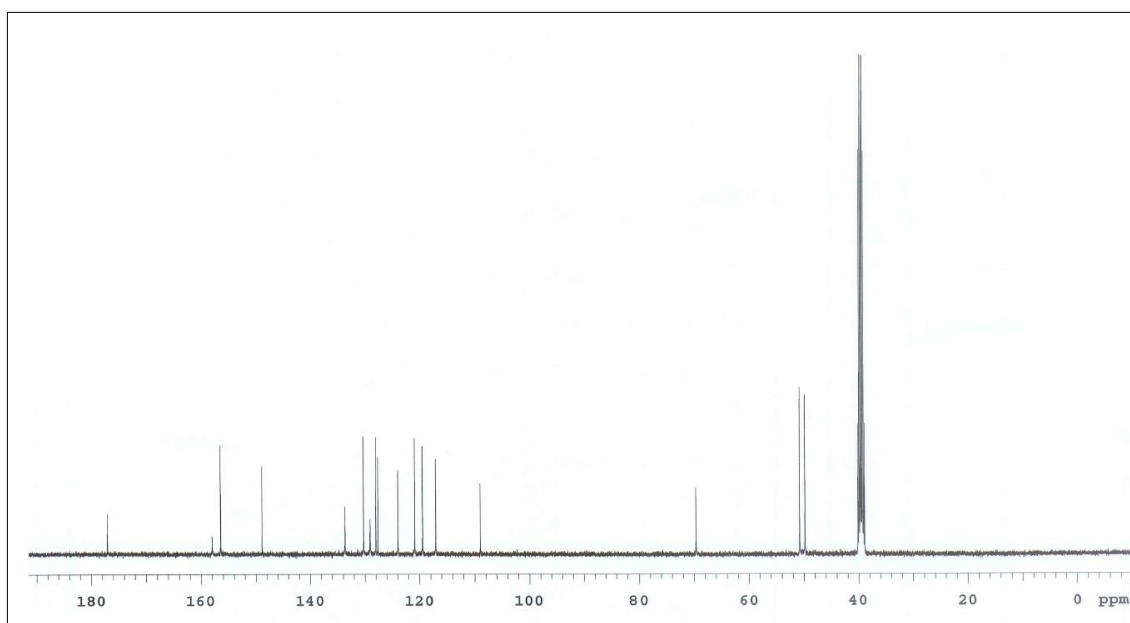

Figure 34. ^{13}C NMR spectrum of Compound **5i**

5-(2-Hydroxyphenyl)-3-{[4-(2,3-dimethylphenyl)piperazin-1-yl]methyl}-1,3,4-oxadi-azole-2(*3H*)-thione (Compound 5j)
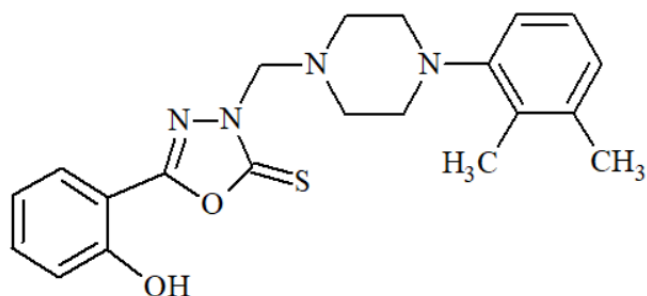
5-(2-Hydroxyphenyl)-1,3,4-oxadiazole-2(*3H*)-thione (0.01 mol, 1.94 g), 1-(2,3-xyxyl)-piperazine (0.01 mol, 1.90 g), formaldehyde (0.01 mol, 0.55 ml) in 15 ml ethanol were reacted according to general synthesis method at 3.1.2.4.

Yield (%)	: 66
Retention factor (R$_f$)	: 0.63 [Toluene: Acetone: Acetic acid (75:25:10)]
Physical appearance	: White powder
Melting point (ºC)	: 133
Solubility	: Highly soluble with acetone and DMSO. Practically insoluble in water

Elemental analysis

Molecular formula	: C$_{21}$H$_{24}$N$_4$O$_2$S
Molecular weight (g/mol)	: 396.50

	C	H	N	S
Calculated (%)	63.61	6.10	14.13	8.09
Found (%)	62.98	6.03	14.37	8.27

Spectral Analysis

Infrared (IR) spectrum

ν_{max} **(cm^{-1}) :** 3364 (O-H stretching); 2948 (aromatic C-H stretchings); 1630 (C=N stretching); 1598, 1492 (aromatic C=C stretchings); 1450 (O-H bending); 1323 (C-O stretching); 1255 (C=S stretching); 746 (2-hydroxyphenyl C-H bendings) (Figure 35).

Figure 35. IR spectrum of Compound **5j**

^{1}H NMR spectrum

δ ppm (400 MHz/DMSO-d_6): 2.09+2.17 (6H, s, phenyl –C$\underline{H}_3$); 2.79-2.91 (8H, m, piperazine H$_2$+H$_3$+H$_5$+H$_6$); 5.1 (2H, s, -N-C$\underline{H}_2$-N-); 6.86 (1H, t, J=8.4 Hz, phenyl H$_5$'); 6.99 (1H, d, J=4.8 Hz; phenyl H$_4$'); 7.00-7.09 (1H, m, phenyl H$_5$); 7.03 (1H, d, J=10.8 Hz, phenyl H$_6$'); 7.05 (1H, d, J=4.8 Hz, phenyl H$_6$); 7.39-7.48 (1H, m, phenyl H$_4$); 7.67 (1H, dd, J=8 J'=1.6 Hz, phenyl H$_3$); 10.58 (1H, bs, -O$\underline{H}$) (Figure 36).
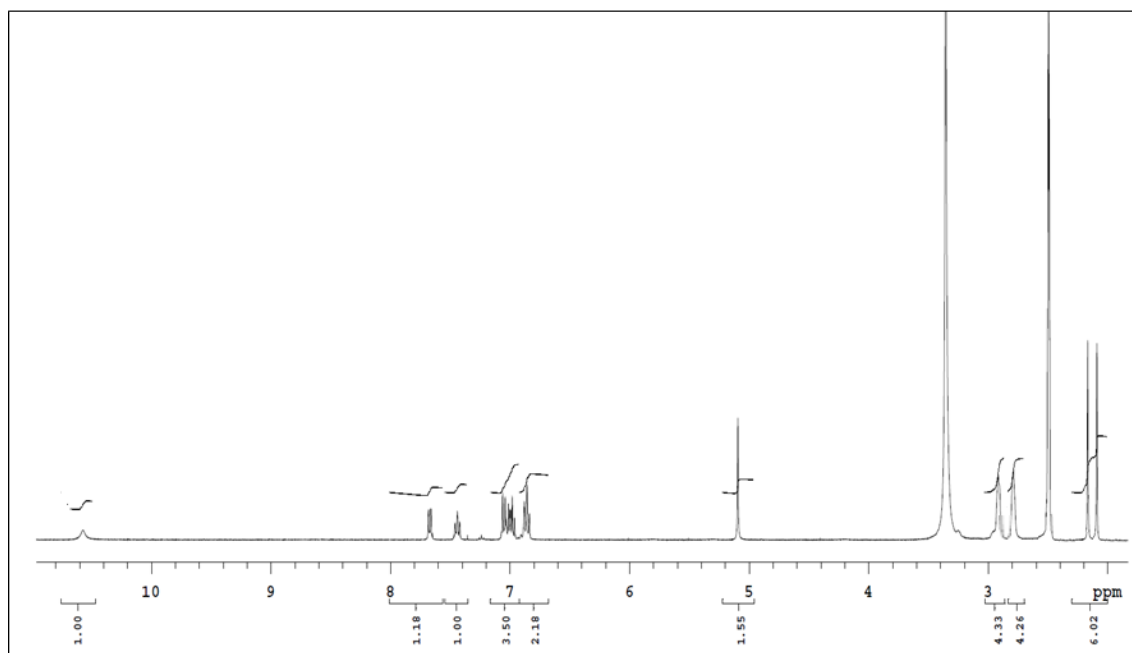
Figure 36. ^{1}H NMR spectrum of Compound **5j**

^{13}C NMR spectrum

δ ppm (400 MHz/DMSO-d_6): 13.66+20.21 (-$\underline{C}H_3$); 50.14 (piperazine C_2+C_6); 51.72 (piperazine C_3+C_5); 69.81 (methylene –$\underline{C}H_2$-); 108.03 (phenyl C_1); 116.44 (phenyl C_3); 117.05 (phenyl C_6'); 119.49 (phenyl C_5'); 124.62 (phenyl C_2'); 125.65 (phenyl C_4); 129.00 (phenyl C_5); 130.44 (phenyl C_6); 130.59 (phenyl C_4'); 137.22 (phenyl C_3'); 151.21 (phenyl C_1'); 156.40 (phenyl C_2); 158.05 ($\underline{C}$=N); 177.14 ($\underline{C}$=S) (Figure 37).
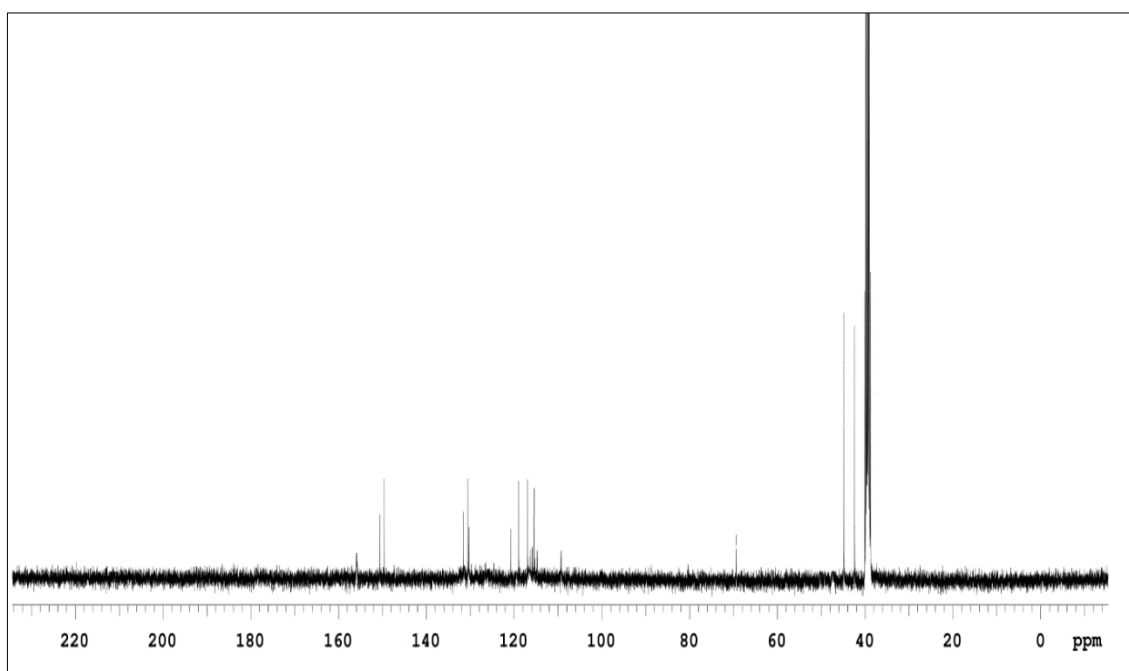

Figure 37. ^{13}C NMR spectrum of Compound **5j**

5-(2-Hydroxyphenyl)-3-{[4-(4-methoxyphenyl)piperazin-1-yl]methyl}-1,3,4-oxadiazole-2(*3H*)-thione (Compound 5k)
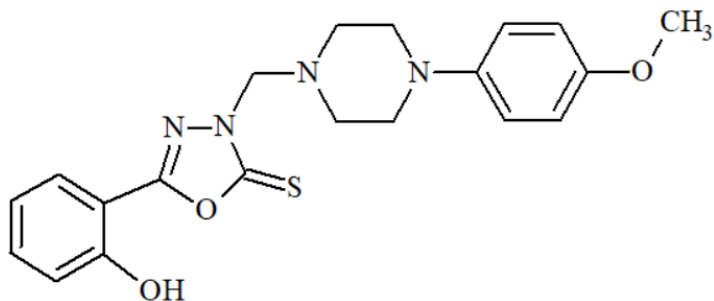
5-(2-Hydroxyphenyl)-1,3,4-oxadiazole-2(*3H*)-thione (0.01 mol, 1.94 g), 1-(4-methoxy-phenyl)piperazine (0.01 mol, 1.92 g), formaldehyde (0.01 mol, 0.55 ml) in 15 ml ethanol were reacted according to general synthesis method at 3.1.2.4.

Yield (%)	: 32
Retention factor (R_f)	: 0.63 [Toluene: Acetone: Acetic acid (75:25:10)]
Physical appearance	: White powder
Melting point (ºC)	: 148
Solubility	: Highly soluble with acetone and DMSO. Practically insoluble in water

Elemental analysis

Molecular formula	: $C_{20}H_{22}N_4O_3S$
Molecular weight (g/mol)	: 398.48

	C	H	N	S
Calculated (%)	60.28	5.56	14.06	8.05
Found (%)	60.13	5.76	14.11	8.17

Spectral Analysis

Infrared (IR) spectrum

ν_{max} **(cm^{-1}) :** 3362 (O-H stretching); 2947 (aromatic C-H stretchings); 1624 (C=N stretching); 1596, 1512 (aromatic C=C stretchings); 1439 (O-H bending); 1322 (C-O stretching); 1249 (C=S stretching); 835 (4-methoxyphenyl C-H bendings); 744 (2-hydroxyphenyl C-H bendings) (Figure 38).
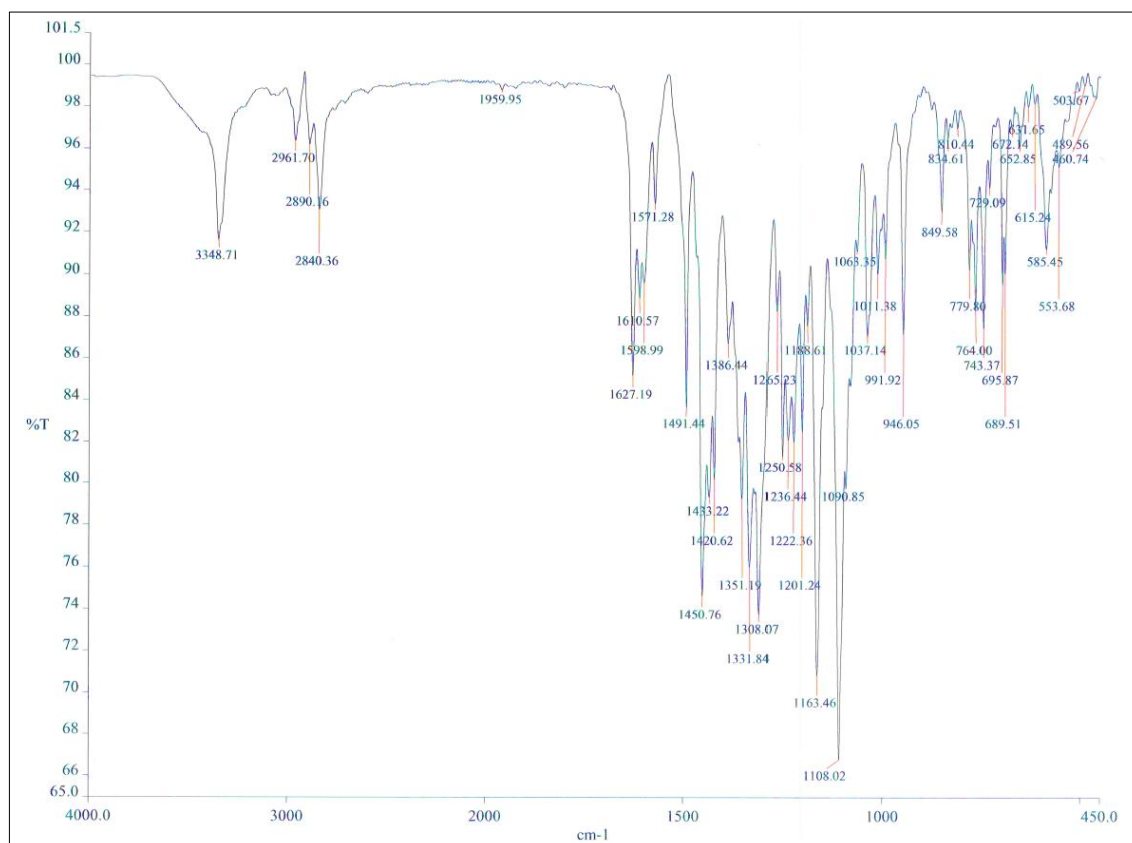

Figure 38. IR spectrum of Compound **5k**

^{1}H NMR spectrum

δ ppm (400 MHz/DMSO-d_6/): 2.88 (4H, bt, J=4.5 Hz, piperazine H$_2$ +H$_6$); 2.99 (4H, bt, J=4.5 Hz, piperazine H$_3$+H$_5$); 3.65 (3H, s, phenyl -OC$\underline{H}_3$); 5.08 (2H, s, -N-C$\underline{H}_2$-N-); 6.77 (2H, bd, J=9 Hz, phenyl H$_2$'+H$_6$'); 6.85 (2H, bd, J=9 Hz, phenyl H$_3$'+H$_5$'); 6.96 (1H, t, J=7.6 Hz; phenyl H$_5$); 7.03 (1H, bd, J=8 Hz, phenyl H$_6$); 7.40-7.45 (1H, m, phenyl H$_4$); 7.65 (1H, dd, J=7.8 J'=1.4 Hz, phenyl H$_3$); 10.52 (1H, bs, -O$\underline{H}$) (Figure 39).
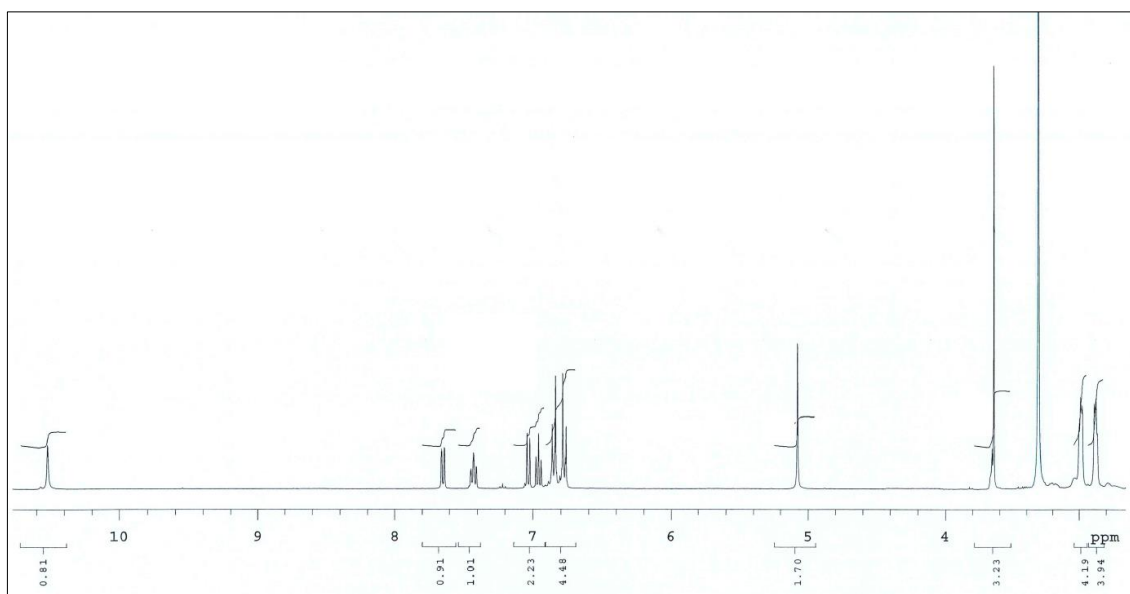
Figure 39. ^{1}H NMR spectrum of Compound **5k**

^{13}C NMR spectrum

δ ppm (400 MHz/DMSO-d_6): 49.69 (piperazine C_2+C_3+C_5+C_6); 55.12 (phenyl -O$\underline{C}H_3$); 69.58 (-N–$\underline{C}H_2$-N-); 108.99 (phenyl C_5); 114.17 (phenyl C_2'+C_6'); 117.05 (phenyl C_4); 117.66 (phenyl C_3'+C_5'); 119.44 (phenyl C_6); 129.15 (phenyl C_3); 133.66 (phenyl C_1); 145.34 (phenyl C_1'); 153.12 (phenyl C_4'); 156.42 (phenyl C_2); 157.94 ($\underline{C}$=N); 177.07 ($\underline{C}$=S) (Figure 40).
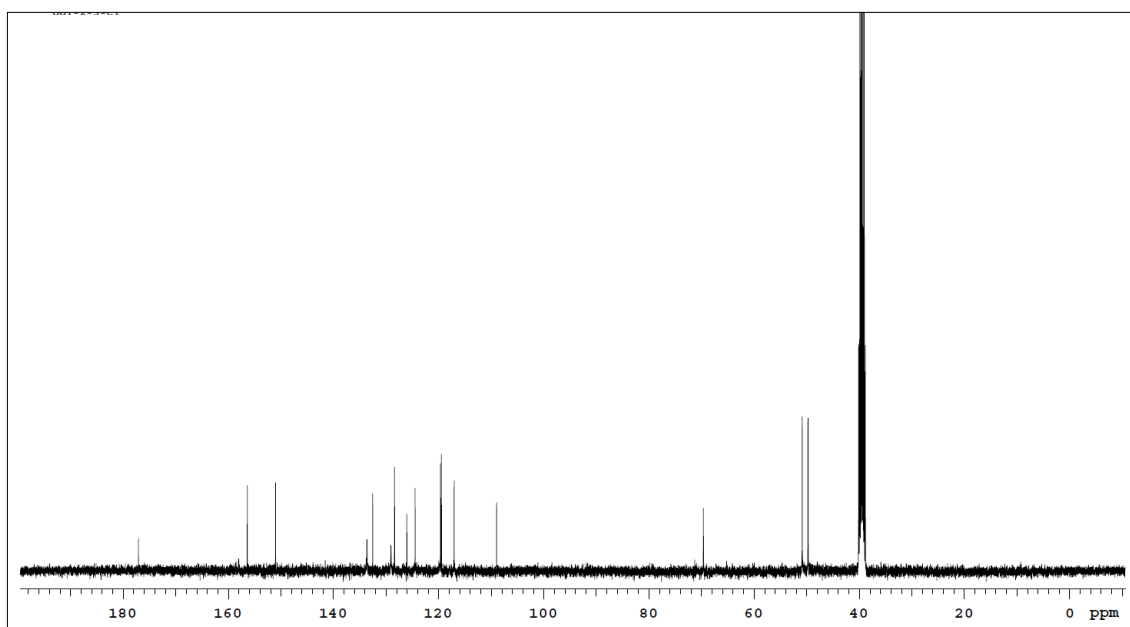

Figure 40. ^{13}C NMR spectrum of Compound **5k**

5-(2-Hydroxyphenyl)-3-{[4-(4-cyanophenyl)piperazin-1-yl]methyl}-1,3,4-oxadiazole-2(*3H*)-thione (Compound 5l)
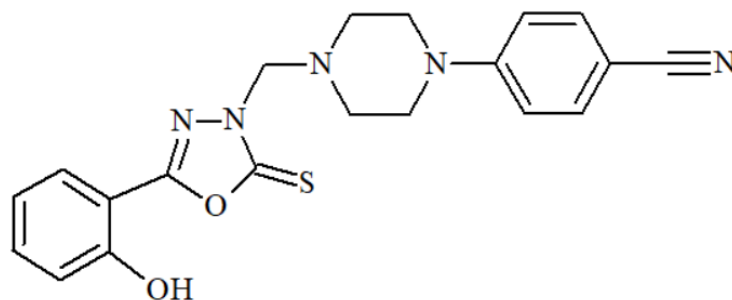
5-(2-Hydroxyphenyl)-1,3,4-oxadiazole-2(*3H*)-thione (0.01 mol, 1.94 g), 4-piperazino-benzonitrile (0.01 mol, 1.87 g), formaldehyde (0.015 mol, 0.55 ml) in 15 ml ethanol were reacted according to general synthesis method at 3.1.2.4.

Yield (%)	: 55
Retention factor (R$_f$)	: 0. 64 [Toluene: Acetone: Acetic acid (75:25:10)]
Physical appearance	: White powder
Melting point (ºC)	: 124
Solubility	: Highly soluble with acetone and DMSO. Practically insoluble in water

Elemental analysis

Molecular formula	: C$_{20}$H$_{19}$N$_5$O$_2$S
Molecular weight (g/mol)	: 393.46

	C	H	N	S
Calculated (%)	61.05	4.87	17.80	8.15
Found (%)	60.47	4.88	17.66	8.25

Spectral Analysis

Infrared (IR) spectrum

ν_{max} (cm^{-1}) : 3304 (O-H stretching); 2943 (aromatic C-H stretchings); 2214 (C≡N stretching); 1626 (C=N stretching); 1605, 1566, 1515, 1488 (aromatic C=C stretchings); 1431 (O-H bending); 1329 (C-O stretching); 1249 (C=S stretching); 819 (4-cyanophenyl C-H bendings); 741 (2-hydroxyphenyl C-H bendings) (Figure 41).
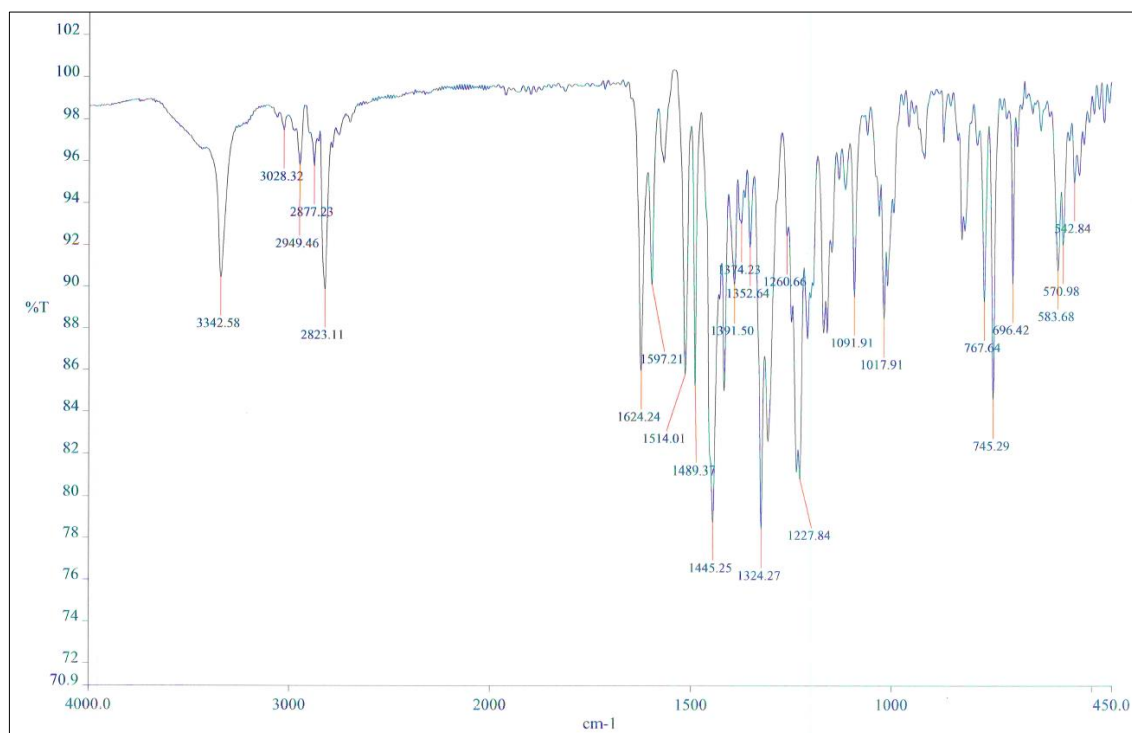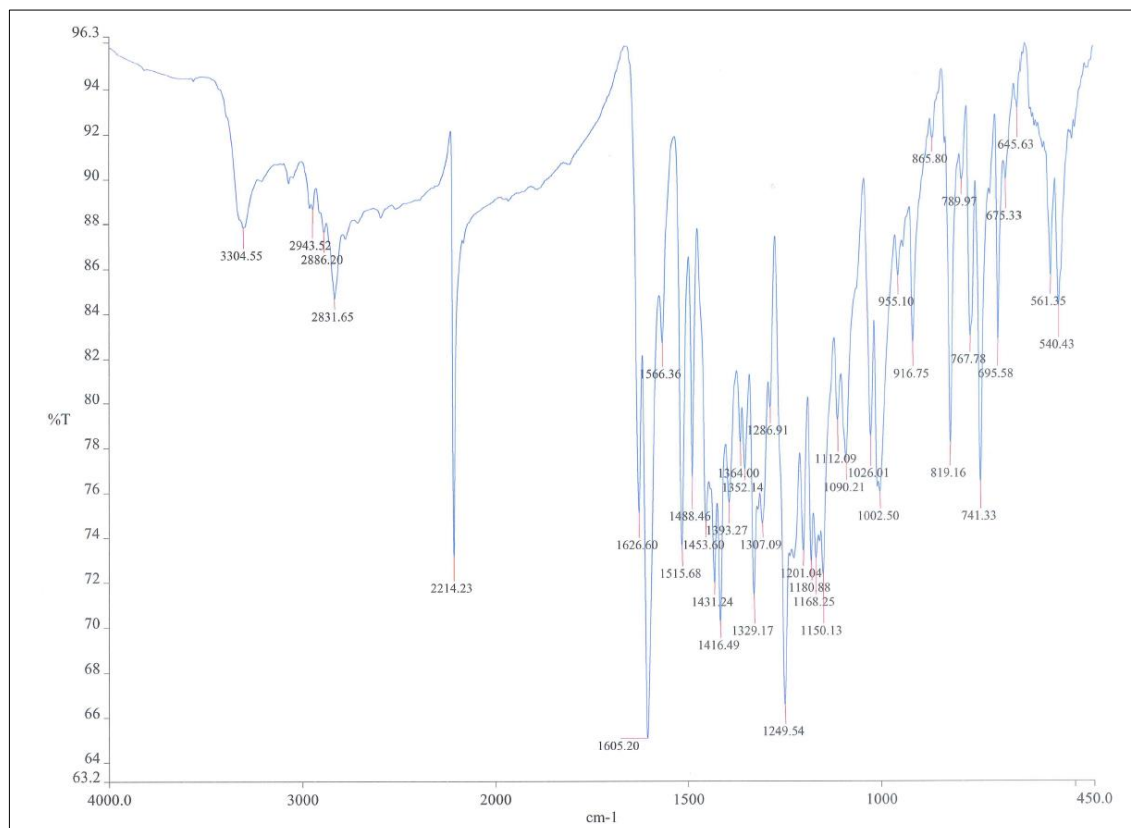

Figure 41. IR spectrum of Compound **5l**

^{1}H NMR spectrum

δ ppm (400 MHz/DMSO-d_6): 2.86 (8H, t, J=5 Hz, piperazine H$_2$+H$_3$+H$_5$+H$_6$); 5.08 (2H, s, -N-CH$_2$-N-); 6.93-6.97 (1H, m, phenyl H$_5$); 6.98 (2H, bd, J=9.2 Hz, phenyl H$_2$'+H$_6$'); 7.02 (1H, bd, J=8 Hz; phenyl H$_6$); 7.39-7.44 (1H, m, phenyl H$_4$); (2H, m, phenyl H$_3$'+H$_5$'); 7.63 (1H, dd, J=8 J'=1.6 Hz, phenyl H$_3$); 10.52 (1H, bs, -OH) (Figure 42).
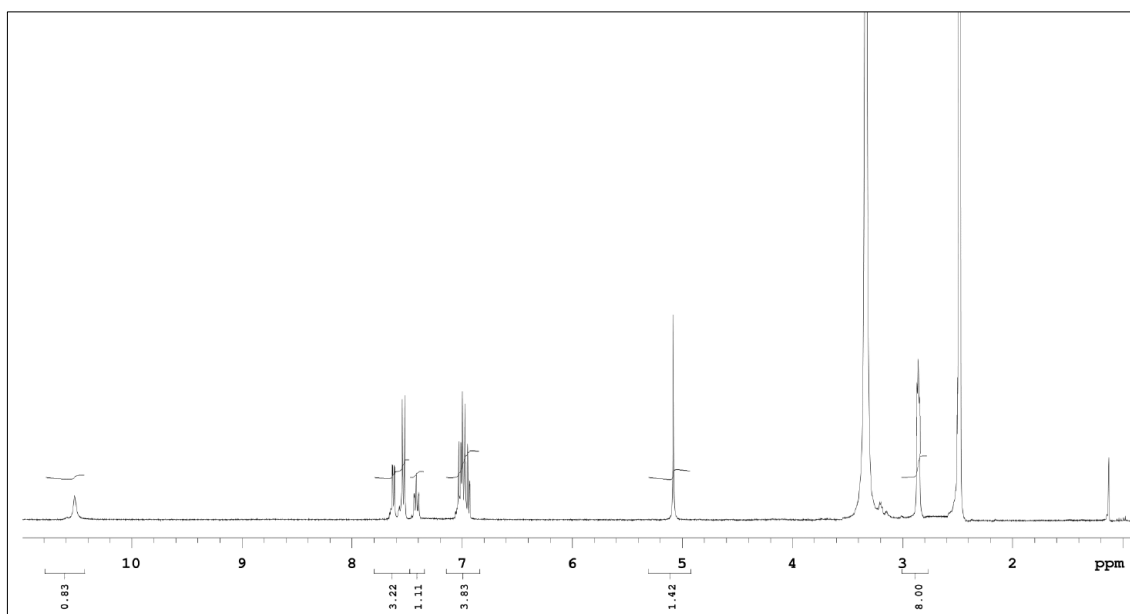
Figure 42. ^{1}H NMR spectrum of Compound **5l**

^{13}C NMR spectrum

δ ppm (400 MHz/DMSO-d_6): 46.26 (piperazine C_2+C_6); 49.16 (piperazine C_3+C_5); 69.38 (-N–$\underline{C}H_2$-N-); 98.23 (phenyl C_4'); 108.91 (phenyl C_5); 114.07 (phenyl C_2'+C_6'); 116.98 (phenyl C_4); 119.36 (phenyl C_6); 119.87 ($\underline{C}$≡N); 129.10 (phenyl C_3); 133.20 (phenyl C_3'+C_5'); 133.62 (phenyl C_1); 152.98 (phenyl C_1'); 156.98 (phenyl C_2); 157.89 ($\underline{C}$=N); 176.99 ($\underline{C}$=S) (Figure 43).
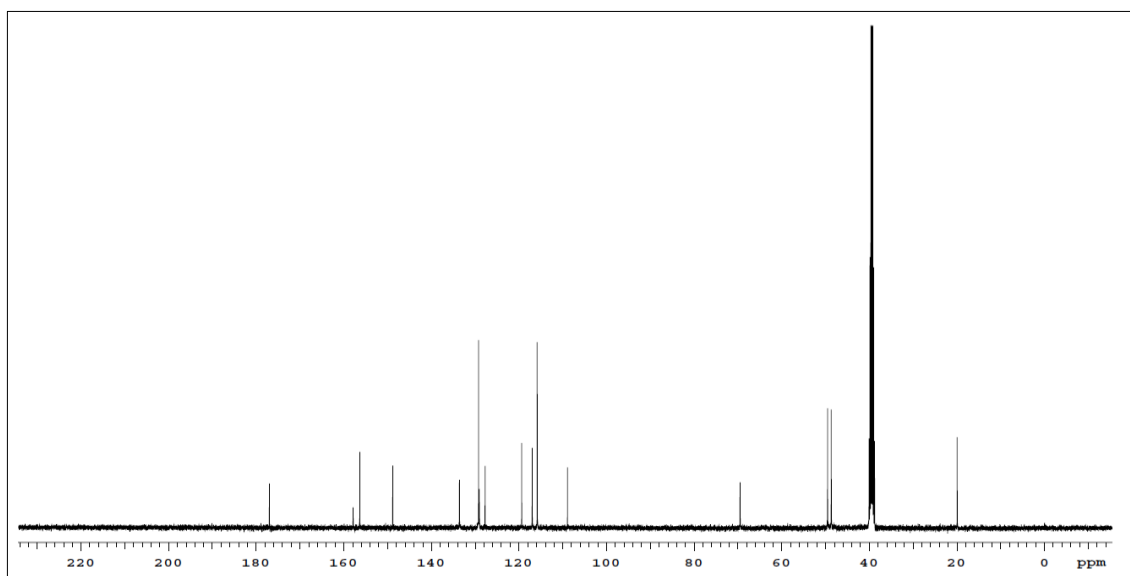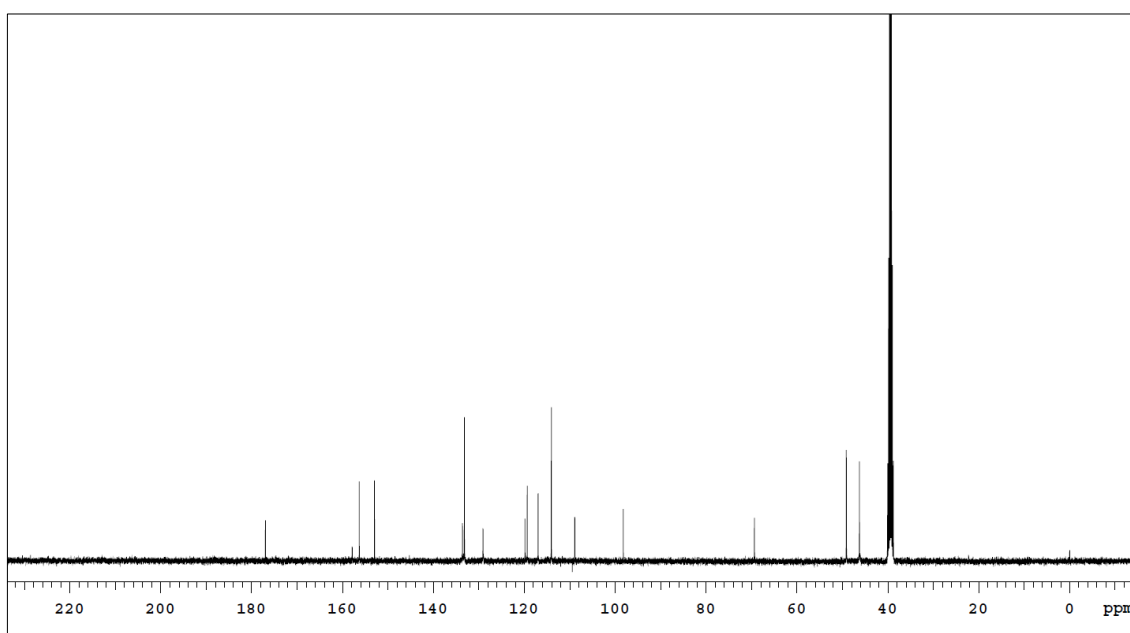

Figure 43. ^{13}C NMR spectrum of Compound **5l**

5-(2-Hydroxyphenyl)-3-{[4-(2-cyanophenyl)piperazin-1-yl]methyl}-1,3,4-oxadiazole-2(*3H*)-thione (Compound 5m)
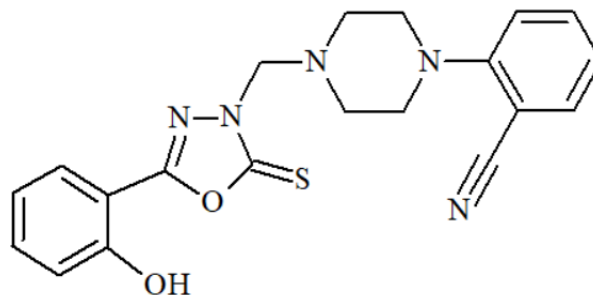
5-(2-Hydroxyphenyl)-1,3,4-oxadiazole-2(*3H*)-thione (0.01 mol, 1.94 g), 1-(2-cyano-phenyl)piperazine (0.01 mol, 1.87 g), formaldehyde (0.015 mol, 0.55 ml) in 15 ml ethanol were reacted according to general synthesis method at 3.1.2.4.

Yield (%)	:	56
Retention factor (R$_f$)	:	0.63 [Toluene: Acetone: Acetic acid (75:25:10)]
Physical appearance	:	White powder
Melting point (ºC)	:	120
Solubility	:	Highly soluble with acetone and DMSO. Practically insoluble in water

Elemental analysis

Molecular formula	:	C$_{20}$H$_{19}$N$_5$O$_2$S
Molecular weight (g/mol)	:	393.46

	C	H	N	S
Calculated (%)	61.05	4.87	17.80	8.15
Found (%)	60.42	4.87	17.65	8.27

Spectral Analysis

Infrared (IR) spectrum

ν_{max} **(cm^{-1}) :** 3336 (O-H stretching); 2964 (aromatic C-H stretchings); 2220 (C≡N stretching); 1625 (C=N stretching); 1595, 1573, 1487 (aromatic C=C stretchings); 1444 (O-H bending); 1322 (C-O stretching); 1250 (C=S stretching); 764 (2-cyanophenyl C-H bendings); 741 (2-hydroxyphenyl C-H bendings) (Figure 44).
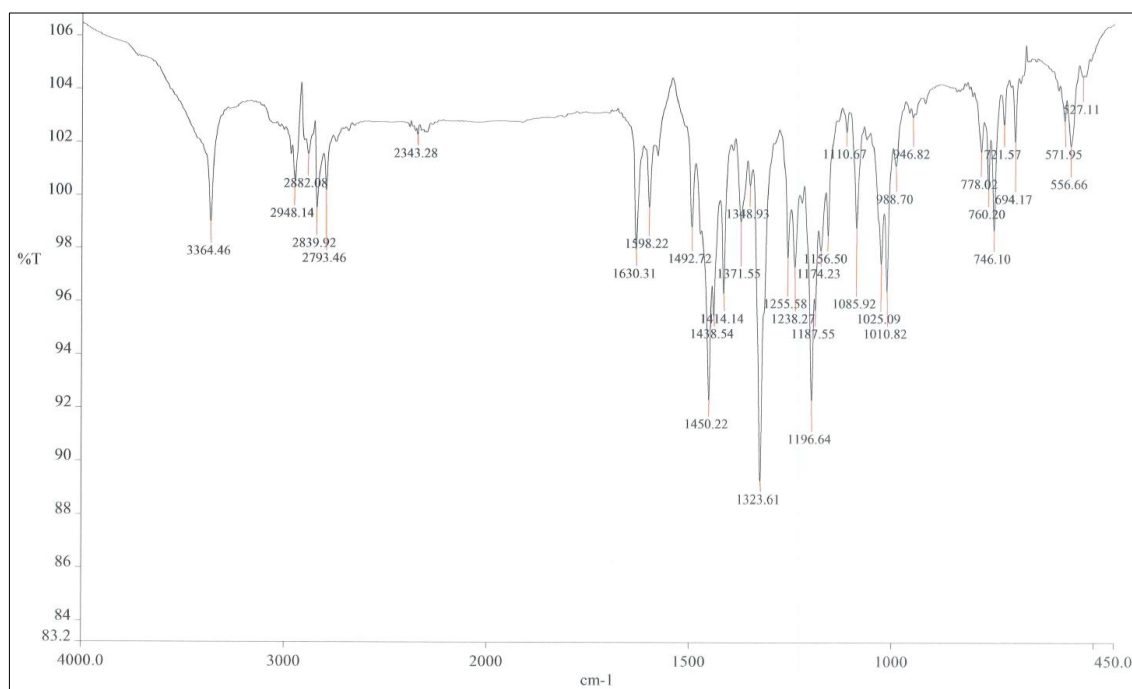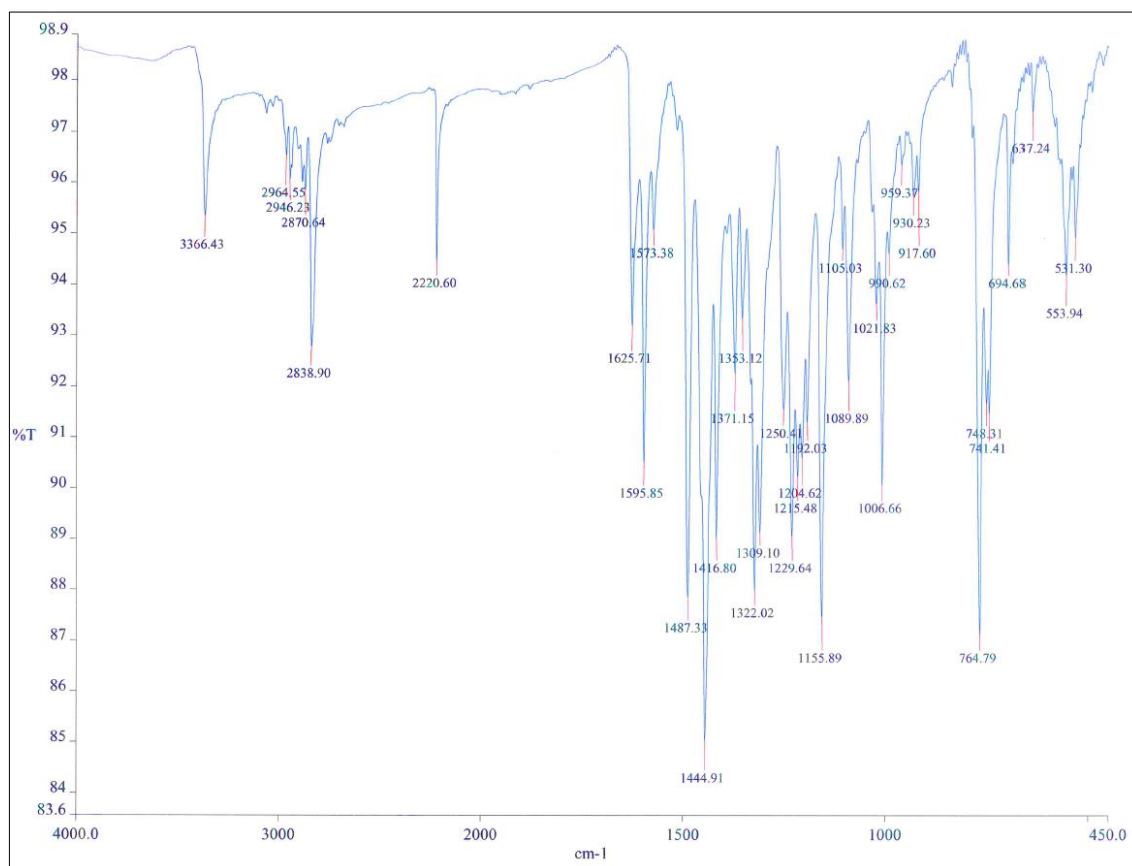

Figure 44. IR spectrum of Compound **5m**

^{1}H NMR spectrum

δ ppm (400 MHz/DMSO-d_6): 2.94 (4H, t, J=4.8 Hz, piperazine H$_2$ +H$_6$); 3.14 (4H, t, J=4.8 Hz, piperazine H$_3$+H$_5$); 5.10 (2H, s, -N-C$\underline{H}_2$-N-); 6.96 (1H, t, J=8 Hz, phenyl H$_5$'); 7.04 (1H, t, J=8 Hz, phenyl H$_6$'); 7.08 (1H, bd, J=7.6 Hz, phenyl H$_6$); 7.14 (1H, bd, J=8 Hz, phenyl H$_3$'); 7.41-7.45 (1H, m, phenyl H$_4$'); 7.55-7.60 (1H, m, phenyl H$_5$); 7.64-7.68 (2H, m, phenyl H$_3$+H$_4$); 10.52 (1H, bs, -O$\underline{H}$) (Figure 45).
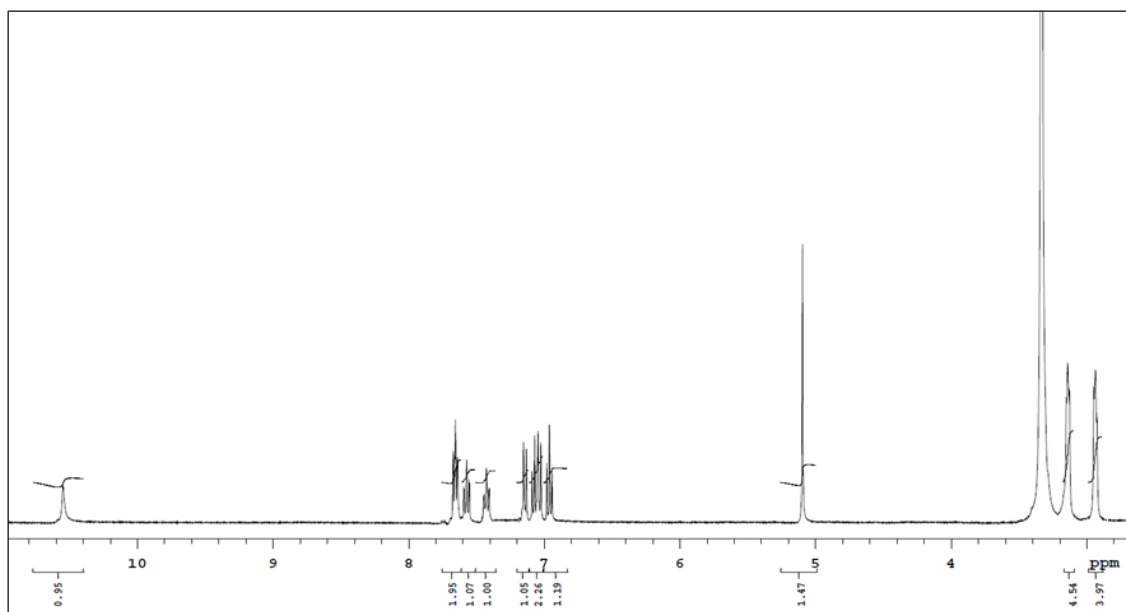
Figure 45. ^{1}H NMR spectrum of Compound **5m**

^{13}C NMR spectrum

δ ppm (400 MHz/DMSO-d_6): 49.67 (piperazine C_2+C_6); 51.11 (piperazine C_3+C_5); 69.55 (-N–$\underline{C}H_2$-N-); 104.78 (phenyl C_2'); 108.98 (phenyl C_1); 117.08 (phenyl C_3); 118.14 (phenyl C_6'); 119.16 (phenyl C_5); 119.47 (phenyl C_4'); 122.10 (phenyl C_6); 129.07 (phenyl C_5'); 133.67 (phenyl C_4); 134.19 (phenyl C_3'+ $\underline{C}$≡N); 134.31 (phenyl C_1'); 155.13 (phenyl C_2); 156.43 ($\underline{C}$=N); 177.10 ($\underline{C}$=S) (Figure 46).
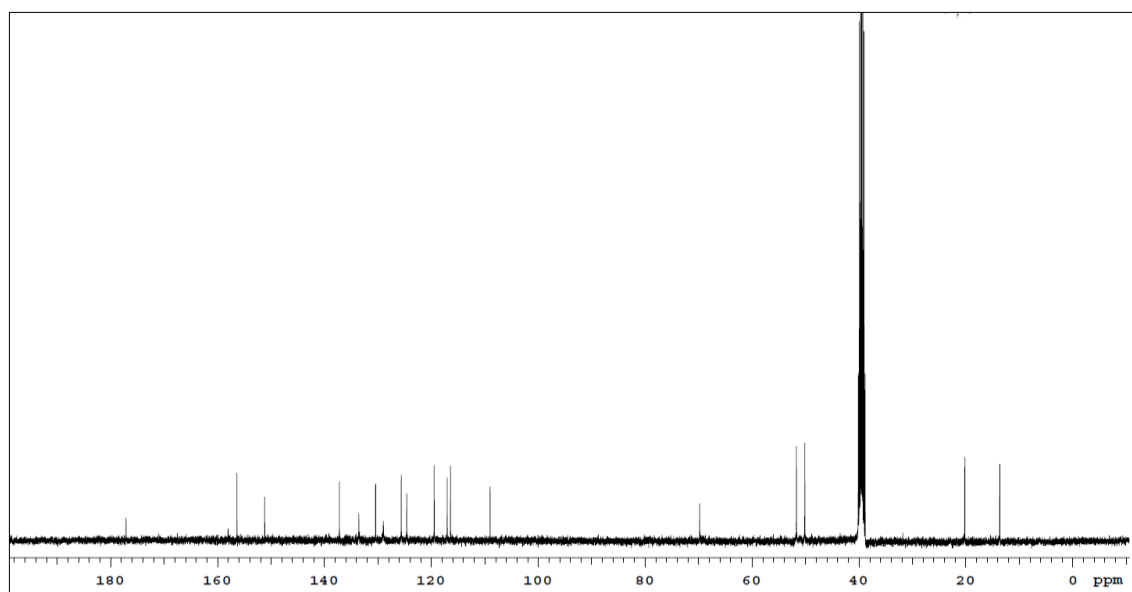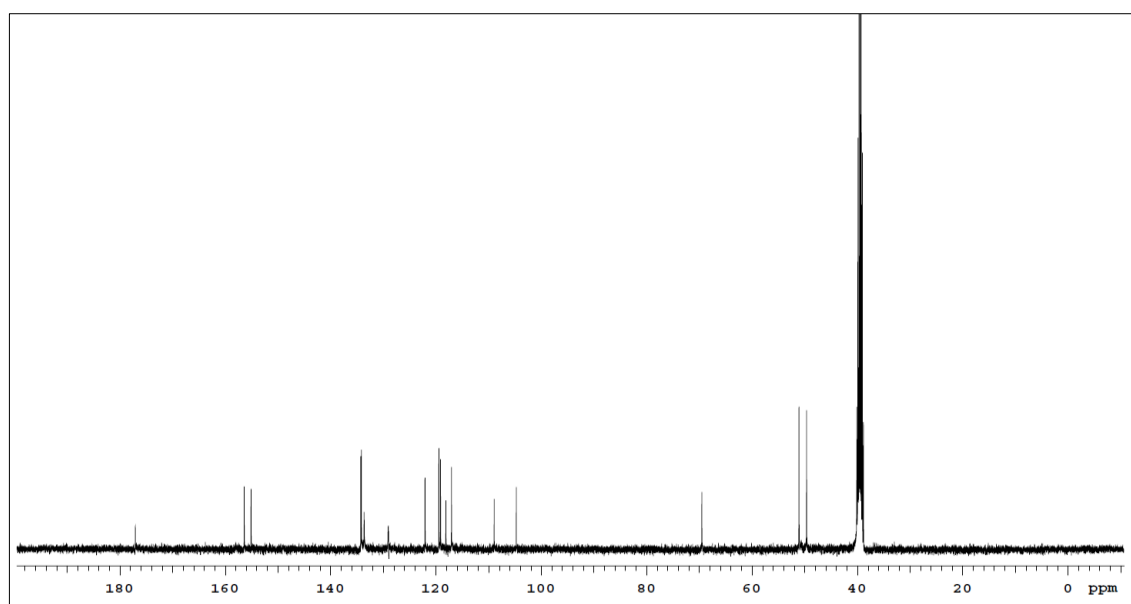

Figure 46. ^{13}C NMR spectrum of Compound **5m**

5-(2-Hydroxyphenyl)-3-{[4-(2-pyridyl)piperazin-1-yl]methyl}-1,3,4-oxadiazole-2-(3H)-thione (Compound 5n)
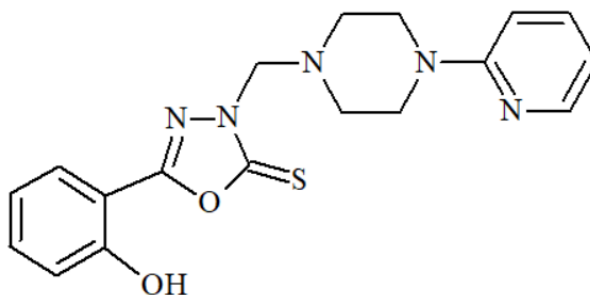
5-(2-Hydroxyphenyl)-1,3,4-oxadiazole-2(3H)-thione (0.01 mol, 1.94 g), 1-(2-pyridyl)-piperazine (0.01 mol, 1.63 g), formaldehyde (0.01 mol, 0.55 ml) in 15 ml ethanol were reacted according to general synthesis method at 3.1.2.4.

Yield (%)	: 59
Retention factor (R$_f$)	: 0.68 [Toluene: Acetone: Acetic acid (75:25:10)]
Physical appearance	: White powder
Melting point (ºC)	: 148
Solubility	: Highly soluble with acetone and DMSO. Practically insoluble in water

Elemental analysis

Molecular formula	: C$_{18}$H$_{19}$N$_5$O$_2$S
Molecular weight (g/mol)	: 369.44

	C	H	N	S
Calculated (%)	58.52	5.18	18.96	8.68
Found (%)	58.80	5.34	18.86	8.72

Spectral Analysis

Infrared (IR) spectrum

ν_{max} **(cm^{-1}) :** 3435 (O-H stretching); 3012 (aromatic C-H stretchings); 1615 (C=N stretching); 1603, 1560, 1484 (aromatic C=C stretchings); 1435 (O-H bending); 1311 (C-O stretching); 1264 (C=S stretching); 772 (2-pyridyl C-H bendings); 743 (2-hydroxyphenyl C-H bendings) (Figure 47).
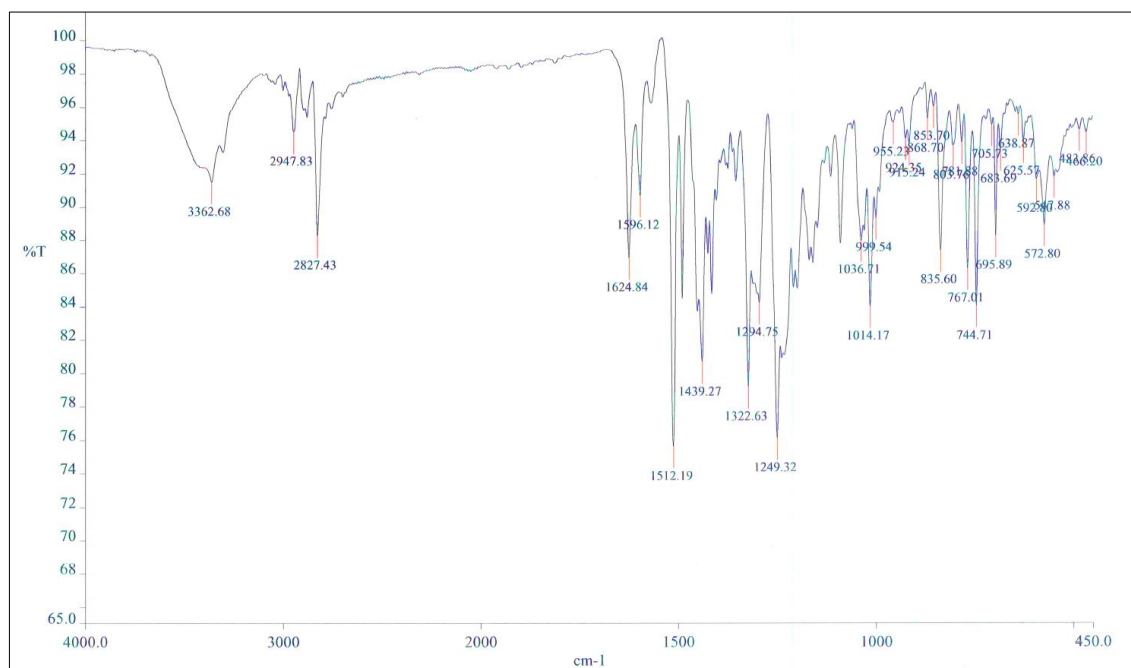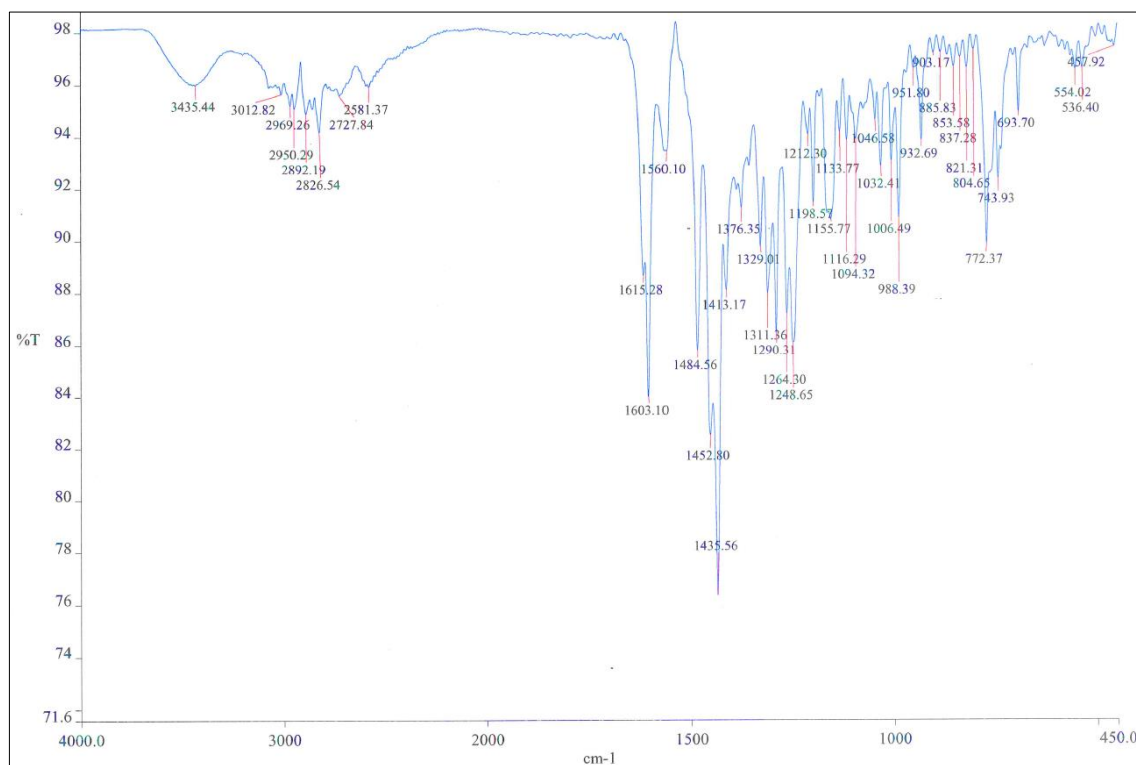

Figure 47. IR spectrum of Compound **5n**

^{1}H NMR spectrum

δ ppm (400 MHz, DMSO-d_6): 2.48 (4H, t, J=5 Hz, piperazine H$_2$ +H$_6$); 3.48 (4H, t, J=5 Hz, piperazine H$_3$+H$_5$); 5.08 (2H, s, -N-C$\underline{H}_2$-N-); 6.57-6.60 (1H, m, pyridyl H$_5$); 6.79 (1H, t, J=8.8 Hz, pyridyl H$_6$); 6.93-6.79 (1H, m, phenyl H$_5$); 7.01 (1H, d, J=8 Hz, phenyl H$_6$); 7.40-7.44 (1H, m, phenyl H$_4$); 7.46-7.50 (1H, m, pyridyl H$_4$); 7.63 (1H, dd, J=7.8 J'=1.8 Hz, phenyl H$_3$); 8.06 (1H, dd, J=4.6 J'=1.8 Hz, pyridyl H$_3$); 10.51 (1H, bs, -O$\underline{H}$) (Figure 48).

Figure 48. [superscript 1]H NMR spectrum of Compound **5n**

[superscript 13]C NMR spectrum
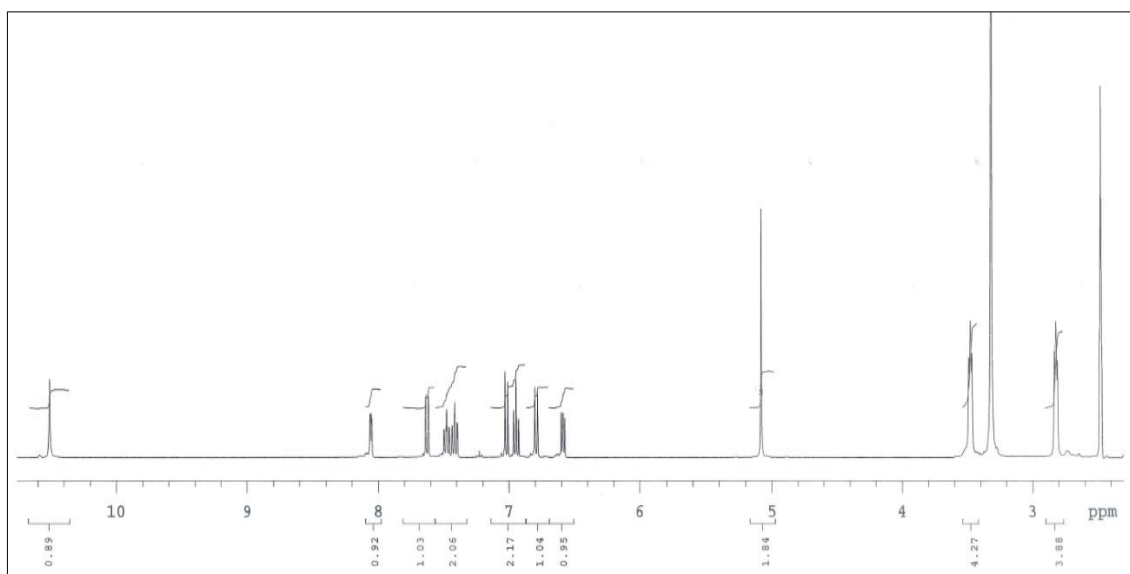
δ ppm (400 MHz/DMSO-d_6): 44.64 (piperazine C_2+C_6); 49.38 (piperazine C_3+C_5); 69.64 (-N–$\underline{C}H_2$-N-); 107.06 (pyridyl C_5); 108.92 (pyridyl C_4); 112.92 (phenyl C_5); 117.01 (phenyl C_4); 119.38 (phenyl C_6); 129.11 (pyridyl C_6); 133.61 (phenyl C_3); 137.38 (phenyl C_1); 147.41 (pyridyl C_3); 156.36 (phenyl C_2); 157.84 (pyridyl C_1); 158.77 ($\underline{C}$=N); 176.98 ($\underline{C}$=S) (Figure 49).
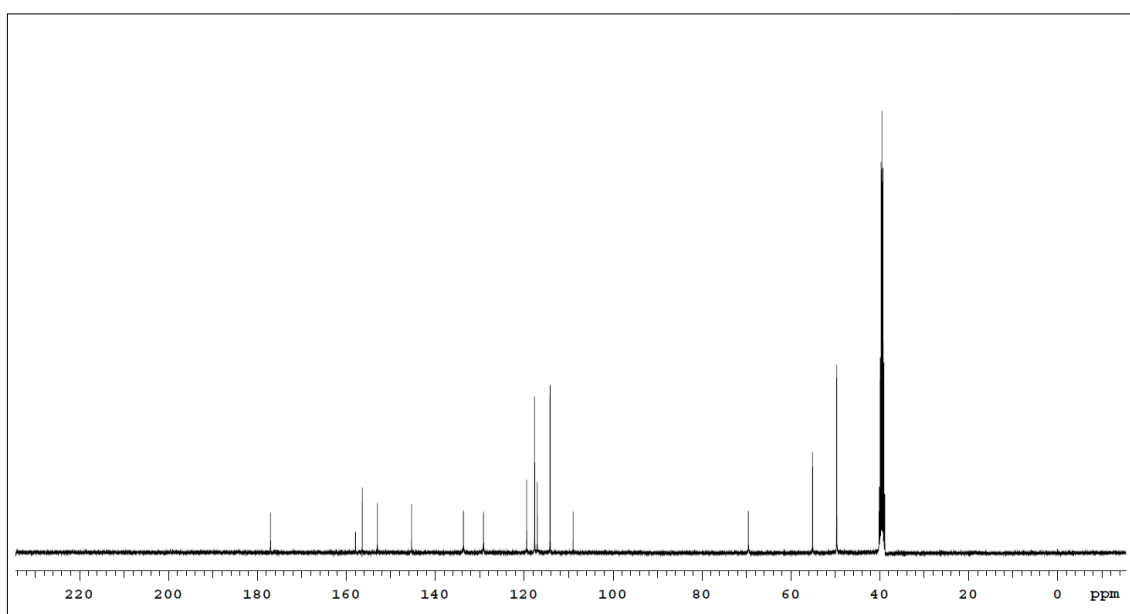

Figure 49. [superscript 13]C NMR spectrum of Compound **5n**

115

5-(2-Hydroxyphenyl)-3-{[4-(2-pyrimidinyl)piperazin-1-yl]methyl}-1,3,4-oxadiazole-2(*3H*)-thione (Compound 5o)
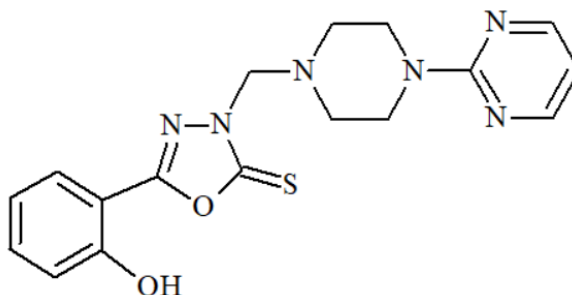
5-(2-Hydroxyphenyl)-1,3,4-oxadiazole-2(*3H*)-thione (0.01 mol, 1.94 g), 1-(2-pyrimi-dinyl)piperazine (0.01 mol, 1.64 g), formaldehyde (0.015 mol, 0.55 ml) in 15 ml ethanol were reacted according to general synthesis method at 3.1.2.4.

Yield (%)	: 60
Retention factor (R$_f$)	: 0.66 [Toluene: Acetone: Acetic acid (75:25:10)]
Physical appearance	: White powder
Melting point (ºC)	: 149
Solubility	: Highly soluble with acetone and DMSO. Practically insoluble in water

Elemental analysis

Molecular formula	: C$_{17}$H$_{18}$N$_6$O$_2$S
Molecular weight (g/mol)	: 370.42

	C	H	N	S
Calculated (%)	55.12	4.90	22.69	8.66
Found (%)	54.65	4.93	22.68	8.84

Spectral Analysis

Infrared (IR) spectrum

ν_{max} **(cm^{-1}) :** 3336 (O-H stretching); 3021 (aromatic C-H stretchings); 1624 (C=N stretching); 1585, 1547, 1489 (aromatic C=C stretchings); 1450 (O-H bending); 1324 (C-O stretching); 1262 (C=S stretching); 798 (2-pyrimidinyl C-H bendings); 742 (2-hydroxyphenyl C-H bendings) (Figure 50).
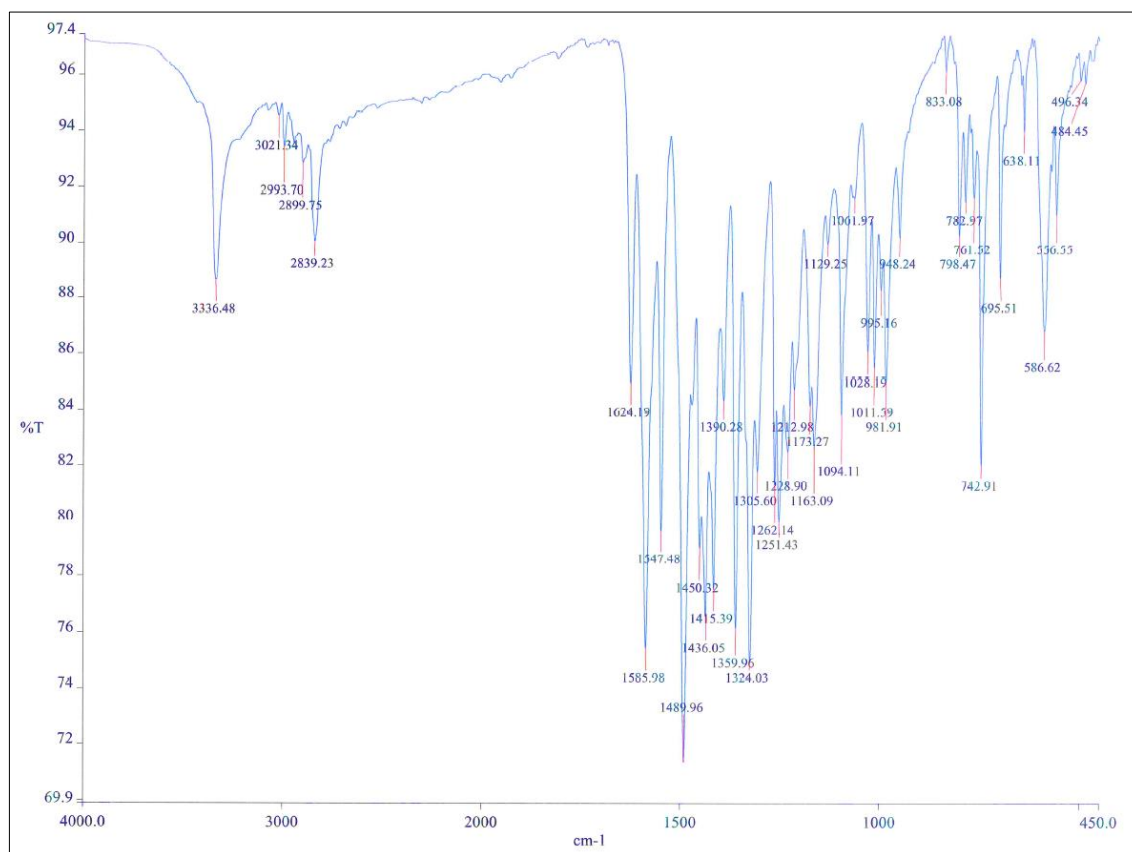
Figure 50. IR spectrum of Compound **5o**

^{1}H NMR spectrum

δ ppm (400 MHz/DMSO-d_6): 2.80 (4H, t, J=5 Hz, piperazine H$_2$ +H$_6$); 3.74 (4H, t, J=5 Hz, piperazine H$_3$+H$_5$); 5.09 (2H, s, -N-C$\underline{H}_2$-N-); 6.59 (1H, t, J=4.8 Hz, pyrimidine H$_4$); 6.95 (1H, m, phenyl H$_5$); 7.02 (1H, bd, J=7.6 Hz, phenyl H$_6$); 7.40-7.44 (1H, m, phenyl H$_4$); 7.63 (1H, dd, J=7.6 J'=1.6 Hz, phenyl H$_3$); 8.32 (2H, d, J=4.8 Hz, pyrimidine H$_3$+H$_5$); 10.48 (1H, bs, -OH) (Figure 51).
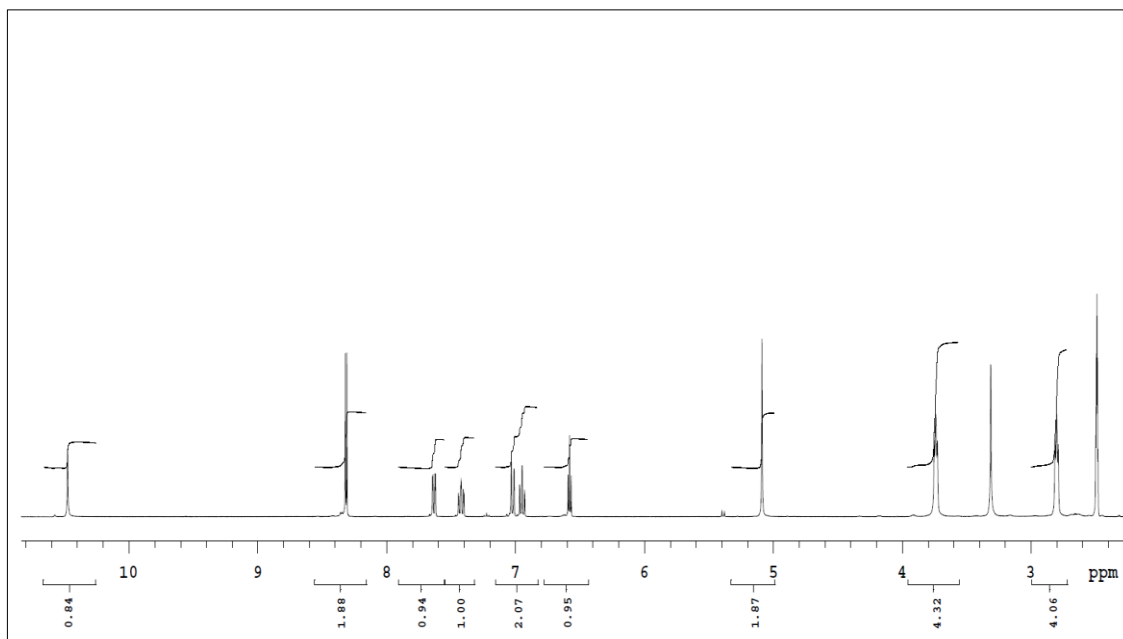
Figure 51. ^{1}H NMR spectrum of Compound **5o**

^{13}C NMR spectrum

δ ppm (400 MHz/DMSO-d_6): 43.13 (piperazine C_2+C_6); 49.44 (piperazine C_3+C_5); 69.73 (-N–$\underline{C}H_2$-N-); 108.99 (phenyl C_5); 110.08 (phenyl C_4); 117.04 (pyrimidine C_4); 119.43 (phenyl C_6); 129.13 (phenyl C_3); 133.62 (phenyl C_1); 156.38 (phenyl C_2); 157.86 (pyrimidine C_3+C_5, $\underline{C}$=N); 161.04 (pyrimidine C_1); 177.01 ($\underline{C}$=S) (Figure 52).
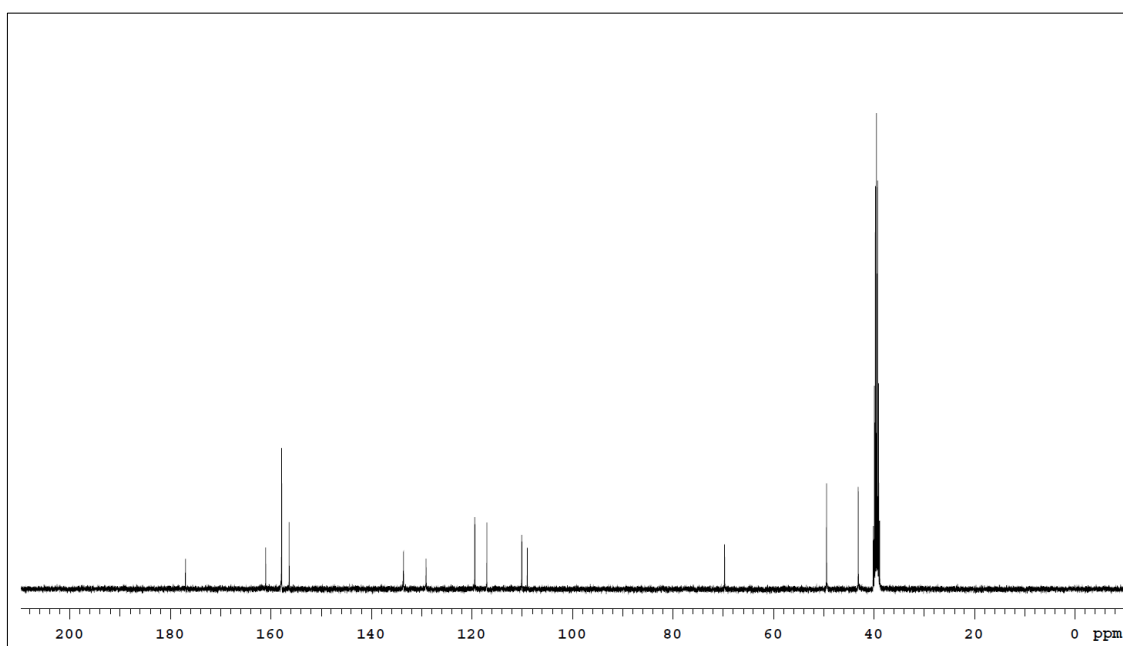
Figure 52. ^{13}C NMR spectrum of Compound **5o**

5-[1-(4-Isobutylphenyl)ethyl]-3-[(4-phenylpiperazin-1-yl)methyl]-1,3,4-oxadiazole-2(3H)-thione (Compound 10a)
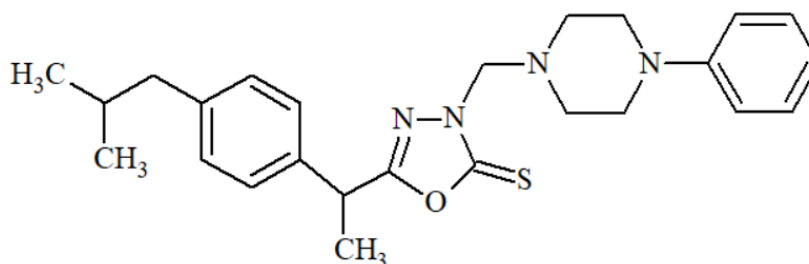
5-[1-(4-Isobutylphenyl)ethyl]-1,3,4-oxadiazole-2(3H)-thione (0.01 mol, 2.62 g), 1-phenylpiperazine (0.01 mol, 1.62 g), formaldehyde (0.015 mol, 0.55 ml) in 15 ml methanol were reacted according to general synthesis method at 3.1.2.4.

Yield (%)	:	72
Retention factor (R$_f$)	:	0.63 [Toluene: Acetone: Acetic Acid (75:25:10)]
Physical appearance	:	White powder
Melting point (ºC)	:	105
Solubility	:	Highly soluble with acetone and DMSO. Practically insoluble in water
Elemental analysis		
Molecular formula	:	C$_{25}$H$_{32}$N$_4$OS
Molecular weight (g/mol)	:	436.61

	C	H	N	S
Calculated (%)	68.77	7.39	12.83	7.34
Found (%)	68.73	7.59	12.88	7.43

Spectral Analysis

Infrared (IR) spectrum

ν_{max} **(cm^{-1}) :** 2952 (aromatic C-H stretchings); 2831 (aliphatic C-H stretchings); 1620 (C=N stretching); 1599, 1506 (aromatic C=C stretchings); 1441 (C-N stretching); 1325 (C-O stretching); 1258 (C=S stretching); 849 (1,4-dialkylphenyl C-H bendings); 756 (phenyl C-H bendings) (Figure 53).
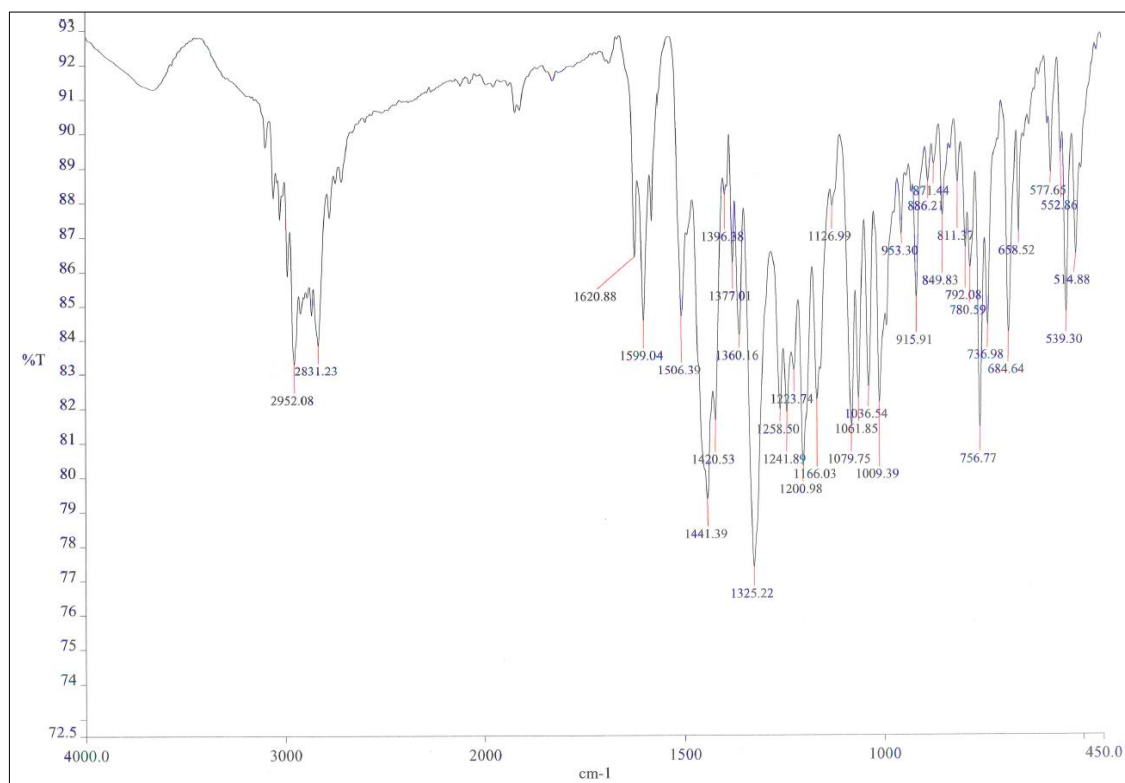
Figure 53. IR spectrum of Compound **10a**

^{1}H NMR spectrum

δ ppm (400 MHz/DMSO-d_6): 0.84 (6H, d, J=6.8 Hz, isobutyl -C$\underline{H}_3$); 1.56 (3H, d, J=6.8 Hz, -CH-C$\underline{H}_3$); 1.78-1.81 (1H, m, isobutyl -C$\underline{H}$-); 2.41 (2H, d, J=7.6 Hz, isobutyl –C$\underline{H}_2$-); 2.84 (4H, t, J=5 Hz, piperazine H$_2$+H$_6$); 3.13 (4H, t, J=5 Hz, piperazine H$_3$+H$_5$); 4.33 (1H, q, J=6.8 Hz, -C$\underline{H}$-CH$_3$,); 5.00 (2H, s, -N-C$\underline{H}_2$-N-); 6.77 (1H, t, J=7.2 Hz, phenyl H$_4$'); 6.91 (2H, d, J=7.8 Hz, phenyl H$_3$+H$_5$); 7.13 (2H, d, J=7.8 Hz, phenyl H$_2$+H$_6$); 7.17-7.21 (4H, m, phenyl H$_2$'+H$_3$'+H$_5$'+H$_6$') (Figure 54).

Figure 54. ^{1}H NMR spectrum of Compound **10a**

^{13}C NMR spectrum

δ ppm (400 MHz/DMSO-d_6): 18.49 (isobutyl –CH-); 22.13+22.14 (isobutyl -CH$_3$); 29.50 (-CH-CH$_3$); 36.09 (isobutyl -CH$_2$-); 44.13 (-CH-CH$_3$); 48.19 (piperazine C$_2$+C$_6$); 49.52 (piperazine C$_3$+C$_5$); 69.43 (-N-CH$_2$-N-); 115.58 (phenyl C$_2$'+C$_6$'); 118.94 (phenyl C$_4$'); 126.99 (phenyl C$_3$+C$_5$); 128.87 (phenyl C$_3$'+C$_5$'); 129.44 (phenyl C$_2$+C$_6$); 136.77 (phenyl C$_4$); 140.51 (phenyl C$_1$); 157.88 (phenyl C$_1$'); 164.10 (C=N); 177.76 (C=S) (Figure 55).

Figure 55. ^{13}C NMR spectrum of Compound **10a**

5-[1-(4-Isobutylphenyl)ethyl]-3-{[4-(4-fluorophenyl)piperazin-1-yl]methyl}-1,3,4-oxadiazole-2(*3H*)-thione (Compound 10b) [17]
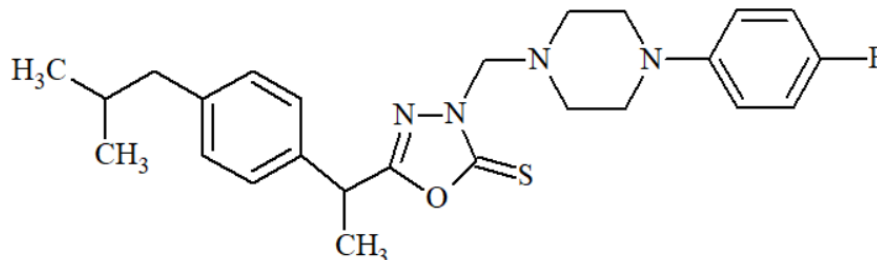
5-[1-(4-Isobutylphenyl)ethyl]-1,3,4-oxadiazole-2(*3H*)-thione (0.01 mol, 2.62 g), 1-(4-fluorophenyl)piperazine (0.01 mol, 1.80 g), formaldehyde (0.015 mol, 0.55 ml) in 15 ml methanol were reacted according to general synthesis method at 3.1.2.4.

Yield (%)	:	69
Retention factor (R$_f$)	:	0.65 [Toluene: Acetone: Acetic Acid (75:25:10)]
Physical appearance	:	White powder
Melting point (ºC)	:	121
Solubility	:	Highly soluble with acetone and DMSO. Practically insoluble in water

Spectral Analysis

Infrared (IR) spectrum

v_{max} **(cm^{-1}) :** 2950 (aromatic C-H stretchings); 2833 (aliphatic C-H stretchings); 1614 (C=N stretching); 1508 (aromatic C=C stretchings); 1447 (C-N stretching); 1330 (C-O stretching); 1254 (C=S stretching); 826 (1,4-dialkylphenyl C-H bending); 780 (4-fluorophenyl C-H bendings) (Figure 56).

Figure 56. IR spectrum of Compound **10b**

^{1}H NMR spectrum

δ ppm (400 MHz/DMSO-d_6): 0.84 (6H, d, J=6.8 Hz, isobutyl -C$\underline{H}_3$); 1.55 (3H, d, J=6.8 Hz, -CH-C$\underline{H}_3$); 1.77-1.81 (1H, m, isobutyl –C$\underline{H}$-); 2.41 (2H, d, J=7.2 Hz, isobutyl –C$\underline{H}_2$-); 2.83 (4H, t, J=5 Hz, piperazine H$_2$+H$_6$); 3.07 (4H, t, J=5 Hz, piperazine H$_3$+H$_5$); 4.33 (1H, q, J=6.4 Hz, -C$\underline{H}$-CH$_3$,); 5.00 (2H, s, -N-C$\underline{H}_2$-N-); 6.93 (2H, dd, J=9.2 J'=4.6 Hz, phenyl H$_2$'+H$_6$'); 7.03 (2H, t, J=8.8 Hz, phenyl H$_3$'+H$_5$'); 7.13 (2H, bd, J=8 Hz, phenyl H$_3$+H$_5$); 7.19 (2H, bd, J=8 Hz, phenyl H$_2$+H$_6$) (Figure 57).

Figure 57. ^{1}H NMR spectrum of Compound **10b**

^{13}C NMR spectrum

δ ppm (400 MHz/DMSO-d_6): 18.48 (isobutyl –$\underline{C}$H-); 22.11+22.13 (isobutyl -$\underline{C}$H$_3$); 29.50 (-CH-$\underline{C}$H$_3$); 36.09 (isobutyl -$\underline{C}$H$_2$-); 44.13 (-$\underline{C}$H-CH$_3$); 48.94 (piperazine C$_2$+C$_6$); 49.48 (piperazine C$_3$+C$_5$); 69.39 (-N-$\underline{C}$H$_2$-N-); 115.09 (phenyl C$_6$'); 115.31 (phenyl C$_2$'); 117.29 (phenyl C$_5$'); 117.36 (phenyl C$_3$'); 126.99 (phenyl C$_3$+C$_5$); 129.43 (phenyl C$_2$+C$_6$); 136.75 (phenyl C$_4$); 140.51 (phenyl C$_1$); 147.74+147.76 (phenyl C$_1$'); 154.86+157.20 (phenyl $\underline{C}$$_4$'-F); 164.07 ($\underline{C}$=N); 177.75 ($\underline{C}$=S) (Figure 58).

Figure 58. ^{13}C NMR spectrum of Compound **10b**

5-[1-(4-Isobutylphenyl)ethyl]-3-{[4-(2-fluorophenyl)piperazin-1-yl]methyl}-1,3,4-oxadiazole-2(*3H*)-thione (Compound 10c)

5-[1-(4-Isobutylphenyl)ethyl]-1,3,4-oxadiazole-2(*3H*)-thione (0.01 mol, 2.62 g), 1-(2-fluorophenyl)piperazine (0.01 mol, 1.80 g), formaldehyde (0.015 mol, 0.55 ml) in 15 ml methanol were reacted according to general synthesis method at 3.1.2.4.

Yield (%)	: 40
Retention factor (R$_f$)	: 0.63 [Toluene: Acetone: Acetic Acid (75:25:10)]
Physical appearance	: White powder
Melting point (ºC)	: 108
Solubility	: Highly soluble with acetone and DMSO. Practically insoluble in water

<u>**Elemental analysis**</u>

Molecular formula	: C$_{25}$H$_{31}$FN$_4$OS
Molecular weight (g/mol)	: 454.60

	C	H	N	S
Calculated (%)	66.05	6.87	12.32	7.05
Found (%)	66.07	7.12	12.35	7.15

Spectral Analysis

Infrared (IR) spectrum

ν_{max} **(cm^{-1}) :** 2950 (aromatic C-H stretchings); 2844 (aliphatic C-H stretchings); 1603 (C=N stretching); 1578, 1500 (aromatic C=C stretchings); 1443 (C-N stretching); 1352 (C-O stretching); 1242 (C=S stretching); 852 (1,4-dialkylphenyl C-H bending); 751 (2-fluorophenyl C-H bendings) (Figure 59).

Figure 59. IR spectrum of Compound **10c**

^{1}H NMR spectrum

δ ppm (400 MHz/DMSO-d_6): 0.85 (6H, d, J=6.8 Hz, isobutyl -C<u>H</u>$_3$); 1.57 (3H, d, J=7.2 Hz, -CH-C<u>H</u>$_3$); 1.77-1.84 (1H, m, isobutyl -C<u>H</u>-); 2.42 (2H, d, J=7.2 Hz, isobutyl –C<u>H</u>$_2$-); 2.86 (4H, t, J=4.8 Hz, piperazine H$_2$+H$_6$); 3.01 (4H, t, J=4.8 Hz, piperazine H$_3$+H$_5$); 4.35 (1H, q, J=7 Hz, -C<u>H</u>-CH$_3$,); 5.00 (2H, s, -N-C<u>H</u>$_2$-N-); 6.94-7.00 (1H, m, phenyl H$_6$'); 7.03 (1H, bd, J=9.2 Hz, phenyl H$_3$'); 7.08-7.12 (2H, m, phenyl H$_4$'+ H$_5$'); 7.15 (2H, bd, J=8.2 Hz, phenyl H$_3$+H$_5$); 7.22 (2H, bd, J=8.2 Hz, phenyl H$_2$+H$_6$) (Figure 60).

Figure 60. ^{1}H NMR spectrum of Compound **10c**

^{13}C NMR spectrum

δ ppm (400 MHz/DMSO-d_6): 18.47 (isobutyl –CH-); 22.12 (isobutyl -CH$_3$); 29.50 (-CH-CH$_3$); 36.11 (isobutyl -CH$_2$-); 44.13 (-CH-CH$_3$); 49.64 (piperazine C$_2$+C$_6$); 49.97 (piperazine C$_3$+C$_5$); 69.49 (-N-CH$_2$-N-); 115.77+115.98 (phenyl C$_6$'); 119.29+119.32 (phenyl C$_3$'); 122.36+122.44 (phenyl C$_4$'); 124.74+124.77 (phenyl C$_5$'); 127.01 (phenyl C$_3$+C$_5$); 129.42 (phenyl C$_2$+C$_6$); 136.77 (phenyl C$_4$); 139.65+139.73 (phenyl C$_1$'); 140.50 (phenyl C$_1$); 153.68+156.11 (phenyl C$_2$'-F); 164.11 (C=N); 177.77 (C=S) (Figure 61).

Figure 61. ^{13}C NMR spectrum of Compound **10c**

5-[1-(4-Isobutylphenyl)ethyl]-3-{[4-(3-(trifluoromethyl)phenyl]piperazin-1-yl}-methyl}-1,3,4-oxadiazole-2(*3H*)-thione (Compound 10d)

5-[1-(4-Isobutylphenyl)ethyl]-1,3,4-oxadiazole-2(*3H*)-thione (0.01 mol, 2.62 g), 1-(3-trifluoromethylphenyl)piperazine (0.01 mol, 2.30 g), formaldehyde (0.015 mol, 0.55 ml) in 15 ml methanol were reacted according to general synthesis method at 3.1.2.4.

Yield (%)	:	56
Retention factor (R$_f$)	:	0.65 [Toluene: Acetone: Acetic Acid (75:25:10)]
Physical appearance	:	White powder
Melting point (ºC)	:	77
Solubility	:	Highly soluble with acetone and DMSO. Practically insoluble in water

Elemental analysis

Molecular formula	:	C$_{26}$H$_{31}$F$_3$N$_4$OS
Molecular weight (g/mol)	:	504.61

	C	H	N	S
Calculated (%)	61.88	6.19	11.10	6.35
Found (%)	61.64	6.49	11.14	6.39

Spectral Analysis

Infrared (IR) spectrum

ν_{max} **(cm^{-1}) :** 2954 (aromatic C-H stretchings); 2886 (aliphatic C-H stretchings); 1610 (C=N stretching); 1512, 1497 (aromatic C=C stretchings); 1447 (C-N stretching); 1329 (C-O stretching); 1242 (C=S stretching); 1169 (C-F stretchings); 851 (1,4-dialkylphenyl C-H bendings); 781 (3-trifluoromethylphenyl C-H bendings) (Figure 62).

Figure 62. IR spectrum of Compound **10d**

^{1}H NMR spectrum

δ ppm (400 MHz/DMSO-d_6): 0.83 (6H, d, J=6.4 Hz, isobutyl -C$\underline{H}_3$); 1.55 (3H, d, J=7.2 Hz, -CH-C$\underline{H}_3$); 1.77-1.81 (1H, m, isobutyl –C$\underline{H}$-); 2.40 (2H, d, J=7.2 Hz, isobutyl –C$\underline{H}_2$-); 2.84 (4H, t, J=4.8 Hz, piperazine H$_2$+H$_6$); 3.23 (4H, t, J=4.8 Hz, piperazine H$_3$+H$_5$); 4.33 (1H, q, J=7 Hz, -C$\underline{H}$-CH$_3$,); 5.01 (2H, s, -N-C$\underline{H}_2$-N-); 7.05 (1H, d, J=7.6 Hz, phenyl H$_6$'); 7.12 (2H, d, J=8 Hz, phenyl H$_3$+H$_5$); 7.15 (1H, bs, phenyl H$_2$'); 7.19 (2H, d, J=8 Hz, phenyl H$_2$+H$_6$); 7.18-7.22 (1H, m, phenyl H$_4$'); 7.40 (1H, t, J=8 Hz, phenyl H$_5$') (Figure 63).
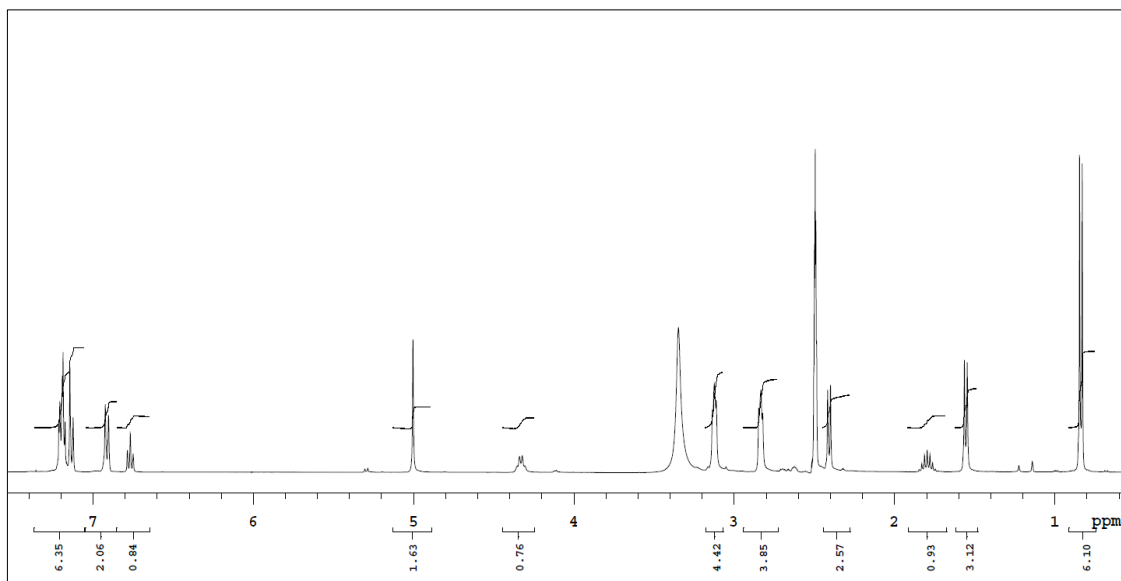
Figure 63. ^{1}H NMR spectrum of Compound **10d**

^{13}C NMR spectrum

δ ppm (400 MHz/DMSO-d_6): 18.49 (Isobutyl –$\underline{C}$H-); 22.13 (isobutyl -$\underline{C}$H$_3$); 29.50 (-CH-$\underline{C}$H$_3$); 36.09 (isobutyl -$\underline{C}$H$_2$-); 44.14 (-$\underline{C}$H-CH$_3$); 49.83 (piperazine C$_2$+C$_6$); 50.72 (piperazine C$_3$+C$_5$); 69.55 (-N-$\underline{C}$H$_2$-N-); 120.94 (phenyl C$_6$'); 122.97+125.68 (-$\underline{C}$F$_3$); 123.96 (phenyl C$_4$'); 126.99 (phenyl C$_3$+C$_5$); 127.58 (phenyl C$_2$'); 128.02 (phenyl C$_5$'); 129.43 (phenyl C$_2$+C$_6$); 130.27 (phenyl $\underline{C}$$_3$'-CF$_3$); 136.82 (phenyl C$_4$); 140.52 (phenyl C$_1$); 148.83 (phenyl C$_1$'); 164.12 ($\underline{C}$=N); 177.76 ($\underline{C}$=S) (Figure 64).
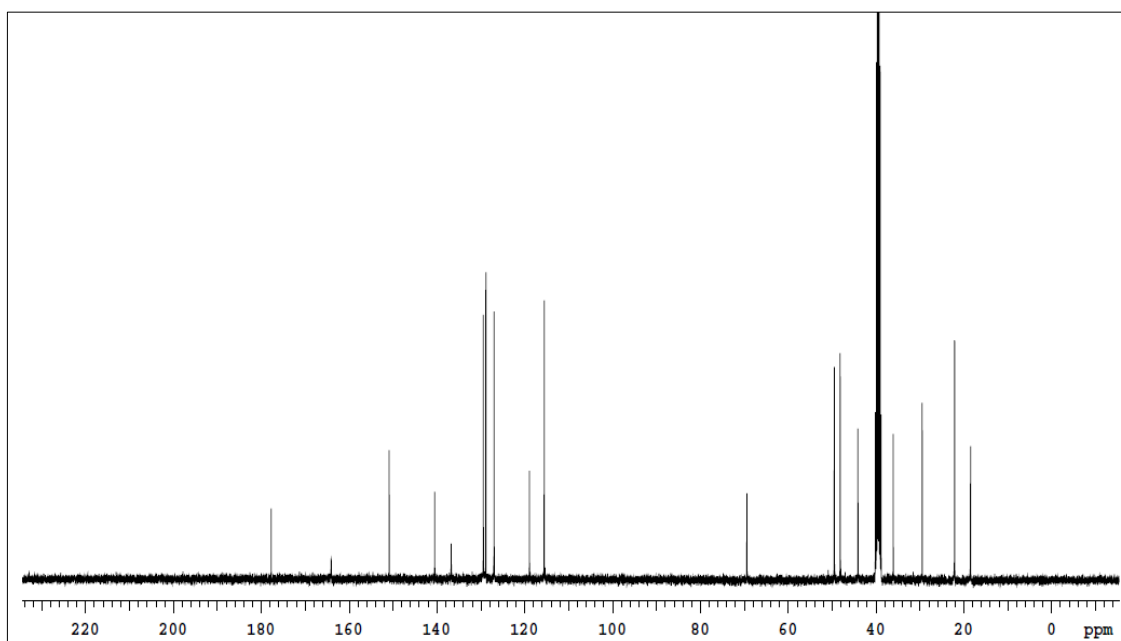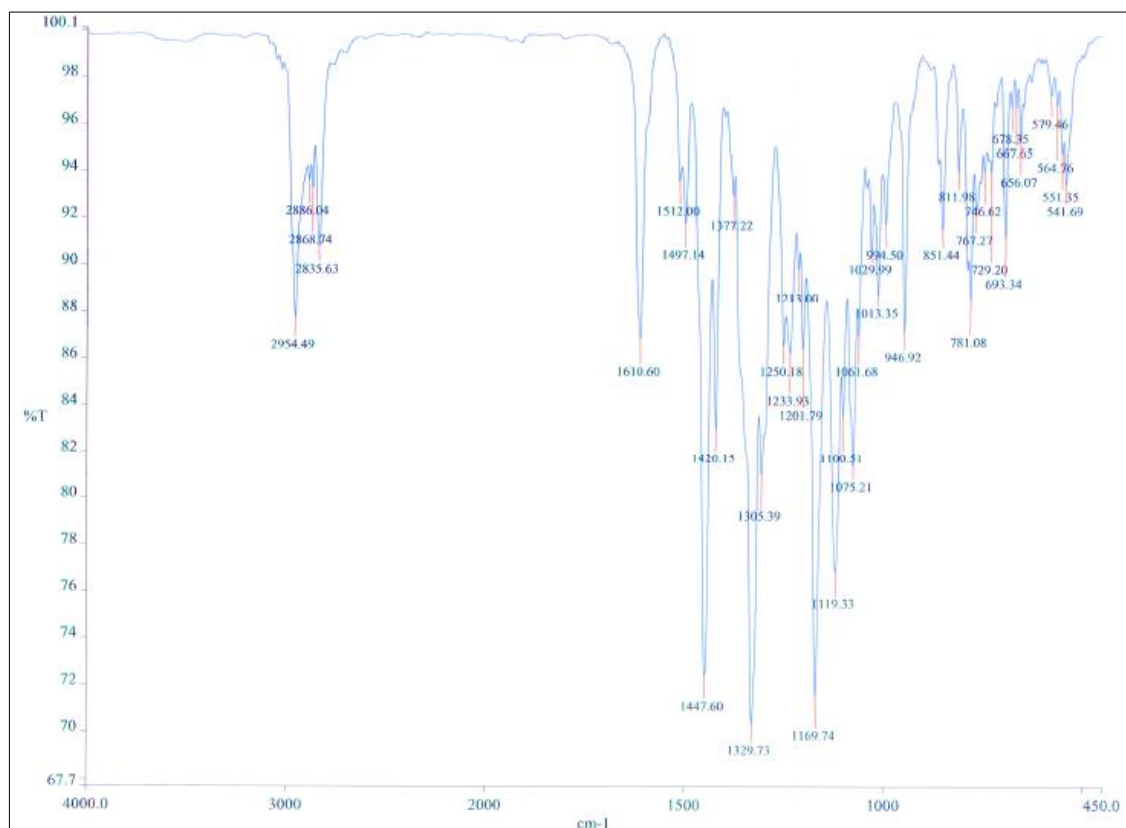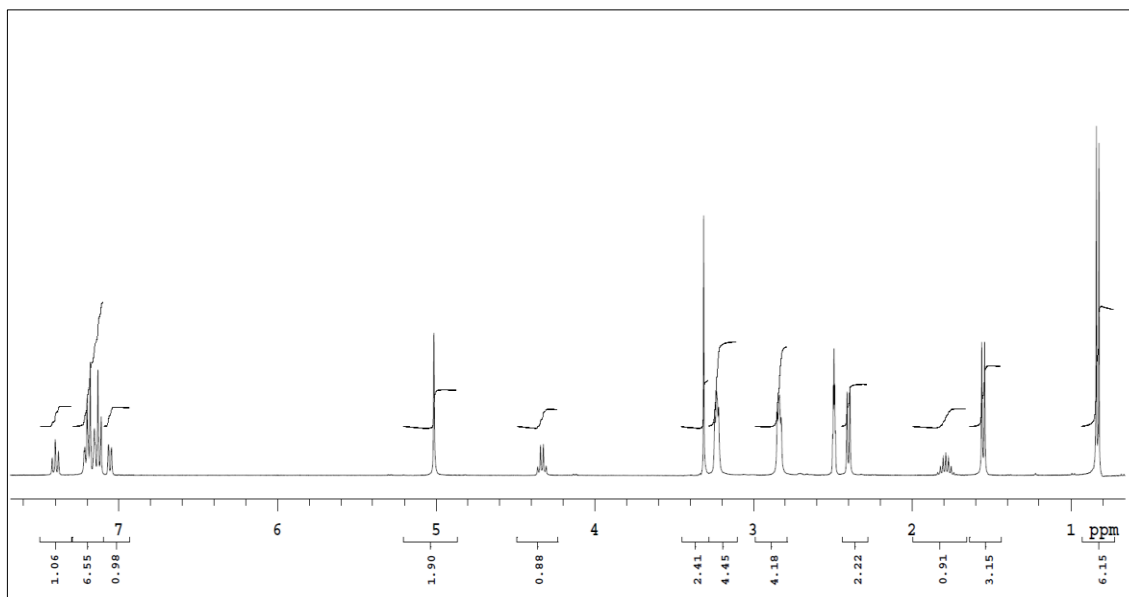

Figure 64. ^{13}C NMR spectrum of Compound **10d**

130

5-[1-(4-Isobutylphenyl)ethyl]-3-{[4-(4-chlorophenyl)piperazin-1-yl]methyl}-1,3,4-oxadiazole-2(*3H*)-thione (Compound 10e) [17]
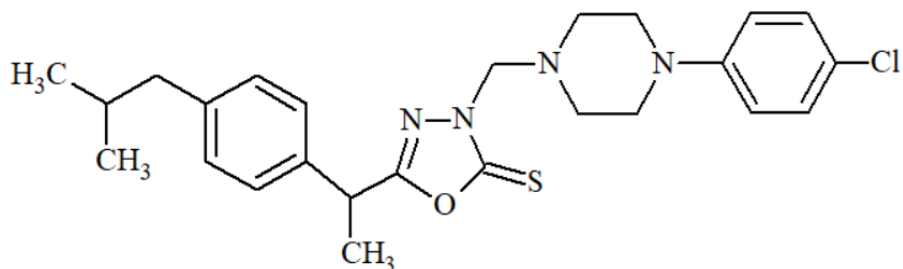
5-[1-(4-Isobutylphenyl)ethyl]-1,3,4-oxadiazole-2(*3H*)-thione (0.01 mol, 2.62 g), 1-(4-chlorophenyl)piperazine (0.01 mol, 1.96 g), formaldehyde (0.015 mol, 0.55 ml) in 15 ml methanol were reacted according to general synthesis method at 3.1.2.4.

Yield (%)	:	54
Retention factor (Rf)	:	0.63 [Toluene: Acetone: Acetic Acid (75:25:10)]
Physical appearance	:	White powder
Melting point (°C)	:	99
Solubility	:	Highly soluble with acetone and DMSO. Practically insoluble in water

Spectral Analysis

Infrared (IR) spectrum

ν_{max} **(cm^{-1}) :** 2949 (aromatic C-H stretchings); 2827 (aliphatic C-H stretchings); 1617 (C=N stretching); 1596, 1496 (aromatic C=C stretchings); 1444 (C-N stretching); 1329 (C-O stretching); 1242 (C=S stretching); 812 (1,4-dialkyl phenyl C-H bendings); 790 (4-chlorophenyl C-H bendings) (Figure 65).
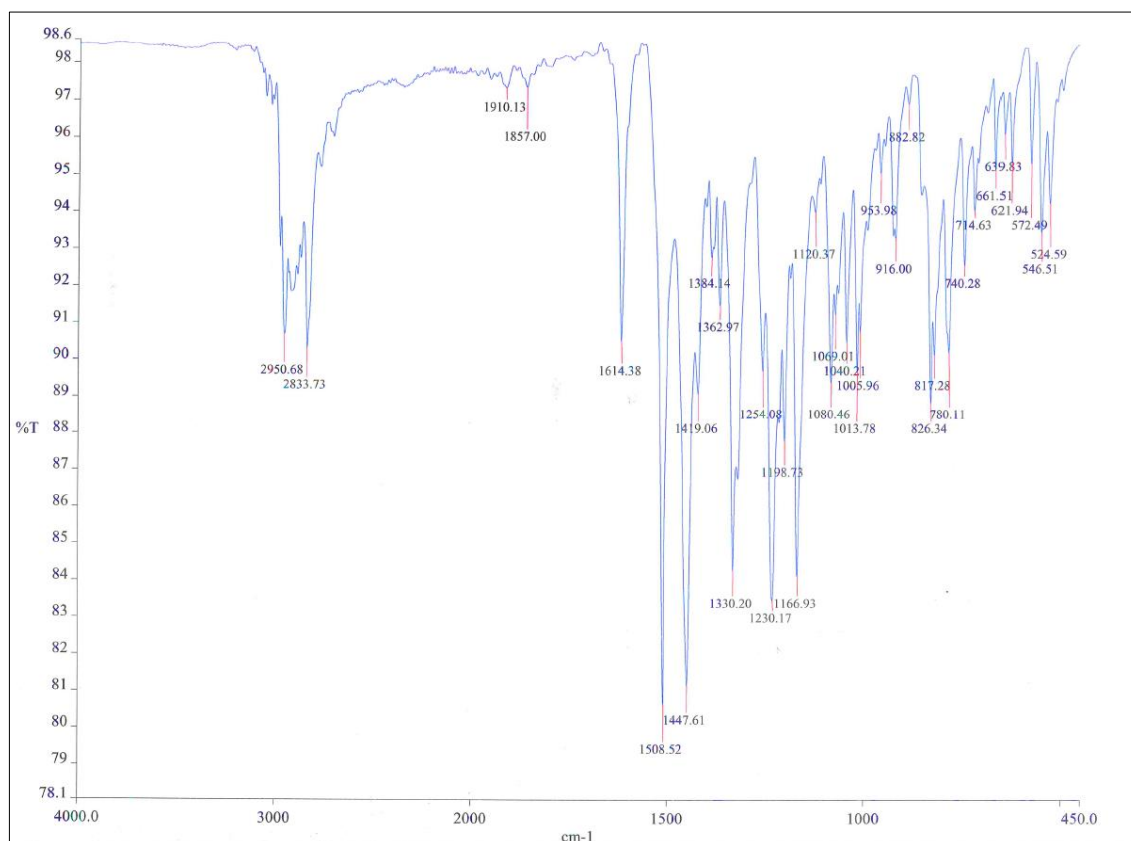

Figure 65. IR spectrum of Compound **10e**

^{1}H NMR spectrum

δ ppm (400 MHz/DMSO-d_6): 0.83 (6H, d, J=6.4 Hz, isobutyl -C$\underline{H}_3$); 1.55 (3H, d, J=7.2 Hz, -CH-C$\underline{H}_3$); 1.77-1.81 (1H, m, isobutyl –C$\underline{H}$-); 2.40 (2H, d, J=6.8 Hz, isobutyl –C$\underline{H}_2$-); 2.87 (4H, t, J=5 Hz, piperazine H$_2$+H$_6$); 3.13 (4H, t, J=5 Hz, piperazine H$_3$+H$_5$); 4.32 (1H, q, J=7.2 Hz, -C$\underline{H}$-CH$_3$,); 4.99 (2H, s, -N-C$\underline{H}_2$-N-); 6.92 (2H, bd, J=9.4 Hz, phenyl H$_2$'+H$_6$'); 7.12 (2H, bd, J=8.6 Hz, phenyl H$_3$+H$_5$); 7.18 (2H, bd, J=8.6 Hz, phenyl H$_2$+H$_6$); 7.21 (2H, bd, J=9.4 Hz, phenyl H$_3$'+H$_5$') (Figure 66).
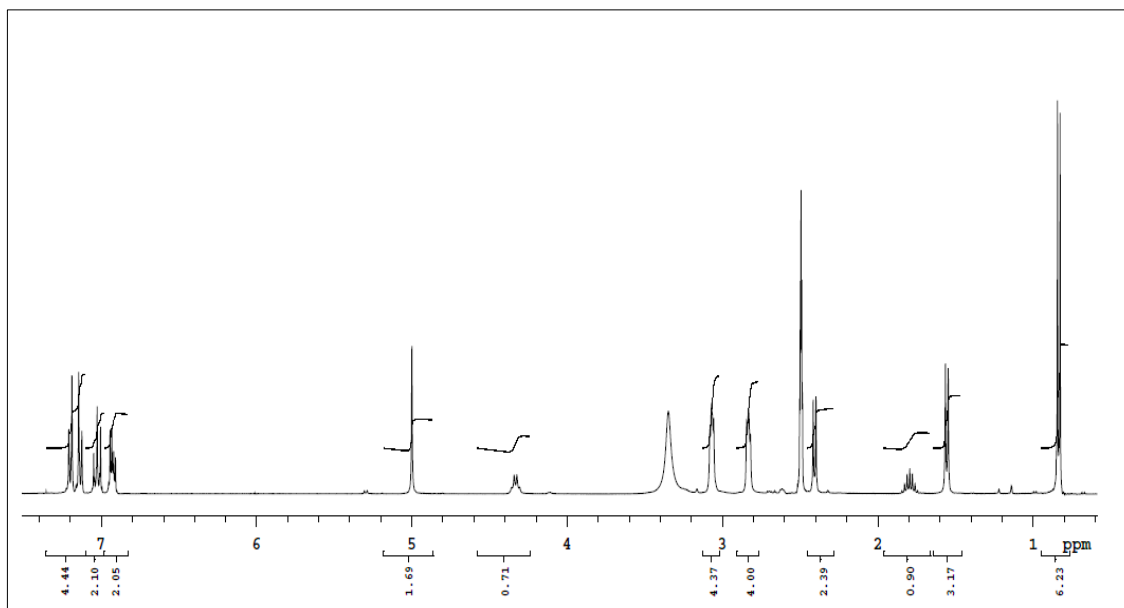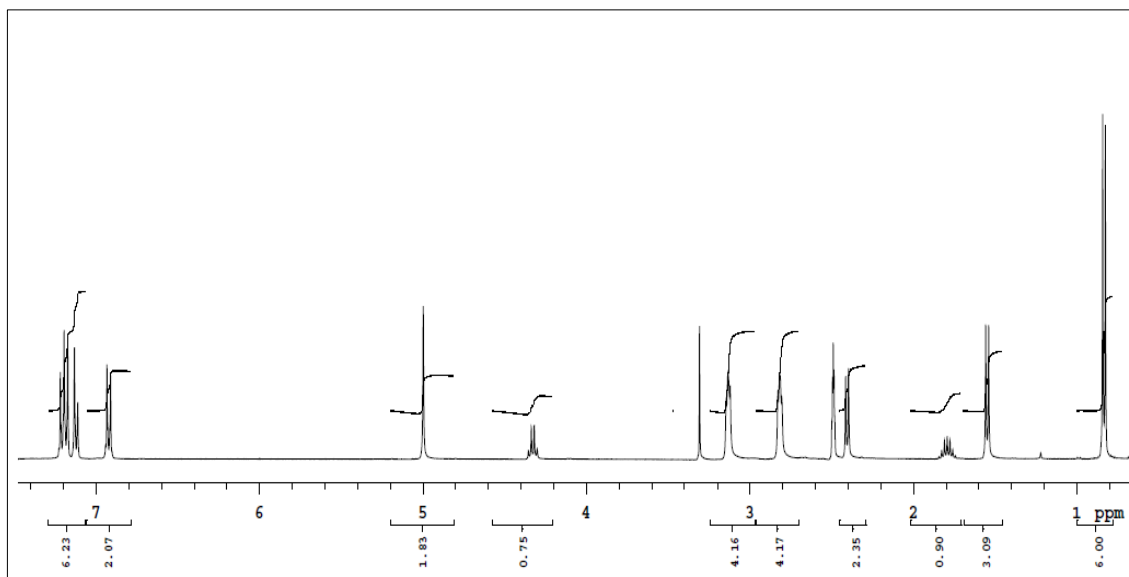
Figure 66. ^{1}H NMR spectrum of Compound **10e**

^{13}C NMR spectrum

δ ppm (400 MHz/DMSO-d_6): 18.48 (isobutyl –$\underline{C}$H-); 22.11+22.13 (isobutyl -$\underline{C}$H$_3$); 29.50 (-CH-$\underline{C}$H$_3$); 36.07 (isobutyl -$\underline{C}$H$_2$-); 44.13 (-$\underline{C}$H-CH$_3$); 47.95 (piperazine C$_2$+C$_6$); 49.27 (piperazine C$_3$+C$_5$); 69.36 (-N-$\underline{C}$H$_2$-N-); 116.97 (phenyl C$_2$'+C$_6$'); 122.36 (phenyl C$_4$'); 126.94 (phenyl C$_3$+C$_5$); 128.56 (phenyl C$_3$'+C$_5$'); 129.43 (phenyl C$_2$+C$_6$); 136.75 (phenyl C$_4$); 140.51 (phenyl C$_1$); 149.59 (phenyl C$_1$'); 164.07 ($\underline{C}$=N); 177.73 ($\underline{C}$=S) (Figure 67).
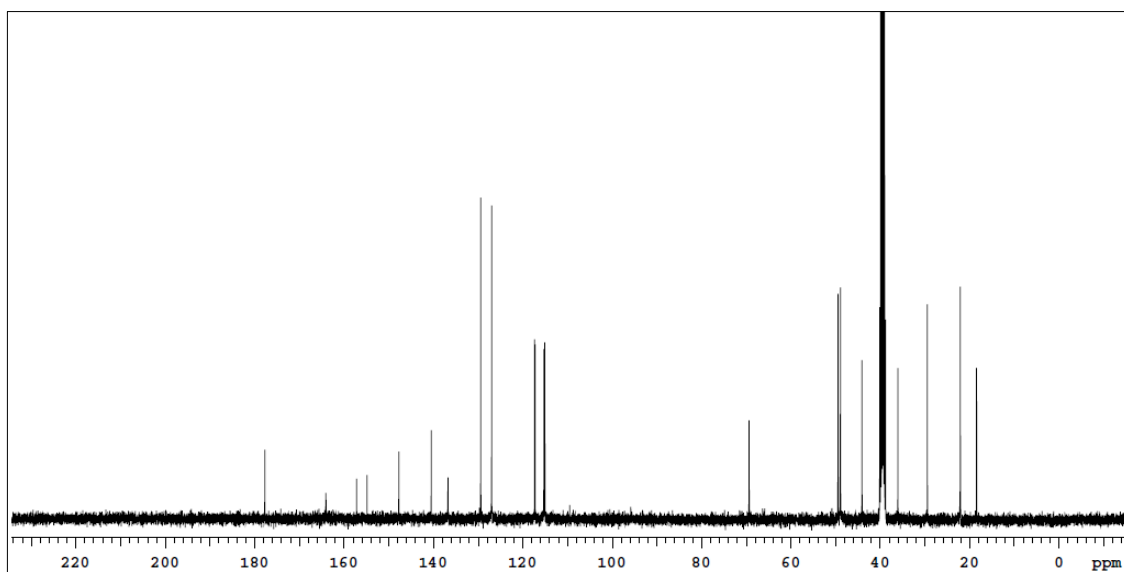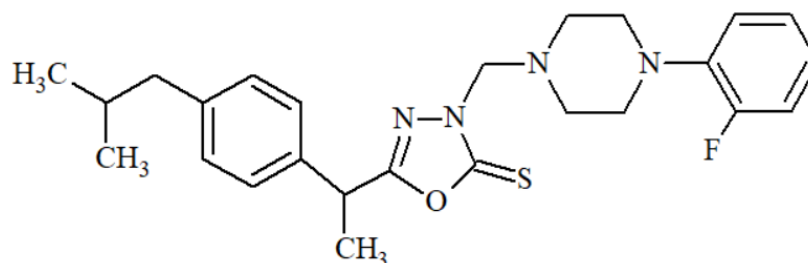

Figure 67. ^{13}C NMR spectrum Compound **10e**

5-[1-(4-Isobutylphenyl)ethyl]-3-{[4-(2-chlorophenyl)piperazin-1-yl]methyl}-1,3,4-oxadiazole-2(*3H*)-thione (Compound 10f)
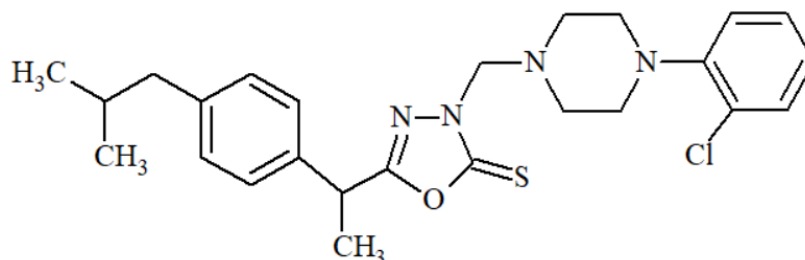
5-[1-(4-Isobutylphenyl)ethyl]-1,3,4-oxadiazole-2(*3H*)-thione (0.01 mol, 2.62 g), 1-(2-chlorophenyl)piperazine monohydrochloride (0.01 mol, 2.33 g), formaldehyde (0.015 mol, 0.55 ml) in 15 ml methanol were reacted according to general synthesis method at 3.1.2.4.

Yield (%)	:	39
Retention factor (Rf)	:	0.61 [Toluene: Acetone: Acetic Acid (75:25:10)]
Physical appearance	:	White powder
Melting point (ºC)	:	94
Solubility	:	Highly soluble with acetone and DMSO. Practically insoluble in water
Elemental analysis		
Molecular formula	:	$C_{25}H_{31}ClN_4OS$
Molecular weight (g/mol)	:	471.06

	C	H	N	S
Calculated (%)	63.74	6.63	11.89	6.81
Found (%)	63.05	6.83	12.12	6.97

Spectral Analysis

Infrared (IR) spectrum

v_{max} **(cm^{-1}) :** 3053 (aromatic C-H stretchings); 2819 (aliphatic C-H stretchings); 1618 (C=N stretching); 1586, 1479 (aromatic C=C stretchings); 1443 (C-N stretching); 1330 (C-O stretching); 1250 (C=S stretching); 845 (1,4-dialkylphenyl C-H bendings); 741 (2-chlorophenyl C-H bendings) (Figure 68).
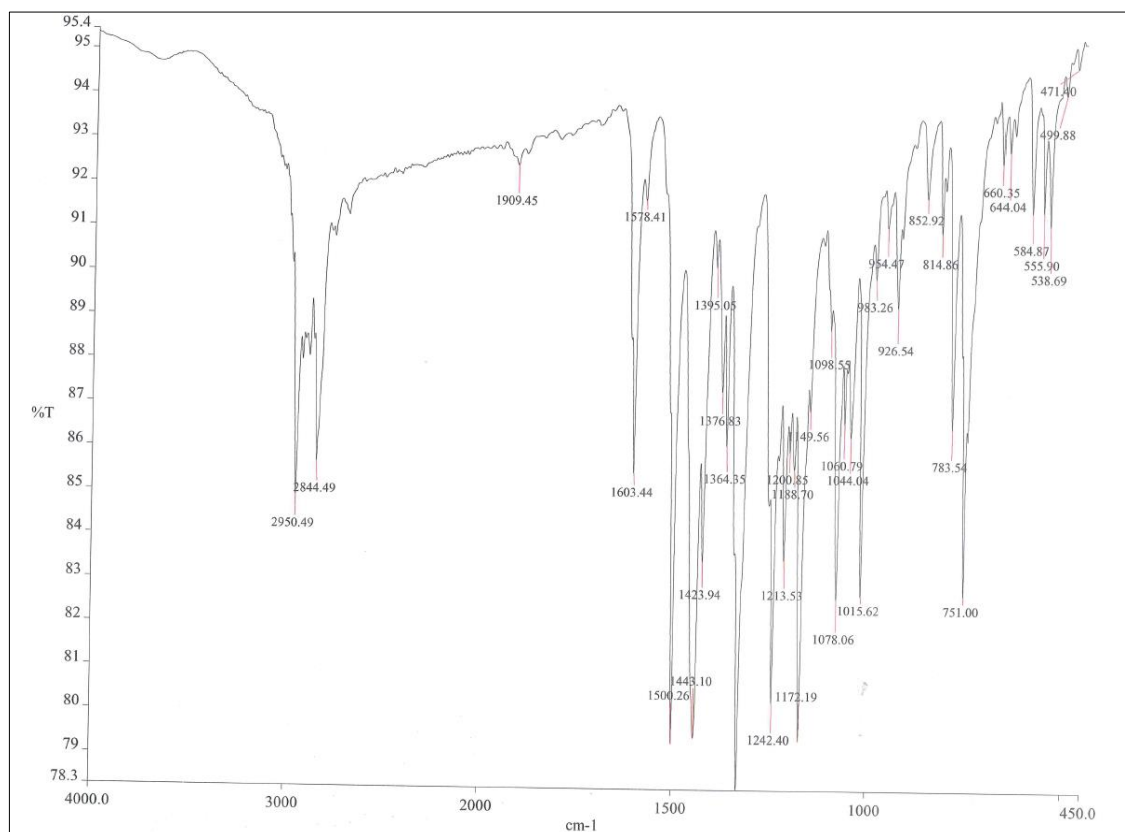

Figure 68. IR spectrum of Compound **10f**

^{1}H NMR spectrum

δ ppm (400 MHz/DMSO-d_6): 0.85 (6H, d, J=6.4 Hz, isobutyl -C$\underline{H}_3$); 1.58 (3H, d, J=7.2 Hz, -CH-C$\underline{H}_3$); 1.79-1.83 (1H, m, isobutyl -C$\underline{H}$-); 2.42 (2H, d, J=7.2 Hz, isobutyl –C$\underline{H}_2$-); 2.87 (4H, d, J=4.4 Hz, piperazine H$_2$+H$_6$); 2.96 (4H, d, J=4.4 Hz, piperazine H$_3$+H$_5$); 4.37 (1H, q, J=7.2 Hz, -C$\underline{H}$-CH$_3$,); 5.01 (2H, s, -N-C$\underline{H}_2$-N-); 7.02-7.06 (1H, m, phenyl H$_5$'); 7.15 (1H, dd, J=8.2 J'=1.8 Hz, phenyl H$_6$'); 7.16 (2H, bd, J=8 Hz, phenyl H$_3$+H$_5$); 7.23 (2H, bd, J=8 Hz, phenyl H$_2$+H$_6$); 7.27-7.31 (1H, m, phenyl H$_4$'); 7.40 (2H, dd, J=8.2 J'=1.4 Hz, phenyl H$_3^{'}$) (Figure 69).
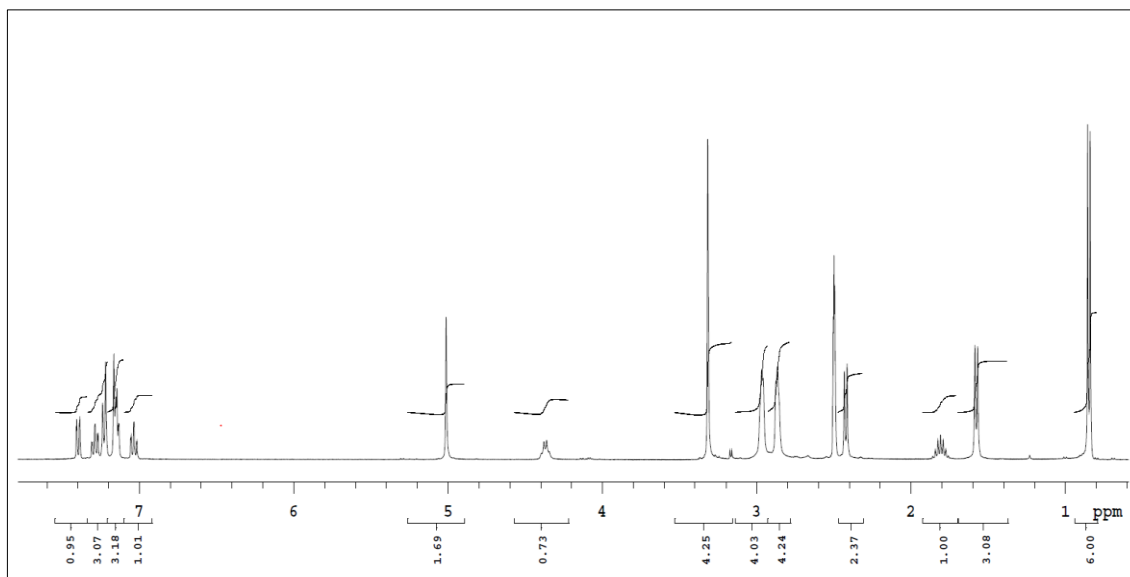
Figure 69. ^{1}H NMR spectrum of Compound **10f**

^{13}C NMR spectrum

δ ppm (400 MHz/DMSO-d_6): 18.50 (isobutyl –CH-); 22.13 (isobutyl -CH$_3$); 29.51 (-CH-CH$_3$); 36.09 (isobutyl -CH$_2$-); 44.14 (-CH-CH$_3$); 49.83 (piperazine C$_2$+C$_6$); 50.72 (piperazine C$_3$+C$_5$); 69.55 (-N-CH$_2$-N-); 120.93 (phenyl C$_4$'); 123.96 (phenyl C$_3$'); 126.99 (phenyl C$_3$+C$_5$); 127.58 (phenyl C$_6$'); 128.03 (phenyl C$_5$'); 129.43 (phenyl C$_2$+C$_6$); 130.28 (phenyl C$_1$); 136.83 (phenyl C$_4$); 140.52 (phenyl C$_1$'); 148.83 (C$_2$'); 164.13 (C=N); 177.78 (C=S) (Figure 70).
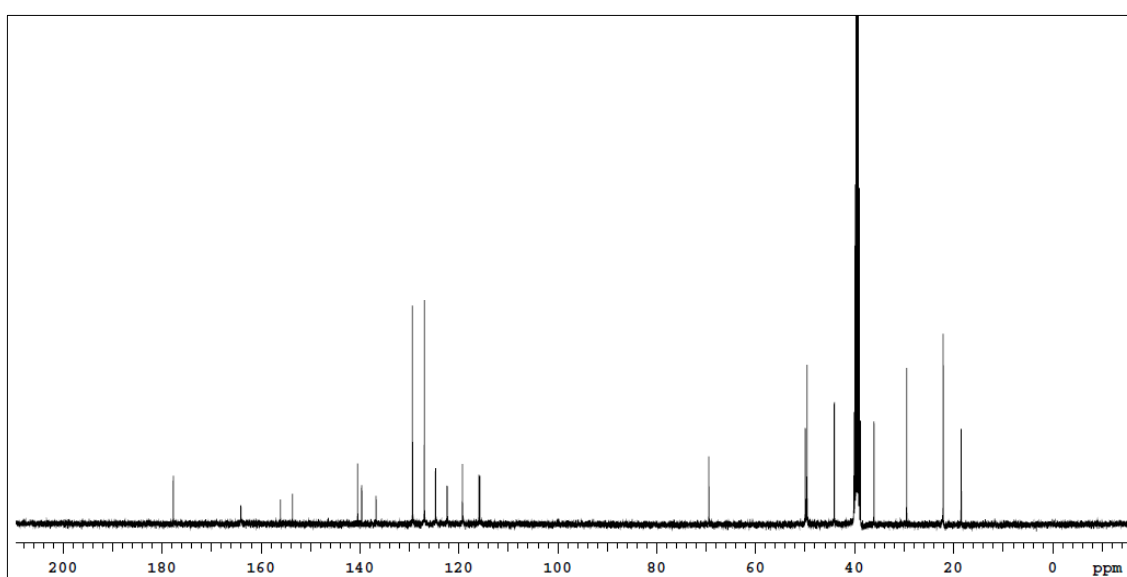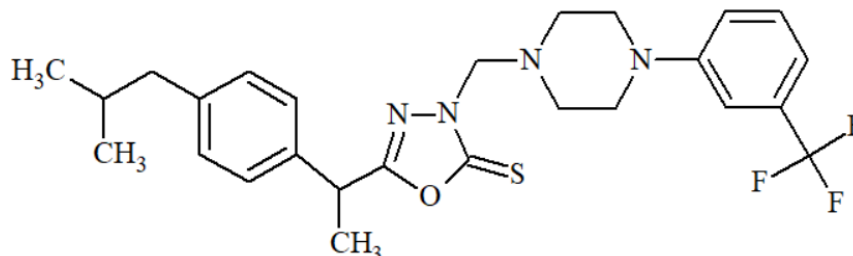

Figure 70. ^{13}C NMR spectrum of Compound **10f**

5-[1-(4-Isobutylphenyl)ethyl]-3-{[4-(3,4-dichlorophenyl)piperazin-1-yl]methyl}-1,3,4-oxadiazole-2(*3H*)-thione (Compound 10g)
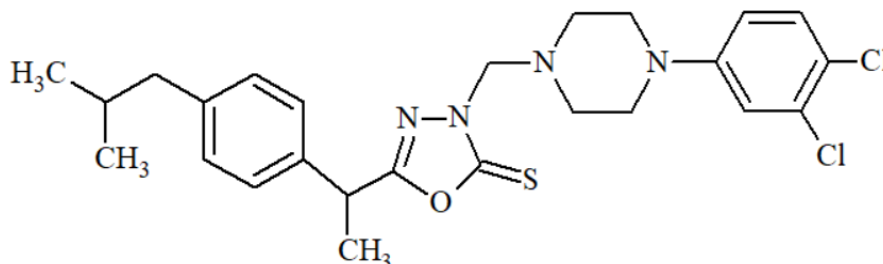
5-[1-(4-Isobutylphenyl)ethyl]-1,3,4-oxadiazole-2(*3H*)-thione (0.01 mol, 2.62 g), 1-(3,4-chlorophenyl)piperazine (0.01 mol, 2.31 g), formaldehyde (0.015 mol, 0.55 ml) in 15 ml methanol were reacted according to general synthesis method at 3.1.2.4.

Yield (%)	:	63
Retention factor (R$_f$)	:	0.60 [Toluene: Acetone: Acetic Acid (75:25:10)]
Physical appearance	:	White powder
Melting point (ºC)	:	116
Solubility	:	Highly soluble with acetone and DMSO. Practically insoluble in water

Elemental analysis

Molecular formula	:	C$_{25}$H$_{30}$Cl$_2$N$_4$OS
Molecular weight (g/mol)	:	505.50

	C	H	N	S
Calculated (%)	59.40	5.98	11.08	6.34
Found (%)	58.78	6.12	11.15	6.40

Spectral Analysis

Infrared (IR) spectrum

ν_{max} **(cm^{-1}) :** 2946 (aliphatic C-H stretchings); 2846 (aliphatic C-H stretchings); 1619 (C=N stretching); 1593, 1551, 1512, 1486 (aromatic C=C stretchings); 1442 (C-N stretching); 1330 (C-O stretching); 1258 (C=S stretching); 835 (1,4-dialkylphenyl C-H bendings); 802 (3,4-dichlorophenyl C-H bendings) (Figure 71).

Figure 71. IR spectrum of Compound **10g**

^{1}H NMR spectrum

δ ppm (400 MHz/DMSO-d_6): 0.83 (6H, d, J=6.4 Hz, isobutyl -C$\underline{H}_3$); 1.54 (3H, d, J=6.8 Hz, -CH-C$\underline{H}_3$); 1.77-1.81 (1H, m, isobutyl -C$\underline{H}$-); 2.40 (2H, d, J=7.2 Hz, isobutyl –C$\underline{H}_2$-); 2.78 (4H, t, J=4.8 Hz, piperazine H$_2$+H$_6$); 3.19 (4H, t, J=4.8 Hz, piperazine H$_3$+H$_5$); 4.32 (1H, q, J=7.2 Hz, -C$\underline{H}$-CH$_3$,); 4.99 (2H, s, -N-C$\underline{H}_2$-N-); 6.91 (1H, dd, J=9.2 J'=2.8 Hz, phenyl H$_6$'); 7.11 (1H, d, J=3.2 Hz, phenyl H$_2$'); 7.12 (2H, d, J=8 Hz, phenyl H$_3$+H$_5$); 7.17 (2H, d, J=8 Hz, phenyl H$_2$+H$_6$); 7.40 (1H, d, J=9.2 Hz, phenyl H$_5$') (Figure 72).
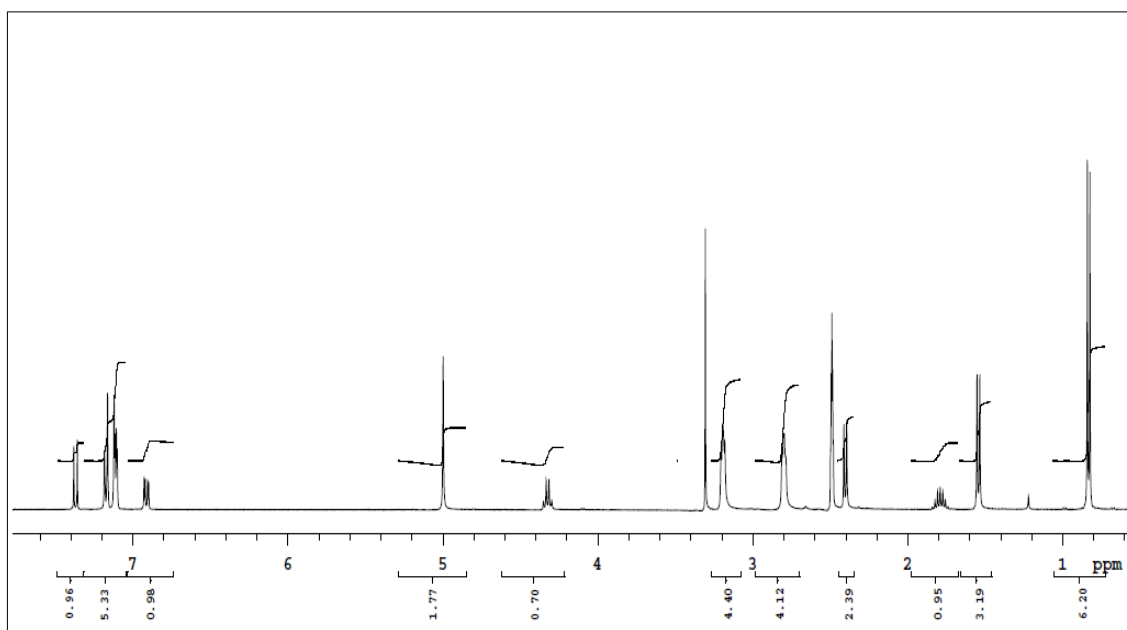
Figure 72. ¹H NMR spectrum of Compound **10g**

¹³C NMR spectrum

δ ppm (400 MHz/DMSO-d_6):18.47 (isobutyl –$\underline{C}$H-); 22.11+22.12 (isobutyl -$\underline{C}$H$_3$); 29.50 (-CH-$\underline{C}$H$_3$); 36.06 (isobutyl -$\underline{C}$H$_2$-); 44.13 (-$\underline{C}$H-CH$_3$); 47.44 (piperazine C$_2$+C$_6$); 49.10 (piperazine C$_3$+C$_5$); 69.30 (-N-$\underline{C}$H$_2$-N-); 115.39 (phenyl C$_6$'); 116.30 (phenyl C$_5$'); 119.54 (phenyl C$_2$'); 126.94 (phenyl C$_3$+C$_5$); 129.41 (phenyl C$_2$+C$_6$); 130.40 (phenyl C$_4$'); 131.45 (phenyl C$_3$'); 136.74 (phenyl C$_4$); 140.50 (phenyl C$_1$); 150.45 (phenyl C$_1$'); 164.07 ($\underline{C}$=N); 177.71 ($\underline{C}$=S) (Figure 73).
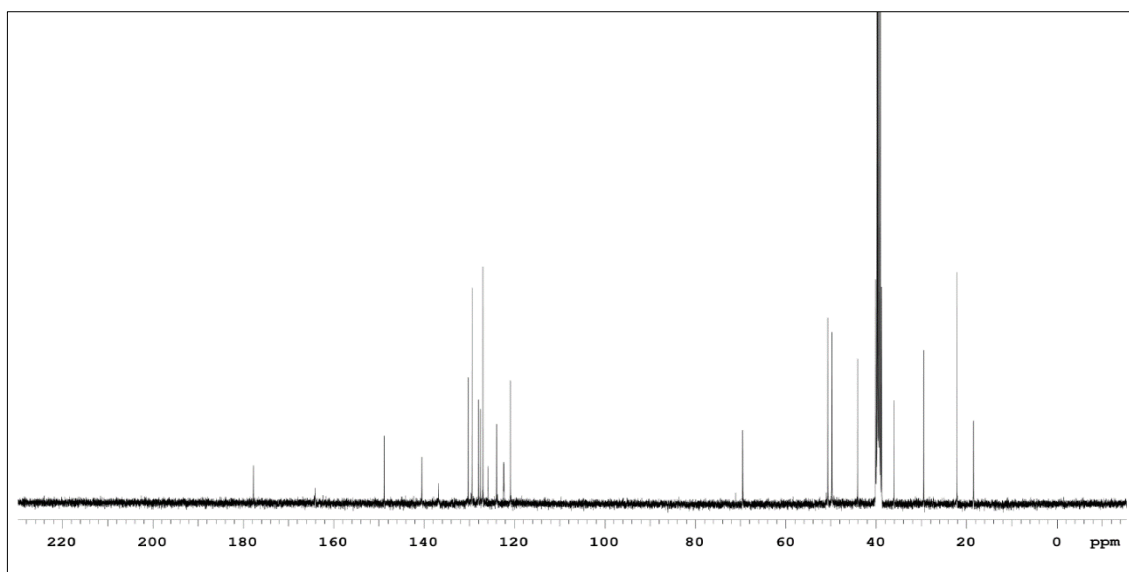

Figure 73. ¹³C NMR spectrum of Compound **10g**

139

5-[1-(4-Isobutylphenyl)ethyl]-3-{[4-(2,3-dichlorophenyl)piperazin-1-yl]methyl}-1,3,4-oxadiazole-2(*3H*)-thione (Compound 10h)
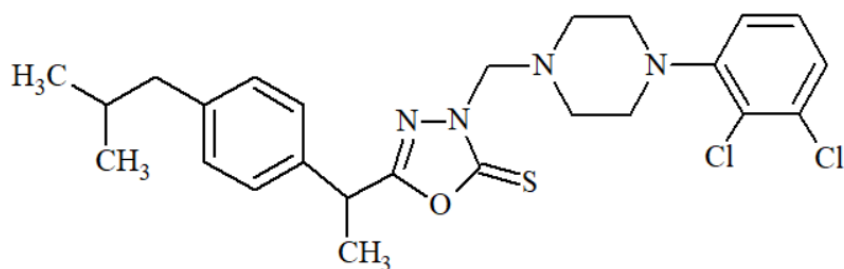
5-[1-(4-Isobutylphenyl)ethyl]-1,3,4-oxadiazole-2(*3H*)-thione (0.01 mol, 2.62 g), 1-(2,3-dichlorophenyl)piperazine hydrochloride (0.01 mol, 2.67 g), formaldehyde (0.015 mol, 0.55 ml) in 15 ml methanol were reacted according to general synthesis method at 3.1.2.4.

Yield (%)	: 52
Retention factor (R_f)	: 0.60 [Toluene: Acetone: Acetic Acid (75:25:10)]
Physical appearance	: White powder
Melting point (ºC)	: 99
Solubility	: Highly soluble with acetone and DMSO. Practically insoluble in water

Elemental analysis

Molecular formula	: $C_{25}H_{30}Cl_2N_4OS$
Molecular weight (g/mol)	: 505.50

	C	H	N	S
Calculated (%)	59.40	5.98	11.08	6.34
Found (%)	58.70	6.11	11.09	6.36

Spectral Analysis

Infrared (IR) spectrum

ν_{max} **(cm^{-1}) :** 2946 (aromatic C-H stretchings); 2845 (aliphatic C-H stretchings); 1619 (C=N stretching); 1593, 1552, 1511, 1486 (aromatic C=C stretchings); 1442 (C-N stretching); 1326 (C-O stretching); 1258 (C=S stretching); 835 (1,4-dialkylphenyl C-H bendings); 802 (2,3-dichlorophenyl C-H bendings) (Figure 74).
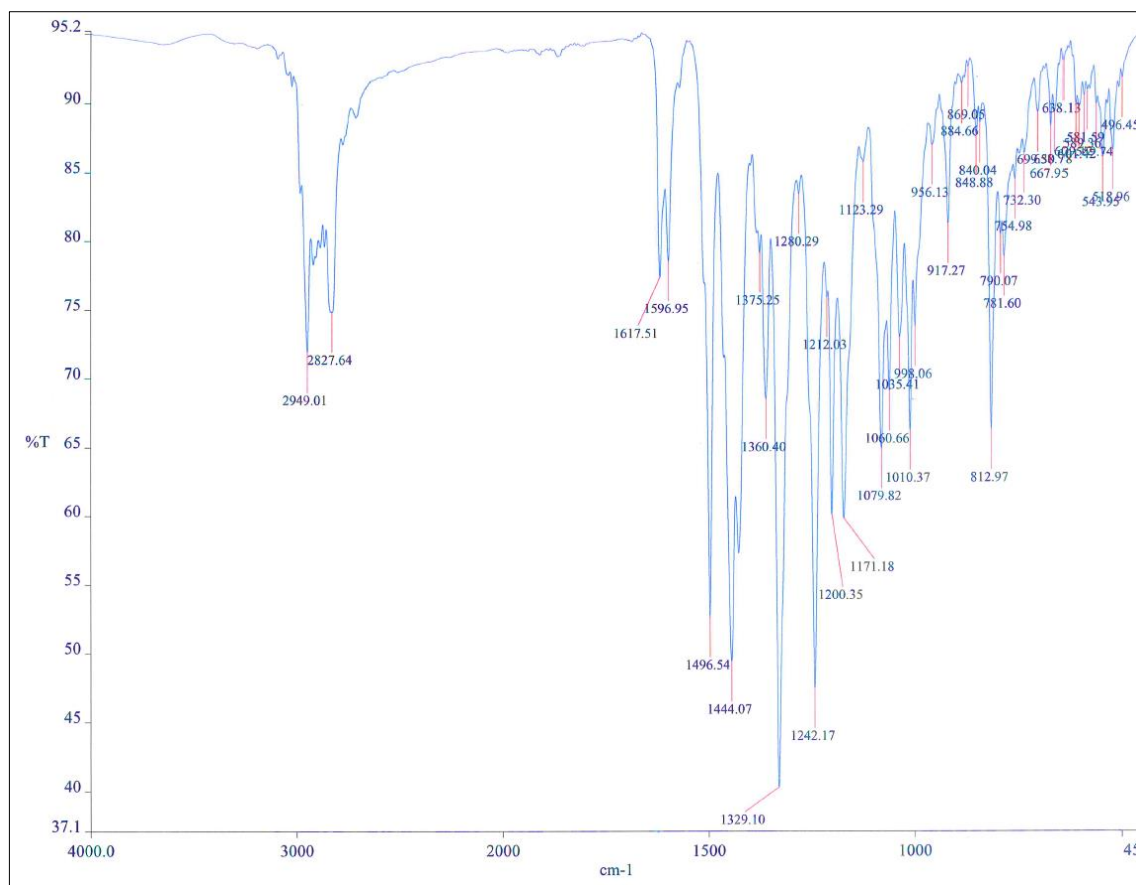

Figure 74. IR spectrum of Compound **10h**

¹H NMR spectrum

δ ppm (400 MHz/DMSO-d_6): 0.84 (6H, d, J=6.4 Hz, isobutyl -C$\underline{H}_3$); 1.57 (3H, d, J=7.6 Hz, -CH-C$\underline{H}_3$); 1.77-1.83 (1H, m, isobutyl -C$\underline{H}$-); 2.41 (2H, d, J=6.8 Hz, isobutyl –C$\underline{H}_2$-); 2.87 (4H, d, J=4.2 Hz, piperazine H_2+H_6); 2.97 (4H, d, J=4.2 Hz, piperazine H_3+H_5); 4.36 (1H, q, J=6.8 Hz, -C$\underline{H}$-CH$_3$,); 5.00 (2H, s, -N-C$\underline{H}_2$-N-); 7.14 (1H, t, J=8 Hz, phenyl H_5'); 7.15 (2H, bd, J=7.4 Hz, phenyl H_3+H_5); 7.22 (2H, bd, J=7.4 Hz, phenyl H_2+H_6); 7.28-7.31 (2H, m, phenyl H_4'+H_6') (Figure 75).
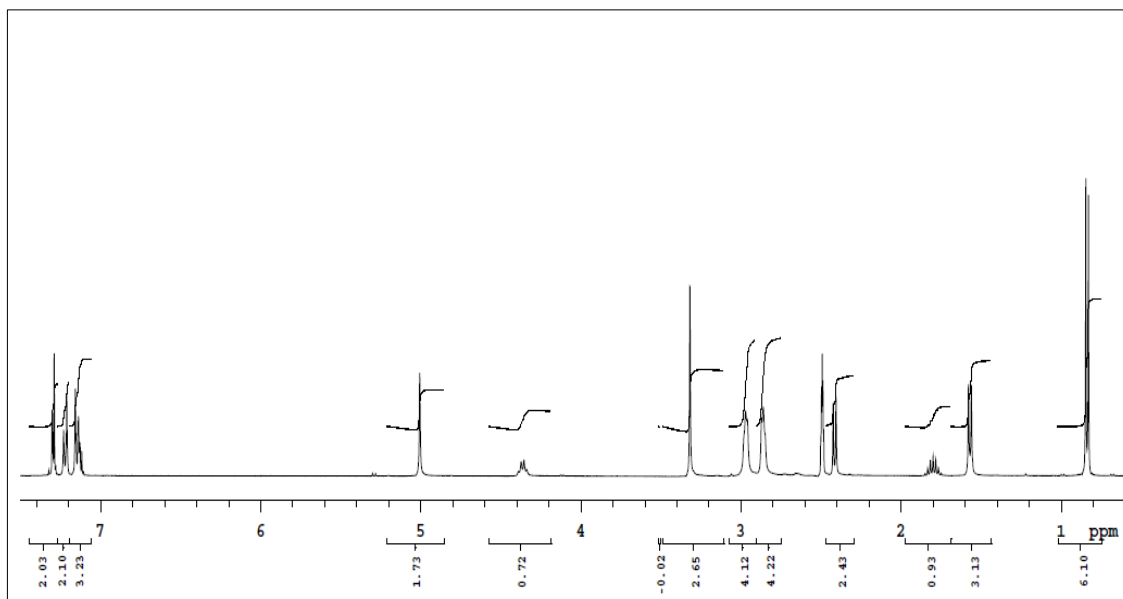
Figure 75. ^{1}H NMR spectrum of Compound **10h**

^{13}C NMR spectrum

δ ppm (400 MHz/DMSO-d_6): 18.48 (isobutyl –CH-); 22.12+22.13 (isobutyl -CH$_3$); 29.50 (-CH-CH$_3$); 36.08 (isobutyl -CH$_2$-); 44.14 (-CH-CH$_3$); 49.77 (piperazine C$_2$+C$_6$); 50.79 (piperazine C$_3$+C$_5$); 69.51 (-N-CH$_2$-N-); 119.68 (phenyl C$_6$'); 124.47 (phenyl C$_4$'); 126.02 (phenyl C$_2$'); 126.99 (phenyl C$_3$+C$_5$); 128.41 (phenyl C$_5$'); 129.43 (phenyl C$_2$+C$_6$); 132.57 (phenyl C$_3$'); 136.81 (phenyl C$_4$); 140.52 (phenyl C$_1$); 150.98 (phenyl C$_1$'); 164.14 (C=N); 177.76 (C=S) (Figure 76).
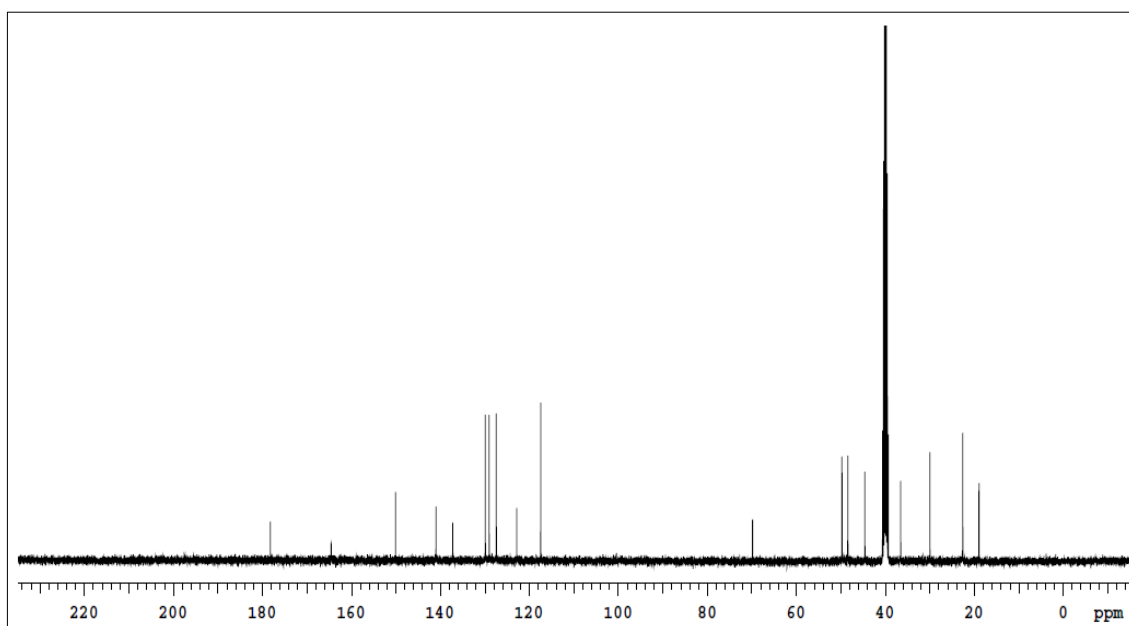

Figure 76. ^{13}C NMR spectrum of Compound **10h**

5-[1-(4-Isobutylphenyl)ethyl]-3-{[4-(4-methylphenyl)piperazin-1-yl]methyl}-1,3,4-oxadiazole-2(*3H*)-thione (Compound 10i)
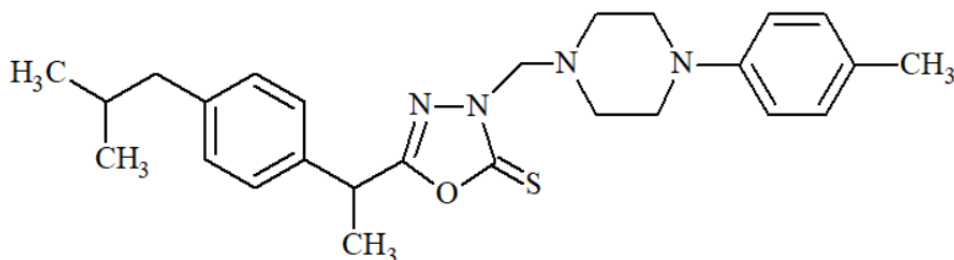
5-[1-(4-Isobutylphenyl)ethyl]-1,3,4-oxadiazole-2(*3H*)-thione (0.01 mol, 2.62 g), 1-(4-methylphenyl)piperazine (0.01 mol, 1.76 g), formaldehyde (0.015 mol, 0.55 ml) in 15 ml methanol were reacted according to general synthesis method at 3.1.2.4.

Yield (%)	: 70
Retention factor (R$_f$)	: 0.64 [Toluene: Acetone: Acetic Acid (75:25:10)]
Physical appearance	: White powder
Melting point (ºC)	: 98
Solubility	: Highly soluble with acetone and DMSO. Practically insoluble in water

Elemental analysis

Molecular formula	: C$_{26}$H$_{34}$N$_4$OS
Molecular weight (g/mol)	: 450.63

	C	H	N	S
Calculated (%)	69.30	7.60	12.43	7.12
Found (%)	69.08	7.67	12.52	7.21

Spectral Analysis

Infrared (IR) spectrum

v_{max} **(cm^{-1}) :** 2948 (aromatic C-H stretchings); 2824 (aliphatic C-H stretchings); 1620 (C=N stretching); 1574, 1519 (aromatic C=C stretchings); 1441 (C-N stretching); 1326 (C-O stretching); 1245 (C=S stretching); 848 (1,4-dialkylphenyl C-H bendings); 807 (4-methylphenyl C-H bendings) (Figure 77).
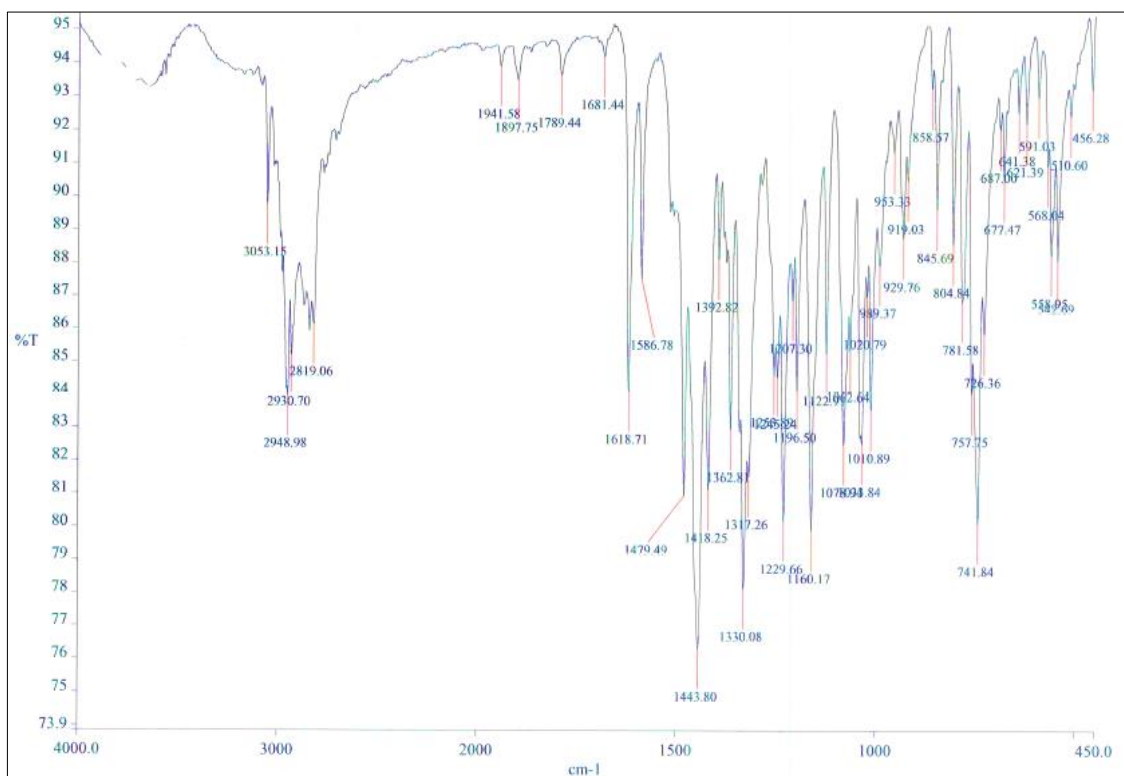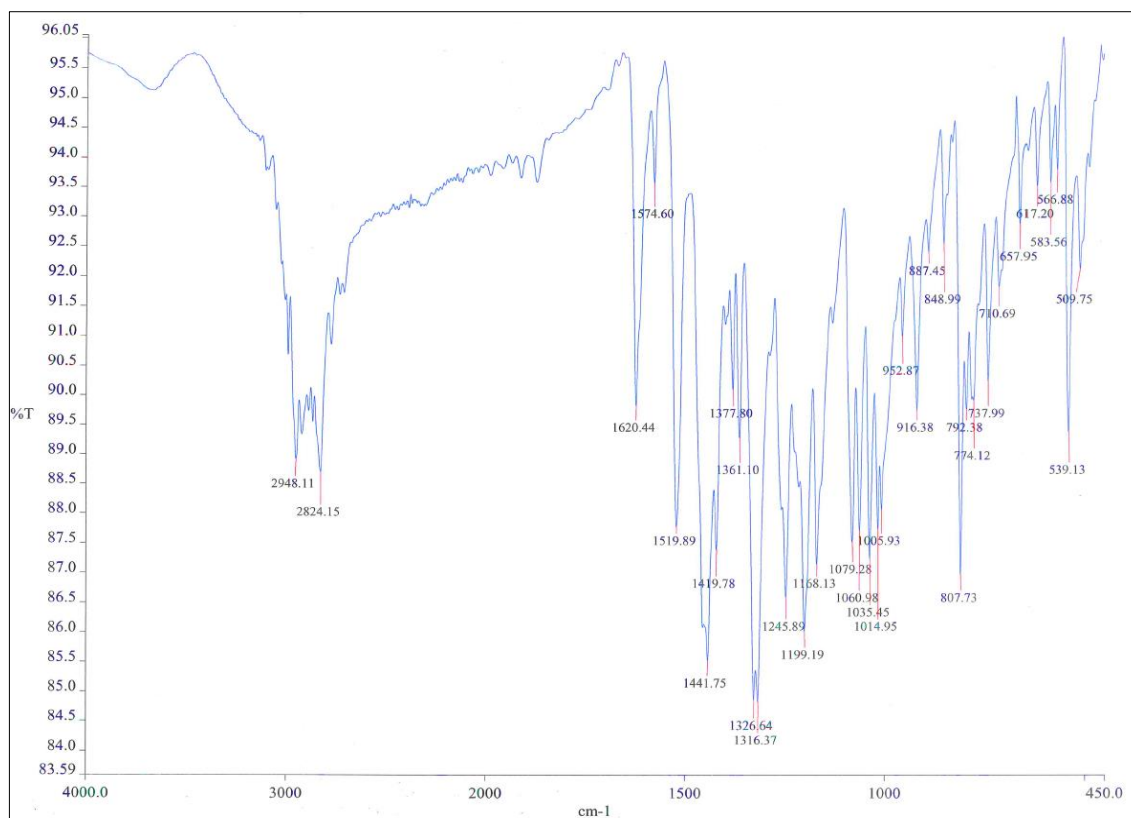

Figure 77. IR spectrum of Compound **10i**

^{1}H NMR spectrum

δ ppm (400 MHz/DMSO-d_6): 0.83 (6H, d, J=6.8 Hz, isobutyl -C$\underline{H}_3$); 1.55 (3H, d, J=7.2 Hz, -CH-C$\underline{H}_3$); 1.77-1.81 (1H, m, isobutyl –C$\underline{H}$-); 2.18 (3H, s, phenyl C$\underline{H}_3$); 2.40 (2H, d, J=7.6 Hz, isobutyl –C$\underline{H}_2$-); 2.83 (4H, t, J=5 Hz, piperazine H$_2$+H$_6$); 3.06 (4H, t, J=5 Hz, piperazine H$_3$+H$_5$); 4.33 (1H, q, J=7.2 Hz, -C$\underline{H}$-CH$_3$); 4.99 (2H, s, -N-C$\underline{H}_2$-N-); 6.81 (2H, d, J=8.8 Hz, phenyl H$_3$'+H$_5$'); 7.01 (2H, d, J=8.8 Hz, phenyl H$_2$'+H$_6$'); 7.13 (2H, d, J=8.2 Hz, phenyl H$_3$+H$_5$); 7.19 (2H, d, J=8.2 Hz, phenyl H$_2$+H$_6$) (Figure 78).
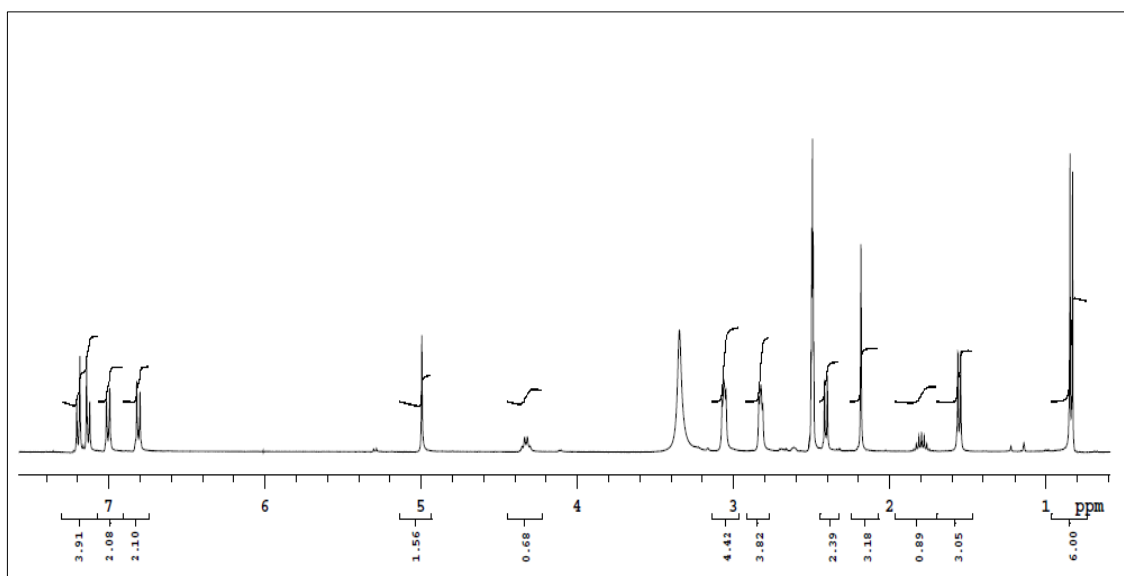
Figure 78. ^{1}H NMR spectrum of Compound **10i**

^{13}C NMR spectrum

δ ppm (400 MHz/DMSO-d_6): 18.49 (isobutyl –$\underline{C}$H-); 20.01 (phenyl -$\underline{C}$H$_3$); 22.13+22.14 (isobutyl -$\underline{C}$H$_3$); 29.50 (-CH-$\underline{C}$H$_3$); 36.09 (isobutyl -$\underline{C}$H$_2$-); 44.14 (-$\underline{C}$H-CH$_3$); 48.65 (piperazine C$_2$+C$_6$); 49.52 (piperazine C$_3$+C$_5$); 69.44 (-N-$\underline{C}$H$_2$-N-); 115.85 (phenyl C$_2$'+C$_6$'); 126.99 (phenyl C$_4$'); 127.73 (phenyl C$_3$+C$_5$); 129.31 (phenyl C$_3$'+C$_5$'); 129.44 (phenyl C$_2$+C$_6$); 136.78 (phenyl C$_4$); 140.51 (phenyl C$_1$); 148.79 (phenyl C$_1$'); 164.07 ($\underline{C}$=N); 177.75 ($\underline{C}$=S) (Figure 79).
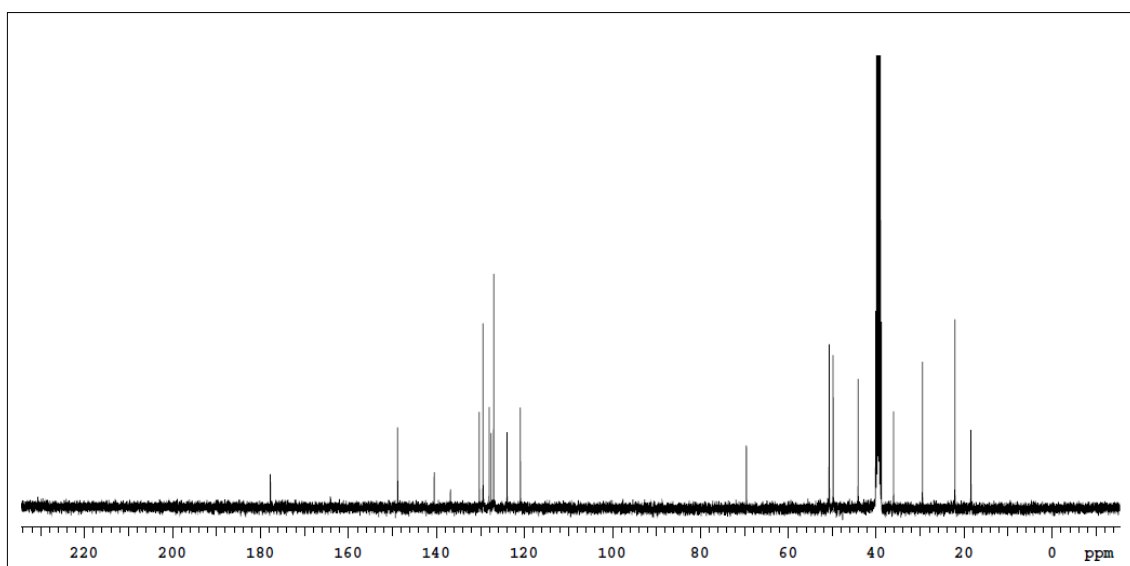

Figure 79. ^{13}C NMR spectrum of Compound **10i**

5-[1-(4-Isobutylphenyl)ethyl]-3-{[4-(2,3-xyxylphenyl)piperazin-1-yl]methyl}-1,3,4-oxadiazole-2(*3H*)-thione (Compound 10j)
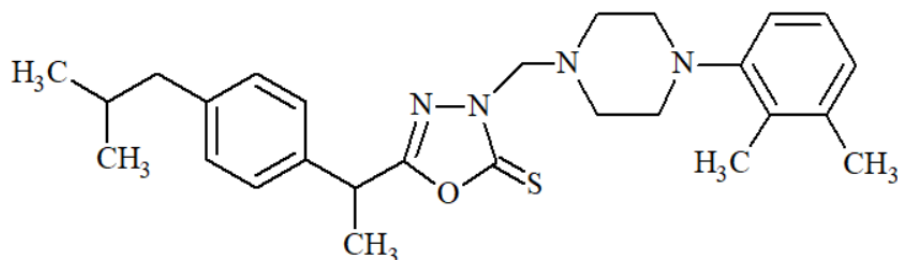
5-[1-(4-Isobutylphenyl)ethyl]-1,3,4-oxadiazole-2(*3H*)-thione (0.01 mol, 2.62 g), 1-(2,3-xyxyl)piperazine (0.01 mol, 1.90 g), formaldehyde (0.015 mol, 0.55 ml) in 15 ml methanol were reacted according to general synthesis method at 3.1.2.4.

Yield (%)	:	45
Retention factor (R_f)	:	0.65 [Toluene: Acetone: Acetic Acid (75:25:10)]
Physical appearance	:	White powder
Melting point (ºC)	:	93
Solubility	:	Highly soluble with acetone and DMSO. Practically insoluble in water

Elemental analysis

Molecular formula	:	$C_{27}H_{36}N_4OS$
Molecular weight (g/mol)	:	464.67

	C	H	N	S
Calculated (%)	69.79	7.81	12.06	6.90
Found (%)	69.01	7.61	12.09	6.85

Spectral Analysis

Infrared (IR) spectrum

ν_{max} **(cm^{-1}) :** 2950 (aromatic C-H stretchings); 2845 (aliphatic C-H stretchings); 1618 (C=N stretching); 1581, 1511, 1470 (aromatic C=C stretchings); 1454 (C-N stretching); 1326 (C-O stretching); 1239 (C=S stretching); 842 (1,4-dialkylphenyl C-H bendings); 776 (2,3-dimethylphenyl C-H bendings) (Figure 80).
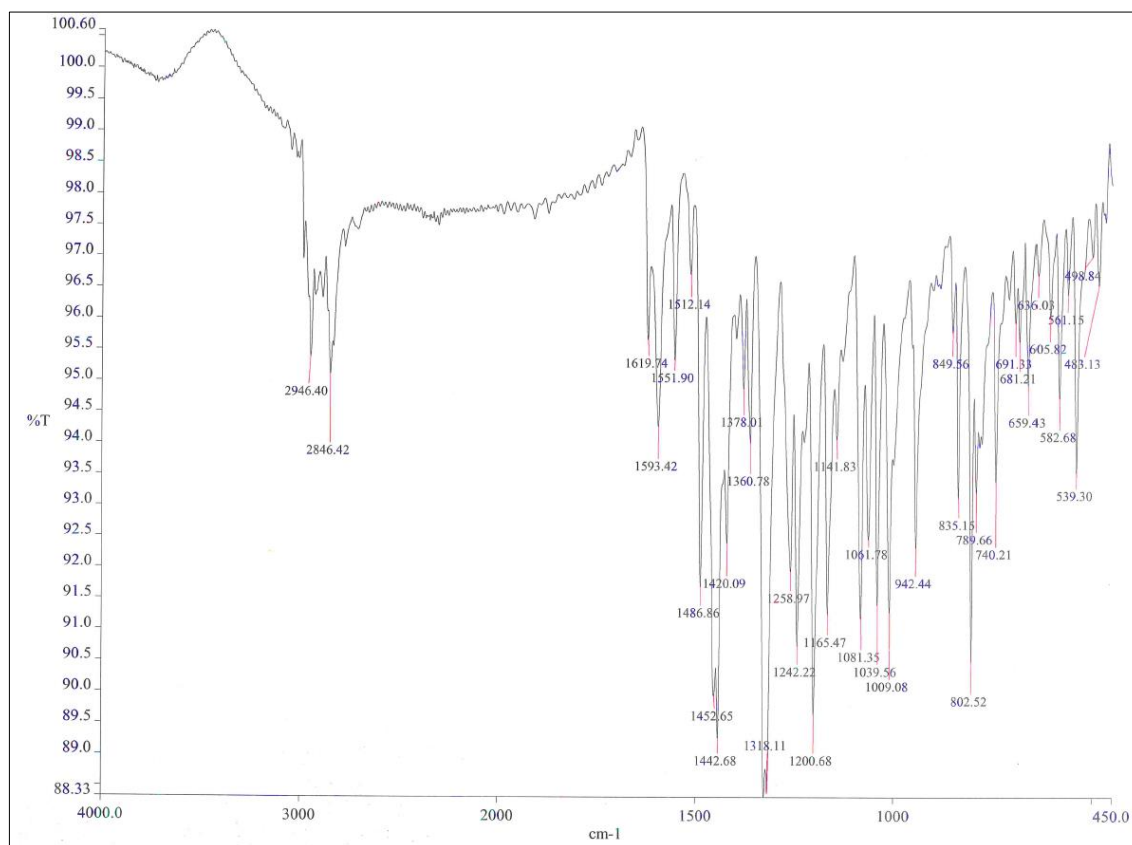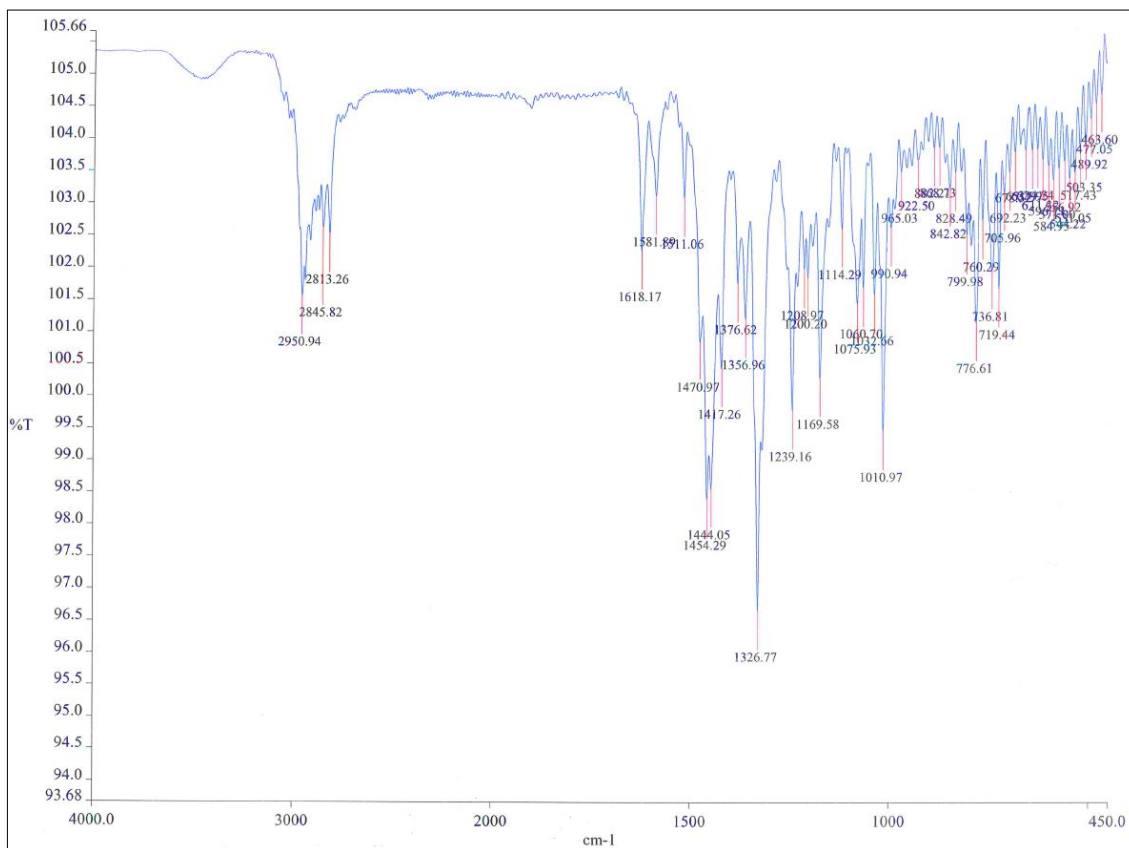

Figure 80. IR spectrum of Compound **10j**

^{1}H NMR spectrum

δ ppm (400 MHz/DMSO-d_6): 0.84 (6H, d, J=6.4 Hz, isobutyl -C$\underline{H}_3$); 1.57 (3H, d, J=7.2 Hz, -CH-C$\underline{H}_3$); 1.78-1.82 (1H, m, isobutyl –C$\underline{H}$-); 2.11+2.19 (6H, s, phenyl -C$\underline{H}_3$); 2.42 (2H, d, J=7.2 Hz, isobutyl –C$\underline{H}_2$-); 2.77 (4H, bd, J=3.6 Hz, piperazine H$_2$+H$_6$); 2.85 (4H, bs, piperazine H$_3$+H$_5$); 4.36 (1H, q, J=7.2 Hz, -C$\underline{H}$-CH$_3$,); 5.00 (2H, s, -N-C$\underline{H}_2$-N-); 6.87 (2H, bd, J=8 Hz, phenyl H$_4$'+H$_6$'); 7.02 (2H, t, J=7.8 Hz, phenyl H$_5$'); 7.15 (2H, d, J=8 Hz, phenyl H$_3$+H$_5$); 7.22 (2H, d, J=8 Hz, phenyl H$_2$+H$_6$) (Figure 81).
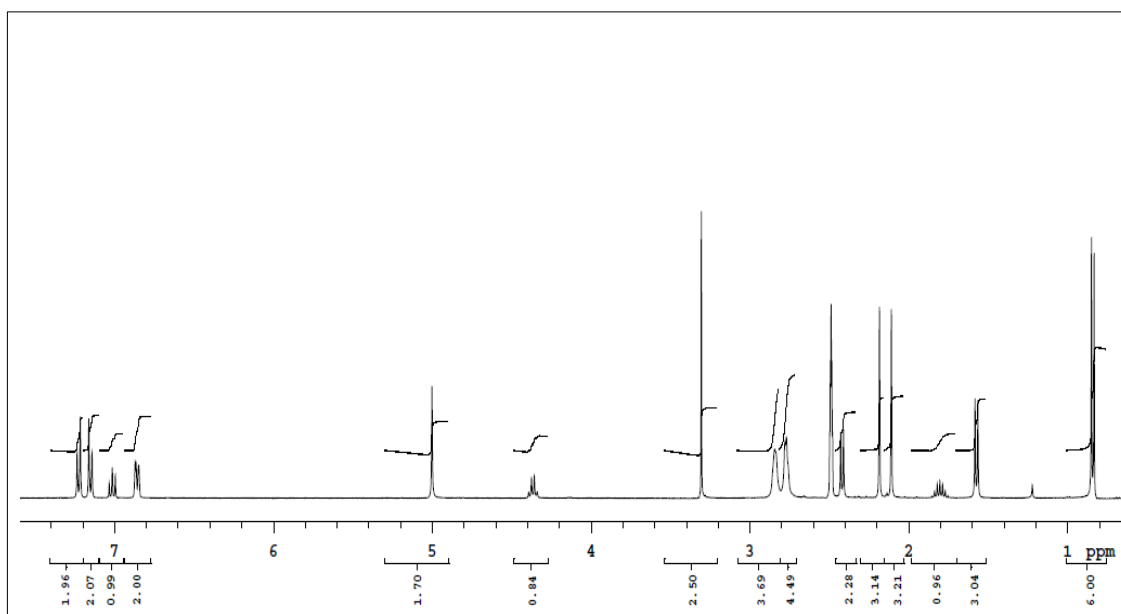
Figure 81. ^{1}H NMR spectrum of Compound **10j**

^{13}C NMR spectrum

δ ppm (400 MHz/DMSO-d_6): 13.57 (phenyl C_4'–$\underline{C}H_3$); 18.50 (isobutyl –$\underline{C}H$-); 20.01 (phenyl C_3'-$\underline{C}H_3$); 22.12+22.13 (isobutyl -$\underline{C}H_3$); 29.52 (-CH-$\underline{C}H_3$); 36.08 (isobutyl -$\underline{C}H_2$-); 44.14 (-$\underline{C}H$-CH$_3$); 50.15 (piperazine C_2+C_6); 51.65 (piperazine C_3+C_5); 60.61 (-N-$\underline{C}H_2$-N-); 116.46 (phenyl C_6'); 124.62 (phenyl C_4'); 125.66 (phenyl C_2'); 126.98 (phenyl C_3+C_5); 129.43 (phenyl C_2+C_6); 130.40 (phenyl C_5'); 136.85 (phenyl C_4); 137.22 (phenyl C_3'); 140.53 (phenyl C_1); 148.79 (phenyl C_1'); 164.07 ($\underline{C}$=N); 177.75 ($\underline{C}$=S) (Figure 82).
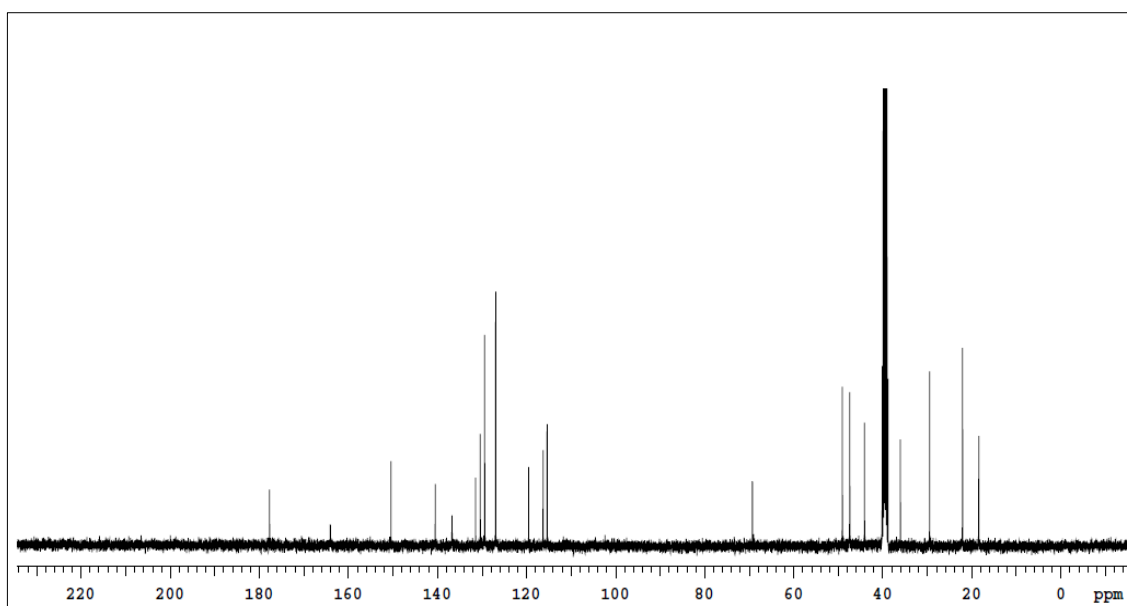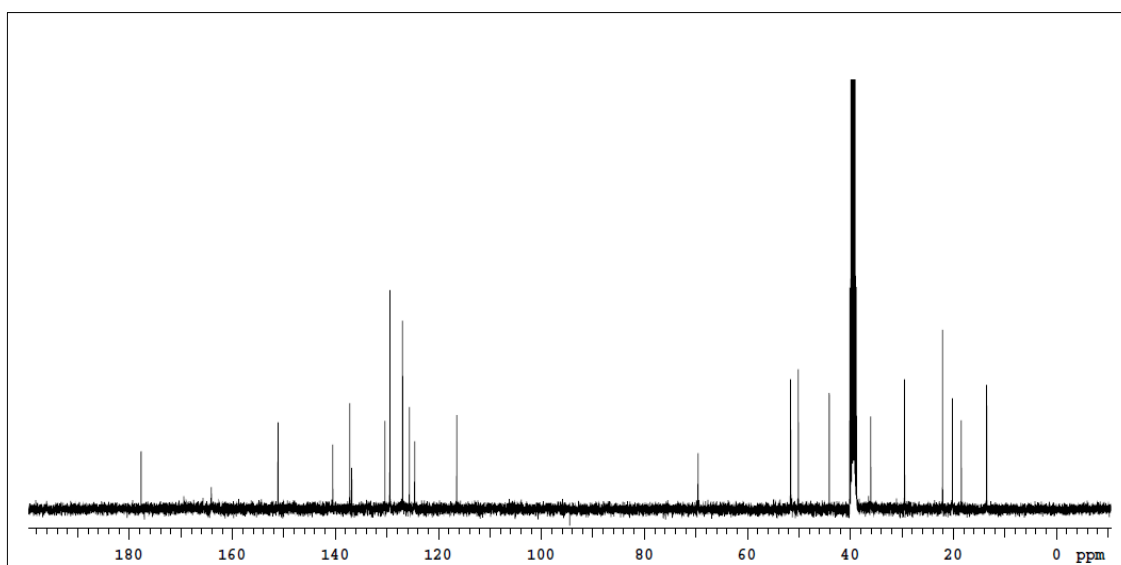

Figure 82. ^{13}C NMR spectrum of Compound **10j**

5-[1-(4-Isobutylphenyl)ethyl]-3-{[4-(4-methoxyphenyl)piperazin-1-yl]methyl}-1,3,4-oxadiazole-2(*3H*)-thione (Compound 10k) [17]
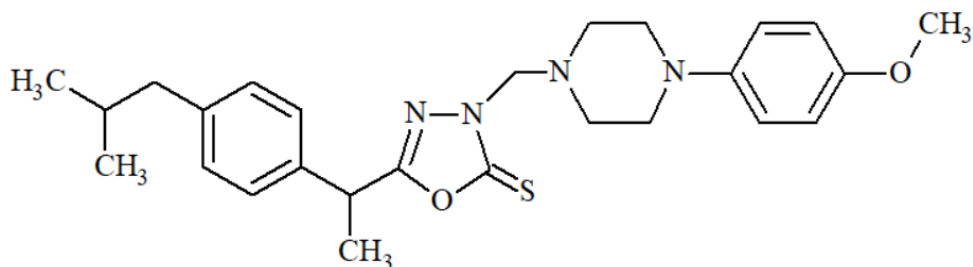
5-[1-(4-Isobutylphenyl)ethyl]-1,3,4-oxadiazole-2(*3H*)-thione (0.01 mol, 2.62 g), 1-(4-methoxyphenyl)piperazine (0.01 mol, 1.92 g), formaldehyde (0.015 mol, 0.55 ml) in 15 ml methanol were reacted according to general synthesis method at 3.1.2.4.

Yield (%)	:	47
Retention factor (R$_f$)	:	0.65 [Toluene:Acetone:Acetic Acid (75:25:10)]
Physical appearance	:	White powder
Melting point (ºC)	:	97
Solubility	:	Highly soluble with acetone and DMSO. Practically insoluble in water

Spectral Analysis

Infrared (IR) spectrum

v_{max} **(cm^{-1}) :** 2950 (aromatic C-H stretchings); 2833 (aliphatic C-H stretchings); 1622 (C=N stretching); 1518 (aromatic C=C stretchings); 1456 (C-N stretching); 1325 (C-O stretching); 1265 (C=S stretching); 820 (1,4-dialkylphenyl C-H bendings); 803 (4-methoxyphenyl C-H bendings) (Figure 83).
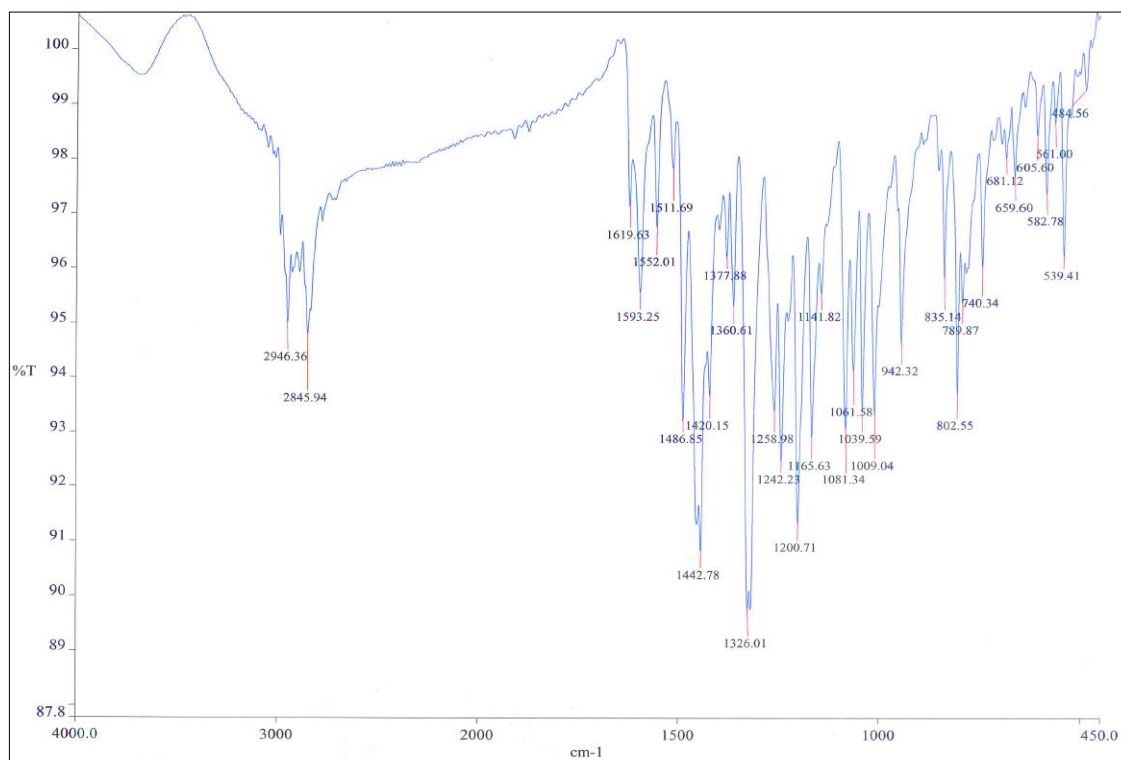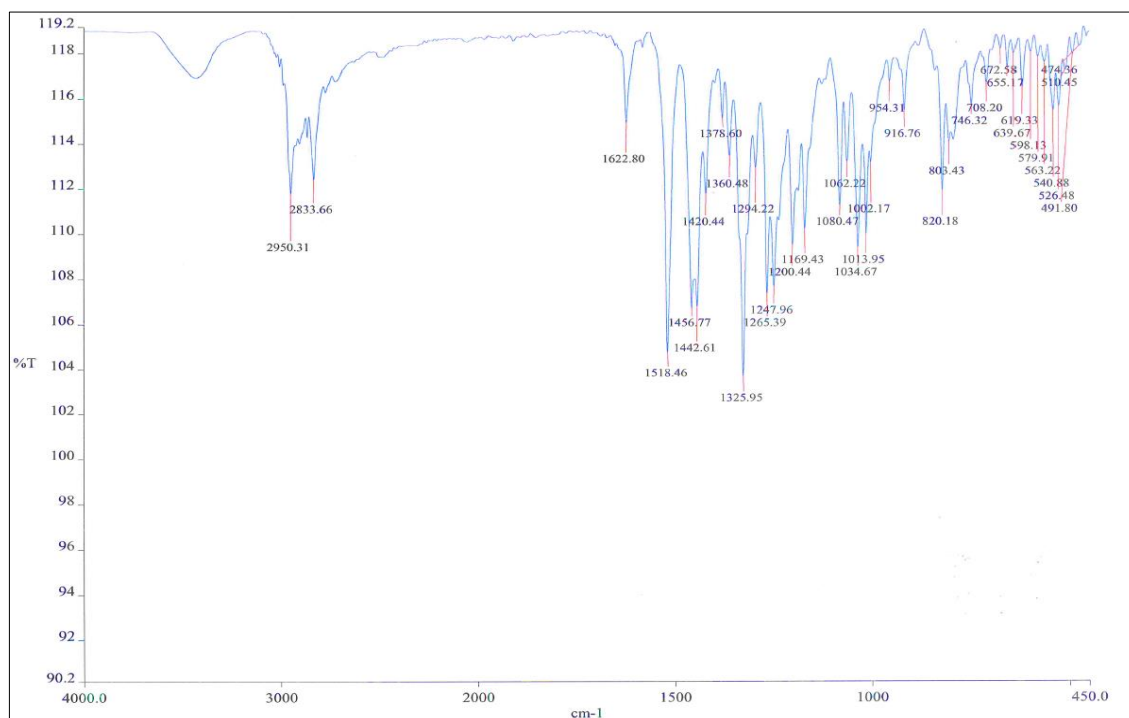

Figure 83. IR spectrum of Compound **10k**

^{1}H NMR spectrum

δ ppm (400 MHz/DMSO-d_6): 0.82 (6H, d, J=6.8 Hz, isobutyl -C$\underline{H}_3$); 1.54 (3H, d, J=6.8 Hz, -CH-C$\underline{H}_3$); 1.77-1.80 (1H, m, isobutyl –C$\underline{H}$-); 2.40 (2H, d, J=7.2 Hz, isobutyl –C$\underline{H}_2$-); 2.82 (4H, t, J=4.6 Hz, piperazine H$_2$+H$_6$); 2.99 (4H, t, J=4.6 Hz, piperazine H$_3$+H$_5$); 3.65 (3H, s, phenyl –OC$\underline{H}_3$); 4.32 (1H, q, J=6.8 Hz, -C$\underline{H}$-CH$_3$,); 4.98 (2H, s, -N-C$\underline{H}_2$-N-); 6.78 (2H, bd, J=9 Hz, phenyl H$_2$'+H$_6$'); 6.85 (2H, bd, J=9 Hz, phenyl H$_3$'+H$_5$'); 7.13 (2H, bd, J=8.4 Hz, phenyl H$_3$+H$_5$); 7.19 (2H, d, J=8.4 Hz, phenyl H$_2$+H$_6$) (Figure 84).
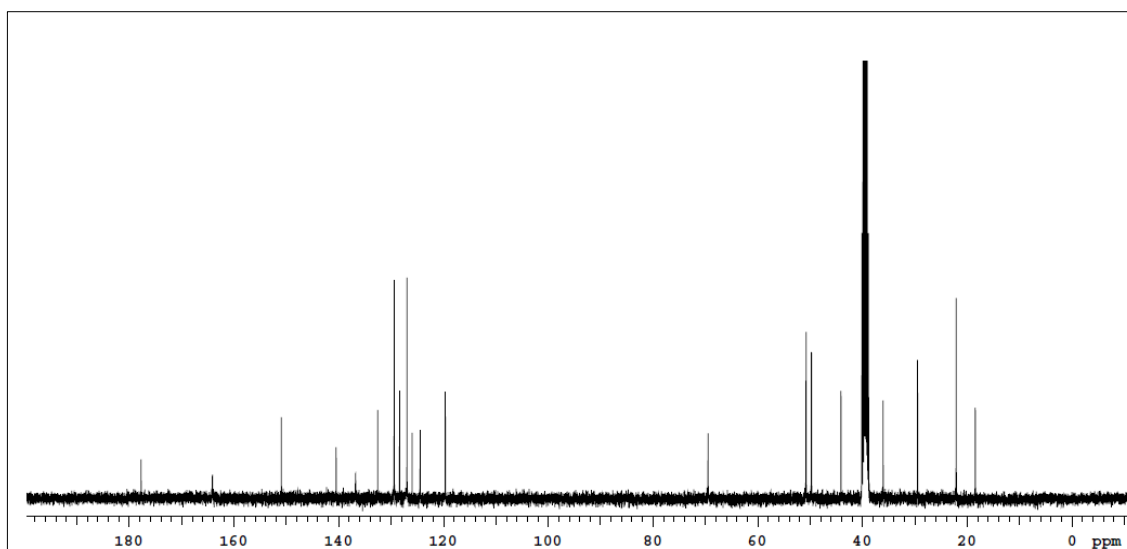
Figure 84. ^{1}H NMR spectrum of Compound **10k**

5-[1-(4-Isobutylphenyl)ethyl]-3-{[4-(3-methoxyphenyl)piperazin-1-yl]methyl}-1,3,4-oxadiazole-2(*3H*)-thione (Compound 10l)
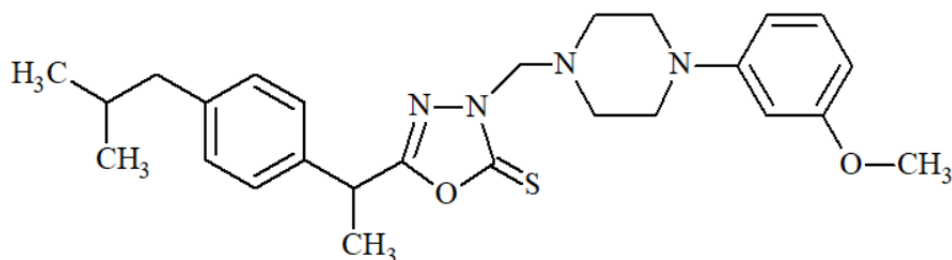
5-[1-(4-Isobutylphenyl)ethyl]-1,3,4-oxadiazole-2(*3H*)-thione (0.01 mol, 2.62 g), 1-(3-methoxyphenyl)piperazine (0.01 mol, 1.92 g), formaldehyde (0.015 mol, 0.55 ml) in 15 ml methanol were reacted according to general synthesis method at 3.1.2.4.

Yield (%)	:	45
Retention factor (R_f)	:	0.65 [Toluene: Acetone: Acetic Acid (75:25:10)]
Physical appearance	:	White powder
Melting point (ºC)	:	93
Solubility	:	Highly soluble with acetone and DMSO. Practically insoluble in water

Elemental analysis

Molecular formula	:	$C_{26}H_{34}N_4O_2S$
Molecular weight (g/mol)	:	466.64

	C	H	N	S
Calculated (%)	66.92	7.34	12.01	6.87
Found (%)	65.91	7.57	12.43	7.01

Spectral Analysis

Infrared (IR) spectrum

ν_{max} **(cm^{-1}) :** 2923 (aromatic C-H stretchings); 2810 (aliphatic C-H stretchings); 1603 (C=N stretching); 1572, 1495 (aromatic C=C stretchings); 1449 (C-N stretching); 1338 (C-O stretching); 1269 (C=S stretching); 836 (1,4-dialkylphenyl C-H bendings); 759 (3-methoxyphenyl C-H bendings) (Figure 85).

Figure 85. IR spectrum of Compound **10l**

^{1}H NMR spectrum

δ ppm (400 MHz/DMSO-d_6): 0.84 (6H, d, J=6.4 Hz, isobutyl C$\underline{H}_3$); 1.56 (3H, d, J=6.8 Hz, -CH-C$\underline{H}_3$); 1.77-1.84 (1H, m, isobutyl –C$\underline{H}$-); 2.41 (2H, d, J=7.2 Hz, isobutyl –C$\underline{H}_2$-); 2.86 (4H, t, J=5 Hz, piperazine H$_2$+H$_6$); 3.13 (4H, t, J=5 Hz, piperazine H$_3$+H$_5$); 4.34 (1H, q, J=7.2 Hz, -C$\underline{H}$-CH$_3$); 5.00 (2H, s, -N-C$\underline{H}_2$-N-); 6.36 (1H, dd, J=8.2 J'=2.2 Hz, phenyl H$_6$'); 6.44 (1H, t, J=2.2 Hz, phenyl H$_2$'); 6.51 (1H, dd, J=8.2 Hz J'=2.2 Hz, phenyl H$_4$'); 7.09 (1H, t, J=8.4 Hz, phenyl H$_5$'); 7.14 (2H, d, J=8.2 Hz, phenyl H$_3$+H$_5$); 7.20 (2H, d, J=8.2 Hz, phenyl H$_2$+H$_6$) (Figure 86).
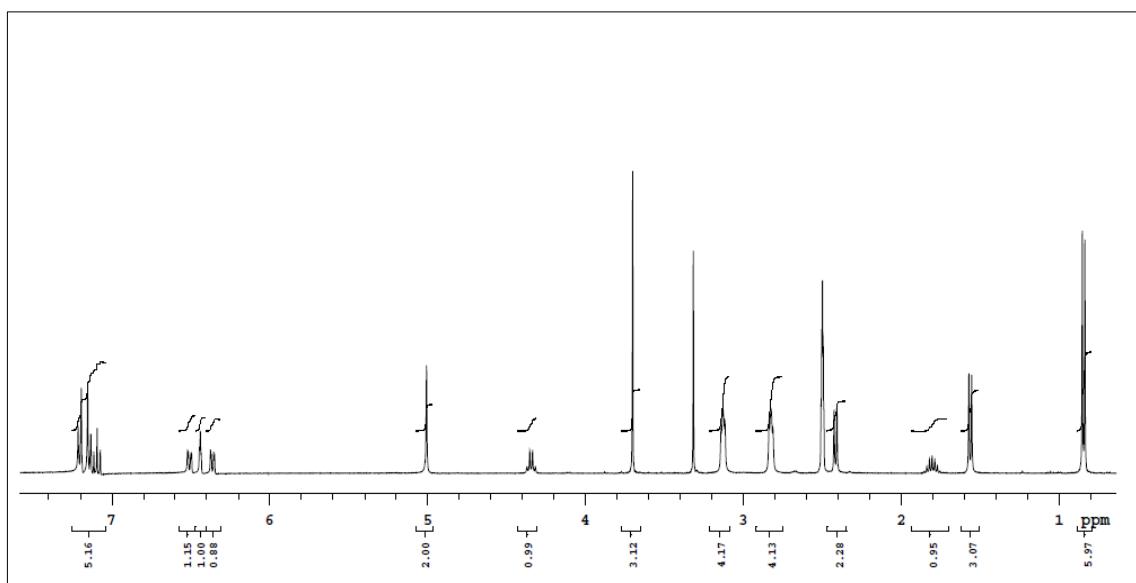
Figure 86. ^{1}H NMR spectrum of Compound **10l**

^{13}C NMR spectrum

δ ppm (400 MHz/DMSO-d_6): 18.49 (-CH-$\underline{C}$H$_3$); 22.13+22.14 (isobutyl -$\underline{C}$H$_3$); 29.50 (isobutyl -$\underline{C}$H-); 36.09 (isobutyl -$\underline{C}$H$_2$-); 44.13 (-$\underline{C}$H-CH$_3$); 48.13 (piperazine C$_2$+C$_6$); 49.49 (piperazine C$_3$+C$_5$); 54.82 (phenyl C$_3$'-O$\underline{C}$H$_3$); 69.42 (-N-$\underline{C}$H$_2$-N-); 101.69 (phenyl C$_2$'); 104.26 (phenyl C$_6$'); 108.18 (phenyl C$_4$'); 126.98 (phenyl C$_2$+C$_6$); 129.44 (phenyl C$_3$+C$_5$); 129.56 (phenyl C$_5$'); 136.76 (phenyl C$_4$); 140.50 (phenyl C$_1$); 152.23 (phenyl C$_1$'); 160.14 (phenyl C$_3$') 164.10 ($\underline{C}$=N); 177.76 ($\underline{C}$=S) (Figure 87).
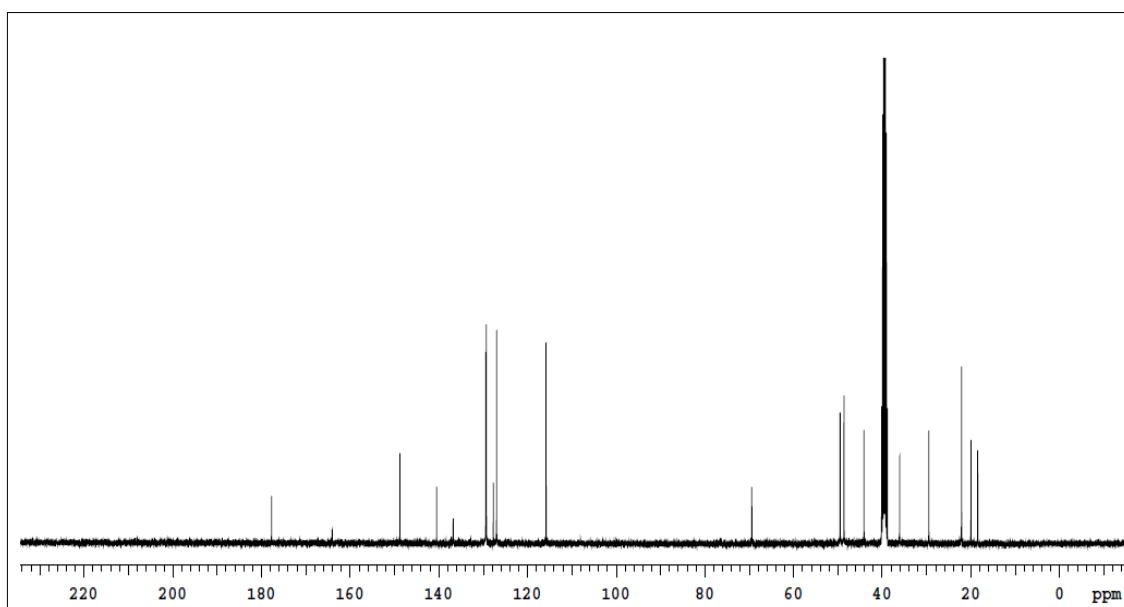

Figure 87. ^{13}C NMR spectrum of Compound **10l**

5-[1-(4-Isobutylphenyl)ethyl]-3-{[4-(2-methoxyphenyl)piperazin-1-yl]methyl}-1,3,4-oxadiazole-2(*3H*)-thione (Compound 10m)
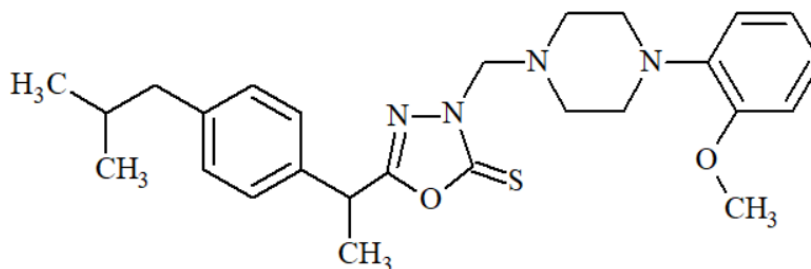
5-[1-(4-Isobutylphenyl)ethyl]-1,3,4-oxadiazole-2(*3H*)-thione (0.01mol, 2.62 g), 1-(2-methoxyphenyl)piperazine (0.01 mol, 1.92 g), formaldehyde (0.015 mol, 0.55 ml) in 15 ml methanol were reacted according to general synthesis method at 3.1.2.4.

Yield (%)	:	41
Retention factor (R$_f$)	:	0.66 [Toluene: Acetone: Acetic Acid (75:25:10)]
Physical appearance	:	White powder
Melting point (ºC)	:	98
Solubility	:	Highly soluble with acetone and DMSO. Practically insoluble in water

Elemental analysis

Molecular formula	:	C$_{26}$H$_{34}$N$_4$O$_2$S
Molecular weight (g/mol)	:	466.64

	C	H	N	S
Calculated (%)	66.92	7.34	12.01	6.87
Found (%)	65.99	7.61	11.92	7.01

Spectral Analysis

Infrared (IR) spectrum

ν_{max} **(cm⁻¹) :** 3049 (aromatic C-H stretchings); 2909 (aliphatic C-H stretchings); 1614 (C=N stretching); 1594, 1498 (aromatic C=C stretchings); 1444 (C-N stretching); 1324 (C-O stretching); 1242 (C=S stretching); 850 (1,4-dialkylphenyl C-H bendings); 737 (2-methoxyphenyl C-H bendings) (Figure 88).

Figure 88. IR spectrum of Compound **10m**

¹H NMR spectrum

δ ppm (400 MHz/DMSO-d_6): 0.85 (6H, d, *J*=6.8 Hz, isobutyl C$\underline{H}_3$); 1.58 (3H, d, *J*=7.6 Hz, -CH-C$\underline{H}_3$); 1.76-1.86 (1H, m, isobutyl –C$\underline{H}$-); 2.42 (2H, d, *J*=7.2 Hz, isobutyl –C$\underline{H}_2$-); 2.85 (4H, bs, piperazine H₂+H₆); 2.95 (4H, bs, piperazine H₃+H₅); 3.76 (3H, s, phenyl C₂'–OC$\underline{H}_3$); 4.37 (1H, q, *J*=7 Hz, -C$\underline{H}$-CH₃); 4.99 (2H, s, -N-C$\underline{H}_2$-N-); 6.86-6.95 (4H, m, phenyl H₃'+H₄'+H₅'+H₆'); 7.16 (2H, bd, *J*=8 Hz, phenyl H₃+H₅); 7.23 (2H, bd, *J*=8 Hz, phenyl H₂+H₆) (Figure 89).
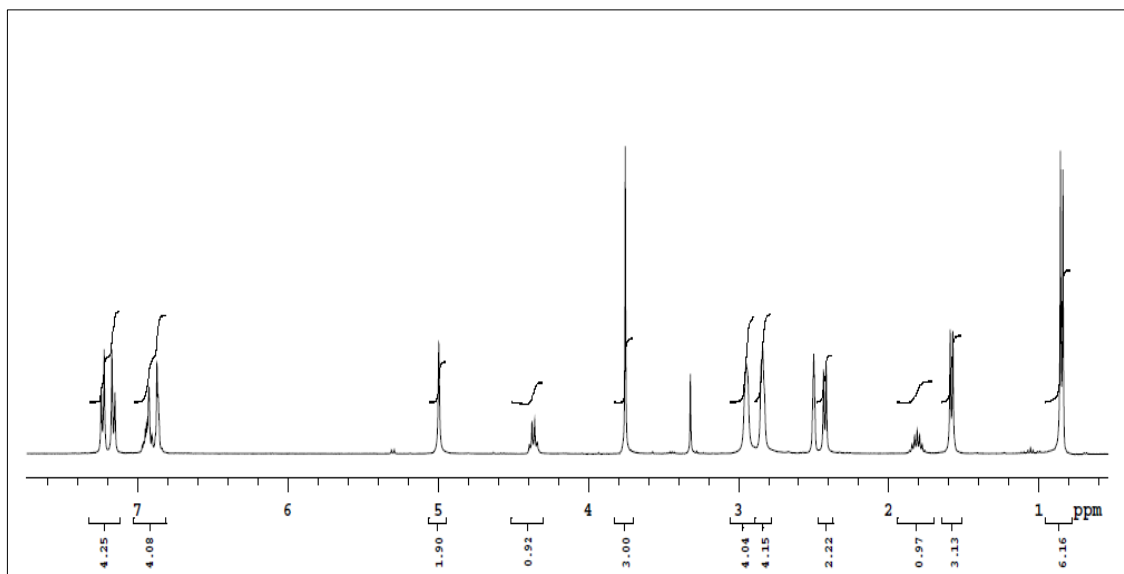
Figure 89. ^{1}H NMR spectrum of Compound **10m**

^{13}C NMR spectrum

δ ppm (400 MHz/DMSO-d_6): 18.49 (-CH-$\underline{C}$H$_3$); 22.12+22.13 (isobutyl -$\underline{C}$H$_3$); 29.50 (isobutyl –$\underline{C}$H-); 36.09 (isobutyl -$\underline{C}$H$_2$-); 44.14 (-$\underline{C}$H-CH$_3$); 49.86 (piperazine C$_2$+C$_6$); 49.93 (piperazine C$_3$+C$_5$); 55.21 (phenyl C$_2$'–O$\underline{C}$H$_3$); 69.66 (-N-$\underline{C}$H$_2$-N-); 111.78 (phenyl C$_6$'); 118.02 (phenyl C$_3$'); 120.75 (phenyl C$_4$'); 122.51 (phenyl C$_5$'); 127.03 (phenyl C$_3$+C$_5$); 129.43 (phenyl C$_2$+C$_6$); 136.79 (phenyl C$_4$); 140.52 (phenyl C$_1$); 140.99 (phenyl C$_1$'); 151.88 (phenyl C$_2$'); 164.11 ($\underline{C}$=N); 177.75 ($\underline{C}$=S) (Figure 90).
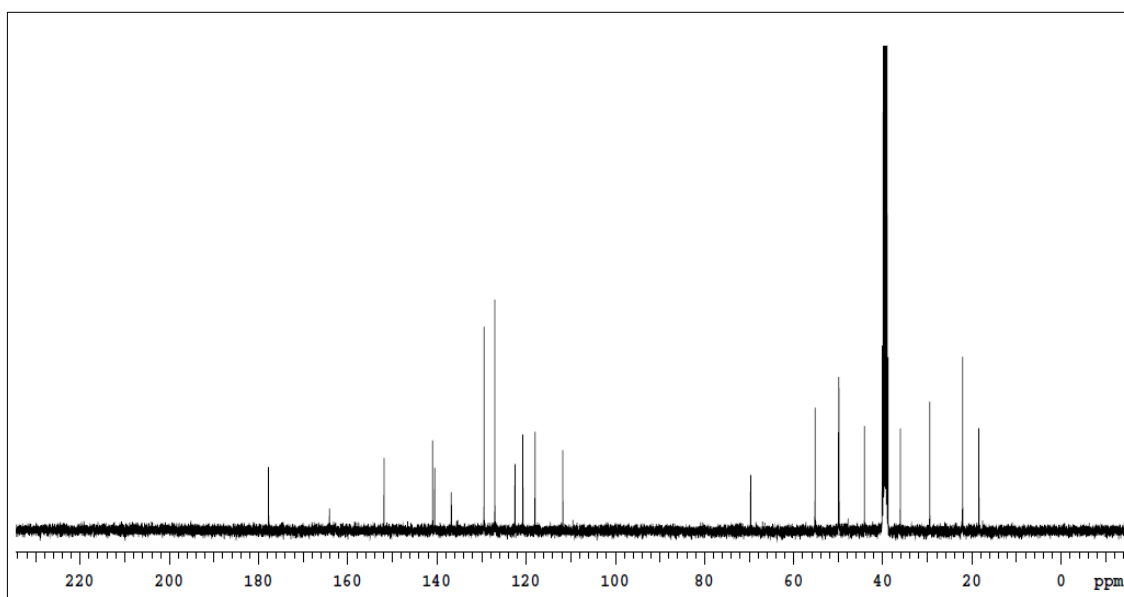
Figure 90. ^{13}C NMR spectrum of Compound **10m**

157

5-[1-(4-Isobutylphenyl)ethyl]-3-{[4-(4-cyanophenyl)piperazin-1-yl]methyl}-1,3,4-oxadiazole-2(*3H*)-thione (Compound 10n)
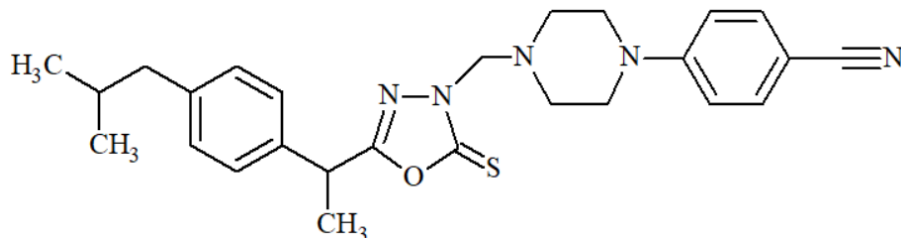
5-[1-(4-Isobutylphenyl)ethyl]-1,3,4-oxadiazole-2(*3H*)-thione (0.01 mol, 2.62 g), 4-piperazinobenzonitrile (0.01 mol, 1.87 g), formaldehyde (0.015 mol, 0.55 ml) in 15 ml methanol were reacted according to general synthesis method at 3.1.2.4.

Yield (%)	:	50
Retention factor (R$_f$)	:	0.66 [Toluene: Acetone: Acetic Acid (75:25:10)]
Physical appearance	:	White powder
Melting point (ºC)	:	50
Solubility	:	Highly soluble with acetone and DMSO. Practically insoluble in water

Elemental analysis

Molecular formula	:	$C_{26}H_{31}N_5OS$
Molecular weight (g/mol)	:	461.62

	C	H	N	S
Calculated (%)	67.65	6.77	15.17	6.95
Found (%)	67.70	6.98	15.20	7.04

Spectral Analysis

Infrared (IR) spectrum

ν_{max} **(cm^{-1}) :** 2946 (aromatic C-H stretchings); 2840 (aliphatic C-H stretchings); 2211 (C≡N stretching); 1604 (C=N stretching); 1513 (aromatic C=C stretchings); 1445 (C-N stretching); 1329 (C-O stretching); 1248 (C=S stretching); 818 (1,4-dialkylphenyl C-H bendings); 789 (4-cyanophenyl C-H bendings) (Figure 91).
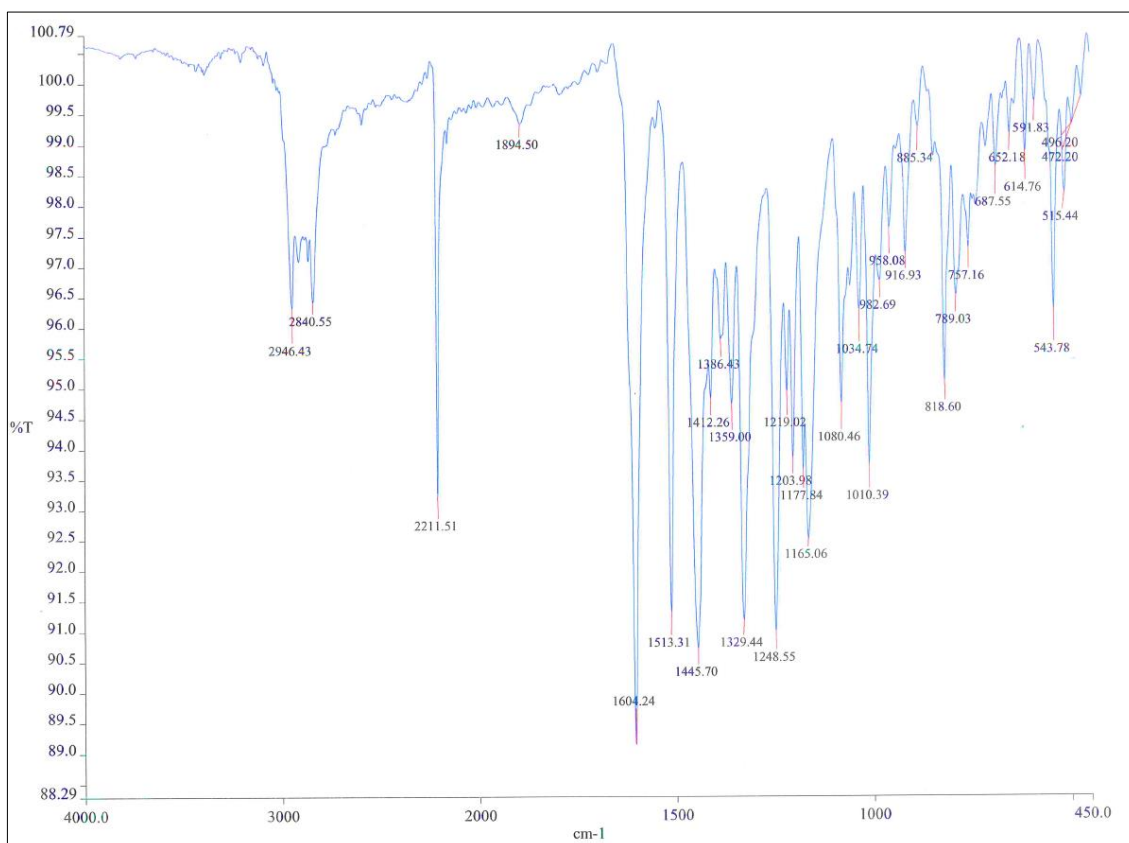
Figure 91. IR spectrum of Compound **10n**

^{1}H NMR spectrum

δ ppm (400 MHz/DMSO-d_6): 0.83 (6H, d, J=6.4 Hz, isobutyl -C$\underline{H}_3$); 1.53 (3H, d, J=6.8 Hz, -CH-C$\underline{H}_3$); 1.76-1.80 (1H, m, isobutyl –C$\underline{H}$-); 2.39 (2H, d, J=7.2 Hz, isobutyl –C$\underline{H}_2$-); 2.80 (4H, bs, piperazine H$_2$+H$_6$); 3.53 (4H, t, J=5 Hz, piperazine H$_3$+H$_5$); 4.31 (3H, q, J=7.2 Hz, -C$\underline{H}$-CH$_3$,); 5.00 (2H, s, -N-C$\underline{H}_2$-N-); 7.01 (2H, bd, J=8.8 Hz phenyl H$_2$'+H$_6$'); 7.09 (2H, bd, J=8 Hz phenyl H$_3$+H$_5$); 7.16 (2H, bd, J=8 Hz, phenyl H$_2$+H$_6$); 7.56 (2H, bd, J=8.8 Hz, phenyl H$_3$'+H$_5$') (Figure 92).
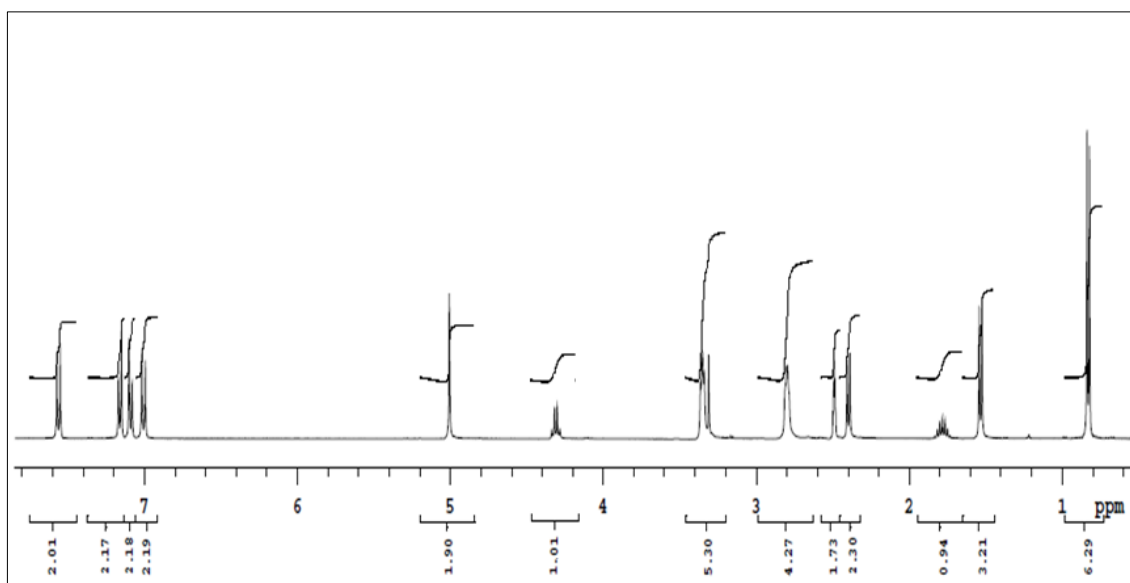
Figure 92. ^{1}H NMR spectrum of Compound **10n**

^{13}C NMR spectrum

δ ppm (400 MHz/DMSO-d_6): 18.47 (isobutyl –$\underline{C}$H-); 20.09+20.13 (isobutyl -$\underline{C}$H$_3$); 29.50 (-CH-$\underline{C}$H$_3$); 36.06 (isobutyl -$\underline{C}$H$_2$-); 44.11 (-$\underline{C}$H-CH$_3$); 46.32 (piperazine C$_2$+C$_6$); 49.07 (piperazine C$_3$+C$_5$); 69.28 (-N-$\underline{C}$H$_2$-N-); 98.26 (phenyl C$_4$'-$\underline{C}$≡N); 114.12 (phenyl C$_2$'+C$_6$'); 119.94 (phenyl C$_4$'); 126.93 (phenyl C$_3$+C$_5$); 129.40 (phenyl C$_2$+C$_6$); 133.29 (phenyl C$_3$'+C$_5$'); 136.73 (phenyl C$_4$); 140.51 (phenyl C$_1$); 152.90 (phenyl C$_1$'); 164.07 ($\underline{C}$=N); 177.71 ($\underline{C}$=S) (Figure 93).
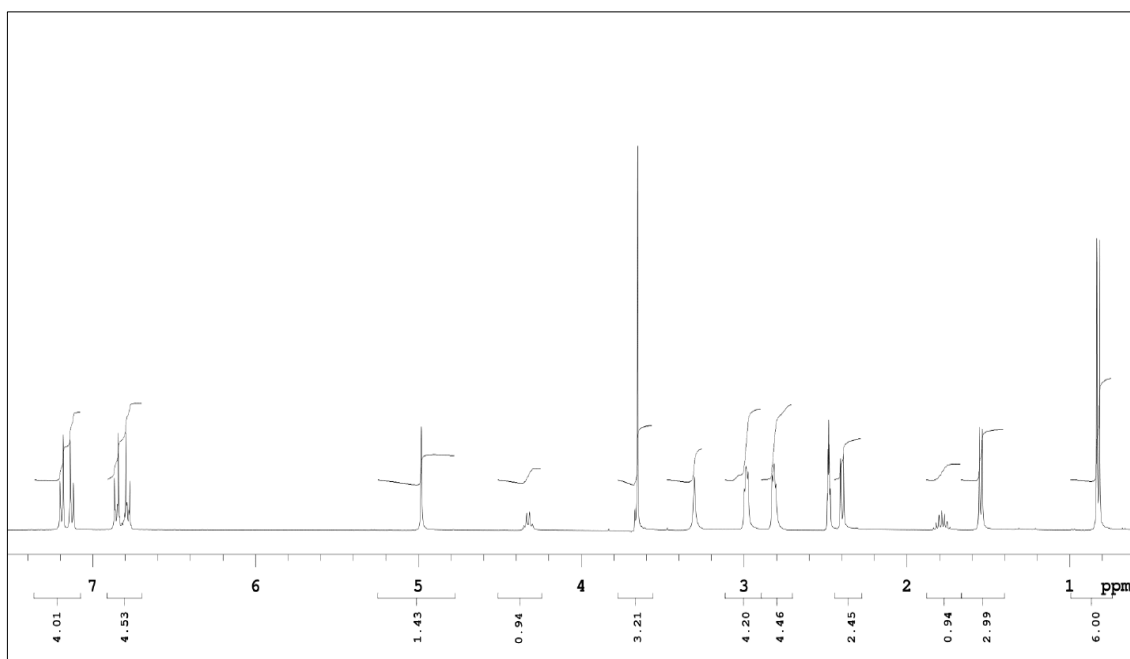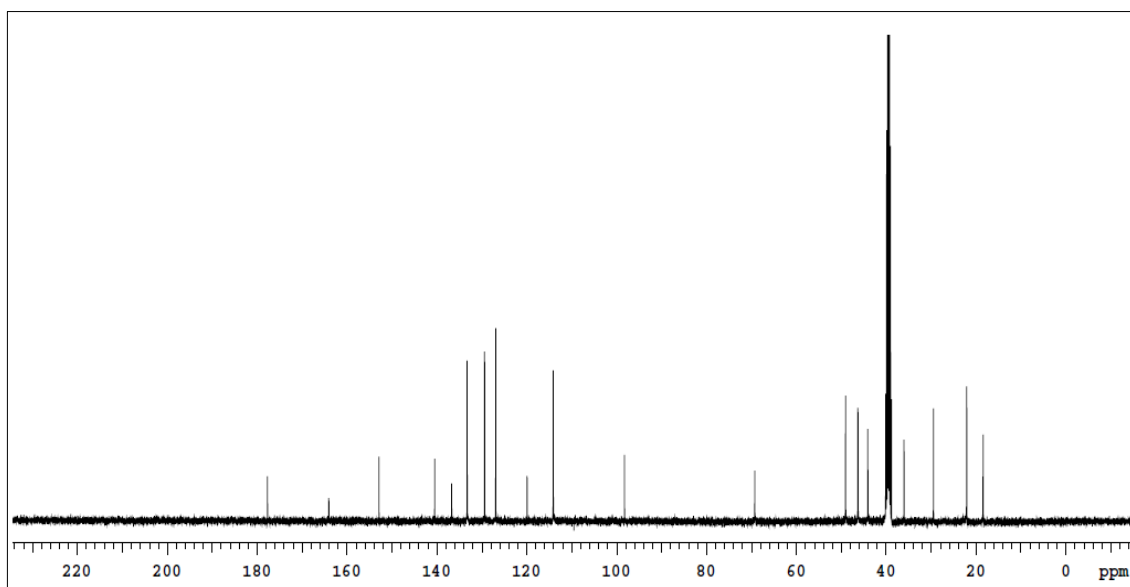

Figure 93. ^{13}C NMR spectrum of Compound **10n**

5-[1-(4-Isobutylphenyl)ethyl]-3-{[4-(2-cyanophenyl)piperazin-1-yl]methyl}-1,3,4-oxadiazole-2(*3H*)-thione (Compound 10o)
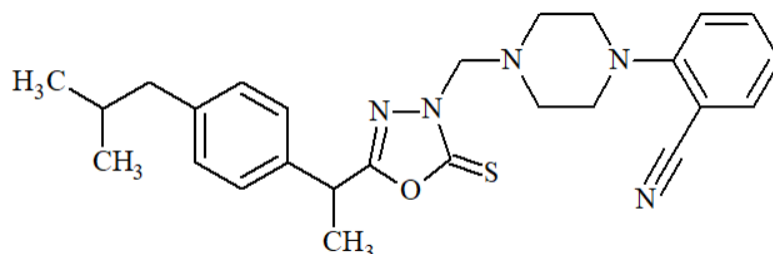
5-[1-(4-Isobutylphenyl)ethyl]-1,3,4-oxadiazole-2(*3H*)-thione (0.01 mol, 2.62 g), 1-(2-cyanophenyl)piperazine (0.01 mol, 1.87 g), formaldehyde (0.015 mol, 0.55 ml) in 15 ml methanol were reacted according to general synthesis method at 3.1.2.4.

Yield (%)	: 52
Retention factor (R$_f$)	: 0.64 [Toluene: Acetone: Acetic Acid (75:25:10)]
Physical appearance	: White powder
Melting point (ºC)	: 80
Solubility	: Highly soluble with acetone and DMSO. Practically insoluble in water

Elemental analysis

Molecular formula	: C$_{26}$H$_{31}$N$_5$OS
Molecular weight (g/mol)	: 461.62

	C	H	N	S
Calculated (%)	67.65	6.77	15.17	6.95
Found (%)	66.91	6.79	15.31	7.09

Spectral Analysis

Infrared (IR) spectrum

ν_{max} **(cm^{-1}) :** 2945 (aromatic C-H stretchings); 2837 (aliphatic C-H stretchings); 2218 (C≡N stretching); 1617 (C=N stretching); 1594, 1569, 1510, 1488 (aromatic C=C stretchings); 1445 (C-N stretching); 1329 (C-O stretching); 1250 (C=S stretching); 847 (1,4-dialkylphenyl C-H bendings); 765 (2-cyanophenyl C-H bendings) (Figure 94).
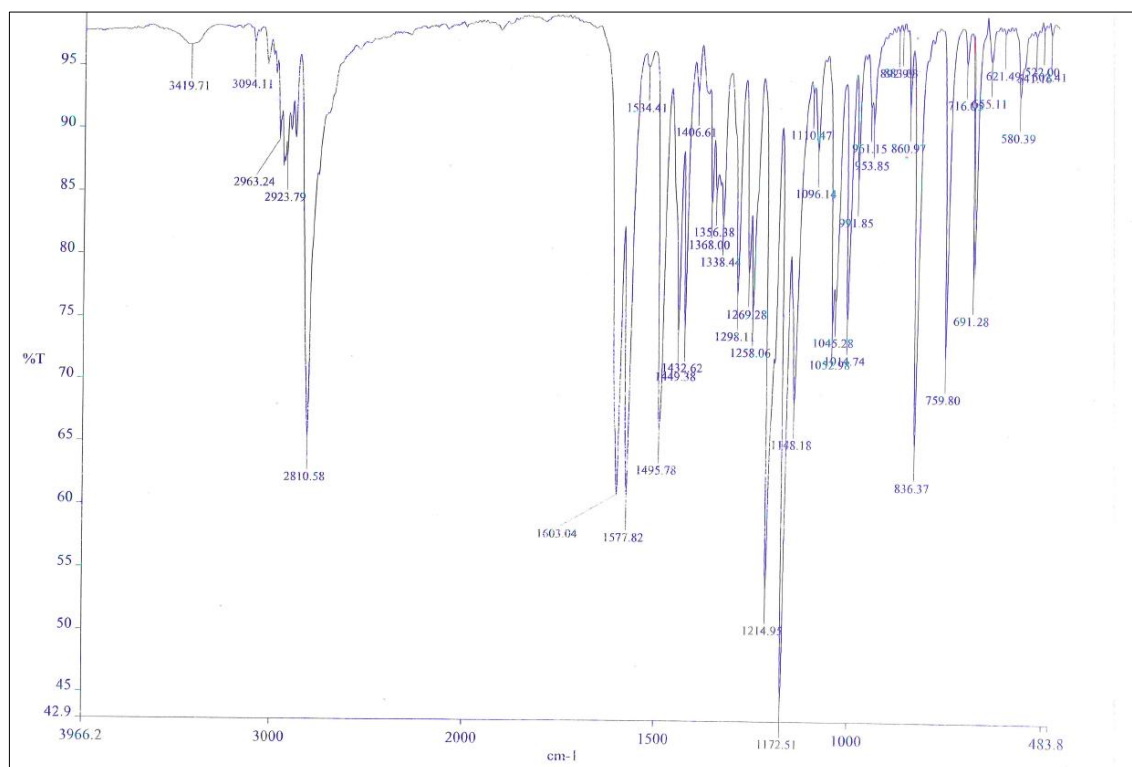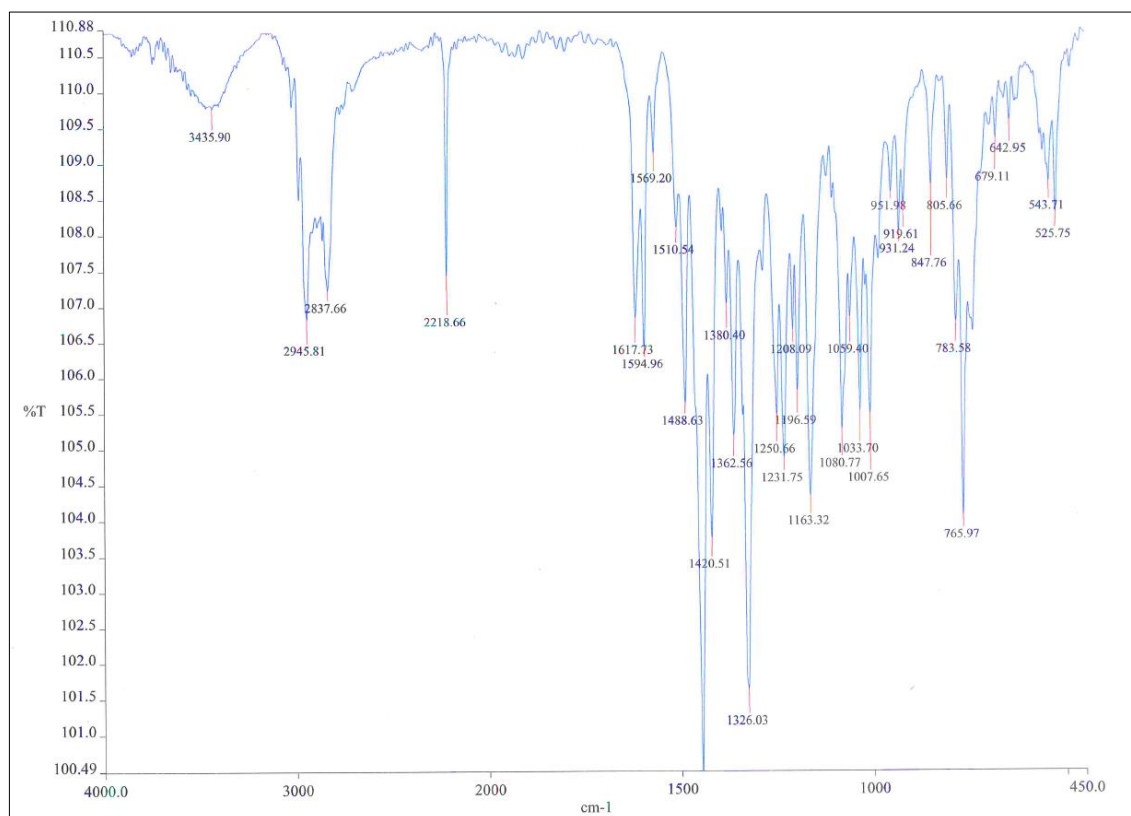

Figure 94. IR spectrum of Compound **10o**

^{1}H NMR spectrum

δ ppm (400 MHz/DMSO-d_6): 0.84 (6H, d, *J*=6.8 Hz, isobutyl -C$\underline{H}_3$); 1.57 (3H, d, *J*=7.2 Hz, -CH-C$\underline{H}_3$); 1.78-1.82 (1H, m, isobutyl –C$\underline{H}$-); 2.41 (2H, d, *J*=7.6 Hz, isobutyl –C$\underline{H}_2$-); 2.90 (4H, t, *J*=3.5 Hz, piperazine H$_2$+H$_6$); 3.14 (4H, t, *J*=3.5 Hz, piperazine H$_3$+H$_5$); 4.37 (3H, q, *J*=7 Hz, -C$\underline{H}$-CH$_3$,); 5.03 (2H, s, -N-C$\underline{H}_2$-N-); 7.10 (2H, t, *J*=7.8 Hz phenyl H$_5$'); 7.15 (3H, d, *J*=8 Hz phenyl H$_3$+H$_5$+H$_6$'); 7.22 (2H, d, *J*=8 Hz, phenyl H$_2$+H$_6$); 7.58-7.62 (1H, m, phenyl H$_4$'); 7.70 (1H, dd, *J*=7.6 *J'*=1.6 Hz, phenyl H$_3$') (Figure 95).
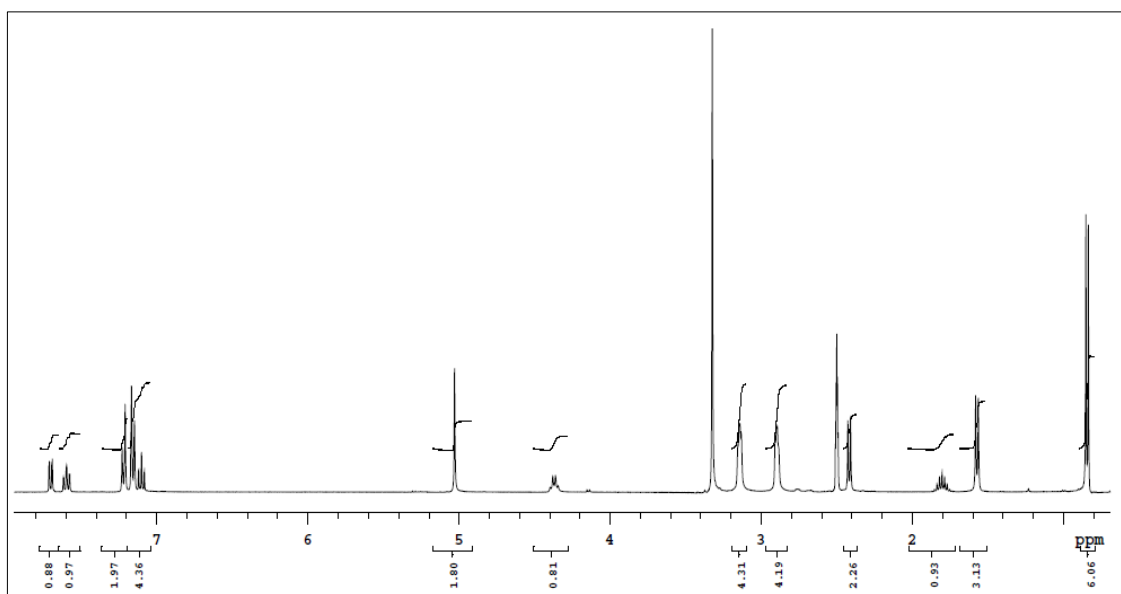
Figure 95. ^{1}H NMR spectrum of Compound **10o**

^{13}C NMR spectrum

δ ppm (400 MHz/DMSO-d_6): 18.51 (isobutyl –CH-); 22.11+22.13 (isobutyl -CH$_3$); 29.49 (-CH-CH$_3$); 36.08 (isobutyl -CH$_2$-); 44.14 (-CH-CH$_3$); 49.66 (piperazine C$_2$+C$_6$); 51.07 (piperazine C$_3$+C$_5$); 69.38 (-N-CH$_2$-N-); 104.88 (phenyl C$_2$'-C≡N); 118.11 (phenyl C$_6$'); 119.19 (phenyl C$_4$'); 122.12 (phenyl C$_2$'); 126.96 (phenyl C$_3$+C$_5$); 129.46 (phenyl C$_2$+C$_6$); 134.18 (phenyl C$_5$'); 136.78 (phenyl C$_4$); 140.50 (phenyl C$_1$); 155.11 (phenyl C$_1$'); 164.15 (C=N); 177.75 (C=S) (Figure 96).
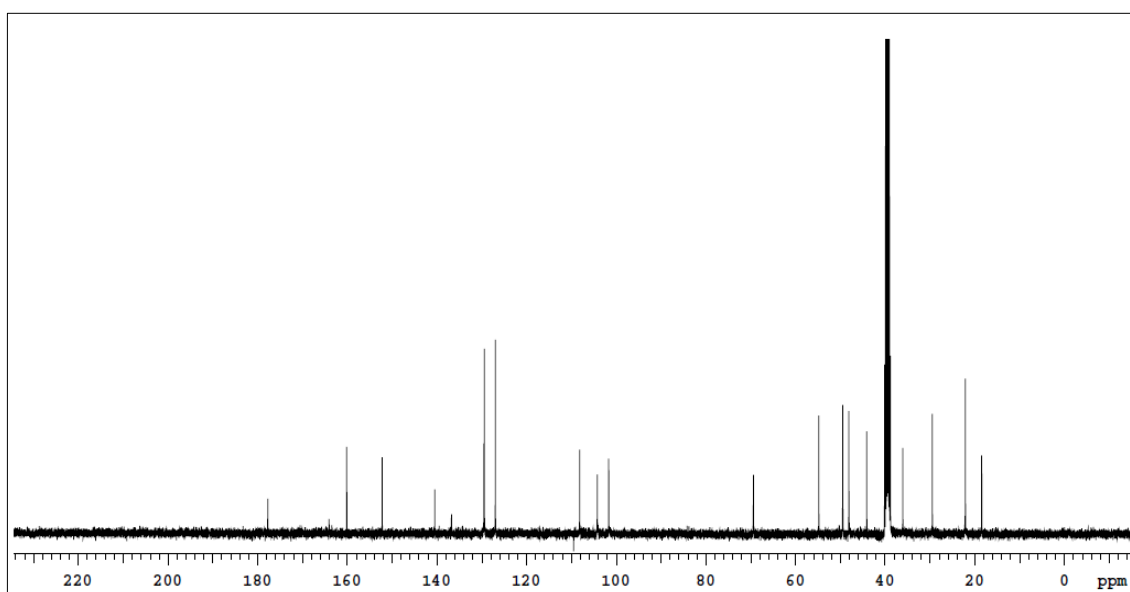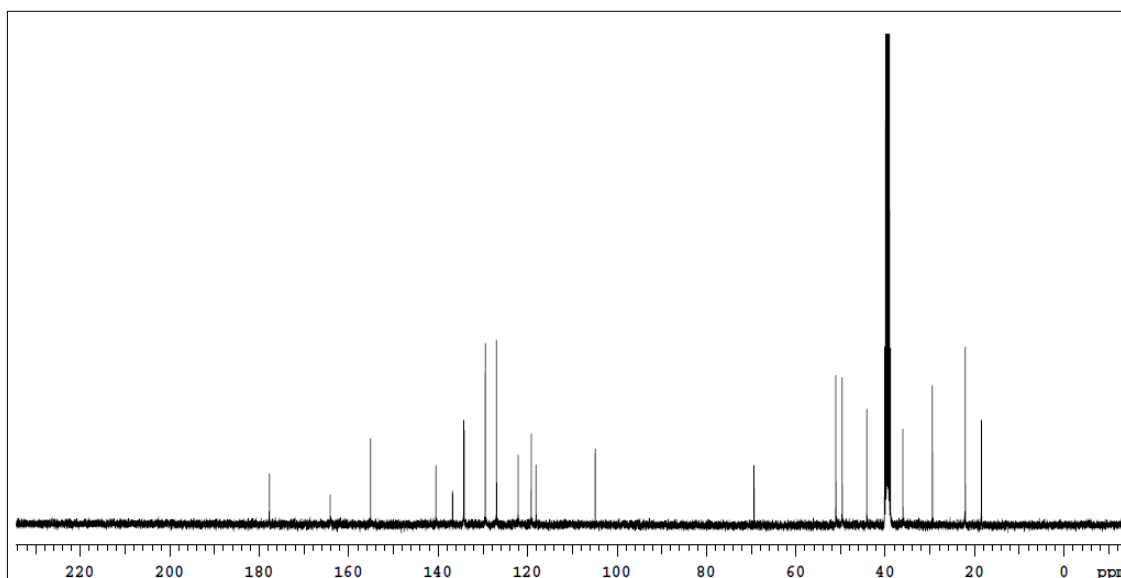

Figure 96. ^{13}C NMR spectrum of Compound **10o**

5-[1-(4-Isobutylphenyl)ethyl]-3-{[4-(2-pyridyl)piperazin-1-yl]methyl}-1,3,4-oxadi-azole-2(*3H*)-thione (Compound 10p)
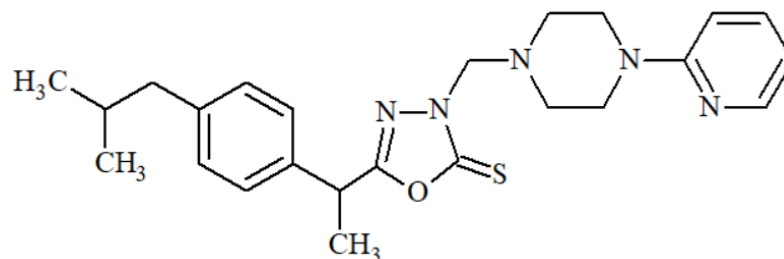
5-[1-(4-Isobutylphenyl)ethyl]-1,3,4-oxadiazole-2(*3H*)-thione (0.01 mol, 2.62 g), 1-(2-pyridyl)piperazine (0.01 mol, 1.63 g), formaldehyde (0.015 mol, 0.55 ml) in 15 ml methanol were reacted according to general synthesis method at 3.1.2.4.

Yield (%)	:	55
Retention factor (R$_f$)	:	0.64 [Toluene: Acetone: Acetic Acid (75:25:10)]
Physical appearance	:	White powder
Melting point (°C)	:	85
Solubility	:	Highly soluble with acetone and DMSO. Practically insoluble in water
Elemental analysis		
Molecular formula	:	C$_{24}$H$_{31}$N$_5$OS
Molecular weight (g/mol)	:	437.60

	C	H	N	S
Calculated (%)	65.87	7.14	16.00	7.33
Found (%)	65.32	7.10	16.12	7.48

Spectral Analysis

Infrared (IR) spectrum

ν_{max} **(cm^{-1}) :** 2951 (aromatic C-H stretchings); 2844 (aliphatic C-H stretchings); 1618 (C=N stretching); 1591, 1563, 1512, 1478 (aromatic C=C stretchings); 1445 (C-N stretching); 1326 (C-O stretching); 1274 (C=S stretching); 843 (1,4-dialkylphenyl C-H bendings); 774 (2-pyridyl C-H bendings) (Figure 97).
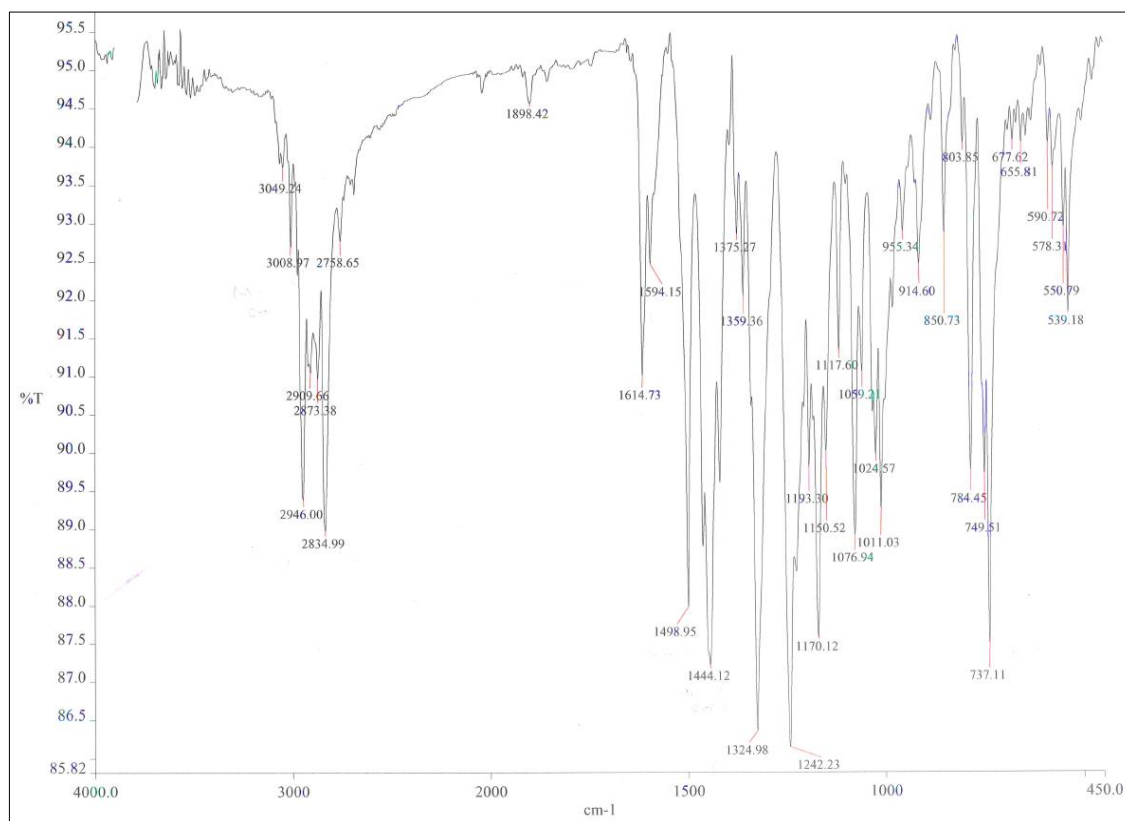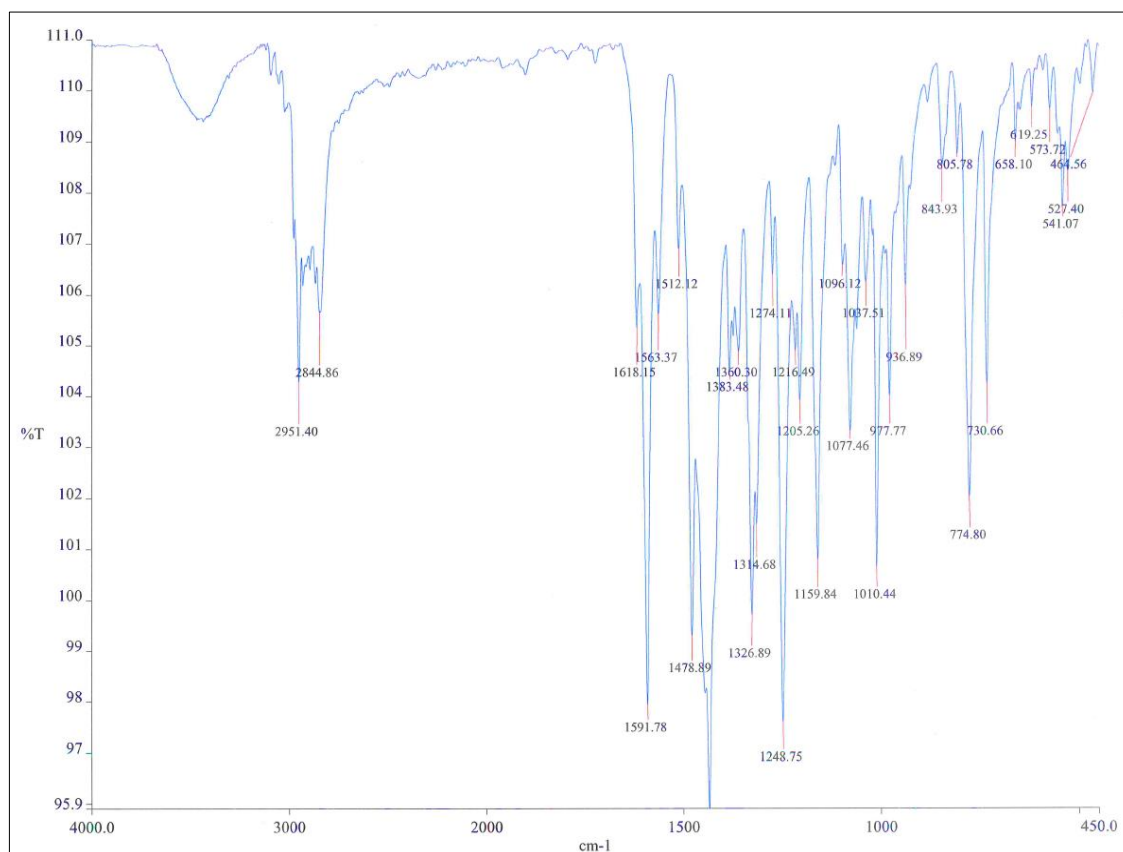

Figure 97. IR spectrum of Compound **10p**

^{1}H NMR spectrum

δ ppm (400 MHz/DMSO-d_6): 0.83 (6H, d, J=6.4 Hz, isobutyl -C$\underline{H}_3$); 1.54 (3H, d, J=6.8 Hz, -CH-C$\underline{H}_3$); 1.74-1.82 (1H, m, isobutyl –C$\underline{H}$-); 2.42 (2H, d, J=7.6 Hz, isobutyl –C$\underline{H}_2$-); 2.78 (4H, t, J=4.8 Hz, piperazine H$_2$+H$_6$); 3.49 (4H, t, J=4.8 Hz, piperazine H$_3$+H$_5$); 4.32 (1H, q, J=7.2 Hz, -C$\underline{H}$-CH$_3$,); 5.00 (2H, s, -N-C$\underline{H}_2$-N-); 6.61-6.64 (1H, m, pyridyl H$_5$); 6.81 (1H, d, J=8.4 Hz, pyridyl H$_6$); 7.11 (2H, d, J=8 Hz, phenyl H$_3$+H$_5$); 7.17 (2H, d, J=8 Hz, phenyl H$_2$+H$_6$); 7.49-7.53 (1H, m, pyridyl H$_4$), 8.09 (1H, dd, J=4.6 J'=1.4 Hz, pyridyl H$_3$) (Figure 98).
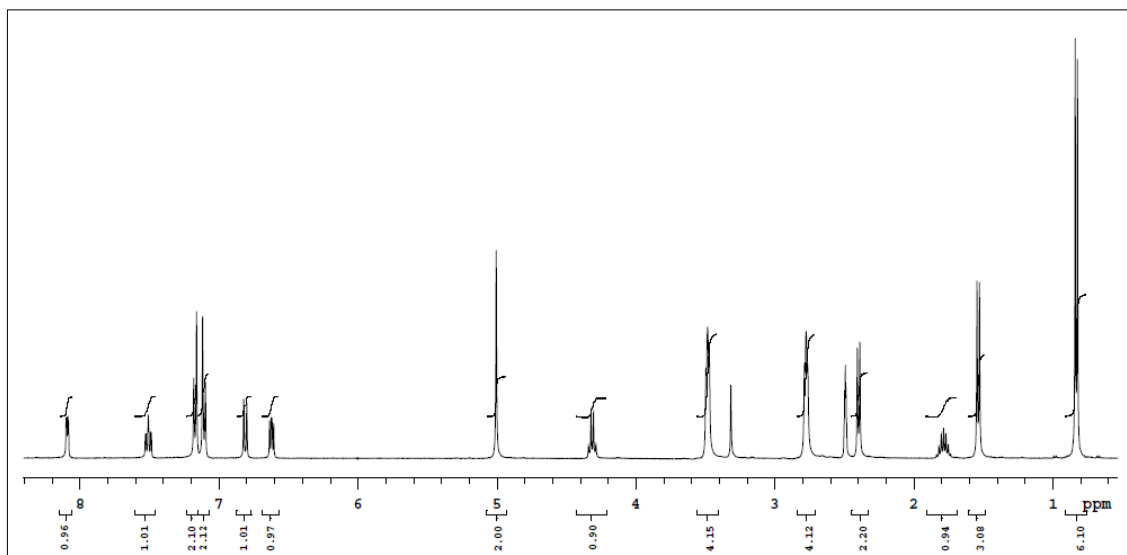
Figure 98. ^{1}H NMR spectrum of Compound **10p**

^{13}C NMR spectrum

δ ppm (400 MHz/DMSO-d_6): 18.45 (isobutyl –C̲H-); 22.11+22.13 (isobutyl -C̲H$_3$); 29.49 (-CH-C̲H$_3$); 36.06 (isobutyl -CH$_2$-); 44.12 (-C̲H-CH$_3$); 44.51 (piperazine C$_2$+C$_6$); 49.34 (piperazine C$_3$+C$_5$); 69.52 (-N-C̲H$_2$-N-); 107.17 (pyridyl C$_6$); 112.99 (pyridyl C$_4$); 126.95 (phenyl C$_3$+C$_5$); 129.41 (phenyl C$_2$+C$_6$); 136.74 (phenyl C$_4$); 137.45 (pyridyl C$_5$); 140.49 (phenyl C$_1$); 147.49 (pyridyl C$_3$); 159.32 (pyridyl C$_1$); 164.58 (C̲=N); 178.22 (C̲=S) (Figure 99).
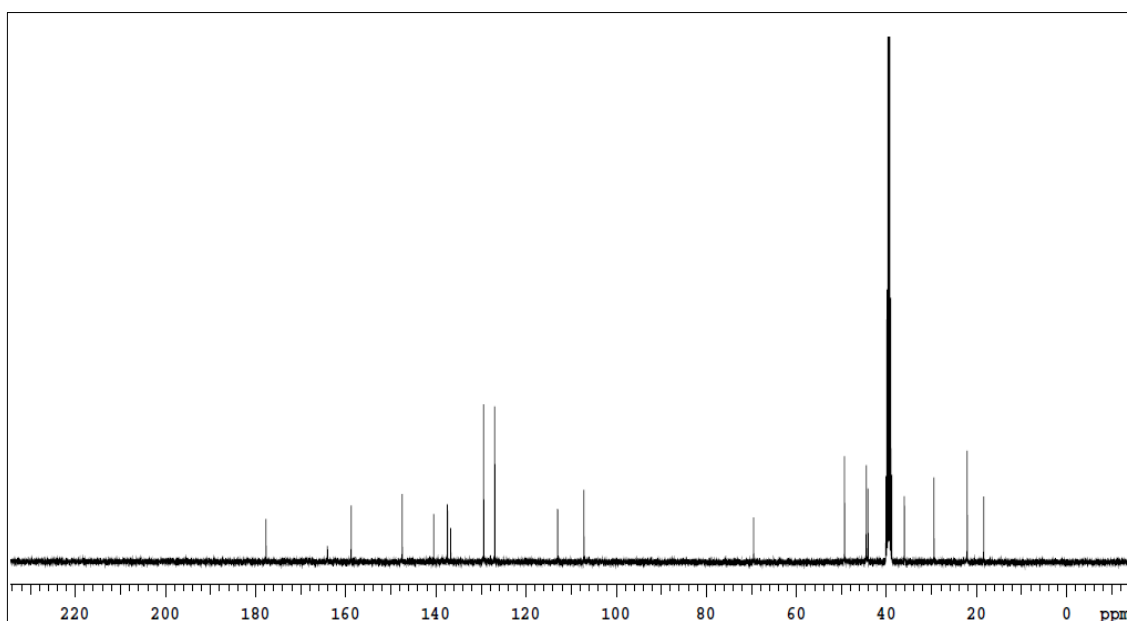
Figure 99. ^{13}C NMR spectrum of Compound **10p**

166

4.2. Biological Studies

4.2.1. Cell Viability

Tested compounds and indomethacin were analyzed for their cytotoxic effects on RAW 264.7 macrophages by using the MTT assay. IC_{50} values of reference and synthesized compounds were given in Table 2.

Table 2. IC_{50} values of compound **5a-5o** and **10a-10p** with reference indomethacin

Compound	IC_{50} (µM)	Compound	IC_{50} (µM)
5a	>100	10a	>100
5b	>100	10b	>100
5c	>100	10c	>100
5d	>100	10d	>100
5e	>100	10e	>100
5f	>100	10f	>100
5g	>50	10g	68.47±1.80
5h	>100	10h	>100
5i	>100	10i	>100
5j	>100	10j	>100
5k	>100	10k	>100
5l	>100	10l	>100
5m	>100	10m	>100
5n	>100	10n	>100
5o	>100	10o	>100
		10p	>100
		Indomethacin	>100

4.2.2. Antiinflammatory Activity

4.2.2.1. COX-1/COX-2 Inhibition

In *vitro* antiinflammatory effect poteantials of tested and reference compounds were done by cyclooxygenase-1 (COX-1)/cyclooxygenase-2 (COX-2) enzyme fluorometric assay kit method. Ibuprofen, SC-560 (selective COX-1 inhibitor) and DuP-687 (selective COX-2 inhibitor) were employed as standart drugs and results were summerized in Table 3 as percentage of enzyme inhibition. All tested samples and standart compounds were applied at 100 μM dose except **5g** and **10g** (50 μM).

Table 3. COX-1 and COX-2 inhibition (%) of compound **5a-5o** and **10a-10p**

Compound	COX-1 inhibition (%)	COX-2 inhibition (%)	Compound	COX-1 inhibition (%)	COX-2 inhibition (%)
5a	**51.3±1.6**	26.9±1.8	**10a**	19.3±1.0	10.2±3.4
5b	24.1±1.0	10.5±1.4	**10b**	**76.4±2.1**	9.9±1.2
5c	24.7±0.8	20.5±0.5	**10c**	35.6±1.1	20.7±2.2
5d	32.3±1.9	25.6±0.7	**10d**	31.5±1.4	13.9±1.0
5e	**50.3±2.1**	39.8±0.6	**10e**	**51.7±2.8**	20.2±2.5
5f	47.9±2.4	20.4±4.1	**10f**	44.2±3.6	35.3±0.5
5g	14.2±2.8	8.6±0.8	**10g**	47±0.8	39.3±0.3
5h	40.4±0.3	18.6±1.9	**10h**	**54.7±2.2**	32.4±0.4
5i	**56.7±0.8**	20.8±1.8	**10i**	9.8±1.1	6.7±1.2
5j	35.2±3.1	14.8±1.9	**10j**	28.4±2.3	23.2±1.4
5k	**51.8±2.6**	19.7±1.2	**10k**	12.8±1.5	6.8±1.5
5l	17.3±2.2	9±2.5	**10l**	31.2±0.6	10.3±1.5
5m	40.8±2.3	28.7±3.2	**10m**	48.3±0.3	20.5±1.1
5n	**56±4.8**	33.8±3.3	**10n**	32.7±1.3	24±4.8
5o	41.8±3.7	18.3±4.2	**10o**	18.2±2.8	12.5±3.7
			10p	26.7±2.0	20.3±4.5
			Ibuprofen	**83.8±1.8**	**62.7±4.0**
			SC-560	**90±2.6**	**NI**
			DuP-697	**NI**	**90±2.6**

4.2.2.2. NO Inhibition

NO inhibition values of synthesized compounds and indomethacin were given in Table 4. All tested and reference compounds were applied at 100 µM doses except **5g** and **10g** (50 µM).

Table 4. LPS-induced nitrite levels of **5a-5o** and **10a-10p** with reference indomethacin

Compound	Nitrite level (µM)	Compound	Nitrite level (µM)
LPS (+)	**41.17±2.96**		
5a	30.32±3.23	**10a**	29.91±4.25
5b	28.93±5.66	**10b**	30.52±6.70
5c	28.44±4.14	**10c**	29.49±5.20
5d	27.47±3.99*	**10d**	**13.16±4.84******
5e	27.33±3.51*	**10e**	**23.77±5.55*****
5f	27.74±4.02*	**10f**	34.38±6.06
5g	30.54±4.91	**10g**	**23.02±1.51******
5h	**20.75±4.40******	**10h**	**14.51±0.13******
5i	30.18±1.69	**10i**	**24.02±3.90*****
5j	31.74±3.37	**10j**	28.16±2.93*
5k	31.95±2.29	**10k**	44.49±7.85
5l	28.93±2.64	**10l**	32.81±7.67
5m	26.13±3.00**	**10m**	32.73±6.35
5n	29.29±2.05	**10n**	37.23±3.38
5o	35.73±2.33	**10o**	37.09±7.69
		10p	27.96±4,83*
		Indomethacin	**24.46±1.80*****

One-way ANOVA, followed by the post-hoc tests by Tukey. The significant differences between groups and control (LPS) were defined with * at $p < 0.05$, ** at $p < 0.01$, *** at $p < 0.001$ and **** at $p < 0.0001$.

4.2.2.3. PGE$_2$ Inhibition

PGE$_2$ inhibition values of synthesized compounds and indomethacin were given in Table 5. All tested and reference compounds were applied at 100 µM doses (except **10g**-50 µM) with three times.

Table 5. LPS-induced PGE$_2$ levels of selected compounds with reference indomethacin.

Compound	PGE$_2$ level (pg/ml)
LPS (+)	**2396±154.8**
5d	2227±14.41
5e	2156±55.78*
5f	2198±42.66
5h	**354.2±36.54****
5k	1521±27.5**
5m	2392±0.1
5n	1659±57.5**
10b	2285±219.5
10d	1982±38.46**
10e	2142±13.85*
10g	2377±76.84
10h	**1026±59.68****
10i	2300±29.76
10j	2330±60.29
10p	2454±31.75
Indomethacin	**22.94±4.26****

One-way ANOVA, followed by the post-hoc tests by Tukey. The significant differences between groups and control (LPS) were defined with * at $p<0.05$, ** at $p<0.01$, *** at $p<0.001$ and **** at $p<0.0001$.

4.2.3. Antioxidant Activity

4.2.3.1. DPPH Scavenging Activity

DPPH scavenging percentages of synthesized compounds and ascorbic acid values were given in Table 6. Ascorbic acid and all tested compounds were applied at 100 µM dose except **5g** and **10g** (50 µM),

Table 6. DPPH radical scavenging percentages of **5a-5o** and **10a-10p** with reference ascorbic acid.

Compounds	DPPH radical scavenging (%)	Compounds	DPPH radical scavenging (%)
5a	34.98±0.97	**10a**	40.22±4.86
5b	**50.60±1.96**	**10b**	35.67±2.65
5c	49.73±3.35	**10c**	40.88±0.83
5d	49.48±1.68	**10d**	47.77±1.38
5e	42.26±2.46	**10e**	39.47±1.25
5f	44.68±1.95	**10f**	33.63±2.46
5g	27.87±0.76	**10g**	19.90±0.99
5h	42.89±0.88	**10h**	37.42±0.99
5i	41.43±3.16	**10i**	42.59±1.61
5j	32.54±1.72	**10j**	30.73±0.09
5k	39.13±1.41	**10k**	17.90±0.88
5l	**50.56±2.29**	**10l**	45.35±0.76
5m	46.22±0.94	**10m**	43.76±0.85
5n	42.26±1.14	**10n**	38.17±2.86
5o	26.66±1.42	**10o**	30.91±0.45
		10p	39.17±0.99
		Ascorbic Acid	**19.09±0.80**

4.3. Docking Studies

4.3.1. COX-1/ COX-2 Docking Scores

Compounds that have more than 50% inhibition against COX-1 enzyme were docked into COX-1 (PDB ID: 5U6X [199]) and COX-2 (PDB ID: 5IKT [200]) enzymes. Docking scores of corresponding samples were given in Table 7.

Table 7. Docking scores of chosen derivatives for COX-1 and COX-2 enzymes

Compound	Docking Score (COX-1)	Docking Score (COX-2)	RMSD
5a	-7.688	-8.03	
5d	-7.668	-8.064	
5e	-7.805	-8.073	
5h	-7.632	-7.324	
5i	-7.863	-8.178	
5k	-7.079	-7.991	
5m	-8.003	-8.483	
5n	-7.444	-8.286	
10b	-8.695	-8.006	
10d	-8.951	-7.5	
10e	-8.658	-7.985	
10g	-8.627	-7.851	
10h	-8.444	-6.602	
10i	-8.106	-7.907	
10m	-7.914	-7.471	
10p	-8.219	-7.531	
Cocrystallized ligand (PDB ID: 5U6X)	-7.715		0.210
Cocrystallized ligand (PDB ID: 5IKT)		-10.165	0.738

5. DISCUSSION and CONCLUSION

5.1. Chemistry

In this study, 5-(2-hydroxyphenyl)-3-[(substitutedpiperazine)methyl]-1,3,4-oxadiazole-2(*3H*)-thione (**5a-5o**) and 5-{1-[4-(isobutyl)phenyl]ethyl}-3-[(4-substituted piperazine)methyl]-1,3,4-oxadiazole-2(*3H*)-thione (**10a-10p**) compounds were synthesized according to reaction pathway depicted in Scheme 7. In the first step, carboxylic acid groups of salicylic acid (**1**) and ibuprofen (**6**) were converted into methyl ester groups (**2**, **7**) from their carboxylic acid moieties in the presence of sulphuric acid and methanol. Subsequently, compounds **2** and **7** were reacted with hydrazine hydrate to produce hydrazide derivatives (Compound **3** and **8**). 1,3,4-Oxadiazole-2(*3H*)-thione ring (compounds **4**, **9**) closure was obtained *via* the reaction of compounds **3** and **8** with carbon disulphide (CS$_2$) and potassium hydroxide (KOH) in hot alcoholic media. Finally compounds **4** and **9** were treated with different piperazines via *Mannich* reaction to afford target compounds **5a-5o** and **10a-10p** in moderate to good yields [17, 84]. After synthesis, compound structures were elucidated with IR, UV, ^{1}H NMR, ^{13}C NMR spectral data and purities were checked by elemental analyses.
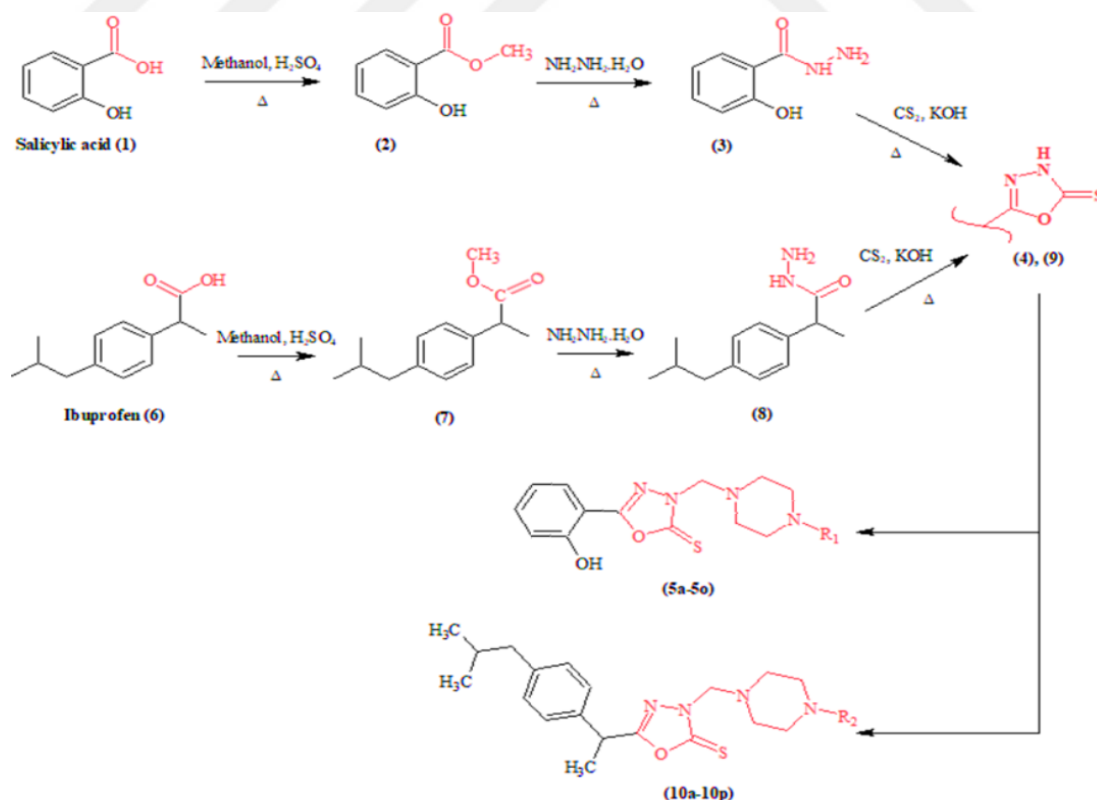
Scheme 7. Chemical synthesis of compound **5a-5o** and **10a-10p**

Final compounds (**5a-5o, 10a-10p**) were obtained by four-step reaction (Scheme 7). For the first step, carboxylic acid groups of salicylic acid and ibuprofen molecules were converted into methyl esters by *Fischer's esterification* mechanism. Reaction work up was easy to handle. The resulting products were pure and in good yields (95-98%). The mechanism of reaction was shown in Scheme 8 as the protonation of carbonyl moiety of carboxylic acid refers formation of a carbocation on carbonyl in which alcohol group attacks on it for the further position. In the next step proton transfer and release of water corresponds to an oxonium ion intermediate. Finally deprotonation provides desired ester product [203].
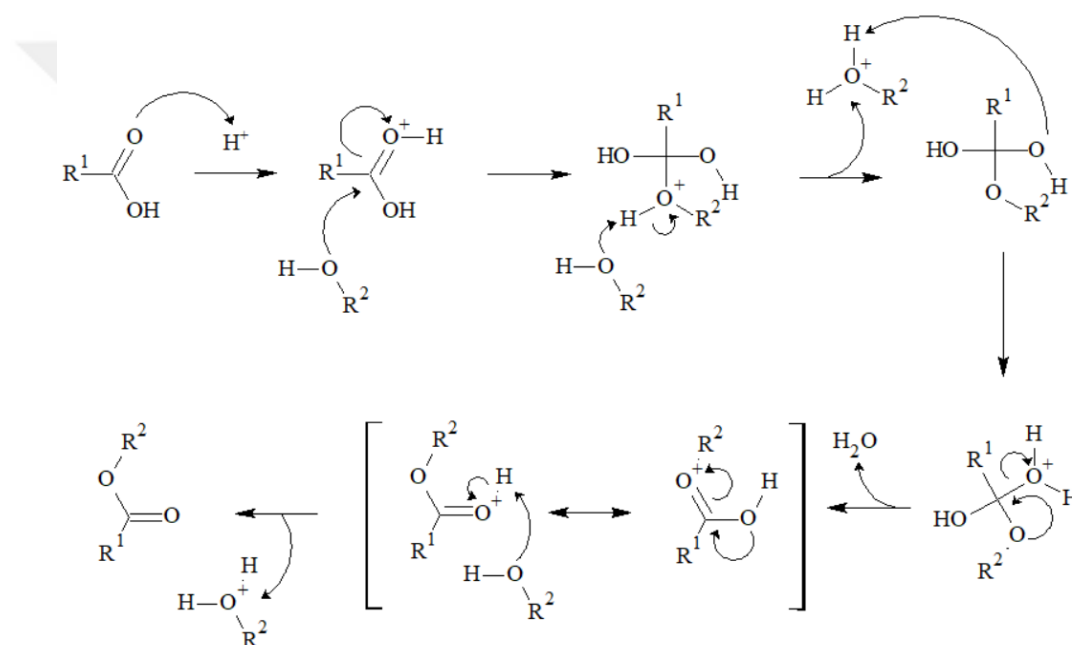
Scheme 8. Mechanism of ester formation from carboxylic acid [203]

For the second step, ester forms of salicylic acid and ibuprofen derivatives were reacted with hydrazine hydrate in the presence of ethanol. Ester compounds and hydrazine hydrate were used with stochiometrically 1:2 mole ratios and the mixture was gently boiled till 12-15 hours. In order to isolate final hydrazides, alcohol was evaporated at reduced pressure [17]. After the generation of an oily compound, iced water was poured onto it. Formed white solids was filtered, washed and dried. Compounds were produced in yields of 40-65%. For the mechanism of ester conversion into hydrazide group (Scheme 9); primary amine group in hydrazine hydrate attacks to carbonyl carbon *via* electrophilic substitution reaction which corresponds to negatively charged oxygen

formation on carbonyl group. Afterwards by the leaving of alkoxy group in the molecule contributes the reformation of carbonyl group again to produce final hydrazide compound [204].
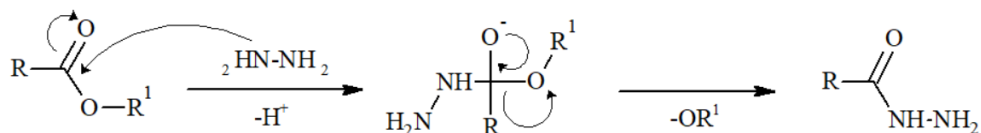
Scheme 9. Mechanism of hydrazide formation from ester group

For the third step, similar synthesis pathway with Manjunatha *et al.* was used [17]. Initially, potassium hydroxide was dissolved in methanol and aryl/alkyl hydrazide was added to the clear solution. While carbondisulphide was treated drop by drop into reaction, dithiocarbamate salts of hydrazide were formed as solid particules in mixture. Untill all solid compounds totally were dissolved in hot reaction media, process was continued (10-15 hours). When the reaction was over, excess solvent was distilled off under reduced pressure and obtained oily-brown compound was quenched with n-hexane. Separated white solid particles were filtered, dried and recrystallized from ethanol. Desired 5-substituted-1,3,4-oxadiazole-2(*3H*)-thiones were yielded in range of 65-85%. Young and Wood explained the mechanism of 1,3,4-oxadiazole ring cyclization in 1955 as, the reaction starts with nucleophilic substitution of carbon in carbondisulphide to primary amine moiety in hydrazide which corresponds to the formation of dithiocarbamate salt. Next step, nucleophilic oxygen attacks to partial positive carbon of dithiocarbamate and molecule becomes cyclized. In the presence of acid catalyst, thiol form of ring is totally tautomerized into thione form as depicted in Scheme 10 [205].
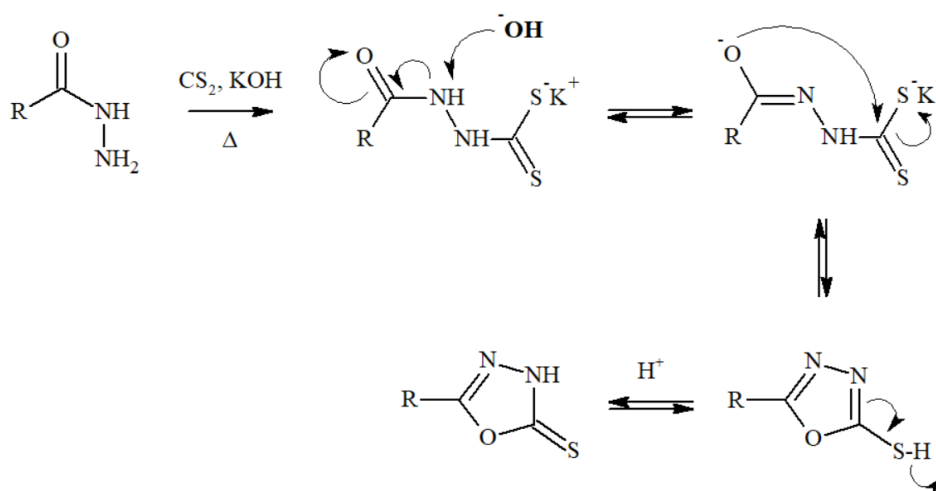
Scheme 10. Mechanism of 1,3,4-oxadiazole-2(*3H*)-thione formation from hydrazide

Last step of target compounds were applied with piperazine derivatives and 5-substituted-1,3,4-oxadiazole-2(*3H*)-thiones by *Mannich* reaction procedure. This reaction is described as a three-component condensation between structurally different substrates (X-H) containing minimum one active hydrogen atom, an aldehyde component and an amine reagent referring to a class of compounds generally known as *Mannich* bases. *Mannich* reactions are also named as aminoalkylation reactions in which if formaldehyde is used as aldehyde component, the substrate is converted into the corresponding *Mannich* base through an aminomethylation process [81]. The proposed mechanisms of our reaction were given as:

The acid-catalyzed *Mannich* reaction,
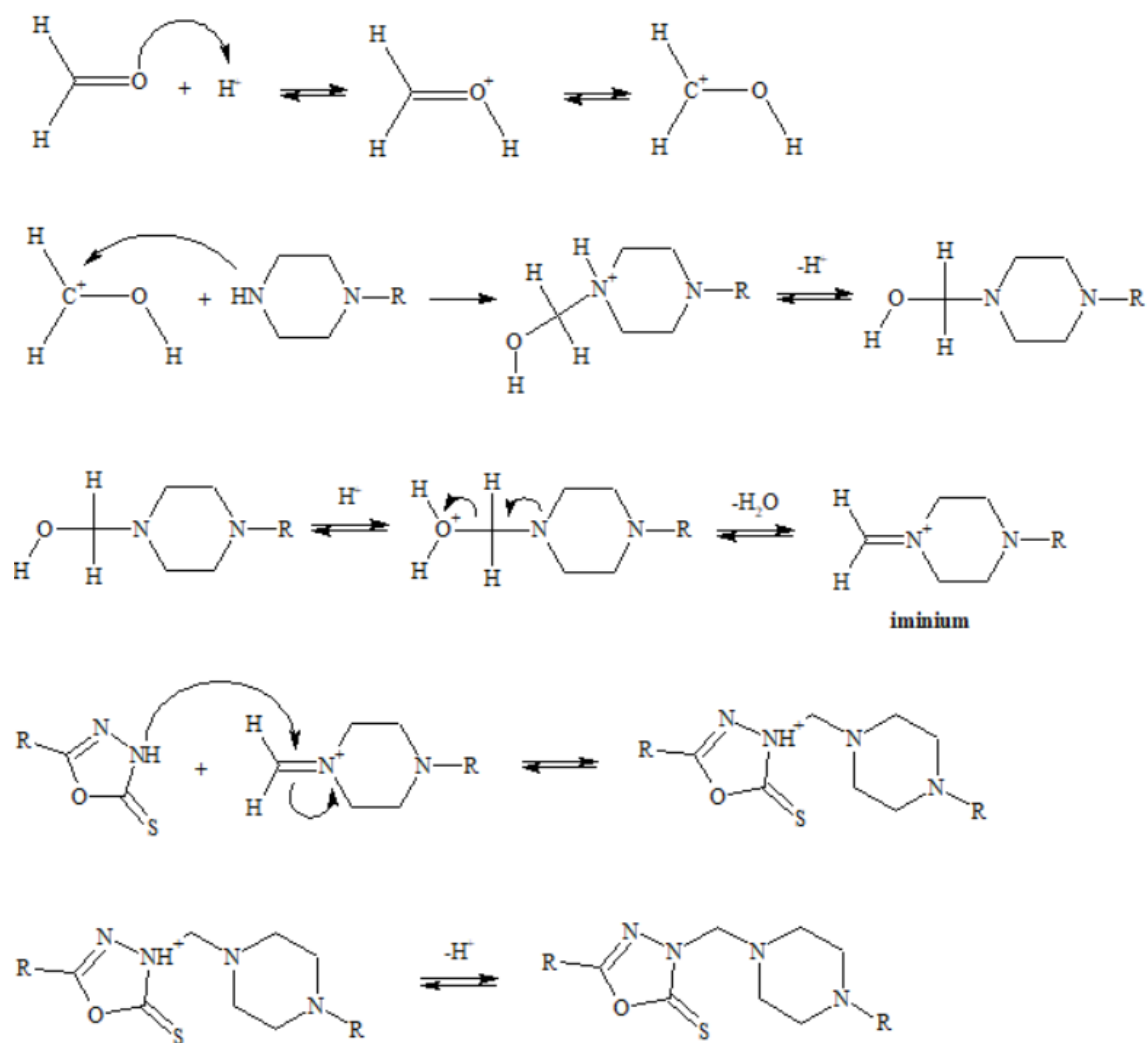
The base-catalyzed *Mannich* reaction,
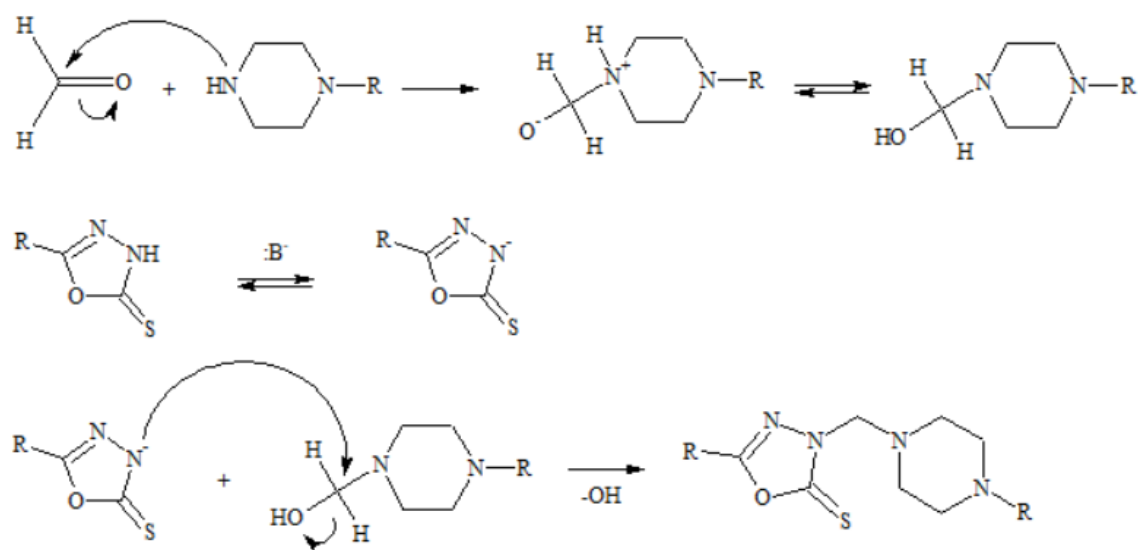
Novel 3,5-disubstituted-1,3,4-oxadiazole-2(*3H*)-thione derivatives **(5a-5o, 10a-10p)** were synthesized in four steps reaction. Piperazine derivatives and third position of 5-substituted-1,3,4-oxadiazole-2(*3H*)-thione ring were combined with a methylene bridge via *Mannich* reaction procedure in the presence of formaldehyde. Desired compounds were yielded in range of **32-84%** for salicylic acid series **(5a-5o)** and **29-72%** for ibuprofen series **(10a-10p).** Particularly para-substituted compounds served higher yields, compared to ortho and meta-substituted ones. Compounds containing halogen groups **(5b-5g, 10b-10g)** evaluated negligible reaction yields according to methyl, methoxy or nitrile containing molecules in both series. With the scores of **84%** and **72%**; compound **5a** and **10a** were found to have highest reaction yields which they have nonsubstituted phenyl piperazine fragments in common.

After the synthesis of compounds, structure elucidation was characterized by different spectral methods. UV spectral data was deteched as strong absorption bands at 208, 255, 315 nm for compound **5a** (Figure 100) and 262 nm for compound **10a** (Figure 101). Observed maximum absorption values refered to n→π* and π→π* transitions of aromatic structures in which these results were parallel with other 5-substitutedphenyl-1,3,4-oxadiazole-2(*3H*)-thione derivatives which were described in previous researches [206-208].
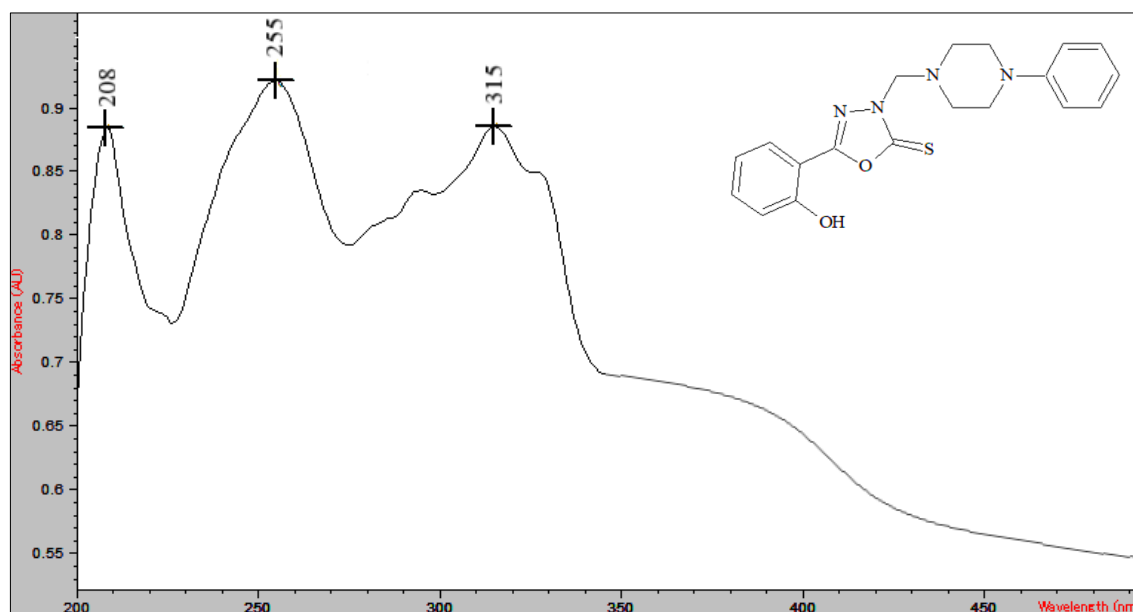
Figure 100. UV spectrum of Compound **5a**
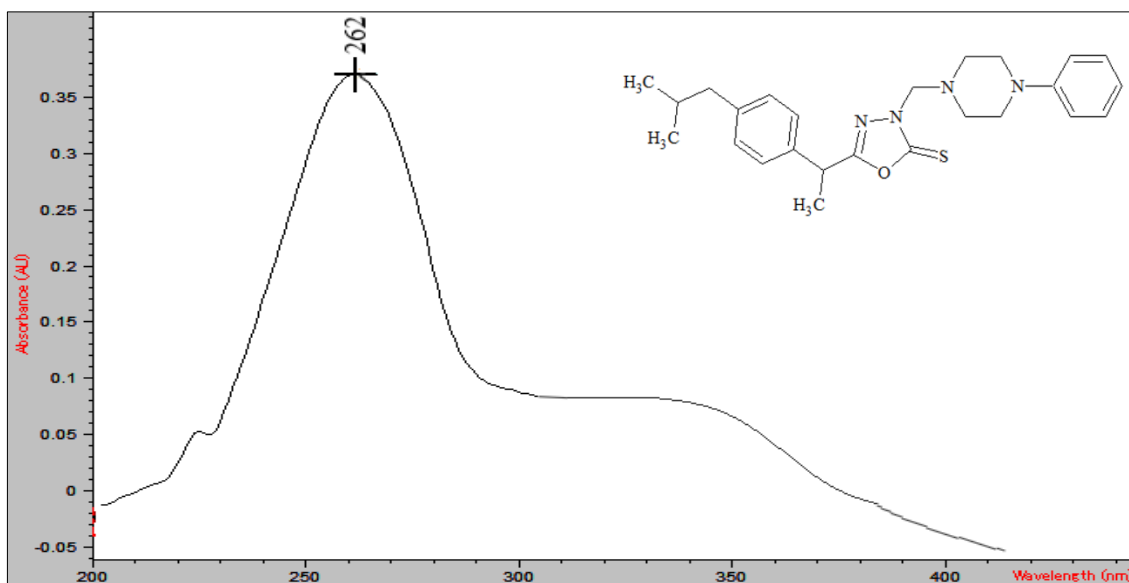
Figure 101. UV spectrum of Compound **10a**

Spesific bond stretchings of salicylic acid **(5a-5o)** and ibuprofen **(10a-10p)** derivatives were also checked *via* FT-IR spectroscopy. Particularly, ring closure of 1,3,4-oxadiazole-2(*3H*)-thione was characterized by using IR, within the disappearance of N-H and emergence of C=N and C=S stretching signals nearly at 3300, 1600-1650 and 1100-1250 cm^{-1} respectively. The signals for C-O stretching in range of 1200-1350 cm^{-1} were also other confirmation for ring closure. Additionally, thione or thiol tautomers of 1,3,4-oxadiazole were indicated by weak signals around 1300 or 2600 cm^{-1} respectively. Aromatic C-H stretchings of **5a-5o** and **10a-10p** were deteched in between 2800-2900 cm^{-1} whereas aromatic C=C stretchings were evaluated around 1450 cm^{-1} in both series. Identically, compound **5a-5o** presented broad O-H band in range of 3304-3436 cm^{-1} depended on hydroxy group of salicylic acid moiety. IR data also indicated loss of N-H stretchings at 3300 cm^{-1} were proposed as the formation of all newly synthesized *Mannich* bases (**5a-5o** and **10a-10p**). IR data of all compounds were found compatible with literature [125]. Representative IR spectrum interpretations were given for the compounds **5g** in Figure 102 and **10d** in Figure 103.
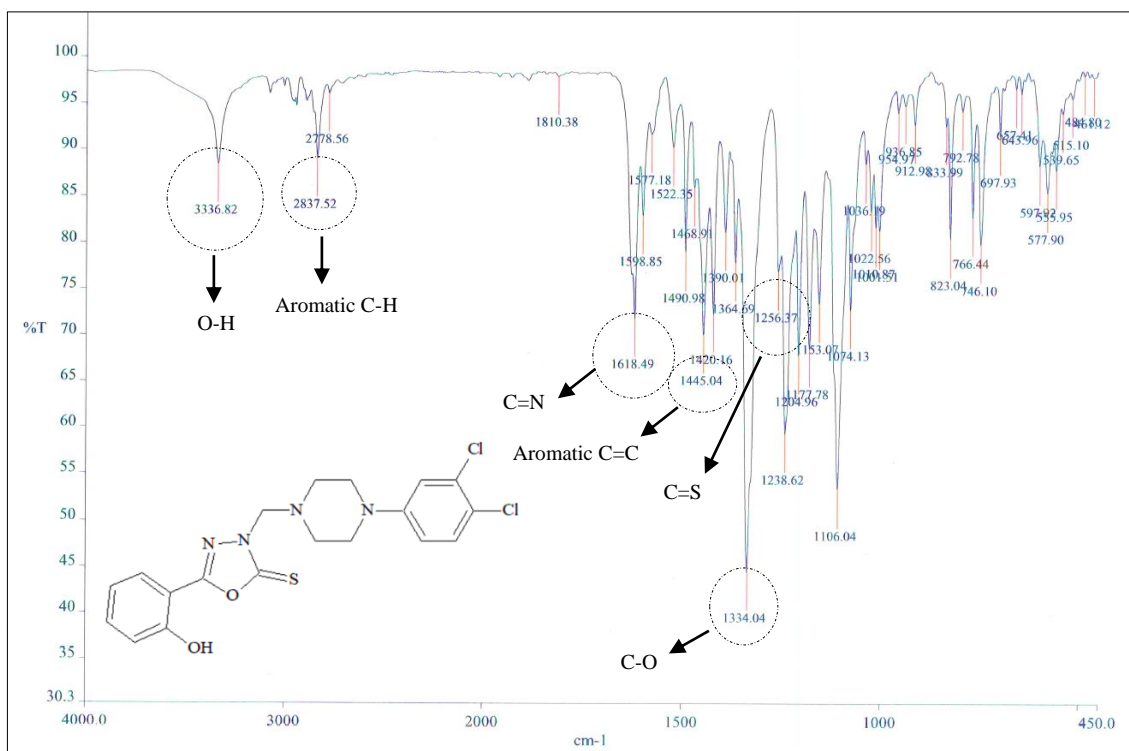
Figure 102. IR characterization of Compound **5g**
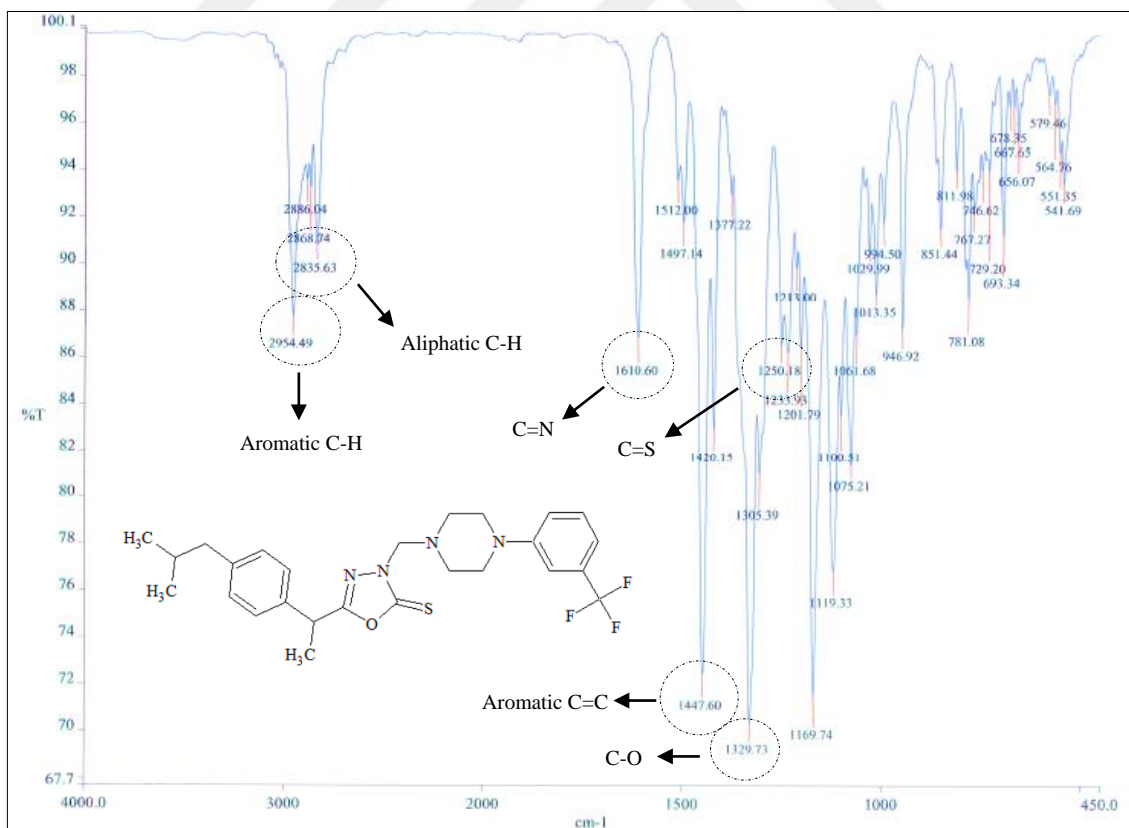
Figure 103. IR characterization of Compound **10d**

To determine the *Mannich* base formation of 1,3,4-oxadiazoles was easy to evaluate by ^{1}H NMR in which spectra signals of all protons related to synthesized compounds were found compatible with estimated chemical shift, multiplicity and coupling constant values in DMSO-*d6*.
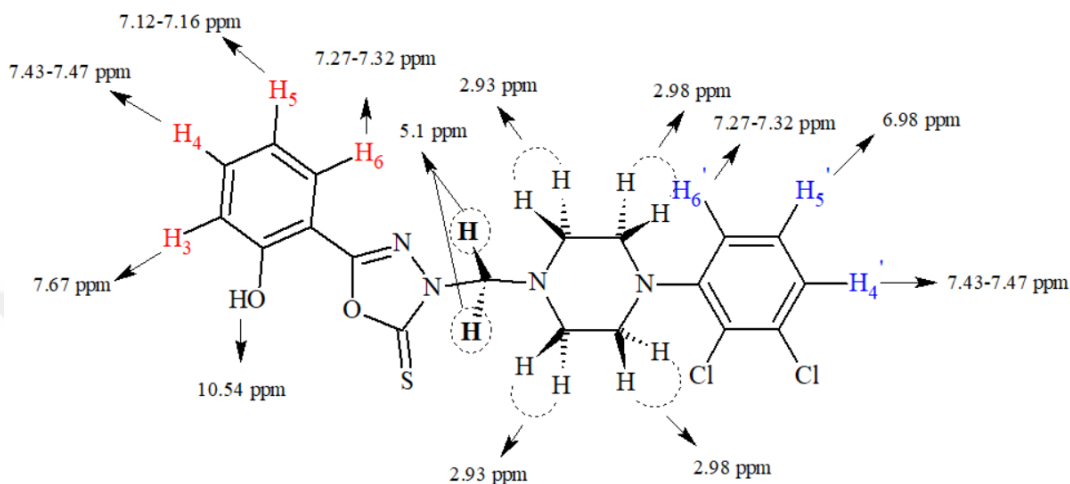
Figure 104. Molecular structure and chemical shifts (ppm) of Compound **5h** in ^{1}H NMR

Particularly descriptive singlet signal of methylene protons that found in range of 4.99-5.10 ppm representing *Mannich* bases of target compounds **(5a-5o, 10a-10p)**. To start with compound **5h** (Figure 104) in salicylic acid serie that possess piperazine hydrogens demonstrated broad doublet signals in region of 2.93-2.99 ppm and methylene protons formed identical singlet signal at 5.1 ppm. For aromatic hydrogens in **5h**; triplet signal at 6.98 ppm (*J*=7.4 Hz) adressed to phenyl H$_5$'; phenyl H$_4$' showed broad doublet signals (*J*=8 Hz) at 7.05 ppm; phenyl H$_5$ and both of phenyl H$_6$+H$_6$' showed multiplet signals in range of 7.12-7.16 and 7.27-7.32 ppm, respectively; also other multipled signals for phenyl H$_4$ were seemed at 7.43-7.47 ppm and phenyl H$_3$, formed a doublet of doublet signal (*J*=7.6, *J'*=1.6 Hz) at 7.67 ppm. Hydroxyl hydrogen of salicylic acid moiety produced a broad singlet signal at 10.54 ppm. Detailed chemical shift values of compound **5h** were given in below (Figure 105, 106, 107, 108).
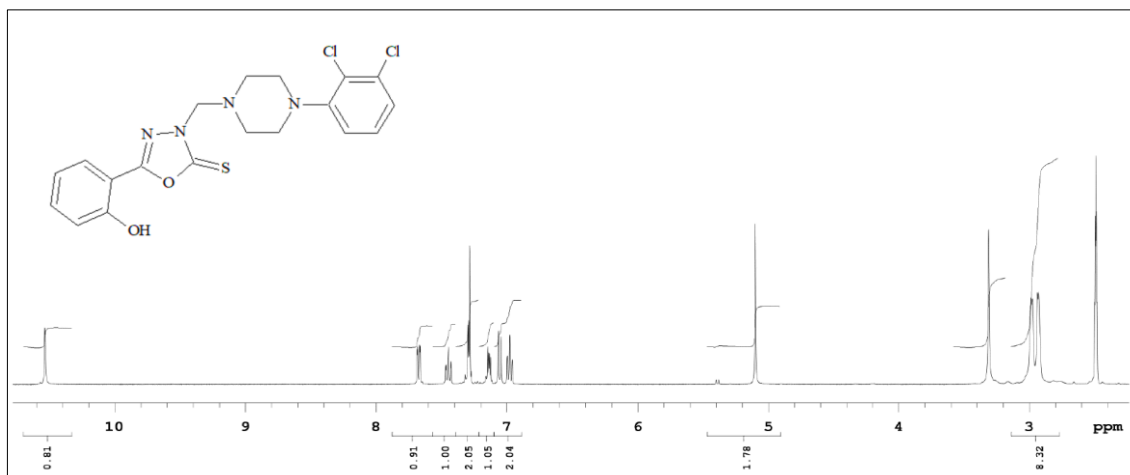
Figure 105. Hydrogen integrations of Compound **5h** in ^{1}H NMR spectra
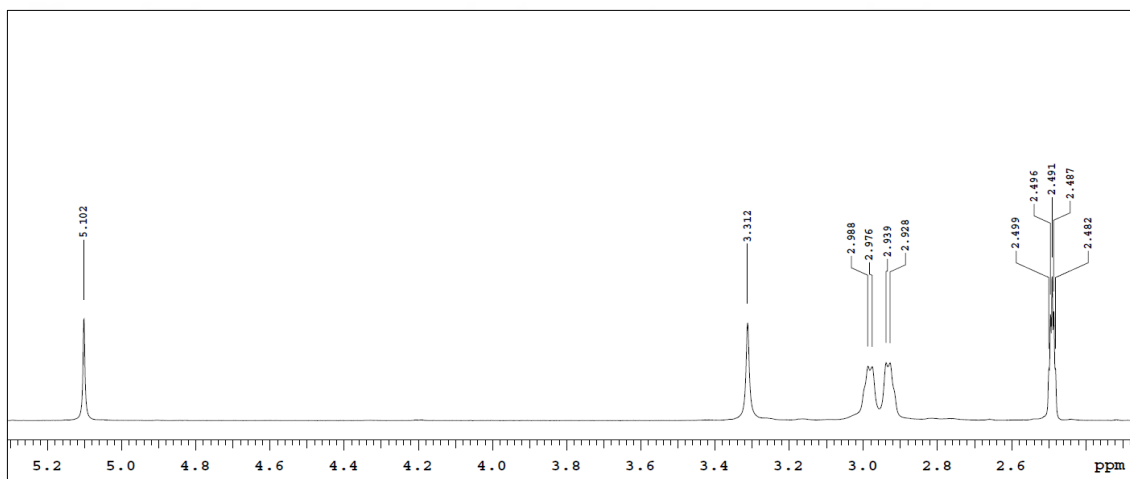
Figure 106. Chemical shift values of Compound **5h** in ^{1}H NMR spectra at 2.0-5.0 ppm
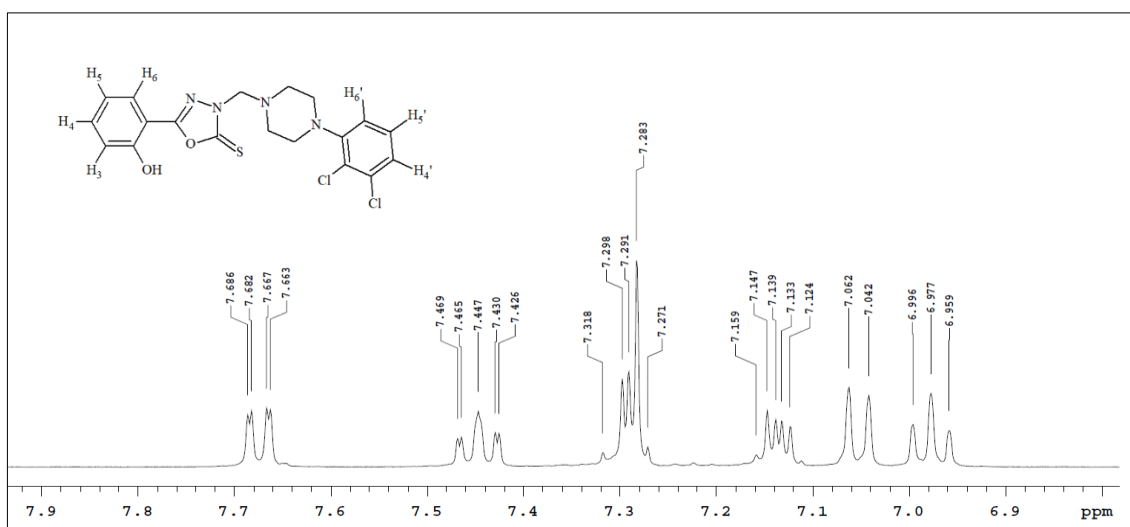
Figure 107. Chemical shift values of Compound **5h** in ^{1}H NMR spectra at 6.5-8.0 ppm

182
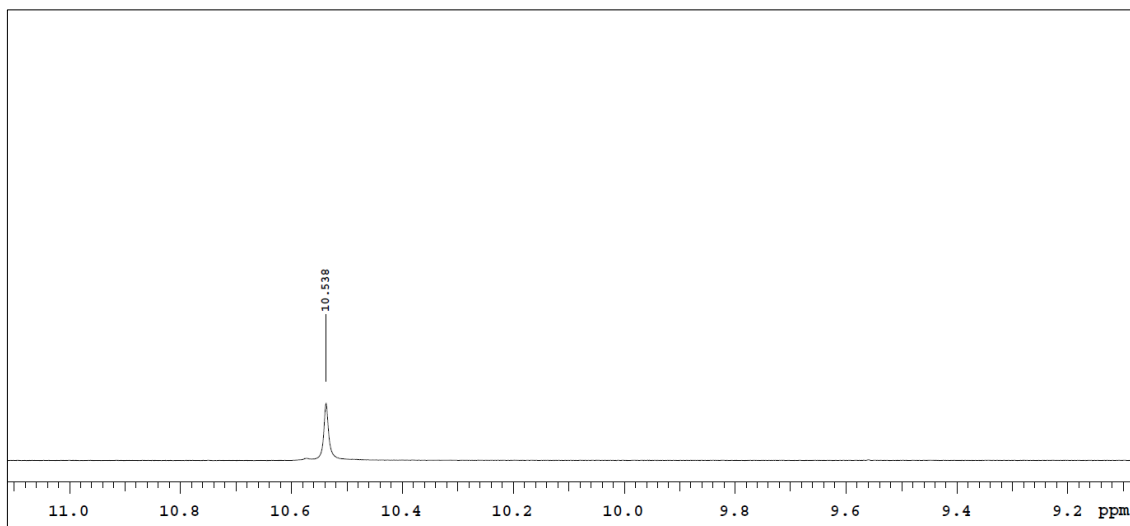
Figure 108. Chemical shift values of hydroxyl peak in Compound **5h** in ^{1}H NMR spectra at 9.0-11.0 ppm

Proton NMR spectra of ibuprofen derivatives (**10a-10p**) revealed that alkyl hydrogens of ibuprofen moiety were shifted more upfield region than aromatic hydrogen signals due to shielded electrons around them (Figure 109).
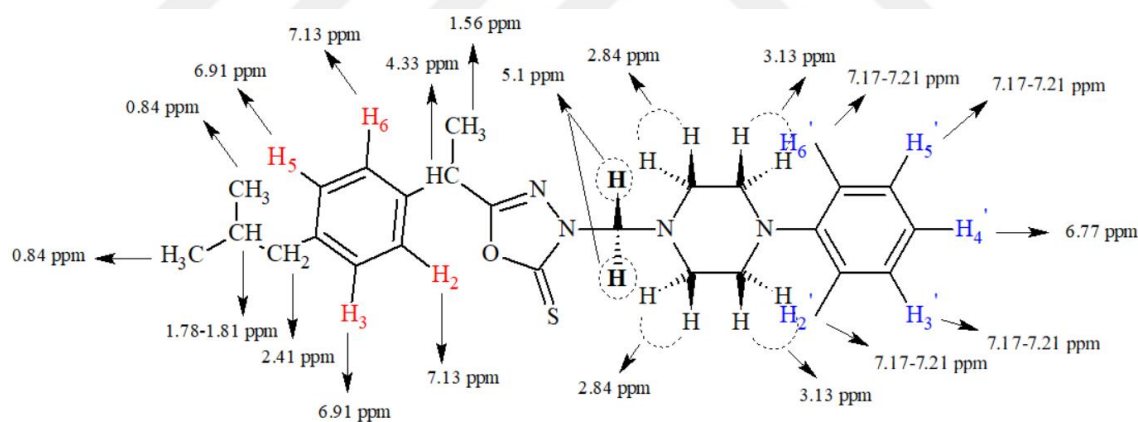
Figure 109. Molecular structure and chemical shifts (ppm) of Compound **10a** in ^{1}H NMR

To exemplified, for compound **10a**, signals of isobutyl and 1-ethyl hydrogens on ibuprofen moiety generated around 0.84-2.41 ppm. In this manner peaks of piperazine hydrogens in **10a** were visualized at more downfield region of scale about 2.84-3.13 ppm as they estimated. *Mannich* base indicator methylene protons produced an identical singlet signal at 5 ppm. ^{1}H NMR scale of compound **10a** also served aromatic hydrogen signals of ibuprofen revealed two similar doublet signals at 6.91-7.13 ppm depended on para-substituted positions. Piperazine bonded phenyl hydrogens formed a triplet peak for

H4' at 6.77 ppm and multiplet signals for H2', H3', H5', H6' in range of 7.17-7.21 ppm were deeply demonstrated in Figures 110, 111, 112 with signal multiplicities.
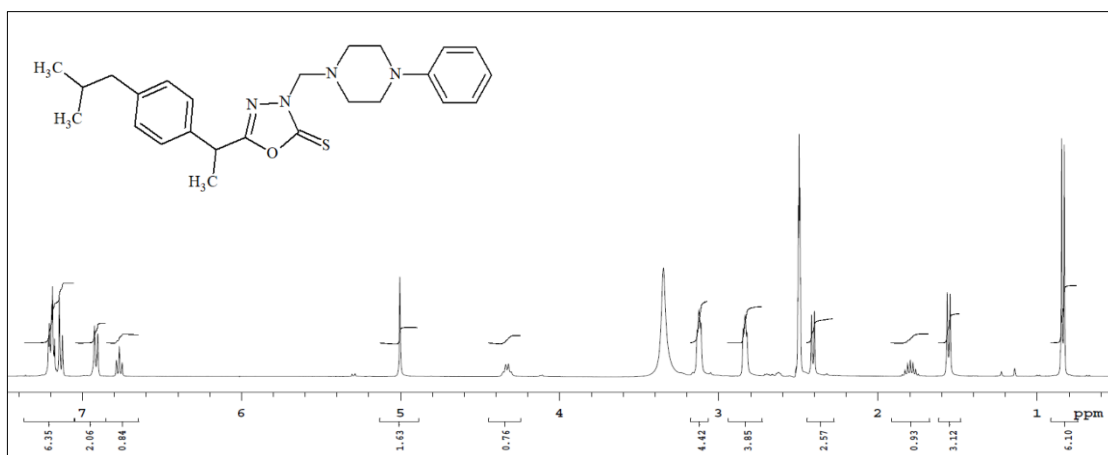
Figure 110. Hydrogen integrations of Compound **10a** in ^{1}H NMR spectra
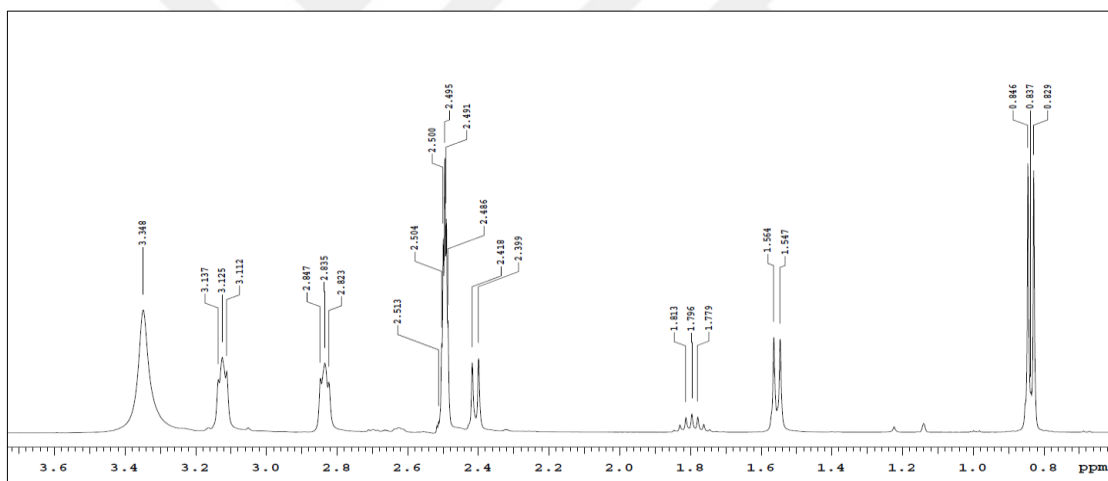
Figure 111. Chemical shift values of Compound **10a** in ^{1}H NMR spectra at 0.8-4.0 ppm
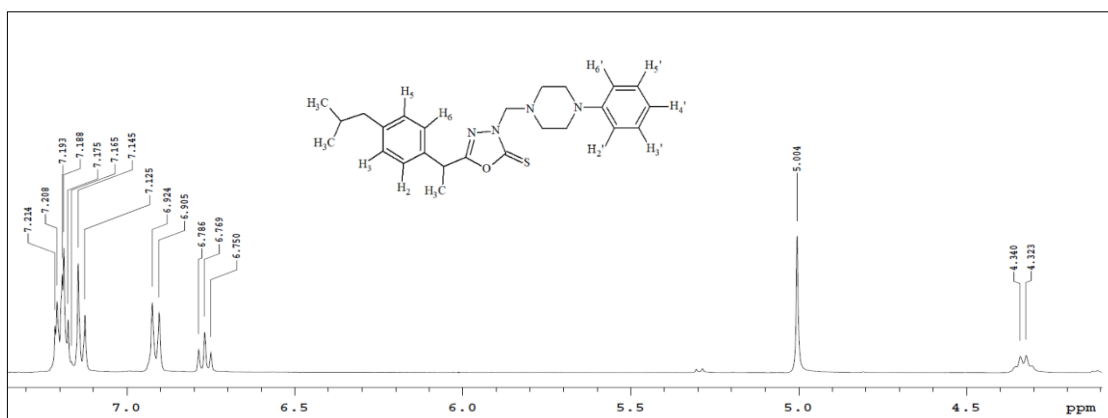
Figure 112. Chemical shift values of Compound **10a** in ^{1}H NMR spectra at 4.0-8.0 ppm

184

Molecular structures of final compounds (**5a-5o**, **10a-10p**) were also supported with ^{13}C NMR spectroscopy data. Based on carbon nucleus under the influence of a high electronegative environment, aromatic carbons linked from fifth position of 1,3,4-oxadiazole-2(*3H*)-thione ring occured at more downfield region in both compound serie. Similar basis also explains peak values of thione (C=S) and imine (C=N) groups in which they appeared at nearly 177 and 155 ppm. In salicylic acid derivatives **(5a-5o)**, chemical shift values of C_2 carbon on phenyl ring that was directly linked to hydroxyl group occured in range of 155-153 ppm. Other carbons of two phenyl rings were sequenced with decreasing values based on their electronic environments. For phenyl piperazine moieties of compound **5a-5o**; para-substituted derivatives **(5b, 5c, 5e, 5i, 5k, 5l)** were presented two double integrated peaks for their C_2'-C_6' and C_3'-C_5' atoms. The situation is strongly correlated with same chemical environments of these carbons. Besides double integrated peaks of chemically same carbons, compound **5b**, **5c** and **5d** represented isotopic peaks due to ^{13}C NMR pulse sequences lack of C-^{19}F decoupling which leads to C-F splittings on NMR scale. Therefore, fluoro and trifluoro moieties in compound **5b**, **5c** and **5d** revealed isotopic peak splittings in their spectrums. Doublet peaks of fluorine (^{19}F-NMR active fluorine) were observed at 158.02 and 157.25 ppm in compound **5c** whereas quartet peaks of trifluoromethyl (C-[19]F_3) group are visualized at 118.39, 118.39, 117.75, 117.43 ppm in compound **5c** depended on "n+1 splitting rule" for ^{13}C NMR spectra (Figure 113, 114).
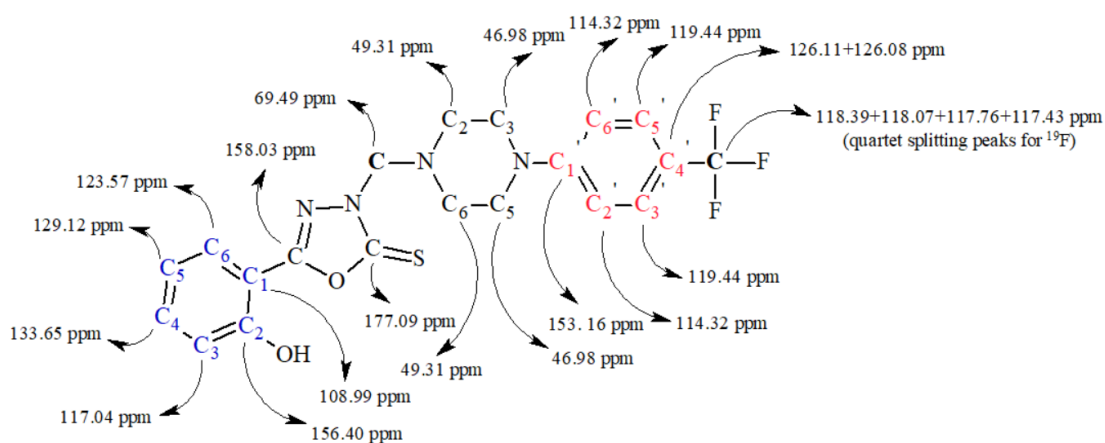
Figure 113. ^{13}C NMR spectral data of Compound **5c**
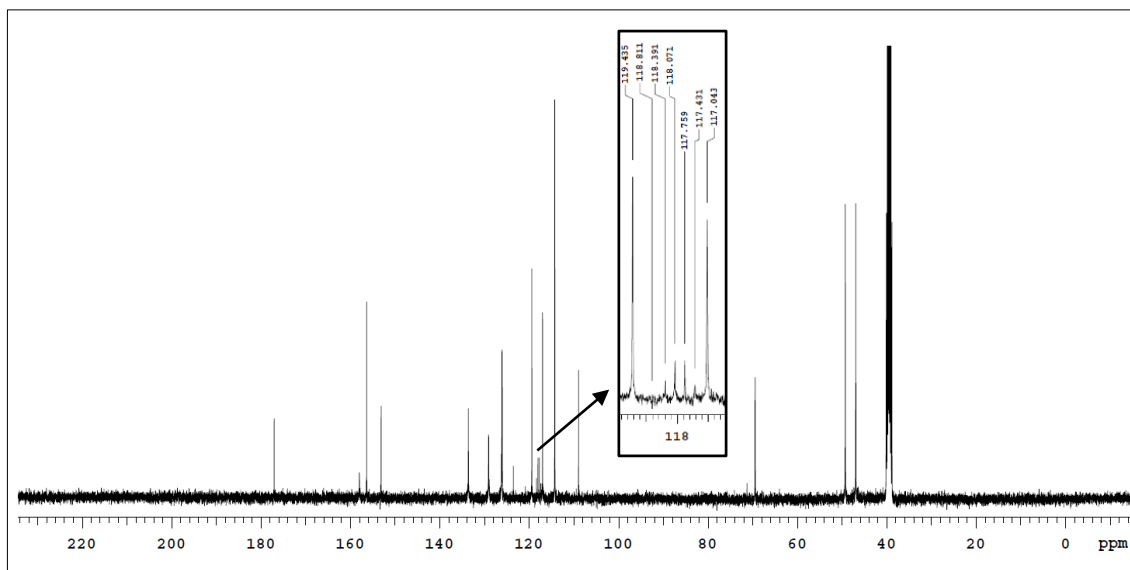
Figure 114. ^{13}C NMR spectrum of Compound **5c** and isotopic splittings of ^{19}F

Also, methylene carbon that combines oxadiazole and piperazine moieties in common for both serie was located at nearly 69 ppm. This spesific peak was an evidence for *Mannich* base compounds **5a-5o** and **10a-10p** were produced succesfully. The carbons of piperazine shifted to 44.85-51.65 ppm values on NMR scale and occured generally as two triplet peaks depended on same C_2-C_6 and C_3-C_5 atoms on the ring.

All data for the compounds of salicylic acid serie, spesific signals were deteched within similar manner for compounds of ibuprofen serie **(10a-10p)**. Thione, imine, aromatic and methylene carbons emerged at similar ppm values (Figure 116). For compound **10d** (Figure 117), ^{19}F-splittings due to trifluoromethyl group are occured *via* a parallel manner as aforementioned for compound **5c** and **5d**. However there are extra carbon shifts which are evaluated in range of 18.47-36.11 ppm, spesifically correspond to aliphalic carbons in molecules **10a-10p** are described in results part. For all newly synthesized original compounds; ^{13}C NMR chemical shift, multiplicity and integration values were suitable with literatures [17, 84].
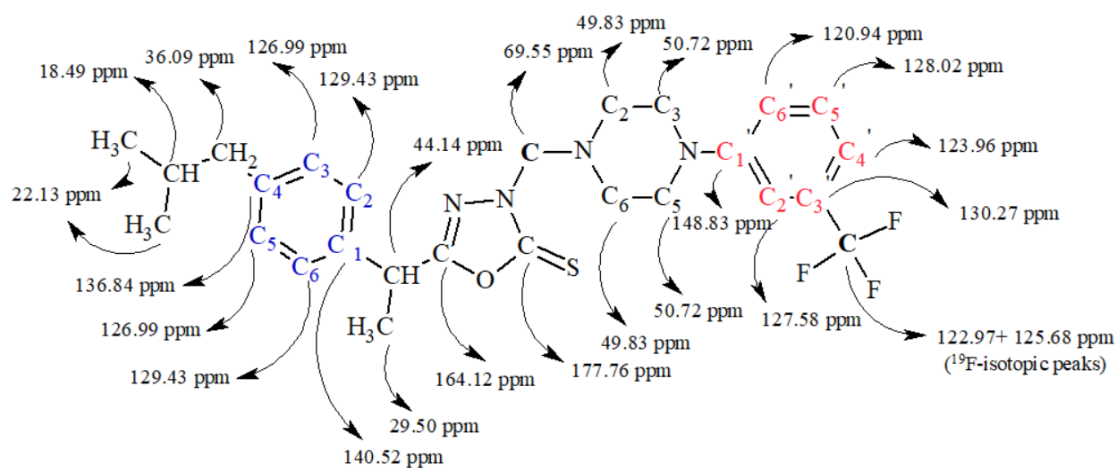
Figure 115. ^{13}C NMR spectral data of Compound **10d**
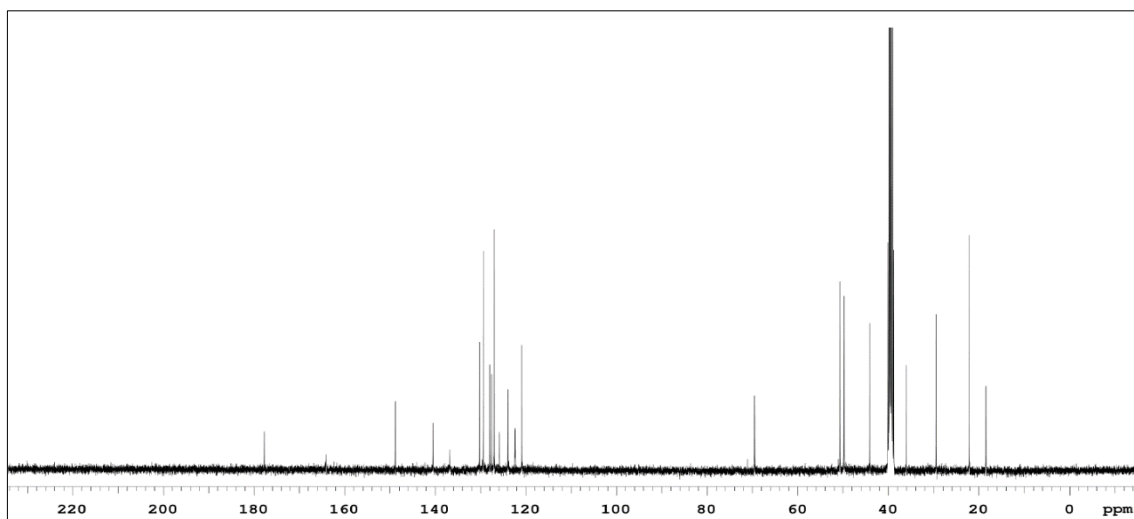
Figure 116. ^{13}C NMR spectrum of Compound **10d**
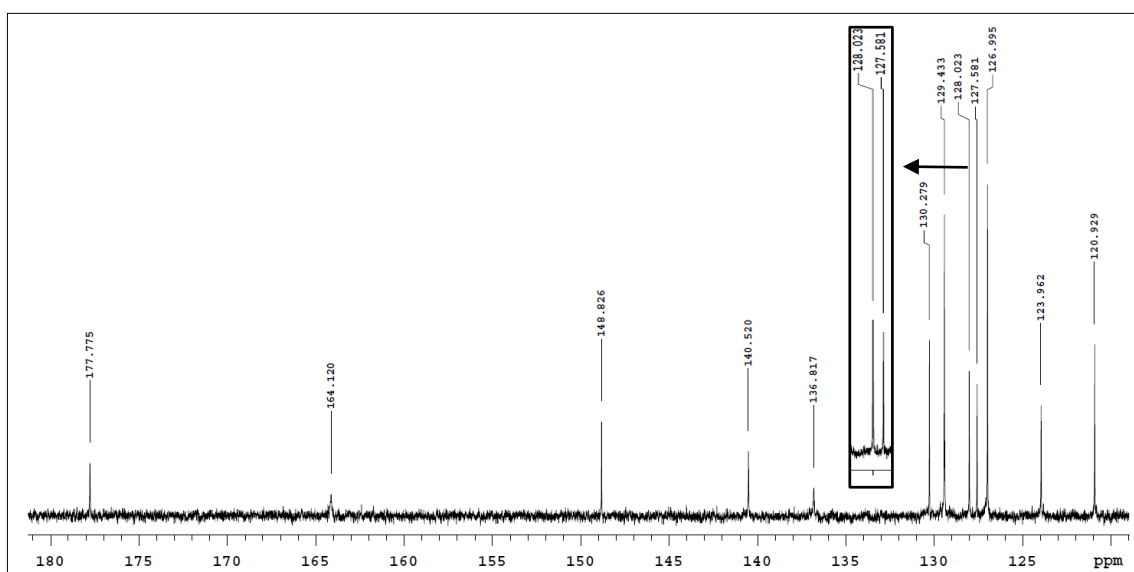
Figure 117. ^{13}C NMR spectrum of Compound **10d** and isotopic splittings of ^{19}F

According to mass spectrometry data, fragmentation patterns of synthesizedcompounds yielded no molecular ion (M⁺) peaks under LC-MS method. Even though, mass analysis of samples were performed with different device modules (low fragmentation-low temperature, low fragmentation-high temperature, high fragmentation-low temperature, high fragmentation-high temperature), none of them provided any M⁺ peaks of tested molecules to evaluate molecular ion peaks of related compound. Based on this case, LC/MS spectra of compound **5c** and **10a** were represented with fragmental base peak as in Figure 118 and Figure 119, respectively. Compound **5c** represented the peak of main fragmentation product at 243 (m/z) and its fragmentation pattern was illustrated in Scheme 11.
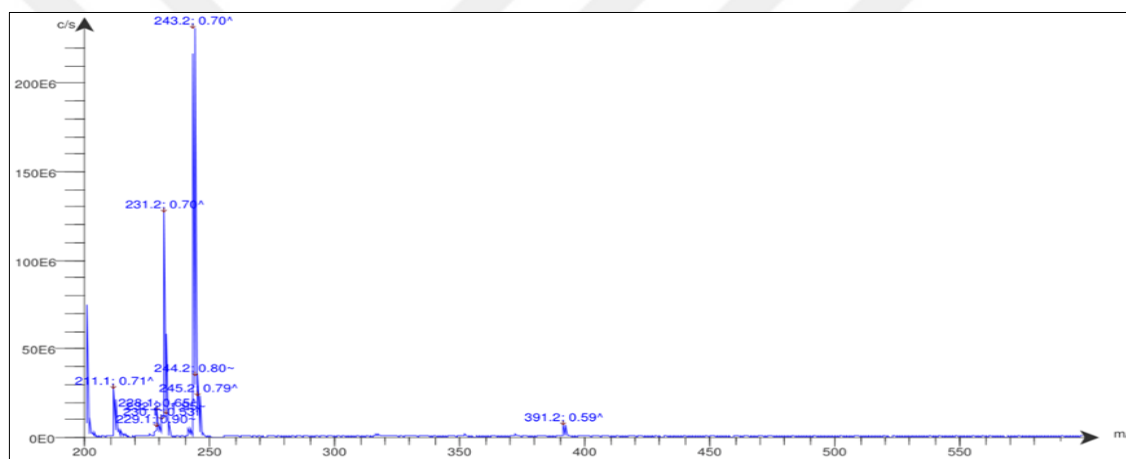
Figure 118. LC-MS fragmentation patterns of Compound **5c**
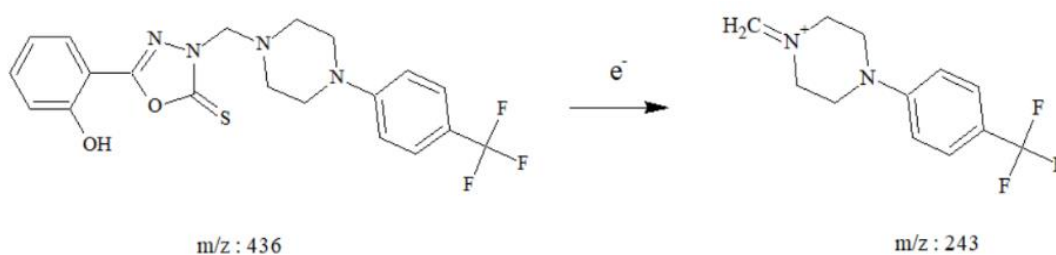
Scheme 11. Mass fragmentation of Compound **5c**

Mass spectrum of ibuprofen derivatives were exemplified with compound **10a** (Figure 119). Fragmentation product gave base peak at 261.1 (m/z) which corresponded to cationic form of 5-substituted-1,3,4-oxadiazole-2(*3H*)-thione structure (Scheme 12).
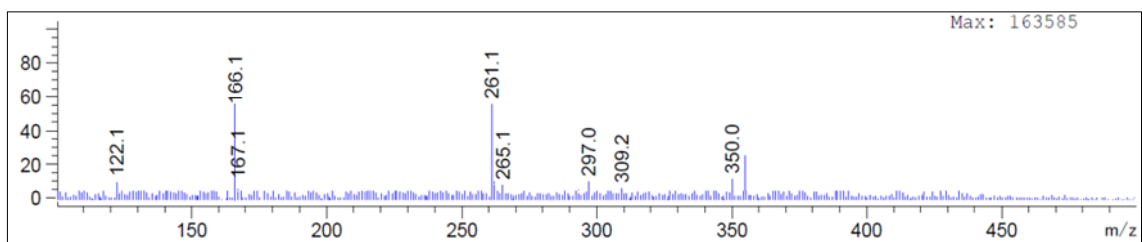
Figure 119. LC-MS fragmentation patterns of Compound **10a**

m/z : 436   m/z : 261
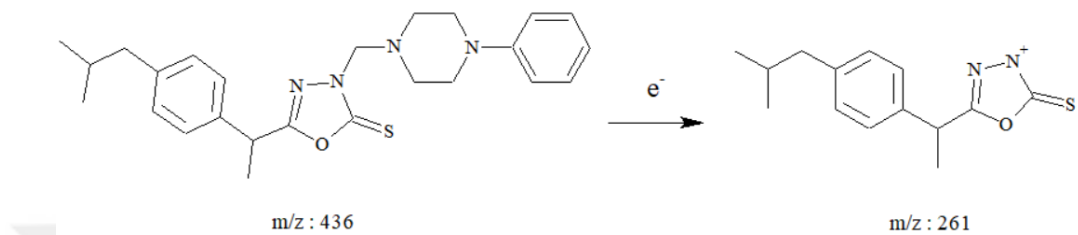
Scheme 12. Mass fragmentation of Compound **10a**

5.2. Biological Evaluation

5.2.1. Cell Viability

IC$_{50}$ values of the tested compounds were found safe at 100 µM concentration except compound **5g** which was safely used at 50 µM for in *vitro* screening assays. IC$_{50}$ value of compound **10g** was found as 68.47±1.80 µM (Table 2). Safe doses of compounds were determined via cell viabilities which were above 70% in comparison to the LPS (+).

5.2.1. Antiinflammatory Activity

5.2.1.1. COX-1/COX-2 Inhibition

Having a developed range of newer 3,5-disubstituted-1,3,4-oxadiazole-2(*3H*)-thione analogues of synthesized **5a-5o** and **10a-10p** compounds were tested for their antiinflammatory action with in *vitro* COX-1/COX-2 inhibition kit assay method.

As a general manner, all tested compounds were evaluated to inhibit COX-1 more selectively than COX-2 enzyme. Especially ibuprofen derived compound **10b** which contains 4-fluorophenyl moiety displayed higher activity than other compounds with 76% for COX-1inhibition. Moreover, molecules **5a, 5e, 5i, 5k, 5n, 10b, 10e** and **10h** showed more than 50% COX-1 inhibitor response. Therefore a glance from Table 3, COX-1 inhibitor potentials of synthesized compounds contributed to make variety of assessments about the relationship between molecular structure-enzyme combinations.

Particularly, COX-1 enzyme inhibition response of **10b** was directly correlated with hydrophobic interactions of ibuprofen moiety on fifth position of 1,3,4-oxadiazole ring and physicochemical advantages of fluoro phenyl fragment contributes COX-1 inhibition response [209-212]. Close inspection of experimental data revealed that however compound **5b** contains the same 4-fluorophenyl fragment like in **10b**, weakened hydrophobic interactions due to salicylic acid moiety in **5b** might explained the decreased level of COX-1 inhibition [107]. It is easy to understand that third and fifth positions of 1,3,4-oxadiazole ring represent important roles for COX-1 enzyme responses. For example, electron-donating groups like methyl (**5i**) and methoxy (**5k**) substituted molecules in salicylic acid serie showed higher inhibitor potential between the compounds **5a-5o** whereas in ibuprofen serie, this response was provided just by electron-withdrawing (halogen) possessed compounds like **10b, 10e** and **10h.** As depicted in Table

3, inserting electron-withdrawing groups to phenyl piperazine moiety (**5a**) in salicylic acid serie, forms compounds **5b** (4-fluoro), **5c** (4-trifluoromethyl), **5d** (3-trifluoromethyl), **5e** (4-chloro), **5f** (2-chloro), **5g** (3,4-chloro), **5h** (2,3-chloro), **5i** (4-cyano), **5m** (2-cyano) and these fragments led to decrease COX-1 inhibitor score according to compound **5a** and this condition might be explained via lowered electron density of molecules. Also salicylic acid moiety probably be other major cause for the suppression of electrons on molecule depended on inductive effect of hydroxyl, so COX-1inhibitory responses of these compounds became reduced with the same manner [107]. For the analogues of **10a-10p**; compared to nonsubstituted phenyl containing derivative (**10a**), insertion of halogen substitutions on phenyl (**10b**, **10c,10d, 10e, 10f, 10g, 10h**) obviously increased COX-1 inhibition whereas methyl (**10i**) and different substituted methoxy (**10l, 10m, 10n**) fragments caused opposite responses. Besides high level hydrophobic bonding capacity of ibuprofen moiety, elecron donating groups in **10i, 10l, 10m** and **10l** might be the reason of exceeding ideal hydrophobic interaction border with target enzyme (COX-1) [107].

Bioisosteric replacement of phenyl (**5a, 10a**) to pyridyl (**5n, 10p**) referred to enhancement of inhibitor activity for both compound series [213]. Particularly in ibuprofen serie, substituting fluorine or chlorine atom(s) displayed more COX-1 inhibitor effect due to chemical advantages of halogen atoms like electron density and less stearic issue properties. Also presence of halogen bond serves crucial roles for the activity [107].

An overview of the screening results represent the fact that substituents on phenyl ring located at para position refers higher COX-1 inhibition scores in general. Surprisingly COX-1 inhibition scores of methoxy-containing compounds **10k, 10l** and **10m** which are substituted from para, meta and ortho positions on phenyl ring respectively resulted that ortho substituted molecule (**10m**) showed more activity against COX-1 enzyme compared to para (**10k**) and meta (**10l**) analogues.

According to our results, these findings are totally correlated with previous researches that explains selective COX-1 inhibition-molecular structure relationship within in *vitro* and in *silico* studies [213]. Common point for all those studies was that specific electron-donating or withdrawing groups play a major role for COX-1 enzyme inhibition. Meanwhile our novel compound series **5a-5o** and **10a-10p** presented moderate COX-1 selective inhibitor potential. Especially halogen containing **5e** (4-chloro), **10b** (4-

fluoro), **10e** (4-chloro) and **10h** (2,3-dichloro); electron-donor containing **5i** (4-methyl) and **5k** (4-methoxy) compounds emerged more that 50% inhibition.

5.2.1.2. NO Inhibition

Macrophages show significant roles in inflammation due to the formation of variety proinflammatory molecules, including nitric oxide (NO). Production of excess NO has been related with several inflammatory diseases like atherosclerosis, ischemic reperfusion, hypertension and septic shock [214, 215]. Recent studies have demonstrated that 1,3,4-oxadiazole containing compounds effectively inhibit inflammatory processes by affecting different molecular targets in which one of them is NO [216, 217]. It is one of a key molecular signal constituent found in inflammatory responses and evaluation of nitrit level is significant approach for inflammatory processes. In this study to detect the antiinflammatory effect of synthesized compounds, LPS-induced NO production was applied with Griess assay method. All compounds and indomethacin were tested at 100 μM doses whereas **5g** and **10g** were applied at 50 μM due to their nontoxic cytotoxic concentrations. Results were summarized in Table 4 and all tested compounds were seemed to able to reduce LPS-induced nitrit levels except **10k** (Figure 120). Particularly compounds **10d** (supressed nitrit level= 13.16±4.84 μM) exhibited excellent nitrite-suppressor activity compared to indomethacin (supressed nitrit level = 24.46±1.80 μM). Besides **10d**; **10e, 10g, 10h, 10i** and **5h** also showed more reducer effect than indomethacin.
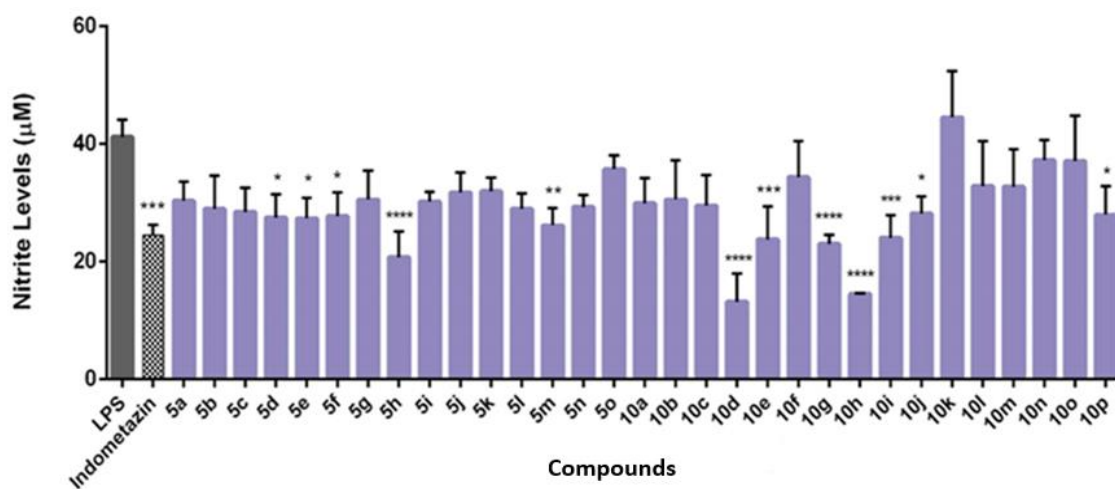
One-way ANOVA, followed by the post-hoc tests by Tukey. The significant differences between groups and control (LPS) were defined with * at p<0.05, ** at p<0.01, *** at p<0.001 and **** at p<0.0001.

Figure 120. Effect of compounds **5a-5o** and **10a-10p** on nitrite levels in LPS-stimulated RAW 264.7 cells.

Molecular structure-biologic response correlation of these active compounds clearly revealed that halogen fragments have significant role for NO suppressing. Especially 3-trifluoromethyl in **10d** and 2,3-dichloro in **5h** and **10h** derivatives demonstrate the importance of halogen atom to obtain desired responce. This relationship was also experienced by Leong and coworkers in 2014. According to their compound model, particularly 2,3-dichloro possesing molecule served highest NO-suppressor effect in which this response strongly support our consequences [218].

Nitrite level inhibition results also showed that ibuprofen derivatives (**10a-10p**) were more active than salicylic acid series (**5a-5o**). Especially compound **10d** and **10h** represented noticeable reducer effect compared to indomethacin. In this part of study, previous researches forced us to correlate the lipophilic properties of compounds and their NO-suppressor responce relationships. In 2005, Erdal and researchers focused on modelling of compounds to develop a selective inhibitor of NOS enzymes. They evaluated that to generate a potent and selective inhibitor, lipophilic character of compounds should be developed first with related molecular modulations [219]. With the same logic, Levesque and researchers in 2008, mentioned the crucial role of lipophilicity for inhibition of NO-producer NOS enzymes [220]. And in 2009, Haitao and coworkers were supported the concept of improved lipophilicity effect on NO suppression. They also contributed the data of halogen advantages for NO-suppressing activity [221]. Therefore it is meaningful to compare nitrite level responses and calculated logP (clogP) values of all synthesized compounds in this study.

In order to look into lipophilicity effect of these compounds on NO-inhibitor response, clogP values were calculated with lipophilicity module of ACD/ChemSketch program. As previous studied mentioned, lipophilicity parameter of compounds is a sensitive indicator of nitrite-suppressor effect. As shown in Table 8, depended on clogP values (lipophilicity degrees) of synthesized compounds, their NO responses were found as majorily compatible. In a general aspect, based on higher clogP values of ibuprofen series (**10a-10p**) than salicylic acid series (**5a-5o**), their superior nitrit-supressor results were obviously supported. Also in both set of compounds, halogenated derivatives were seemed to have more lipophilic properties (higher clogP values) in which this situation revealed to elevated level of their NO inhibitor effect. Particularly, 3-trifluoromethyl (**10d**) and 2,3-dichloro (**10h**) substituted derivatives were found as strong examples to support this approach. Although based on the clogP score, compound **10g** was expected

to reduce the nitrite level more than compound **10d** but it could not, possibly associated with safe dose of **10g** which leads to its study at a lower concentration (50 μM).

Table 8. Nitrit level (μM) and clogP values of synthesized compounds **5a-5o** and **10a-10p**

Salicylic acid derivatives (5a-5o)			Ibuprofen derivatives (10a-10p)		
Compound	Nitrite level (μM)	clogP	Compound	Nitrite level (μM)	clogP
5a	30.32±3.23	2.11±0.99	**10a**	29.91±4.25	5.09±0.71
5b	28.93±5.66	2.20±1.27	**10b**	30.52±6.70	5.18±1.06
5c	28.44±4.14	3.36±1.02	**10c**	29.49±5.20	5.45±0.77
5d	27.47±3.99	3.43±1.02	**10d**	13.16±4.84	6.41±0.75
5e	27.33±3.51	2.84±1.03	**10e**	23.77±5.55	5.82±0.76
5f	27.74±4.02	3.07±1.00	**10f**	34.38±6.06	6.04±0.73
5g	30.54±4.91	3.67±1.04	**10g**	23.02±1.51	6.65±0.77
5h	20.75±4.40	3.90±1.01	**10h**	14.51±0.13	6.87±0.74
5i	30.18±1.69	2.57±0.99	**10i**	24.02±3.90	5.55±0.72
5j	31.74±3.37	3.03±1.00	**10j**	28.16±2.93	6.01±0.72
5k	31.95±2.29	3.03±1.00	**10k**	44.49±7.85	4.89±0.72
5l	28.93±2.64	1.99±1.04	**10l**	32.81±7.67	4.99±0.84
5m	26.13±3.00	1.55±1.23	**10m**	32.73±6.35	5.10±0.74
5n	29.29±2.05	1.19±1.00	**10n**	37.23±3.38	4.97±0.78
5o	35.73±2.33	1.39±0.99	**10o**	37.09±7.69	4.53±1.02
			10p	27.96±4.83	4.17±0.73
Indomethacin				**24.46±1.80**	**4.27**

Calculated logP (clogP) values of compounds were obtained with ACD/ChemSketch program in which Log*P* predictions are used as input variables in many of PhysChem and ADME prediction algorithms.

To find out the linearity of relationship between nitrite level-clogP scores; Pearson correlation coefficient (r) was preferred in which this method is used to determine the association between two continuous variables. To describe the correlation strength of these variants, , r value is scored in between +1 or -1. Achieving scores in +1 or -1 means that all data points are included on the line of best fit – there are no data points that show any variation away from this line [222, 223]. Depended on this origin, base plot distributions were represented in Figure 121-124, considering nitrite level and clogP values of compounds on *x*- and *y*-axis, respectively. According to consequences, nitrit

level-clogP association of all tested compounds including indomethacin was found in weak correlation with r= -0.275 and p>0.05 values in which related plots of measured compounds were seemed entirely distributed on correlation graph (Figure 121). As experienced by Levesque and coworkers, this misleaded case was solved by dividing the data sets based on their derivative types and so, r scores of salicylic acid -0.475 (Figure 122) and ibuprofen compounds -0.703 (Figure 123) demonstrated that ibuprofen derivatives had better nitrite level-clogP correlation than salicylic acid compounds [220]. Representing significant correlation value ($p<0.01^{**}$) was also another evidence for good nitrite level-clogP relationship of ibuprofen compounds (**10a-10p**). Depending on this manner, weak correlation response of all tested compound possesing indomethacin was thought as because of inaccurant correlation effect of salicylic acid serie (**5a-5o**). Furthermore, active nitrite-reducer compounds (**5d, 5e, 5f, 5h, 5m, 10d, 10e, 10g, 10h, 10i, 10j, 10p**) with reference indomethacin and their clogP scores were also measured and obtained results (r= -0.593, $p<0.05^*$) were found in desired range (Figure 124). Additionally, negative relationship between nitrite level and clogP values was evaluated from negative correlation graphs (Figure 121-124) for all data sets as we estimated.
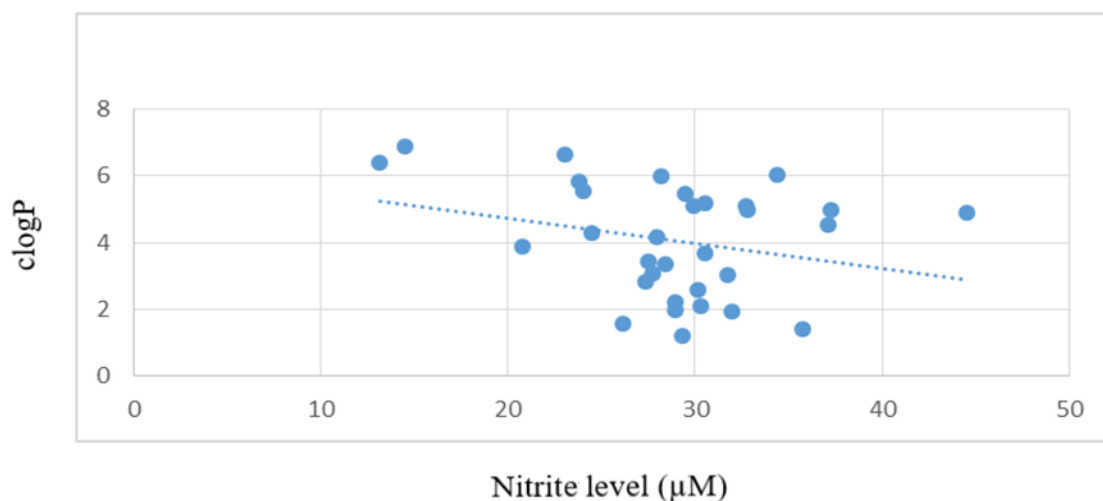
Figure 121. clogP-nitrite level distribution of salicylic acid, ibuprofen derivatives and indomethacin (**r= -0.275, p>0.05**)
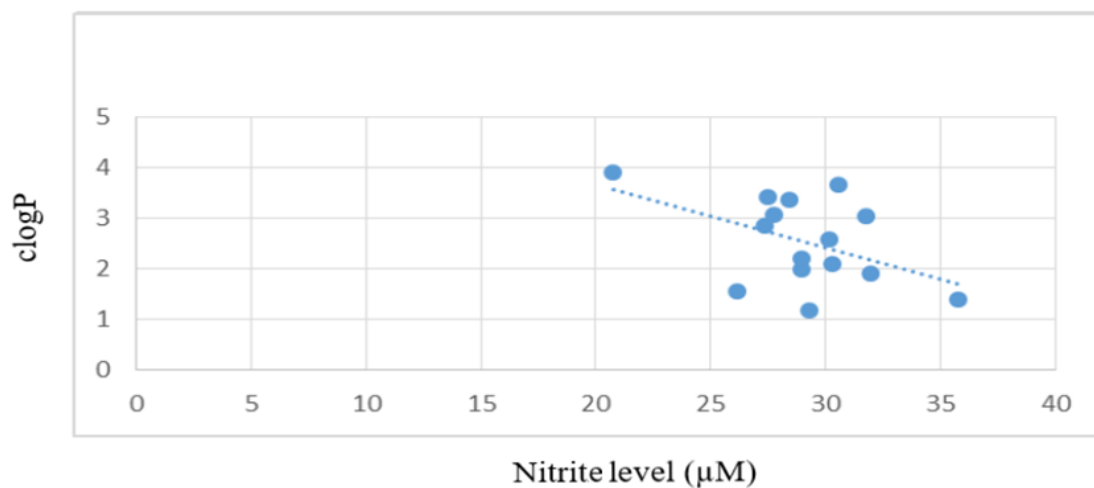
Figure 122. clogP-nitrite level distribution of salicylic acid derivatives (**r= -0.475, p>0.05**)
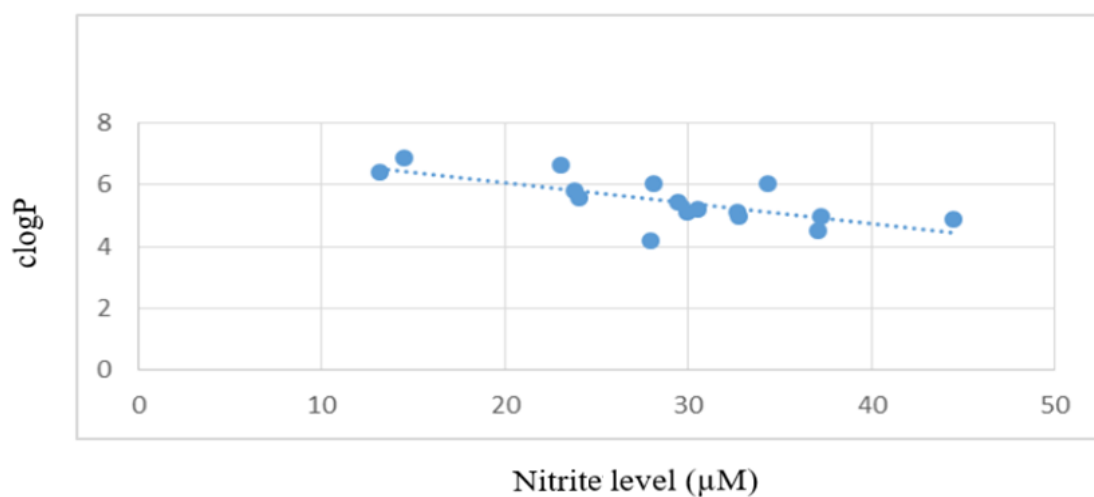
Figure 123. clogP-nitrite level distribution of ibuprofen derivatives (**r= -0.703, p<0.01****)
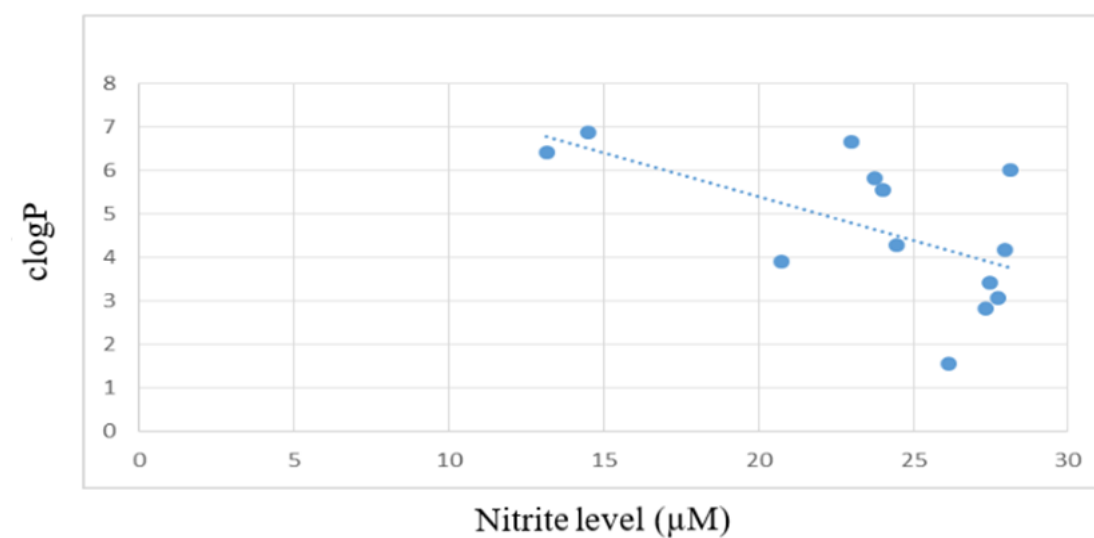
Figure 124. clogP-nitrite level distribution of active nitrit-supressor compounds and indomethacin (**r= -0.593, p<0.05***)

5.2.1.3. Prostaglandin E_2 (PGE$_2$) inhibition

Nitric oxide (NO) which is metabolic product of NOS, interacts with inducible COX in pathologic conditions and enhances the formation of PGE$_2$ prostanoid [224]. PGE$_2$ is involved in many processes leading to the general symptoms of inflammation: redness, swelling and pain. Redness and edema emerge from increased blood flow into the inflamed tissue depend on PGE$_2$-mediated arterial dilatation and increased microvascular permeability. This means PGE$_2$ inhibition plays another crucial role in removal of inflammation, thus eventually contributing to tissue remodeling [225, 226]. Depended on the cooperation between NO and PGE$_2$, synthesized compounds were chosen based on their nitrite-suppression potentials and studied futher for PGE$_2$ responses. LPS-induced PGE$_2$ levels in macrophage RAW 264.7 cells of synthesized compounds were tested at 100 µM doses (except **10g**-50 µM) according to indomethacin (100 µM) and results clearly revealed that PGE$_2$-supression scores of the tested compounds which are also able to reduce nitrite levels (**5d, 5e, 5f, 5h, 5m, 10d, 10e, 10g, 10h, 10i, 10j, 10p**) were found in moderate to good values according to indomethacin except **5i** (Table 5). Especially compound **5h** was seemed to the most active compound in lowering the LPS-induced PGE$_2$ level. Compound **10h** was found as the second potent PGE$_2$-supressor sample in which both of compound **5h** and **10h** have 2,3-dichlorophenyl moieties in common. According to previous studies, dichlorophenyl fragment was evaluated as to reduce the PGE$_2$ level as the same with our consequences [227].
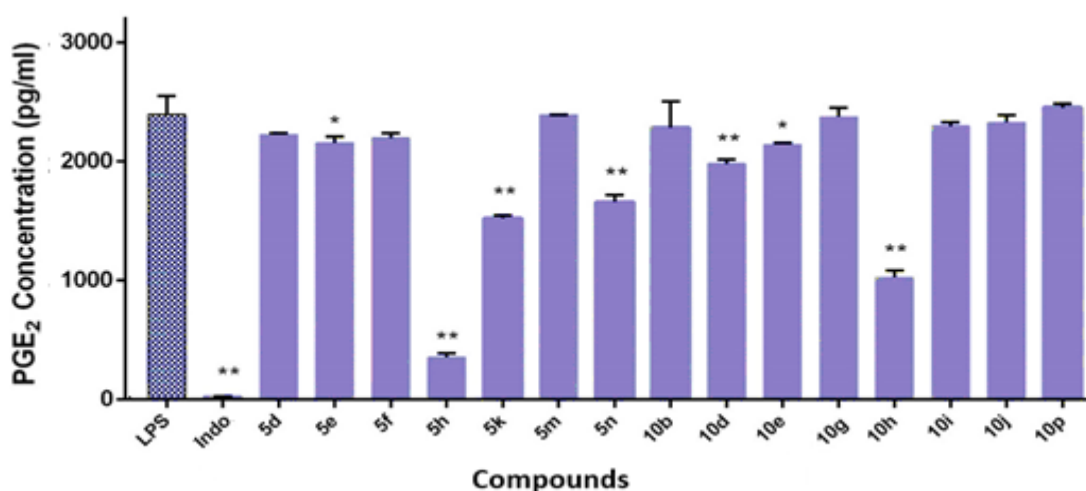
One-way ANOVA, followed by the post-hoc tests by Tukey. The significant differences between groups and control (LPS) were defined with * at $p<0.05$, ** at $p<0.01$, *** at $p<0.001$ and **** at $p<0.0001$.

Figure 125. PGE$_2$-supressor effects of tested compounds in LPS-stimulated RAW 264.7 macrophage cells.

In our study, compounds **5a-5o** and **10a-10p** were evaluated for their antiinflammatory properties [213, 214]. In this regard, compounds were used to investigate whether the NO-inhibitory compounds also interfere with production of PGE$_2$. Effects of tested compounds on NO and PGE$_2$ production were compared with effects of indomethacin that is recognized as therapeutically used for inhibition of inflammatory mediators. Overall, some of studied compounds were found as structure-dependent inhibitors of NO and PGE$_2$ production. On the other hand, the relationship between COX-1 and PGE$_2$ inhibition was also studied in which compounds that have more than 50% inhibition potential on COX-1 enzyme and having weak nitrit-reducer property (**5k, 5n, 10b**) were applied for PGE$_2$ assay. According to test results, it was difficult to set a definite correlation between COX-1 and PGE$_2$ responses as experienced by Brenneis and coworkers [228]. This phenomenon was supported within the cases that strong COX-1 inhibitor **10b** responsed weak for PGE$_2$ inhibition whereas compound **5k** and **5n** were seemed to moderately reduce PGE$_2$ level as depicted in Figure 125. Particularly according to LPS-induced NO and PGE$_2$ level scores of compound **10h** that contain 2,3-dichlorophenyl piperazine moiety showed best supressor effect on NO and PGE$_2$ levels in which same compound showed moderate inhibitor potential on COX-1 enzyme. Consequently, compound **10h** which have dual inhibitor property of NO and PGE$_2$ production may decrease severity of inflammation and thus deserve further preclinical studies.

In the process of inflammatory situations, leukocytes and mast cells are activated in damaged regions which directed to a "respiratory burst" as a result of enhanced oxygen uptake, therefore production and secretion of reactive oxygen species (ROS) might induce at probable inflammatory site [229, 230]. In order to balance the level of these free radicals in the body, natural antioxidant defense mechanism should be activated. Otherwise disturbance of this equilibrum causes oxidative stress and numerous diseases like diabetes, cardiovascular diseases, inflammation, cancer, degenerative diseases, ischemia, and anemia [231, 232]. In order to compansate insufficient activity of antioxidant mechanism, compounds **5a-5o** and **10a-10p** were evaluated *in vitro* by α, α-diphenyl-β-picrylhydrazyl (DPPH) assay to determine their antioxidant properties in comparison with ascorbic acid at 100μM dosage (except **5g** and **10g**). According to DPPH radical scavenging assay, majority of compounds revealed higher potential than ascorbic acid. Average antioxidant potentials of each series represented that salicylic acid

derivatives (**5a-5o**) showed more radical scavenger effect compared to ibuprofen derivatives (**10a-10p**). This situation may be associated with structural advantages of salicylic acid derivatives. Based on the assay mechanism, stable DPPH radical was able to take hydrogen atom from hydroxyl group on phenyl ring and reduced itself [197]. Compounds **5b, 5c, 5d, 5l** that include 4-fluoro, 4-trifluoromethyl, 3-trifluoromethyl and 4-cyano groups linked to phenyl respectively, served the most antioxidant potencies according to reference compound. Furthermore para-substituted electron-withdrawing (**5b, 5c, 5e, 5l**) or donating (**5i**) groups revealed higher scores compared to related ortho or meta-substituted analogues (**5d, 5f, 5h, 5j, 5m**) in salicylic acid series. DPPH scavencing potency of phenyl in compound **5a** became higher when it shifted with pyridyl in compound **5n**. In ibuprofen serie, compounds scavenger property scores were not suitable to classified them according to molecular structures. But interesting point was, meta substituted compounds **10d** and **10l** represented highest antioxidant properties in this serie. Ortho-substituted compounds **10c**, **10f** and **10l** decreased activity according to their para-substituted analogues whereas **10k** seemed to increase. As a general idea related to ibuprofen derivates; scavenger responses were viewed as to emerge by an independent mechanism of different substituents on phenyl piperazine moieties even if these groups are able to change electron densities of molecules or their binding models to desired targets. To exemplify, while compounds **10b** and **10c** (fluoro-containing) presented severe potential, interestingly compounds **10l** and **10m** also evaluated similar potencies in which they have conversely electron-donating methoxy groups. All of the synthesized compounds have higher scores than ascorbic acid at 100 μM except **10k** depended on their nontoxic doses as tabulated in Table 6.

5.3. Docking Studies

5.3.1. Docking Studies on COX-1 Enzyme

Binding to COX-1 enzyme generally occurs by interaction with Arg120, Tyr355 and catalytic Tyr385 residues. The conformer with lowest docking score and most stable binding pose (-7.715, rmsd: 0.210) made π-π interaction with Tyr355 from isoxazole ring re-docking studies performed on the cocrystallized ligand in X-ray data of 5U6X [199]. Compound also makes halogen bond with the Arg120 residue known to be crucial for COX-1 binding.
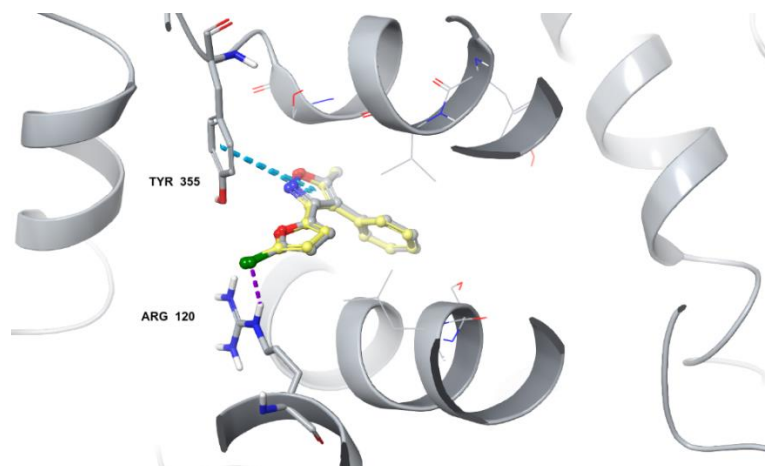
Figure 126. X-ray structure of COX-1 (PDB ID: 5U6X) with the co-crystallized ligand and the generated conformer

Docking studies on the COX-1 enzyme has shown that S isomer of compound **10b** (docking score: -8.695) can make two H-bonds with Arg120 in addition to the π-π interaction with Tyr355 from oxadiazole ring, which may explain its high inhibition observed by *in vitro* studies. The active compound could also interact with the Trp387 by π-π interactions from 4-fluorophenyl group.
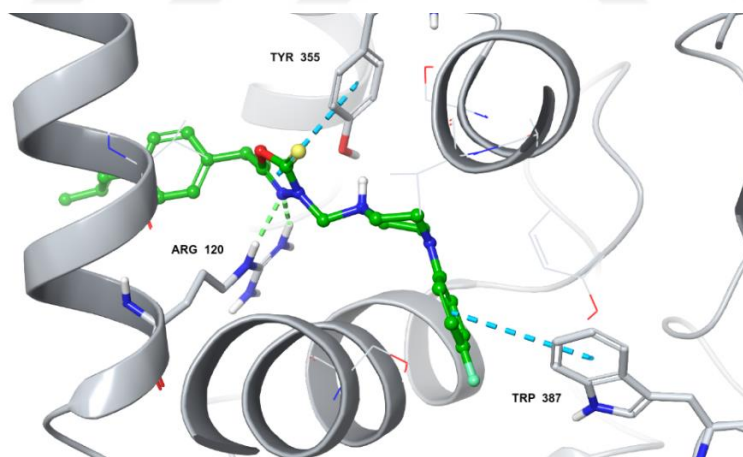
Figure 127. Docking pose of **10b** (PDB ID: 5U6X)

Compound **10b** was also analyzed for the effect of chirality on COX-1 binding. Docking studies revealed that R isomer of the compound can make an additional π-cation interaction with Arg 120. However, the docking score becomes higher (-8.386) due to one less H-bond between oxadiazole and the arginine residue.

200
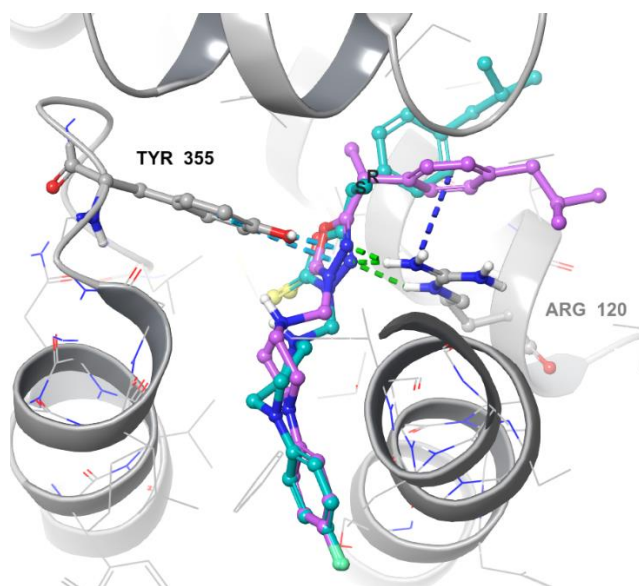
Figure 128. Docking poses of **10b-S (cyan) and 10b-R (violet)** (PDB ID: 5U6X)

5.3.2. Docking Studies on COX-2 Enzyme

Mutation studies proved that interaction with Arg120 is not as crucial for binding to COX-2 enzyme as COX-1 [233]. The conformer with lowest docking score and most stable binding pose (-10.165, rmsd: 0.738) made H-bonds with Tyr385 and Ser530 through free carboxylate group within the re-docking studies performed on the cocrystallized ligand in X-ray data of 5IKT [200].
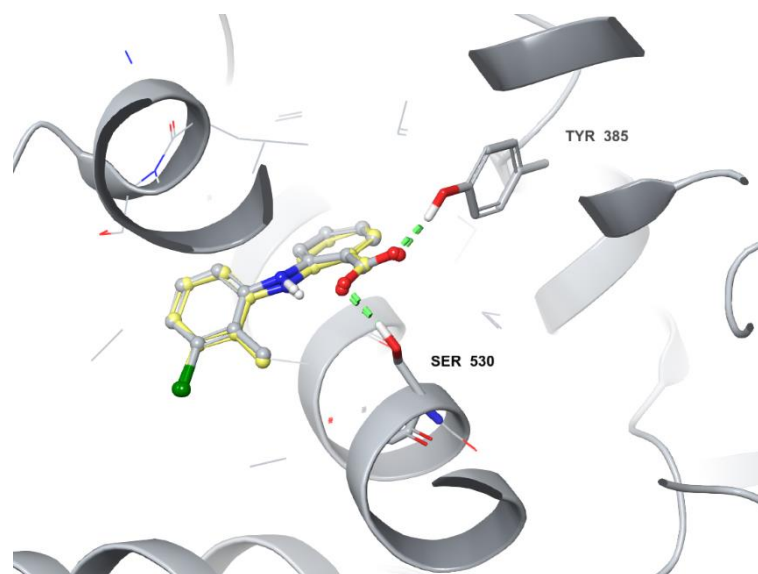
Figure 129. X-ray structure of COX-2 (PDB ID: 5IKT) with the co-crystallized ligand and the generated conformer

Docking studies on the COX-2 enzyme has shown that S isomer of compound **10b** (docking score: -8.006) cannot interact with Tyr385 or Ser530 which may explain its selective inhibition against COX-1 enzyme observed by *in vitro* studies. However, compound can make a π-cation interaction with Arg120 in addition to the π-π interaction with Tyr355 from oxadiazole ring. Further analysis of compound **10b** for the effect of chirality on COX-2 binding revealed that both enantiomers can interact with the receptor in a similar manner.
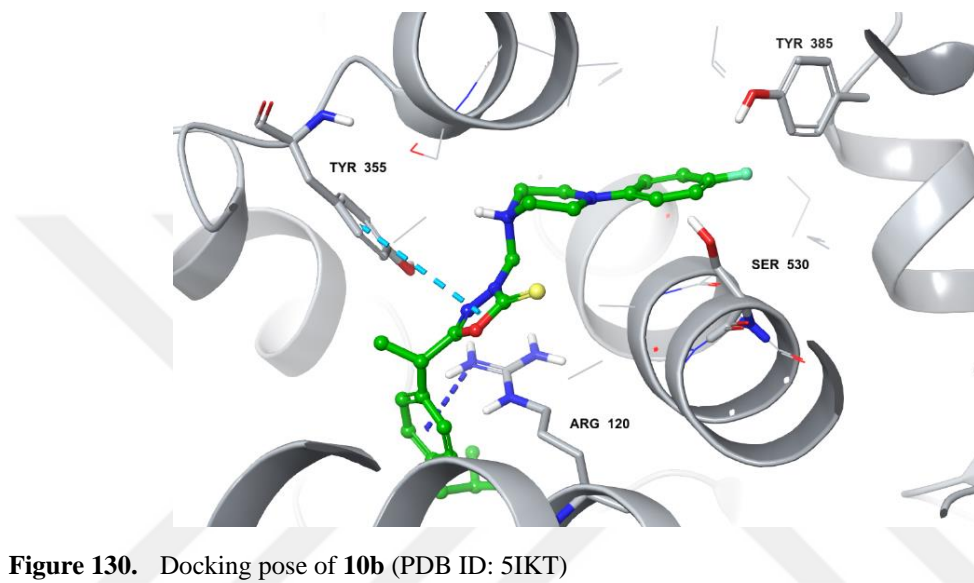
Figure 130. Docking pose of **10b** (PDB ID: 5IKT)
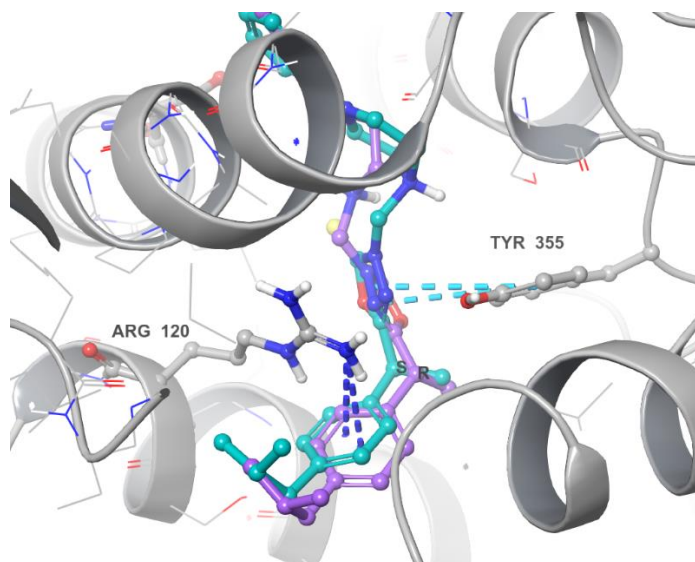
Figure 131. Docking poses of **10b-S (cyan)** and **10b-R (violet)** (PDB ID: 5IKT)

6. REFERENCES

1) Nathan, C. and A. Ding, Nonresolving inflammation. Cell, 2010. 140(6): p. 871-82.

2) Majno, G. and I. Joris, *Cells*. Tissues and Disease: Oxford University; 2004.

3) Medzhitov R. Origin and physiological roles of inflammation. *Nature*, 2008. 454 (24): p. 428-435.

4) Abdellatif, K.R.A., Abdelgawad, M.A., Elshemy, H.A.H., Alsayed, S.S.R., Design, synthesis and biological screening of new 4-thiazolidinone derivatives with promising COX-2 selectivity, anti-inflammatory activity and gastric safety profile. Bioorg Chem, 2016. 64: p. 1–12.

5) Al-Hourani, B.J., Sharma, S.K., Mane, J.Y. et al. Synthesis and evaluation of 1,5-diaryl-substituted tetrazoles as novel selective cyclooxygenase-2 (COX-2) inhibitors. Bioorg Med Chem Lett, 2011; 21: 1823–1826.

6) Allison, M.C., Howatson, A.G., Torrance, C.J., Lee, F.D., Russell, R.I., Gastrointestinal damage associated with the use of nonsteroidal antiinflammatory drugs. N Engl J Med, 1992. 327: p. 749–754.

7) Halter, F., Rainsford, K.D., Sirko, S.P., Schmassmann, A., NSAID-induced mucosal injury: analysis of gastric toxicity with new generation NSAIDs: ulcerogenicity compared with ulcer healing. Yale J Biol Med, 1997. 70: p. 33–43.

8) Bala, S., Kamboj, S., Saini, V., et al. Antiinflammatory, analgesic evaluation and molecular docking studies of N-phenyl anthranilic acid-based 1,3,4-oxadiazole analogues. J Chem, 2013; DOI: 10.1155/2013/412053.

9) Abuo-Rahma, Gel-D., Abdel-Aziz, M., Beshr, EA., Ali, TF., 1,2,4-Triazole/oxime hybrids as new strategy for nitric oxide donors: synthesis, antiinflammatory, ulceroginicity and antiproliferative activities. Eur J Med Chem, 2014. 71: p. 185–198.

10) Metwally, K.A., Yaseen, S.H., Lashine, S.M., El-Fayomi, H.M., El-Sadek, M.E., Non-carboxylic analogues of arylpropionic acids: synthesis, anti-inflammatory activity and ulcerogenic potential. Eur J Med Chem, 2007. 42: p. 152–160.

11) Penning TD, Talley JJ, Bertenshaw SR, et al. Synthesis and biological evaluation of the 1,5-diarylpyrazole class of cyclooxygenase-2 inhibitors: identification of 5-(4-methylphenyl)-3-(trifluoromethyl)-1H-pyrazol-1-yl)benze nesulfonamide (SC-58635, celecoxib). J Med Chem. 1997; 40: 1347–1365.

12) Langman MJ, Jensen DM, Watson DJ, et al. Adverse upper gastrointestinal effects of rofecoxib compared with NSAIDs. JAMA. 1999; 282: 1929–1933.

13) Dallob A, Hawkey CJ, Greenberg H, et al. Characterization of etoricoxib, a novel, selective COX-2 inhibitor. J Clin Pharmacol. 2003; 43: 573–585.

14) Talley JJ, Brown DL, Carter JS, et al. 4-5- Methyl-3-phenylisoxazol-4-yl)-benzenesulfonamide, valdecoxib: a potent and selective inhibitor of COX-2. J Med Chem. 2000; 43: 775–777.

15) Laine, L. The gastrointestinal effects of nonselective NSAIDs and COX-2-selective inhibitors. *Seminars in Arthritis Rheumatism,* 2002. 32: p. 25–32.

16) Bhandari, S.V., Bothara, K.G., Raut, M.K., Design, synthesis and evaluation of antiinflammatory, analgesic and ulcerogenicity studies of novel S-substituted phenacyl-1,3,4-oxadiazole-2-thiol and schiff bases of diclofenac acid as nonulcerogenic derivatives. Bioorg Med Chem, 2008. 16: p. 1822–1831.

17) Manjunatha, K., Poojary, B., Lobo, P.L., Fernandes, J.N., Kumari, S., Synthesis and biological evaluation of some 1,3,4-oxadiazole derivatives. Eur J Med Chem, 2010. 45: p. 5225-5233.

18) Huether, S.E. and K.L. McCance, *Understanding Pathophysiology*. Elsevier Health Sciences: Förlag; 2015.

19) Anwikar, S. and M. Bhitre, Study of the synergistic anti-inflammatory activity of Solanum xanthocarpum. J Ayurveda Res, 2010. 1(3): p. 167.

20) Sharma, J.N., Al-Omran, A., Parvathy, S.S., Role of nitric oxide in inflammatory diseases. Inflammopharmacology, 2007. 15: p. 252–259.

21) Tiemann, F. and P. Kruger, Ueber amidoxime und azoxime. Ber Dtsch Chem Ges, 1884. 17: p. 1685.

22) Gupta, R.R., Kumar, M., Gupta, V., ed. *Heterocyclic Chemistry: Five Membered Heterocycles with more than two heteroatoms*, 1st ed.; Springer: India; 2005.

23) Clapp, LB. 1, 2, 4-Oxadiazoles. *Advances in Heterocyclic Chemistry*, 1976. 20: p. 65-116.

24) Lima, L.M., and E.J. Barreiro, Bioisosterism: A useful strategy for molecular modification and drug design. Curr Med Chem, 2005. 12: p. 23-49.

25) Bostrom, J., Hogner, A., Schmitt, S., Do structurally similar ligands bind in a similar fashion. J Med Chem, 2006. 49: p. 6716-6725.

26) Moussebois, C., and J.F.M. Oth, Helv Chim Acta, 1964. 47: p. 942.

27) Trifonov, R.E. and V.A. Ostrovskii, Basicity of 2-phenyl-(5R)-1,3,4-oxadiazoles. Chem Heterocycl Compd, 2006. 42: p. 657.

28) Li, A.F., Ruan, Y.B., Jiang, Q.Q., He, W.B., Jiang, Y.B., Molecular logic gates and switches based on 1,3,4-oxadiazoles triggered by metal ions. Chem Eur J, 2010. 16: p. 5794-5802.

29) Ma, J.C., and D.A. Dougherty, The Cation-π interaction. Chem Rev, 1997. 97: p. 1303.

30) Taha M, Ismail NH, Imran S, et al. Synthesis, molecular docking and a-glucosidase inhibition of 5-aryl-2-(6'-nitrobenzofuran-2'-yl)-1,3,4-oxadiazoles. Bioorg Chem. 2016; 66: 117-123.

31) Dabiri, M., Salehi, P., Baghbanzadeh, M., Zolfigol, M.A., Bahramnejad, M., Silica sulfuric acid: an efficient and versatile acidic catalyst for the rapid and ecofriendly synthesis of 1,3,4-oxadiazoles at ambient temperature. Synth Commun, 2007. 37: p. 1201-1209.

32) Dabiri, M., Salehi, P., Baghbanzadeh, M., Bahramnejad, M., Alum (KAlSO$_4$)$_2$ · (12H$_2$O): An efficient and inexpensive catalyst for the one-pot synthesis of 1,3,4-oxadiazoles under solvent-free conditions. Monatshefte fur Chemie, 2007. 138: p. 1253–1255.

33) Polshettiwar, V., and R.S. Varma, Greener and rapid access to bio-active heterocycles: one-pot solvent-free synthesis of 1,3,4-oxadiazoles and 1,3,4-thiadiazoles. Tetrahedron Lett, 2008. 49: p. 879–883.

34) Montgomery JI, Toogood PL, Hutchings KM, et al. Discovery and SAR of benzyl phenyl ethers as inhibitors of bacterial phenylalanyl-tRNA synthetase. Bioorg Med Chem Lett. 2009; 19: 665–669.

35) Bethel PA, Gerhardt S, Jones EV, et al. Design of selective Cathepsin inhibitors. Bioorg Med Chem Lett. 2009; 19: 4622–4625.

36) Ramazani, A., Ahmadi, Y., Rouhani, M., Shajari, N., Souldozi, A., The reaction of N-(isocyanimino) triphenylphosphorane with an electron-poor α-haloketone in the presence of aromatic carboxylic acids: A novel three-component reaction for the synthesis of disubstituted 1,3,4-oxadiazole derivatives. Heteroatom Chem, 2010. 21: p. 368-372.

37) Ramazani, A., Rouhani, M., Rezaei, A., Shajari, N., Souldozi, A., Helv Chim Acta, 2011. 94: p. 282-288.

38) Adib, M., Kesheh, M.R., Ansari, S., Bijanzadeh, H.R., Reaction between n-isocyaniminotriphenylphosphorane, aldehydes, and carboxylic acids: a one-pot and three-component synthesis of 2-aryl-5-hydroxyalkyl-1,3,4-oxadiazoles. Synlett, 2009. 10: p. 1575–1578.

39) Souldozi, A. and A. Ramazani, The reaction of N-isocyanimino)triphenyl phosphorane with benzoic acid derivatives: a novel synthesis of 2-aryl-1,3,4-oxadiazole derivatives. Tetrahedron Lett, 2007. 48: p. 1549-1551.

40) Mickevicius, V., Vaickelioniene, R., Sapijanskaite, B., Synthesis of substituted 1,3,4-oxadiazole derivatives. Chem Heterocyc Comp, 2009. 45(2): p. 215-218.

41) Jansen M, Rabe H, Strehless A, et al. Synthesis of GABA-a receptor agonists and evaluation of their α-subunit selectivity and orientation in the gaba binding site. J Med Chem. 2008; 51: 4430–4448.

42) Tabatabai, S.A., Lashkari, S.B., Zarrindast, M.R., Gholibeikian, M., Shafiee, A., Design, synthesis and anticonvulsant activity of 2-2-phenoxy)phenyl-1,3,4-oxadiazole derivatives. Iran J Pharm Res, 2013. 12: p. 105-111.

43) Ningaiah, S., Bhadraiah, U.K., Doddaramappa, S.D., Shridevi, D., Keshavamurthy, S., Javarasetty, C., Novel pyrazole integrated 1,3,4-oxadiazoles: Synthesis, characterization and antimicrobial evaluation. Bioorg Med Chem Lett, 2014. 24: p. 245–248.

44) Dabiri, M., Salehi, P., Baghbanzadeh, M., Bahramnejad, M., A facile procedure for the one-pot synthesis of unsymmetrical 2,5-disubstituted-1,3,4-oxadiazoles. Tetrahedron Lett, 2006. 47(39): p. 6983-6986.

45) Desai, A.R and K.R. Desai, Heterocyclic Synthesis: A convenient route to some 2-mercepto-1,3,4-oxadiazole and green chemistry microwave-induced one-pot synthesis of 2-aryl 1,3,4-oxadiazole in quinazolone and their antibacterial and antifungal activity. J Heterocyclic Chem, 2005. 42: p. 995-997.

46) Ahsan MJ, Samy JG, Khalilullah H, et al. Molecular properties prediction and synthesis of novel 1,3,4-oxadiazole analogues as potent antimicrobial and antitubercular agents. Bioorg Med Chem Lett. 2011; 21(24): 7246-7250.

47) Rane R.A., Gutte S.D., Sahu N.U., Synthesis and evaluation of novel 1,3,4-oxadiazole derivatives of marine bromopyrrole alkaloids as antimicrobial agent. Bioorg Med Chem Lett, 2012. 22: p. 6429–6432.

48) Ramazani, A., Ahmadi, Y., Mahyari, A., One-pot efficient synthesis of fully substituted 1,3,4-oxadiazole derivatives from N-(isocyanoimino) triphenylphosphorane, carboxylic acids and aromatic bis-aldehytes. Synth Commun, 2011. 41: p. 2273-2282.

49) Lai H, Dou D, Arapavalli S, et al. Design, synthesis and characterization of novel 1,2-benzoisoxazol-3(*2H*)-one and 1,3,4-oxadiazole hybrid derivatives: potent inhibitors of Dengue and West Nile virus NS2B/NS3 proteases. Bioorg Med Chem. 2013; 21(1): 102-113.

50) Cao, S., Qian, X., Song, G., Chai, B., Jiang, Z., Synthesis and antifeedant activity of new oxadiazolyl-3(2H)-pyridazinones. J Agric Food Chem, 2003. 51: p. 152-155.

51) El Din., M.M., El-Gamal, M.I., Abdel-Maksoud, M.S., Yoo, K.H., Oh, C.H., Synthesis and in vitro antiproliferative activity of new 1,3,4-oxadiazole derivatives possesing sulfonamide moiety. Eur J Med Chem, 2014. 27: p. 45-52.

52) Singh, A.K., Lohani, M., Parthsarthy, R., Synthesis, characterization and anti-inflammatory activity of some 1,3,4-oxadiazole derivatives. Iran J Pharm Res, 2013. 12(3): p. 319-323.

53) Asghar, S.F., Yasin, K.A., Rehman, H., Aziz, S., Synthesis and cyclisation of 1,4-disubstituted semicarbazides. Nat Prod Res, 2008. DOI: 10.1080/14786410 802435935.

54) Al-Zobaydi, S.F., Bushra Karim, B., Al-Sahib, S.A., Ismael, B.D., Synthesis, characterization of some New 1, 3, 4-oxadiazole derivatives based on 4- amino benzoic acid. Baghdad Sci J, 2016. 13(2): p. 289-297.

55) Hill, J., Katritzky, A.R., Rees, C.W., Comprehensive Heterocyclic Chemistry I', Eds.; Pergamon Press, Oxford, 1984.

56) Bala, S., Kamboj, S., Kajal, A., Saini, V., Prasad D.N., 1,3,4-oxadiazole derivatives: synthesis, characterization, antimicrobial potential, and computational studies. BioMed Res Int, 2014. DOI: 10.1155/2014/172791.

57) Kostyuchenko, A.S., Yurpalov, V.L., Kurowska, A., Domagala, W., Pron, A., Fisyuk A.S., Synthesis of new, highly luminescent bis(2,2'-bithiophen-5-yl) substituted 1,3,4-oxadiazole, 1,3,4-thiadiazole and 1,2,4-triazole. Beilstein J Org Chem, 2014. 10: p. 1596–1602.

58) Nazarbahjat, N., Abdullah, Z., Abdulla, M.A., Ariffin, A., Synthesis and characterization of 2,5-disubstituted-1,3,4-oxadiazole derivatives with thioether. Asian J Chem, 2014. 26(24): p. 17872- 17872.

59) Rajaka HS, Thakura BS, Parmara P, et al. Synthesis and antimicrobial properties of novel 2,5-disubstituted-1,3,4-oxadiazoles. Der Chemica Sinica. 2011; 2(4):115-122.

60) Singh, P., Sharma, P.K., Sharma, J.K., Upadhyay, A., Kumar, N., Synthesis and evaluation of substituted diphenyl 1,3,4-oxadiazole derivatives for central nervous system depressant activity. Org Med Chem Lett, 2012. 2: p. 8. DOI: 10.1186/2191-2858-2-8.

61) Mayer, J.M. Understanding hydrogen atom transfer: From bond strengths to marcus theory. *Accounts of Chemical Research,* 2011. 44: p. 36-46.

62) Maupin CM, Castillo N, Taraphder S, et al. Chemical rescue of enzymes: proton transfer in mutants of human carbonic anhydrase II. J Am Chem Soc. 2011; 133: 6223-6234.

63) Zhang, M.T., Irebo, T., Johansson, O., Hammarström, L., Proton-coupled electron transfer from tyrosine: A strong rate dependence on intramolecular proton transfer distance. J Am Chem Soc, 2011. 133: p. 13224–13227.

64) Weinberg DR, Gagliardi CJ, Hull JF, et al. Proton-coupled electron transfer. Chem Rev. 2012; 11(27): 4016-4093.

65) Raper, E.S. Complexes of heterocyclic thionates Part 2: complexes of bridging ligands. *Coordination Chemistry Reviews*, 1997. 165: p. 475-567.

66) Aydogan, F., Turgut, Z., Ocal, N., Synthesis and electronic structure of new aryl- and alkyl-substituted 1,3,4-oxadiazole-2-thione derivatives,. Turk J Chem, 2002. 26: p. 159-168.

67) Charistos, D.A., Vagenas, G.V., Tzavellas, L.C., Tsoleridis, C.A., Rodios, N.A., Synthesis and a UV and IR spectral study of some 2-aryl-1,3,4-oxadiazoline-5-thiones. Heterocycl Chem, 1994. 31: p. 1593-1598.

68) Tsoleridis, C.A., Charistos, D.A., Vagenas, G.V., UV and MO study on the deprotonation of some 2-aryl-1,3,4-oxadiazoline-5-thiones. J Heterocycl Chem, 1997. 34: p. 1715-1719.

69) Koparır, M., Cetin, A., Cansız, A., 5-Furan-2-yl-1,3,4-oxadiazole-2-thiol, 5-furan-2-yl-4H-1,2,4-triazole-3-thiol and their thiol-thione tautomerism. Molecules, 2005. 10: p. 475-480.

70) Arslan NB, Ozdemir N, Dayan O, et al. Direct and solvent-assisted thione–thiol tautomerism in 5-thiophen-2-yl)-1,3,4-oxadiazole-23H)-thione: Experimental and molecular modeling study. Chem Phy. 2014; 439: 1–11.

71) Young, R.W. and K.H. Wood, J Am Chem Soc, 1955. 77: p. 499.

72) Molina, P., Tarraga, A., Espinosa, A., Alkyl 2-methyldithiocarbazates in heterocyclic synthesis. Preparation of 2-(alkylthio)-1,3,4-thiadiazolium cations and 2-thioxo-2,3-dihydro-1,3,4-oxadiazole derivatives. Synthesis, 1988, 9: p. 690-693.

73) Loetchutinat, C., Chau, F., Mankhetkorn, S., Synthesis and Evaluation of 5-Aryl-3-(4-hydroxyphenyl)-1,3,4-oxadiazole-2(*3H*)-thiones as P-Glycoprotein Inhibitors. Chem Pharm Bull, 2003. 5(16): p. 728-730.

74) Macaev F, Rusu G, Pogrebnoi S, Gudima A, Stingaci E, et al. Synthesis of novel 5-aryl-2-thio-1,3,4-oxadiazoles and study of their structure antimycobacterial activities. Bioorg Med Chem. 2005; 13: 4842-4850.

75) Châabane, R.B. and A. Hedhli, Synthesis and characterization of fluorinated 1,3,4-oxadiazole-2-thiones. J Soc Chim Tun, 2014. 16: p. 25-28.

76) Horning, D.E. and J.M. Muchowski, Five-membered Heterocyclic Thiones. Part I. 1,3,4-Oxadiazole-2-thione. Can J Chem, 1972. 50: p. 3079.

77) http://www.science-and-fun.de/tools/1h-nmr.html

78) http://webcache.googleusercontent.com/search?q=cache:http://shodhganga.inf libnet.ac.in/bitstream/10603/101063/13/13_chapter%25204.pdf

79) Ram, V.J. and H.N. Pandey, Synthesis of bis 1,2,4-triazoles, 1,3,4-oxadiazoles, 1,3,4-thiadiazoles) and related compounds. Agric Biol Chem, 1977. 41: p. 137-142.

80) Belkadi, M. and A.A. Othman, A common route to the synthesis of 1,3,4-oxadiazole-2-thione and 1,2,4-triazole-3-thiols derivatives of trioses and pentoses as models for acyclic C-nucleosides. ARKIVOC, 2006. 11: p. 183-195.

81) Roman G., *Mannich* bases in medicinal chemistry and drug design, Eur J Med Chem, 2015. 89: p. 743-816.

82) Siddiqui, S. M., Salahuddin, A., Azam, A., *Mannich* base derivatives of 1,3,4-oxadiazole: synthesis and screening against *Entamoeba histolytica.* Med Chem Res, 2012. DOI: 10.1007/s00044-012-0108-9.

83) Soni, N., Barthwal, J.P., Saxena, A.K., Bhargava, K.P., Monoamine oxidase and succinate dehydragenase inhibitory properties of substituted 1,3,4-oxadiazole-2-thiones. J Hetero Chem, 1982. 19: p. 29-32.

84) Aboraia, A.S., Abdel-Rahman, H.M., Mahfouz, N.M., El-Gendy, M.A., Novel 5-(2-hydroxyphenyl)-3-substituted-2,3-dihydro-1,3,4-oxadiazole-2-thione deri vatives: Promising anticancer agents. Bioorg Med Chem, 2006. 14: p. 1236–1246.

85) Kumar, G.V.S., Prasad, R. Y., Mallikarjuna, B. P., Chandrashekar, S. M., Synthesis and pharmacological evaluation of clubbed isopropylthiazole derived triazolothiadiazoles, triazolothiadiazines and *Mannich* bases as potential antimicrobial and antitubercular agents. Eur J Med Chem, 2010. 45: p. 5120-5129.

86) Naveena, C.S., Boja, P., Kumari, N.S., Synthesis, characterization and antimicrobial activity of some disubstituted 1,3,4-oxadiazoles carrying 2-(aryloxymethyl)phenyl moiety. Eur J Med Chem, 2010. 45: p. 4708-4719.

87) Ozyanik, M., Demirci, S.,, Bektas, H., Demirbas, A., Alpay-Karaoglu, Sengul., Preparation and antimicrobial activity evaluation of some quinoline derivatives containing an azole nucleus. Turk J Chem, 2012. 36: p. 233–246.

88) Naganagowda, G. and A. Petsom, Synthesis and antimicrobial activity of some new 5-(3-chloro-1-benzothiophen-2-yl)-1,3,4-oxadiazole-2-thiol and their derivatives. Phosphorus, Sulfur, and Silicon, 2011. 186: p. 2112–2121.

89) Frank P.V., Poojary, M.M., Damodara, N., Chikkanna, C., Synthesis and antimicrobial studies of some *Mannich* bases carrying imidazole moiety. Acta Pharm, 2013. 63: p. 231–239.

90) Grover J, Bhatt N, Kumar V, et al. 2,5-Diaryl-1,3,4-oxadiazoles as selective COX-2 inhibitors and anti-inflammatory agents. RSC Advances. 2015; DOI: 10.1039/C5RA01428J.

91) Akhter, M., Akhter, N., Alam, M.M., Zaman, M.S., Saha, R, Kumar, A., Synthesis and biological evaluation of 2,5-disubstituted 1,3,4-oxadiazole derivatives with both COX and LOX inhibitory activity. J Enzyme Inhib Med Chem, 2011. 26(6): p. 767–776.

92) Nagalakshmi, G. Synthesis, antimicrobial and antiinflammatory activity of 2,5-disubstituted-1,3,4-oxadiazoles. *Indian Journal of Pharmaceutical Sciences*, 2008. 70(1): p. 49-55.

93) Sawhney, S.N. and P.K. Sharma, Synthesis and antiinflammatory activity of some 3-heterocyclyl-1,2-benzothiazoles. Bioorg Med Chem Lett, 1993. 3(8): p. 1551-1554.

94) Durgashivaprasad, E., Mathew, G., Sebastian, S., Manohar Reddy, S.A, Mudgal, J., Nampurath, G.T., Novel 2,5-disubstituted-1,3,4-oxadiazoles as antiinflammatory drugs. Ind J Pharm. 2014. 46(5): p. 521-526.

95) Husain, A., Ahmad, A., Alam, M.M., Ajmal, M., Ahuja, P., Fenbufen based 3-(5-substitutedaryl-1,3,4-oxadiazol-2-yl-1-(biphenyl-4-yl)propan-1-ones as safer antiinflammatory and analgesic agents. Eur J Med Chem, 2009. 44: p. 3798–3804.

96) Kotaiah, Y., Harikrishna, N., Nagaraju, K., Rao, CV., Synthesis and antioxidant activity of 1,3,4-oxadiazole tagged thieno(2,3-d)pyrimidine derivatives. Eur J Med Chem, 2012. 58: p. 340-345.

97) Mihailovic N, Markovic V, Mati IZ, et al. Synthesis and antioxidant activity of 1,3,4-oxadiazoles and their diacylhydrazine precursors derived from phenolic acids. RSC Adv, 2017. 7: p. 8550.

98) Reddy, G.M., Muralikrishna, A., Padmavathi, A., Padmaja, A., Tilak, T.K., Rao, C.A., Synthesis and antioxidant activity of styrylsulfonylmethyl-1,3,4-oxadiazoles, pyrazolyl/isoxazolyl-1,3,4-oxadiazoles. Chem Pharm Bull, 2013. 61(12): p. 1291–1297.

99) Mohana, K.N. and C.B.P. Kumar, Synthesis and antioxidant activity of 2-amino-5-methylthiazol derivatives containing 1,3,4-oxadiazole-2-thiol moiety. ISRN Org Chem Vol, 2013. DOI: 10.1155/2013/620718.

100) Husain, A. and M. Ajmal, Synthesis of novel 1,3,4-oxadiazole derivatives and their biological properties. Acta Pharm, 2009. 59: p. 223–233.

101) Bhardwaj, S., Parashar, B., Parashar, N., Sharma, V.K., Microwave assisted synthesis and pharmacological evaluation of some 1,3,4-oxadiazole derivatives. Arch Appl Sci Res, 2011. 3(2): p. 558-567.

102) Amir, M. and K. Shikha, Synthesis and antiinflammatory, analgesic, ulcerogenic and lipid peroxidation activities of some new 2-((2,6-dichloroanilino)phenyl)acetic acid derivatives. Eur J Med Chem, 2004. 39(6): p. 535–545.

103) Panda, J., Patro, V.J., Panda, C.S., Mishra, J., Synthesis, characterization, antibacterial and analgesic evaluation of some 1,3,4-oxadiazole derivatives. Der Pharma Chemica, 2011. 3(2): p. 485-490.

104) Ahsan, M. J., Sharma, J., Bhatia, S., Goyal, P.K., Shank-hala, K., Didel, M., Synthesis of 2,5-disubstituted-1,3,4-oxadiazole analogs as novel anticancer and antimicrobial agents. Lett Drug Des Discov, 2014. 11: p. 413-419.

105) Kumar, S., Synthesis and biological activity of 5-substituted-2-amino-1,3,4-oxadiazole derivatives, *Turkish Journal of Chemistry*, 2011. 35: p. 99-108.

106) Banday, M.R., Mattoo, R.H., Rauf A., Synthesis, characterization and anti-bacterial activity of 5-alkenyl)-2-amino- and 2-(alkenyl)-5-phenyl-1,3,4-oxadiazoles. J Chem Sci, 2010. 122(2): p. 177–182.

107) Polkam N, Kummari B, Rayam P, et al. Synthesis of 2,5-disubstituted-1,3,4-oxadiazole derivatives and their evaluation as anticancer and antimycobacterial agents. Chem Select, 2017. 2: p. 5492–5496.

108) Salahuddin, Mazumder, A., Shaharyar, M., Synthesis, characterization, and ın vitro anticancer evaluation of novel 2,5-disubstituted 1,3,4-oxadiazole analogue. Hindawi Publishing Corp BioMed Res Int, 2014. Article ID 491492, DOI: 10.1155/2014/491492.

109) Amir, M., Javed, S.A., Kumar, H., Synthesis of some 1,3,4-oxadiazole derivatives as potential anti-inflammatory activity. Ind J Chem, 2007. 46: p. 1014-1019.

110) Jakubkiene, V., Burbuliene, M.M., Mekuskiene, G., Udrenaite, E., Gaidelis, P., Vainilavicius, P. Synthesis and anti-inflammatory activity of 5-6-methyl-2-

substituted-4-pyrimidinyloxymethyl)-1,3,4-oxadiazole-2-thiones and their 3-morpholinomethyl derivatives. Il Farmaco, 2003. 58: p. 323-328.

111) El Sayed H, El Tamany H, El Fattah A, et al. Immunomodulatory properties of S- and N-alkylated 5-(1H-indol-2-yl)-1,3,4-oxadiazole-2(*3H*)-thione. J Enzyme Inhib Med Chem, 2013. 28: p. 105-112. DOI: 10.3109/14756366.2011 .636361

112) Burbuliene, M.M., Jakubkiene, V., Mekuskiene, G., Udrenaite, E., Smicius, R., Vainilavicius, R., Synthesis and anti-inflammatory activity of derivatives of 5-(2-disubstitutedamino-(6-methyl-pyrimidin-4-yl)-sulfanylmethyl)-*3H*-1,3,4-oxadiazole-2-thiones. IL Farmaco, 2004. 59: p. 767–774.

113) El-Azzouny, A.A., Maklad, Y.A., Bartsch, H., Zaghary, W.A., Ibrahim, W.M., Mohamed, M.S., Synthesis and pharmacological evaluation of fenamate analogues: 1,3,4-oxadiazol-2-ones and 1,3,4- oxadiazole-2-thiones. Sci Pharm, 2003. 71: p. 331-356.

114) Mullican, M.D., Wilson, M.W., Connor, D.T., Kostlan, C.R., Schier, D.J., Dyer, R.D., Design of 5-3,5-Di-tert-butyl-4-(hydroxyphenyl)-1,3,4-thiadiazoles, -1,3,4-oxadiazole and -1,2,4-triazole as orally-active, nonulcerogenic antiinflammatory agents. J Med Chem, 1990. 36(8): p. 1090-1099.

115) Boschelli, D.H., Connor, D.T., Hoefle, M., Bornemeier, D.A., Dyer, R.D., Conversion of NSAIDS into balanced dual inhibitors of cyclooxygenase and 5-lipoxygenase. Bioorg Med Chem Lett, 1992. 2: p. 69–72.

116) Sahoo, B.M, Dinda, S.C., Ravi Kumar, B.V.V., Panda J., Brahmkshatriya, P.S., Design, green synthesis, and anti-inflammatory activity of Schiff base of 1,3,4-oxadiazole analogues. Lett Drug Des Discov, 2014. 11: p. 82-89.

117) Alp, A.S., Kılcıgil, G., Ozdamar, E.D., Çoban, Eke B., Synthesis and evaluation of antioxidant activities of novel 1,3,4-oxadiazole and imine containing 1*H*-benzimidazoles. Turk J Chem, 2015. 39: p. 42-53.

118) Nazarbahjat N, Ariffin A, Abdullah Z, et al. Synthesis, characterization, drug-likeness properties and determination of the in vitro antioxidant and cytotoxic activities of new 1,3,4-oxadiazole derivatives. Med Chem Res. 2016; DOI 10.1007/s00044-016-1660-5.

119) Almasirad A, Shafiee A, Abdollahi M, et al. Synthesis and analgesic activity of new 1,3,4-oxadiazoles and 1,2,4-triazoles. Med Chem Res. 2011; 20: 435–442.

120) Desai, S.R., Laddi, U., Bennur, R.S., Patil, P.A., Bennur, S., Synthesis and pharmacological activities of some new 5-substituted-2-mercapto-1,3,4-oxadiazoles. Indian J Pharm Sci, 2011. 73(5): p. 593-596.

121) Thore, S.N., Gupta, S.V., Baheti, K.G., Synthesis and pharmacological evaluation of 5-methyl-2-phenylthiazole-4-substituted heteroazoles as a potential anti-inflammatory and analgesic agents. J Saudi Chem Soc, 2016. 20: p. 46–52.

122) Sahin, G., Palaska, E., Ekizoglu M., Ozalp, M., Synthesis and antimicrobial activity of some 1,3,4-oxadiazole derivatives. Il Farmaco, 2002. 57: p. 539–542

123) Sonar, V.N. and N. Sreenivasulu, New *Mannich* bases from oxadiazolylindoles and their antibacterial activity. Indian J Heterocycl, 1995. 4: p. 203.

124) Grover, G. and G. Kini, Synthesis and evaluation of new 1,3,4-oxadiazoles and 1,3,4-oxadiazole-2-thione derivatives of nalidixic acid as potential antibacterial and antifungal agents. Ind J Heterocyc Chem, 2003. 12(3): p. 289-290.

125) Gudipati, R., Anreddy, R.N.R., Manda, S., Synthesis, characterization and anticancer activity of certain 3-{4-(5-mercapto-1,3,4-oxadiazole-2-yl)phenylimino}indolin-2-one derivatives. Saudi Pharm J, 2011. 19: p. 153–158.

126) Feng, C.T., Wang, L.D., Yan, Y.G., Liu, J., Li, S.H., Synthesis and antitumor evaluation of some 1,3,4-oxadiazole-2(*3H*)-thione and 1,2,4-triazole-5(*1H*)-thione derivatives. Med Chem Res, 2012. 21: p. 315–320.

127) Thore, S.N., Gupta, S.V., Baheti, K.G., Docking, synthesis, and pharmacological investigation of novel substituted thiazole derivatives as non-carboxylic, antiinflammatory and analgesic agents. Med Chem Res, 2013. 22: p. 3802-3811.

128) Ma L, Xiao Y, Li C, et al. Synthesis and antioxidant activity of novel Mannich base of 1,3,4-oxadiazole derivatives possessing 1,4-benzodioxan. Bioorg Med Chem. 2013; 21: 6763-6770.

129) Akram M, Rauf A, Saeed A, et al. Synthesis, biological evaluation and molecular docking studies of *Mannich* bases derived from 1,3,4-oxadiazole-2-thiones as potential urease inhibitors. Trop J Pharm Res. 2018; 17(1): 127-134.

130) Rahul, R., Jat, R.K., Saravanan, J., Synthesis, characterization & biological evaluation of 1,3,4- oxadiazoles as antioxidant agents. JIPBS, 2016. 3(3): p. 104-113.

131) Selvakumar, K., Joysa Ruby, J., Rajamanickam, V., Vignesh, M., Parkavi, V., Muthumohamed, J., Jesindha Beyatrics, K., Synthesis, characterization and analgesic activity of 1,3,4-oxadiazole derivatives. Ind J Pharm Ind Res, 2012. 21.

132) Ali, M.A. and M. Shaharyar, Oxadiazole *Mannich* bases: synthesis and antimycobacterial activity. Bioorg Med Chem Lett, 2007. 17: p. 3314-3316.

133) Nimbalkar, U.D., Tupe, S.G., Vazquez, J.A.S., Khan, F.A.K., Sangshetti, J.N., Nikalje, A.P.G., Ultrasound- and molecular sieves-assisted synthesis, molecular docking and antifungal evaluation of 5-(4-benzyloxy)-substitutedphenyl)-3-phenylamino)methyl)-1,3,4-oxadiazole-2(*3H*)-thiones. Molecules, 2016. 21: p. 484. DOI:10.3390/molecules 21050484.

134) Al-Omar, M.A., Synthesis and antimicrobial activity of new 5-(2-thienyl)-1,2,4-triazoles and 5-(2-thienyl)-1,3,4-oxadiazoles and related derivatives. *Molecules*, 2010. 15: p. 502-514.

135) Desai, N.C., Bhatt, N., Somani, H., Trivedi, A., Synthesis, antimicrobial and cytotoxic activities of some novel thiazole clubbed 1,3,4-oxadiazoles. Eur J Med Chem, 2013. 67: p. 54-59.

136) Rahman, D.E.A., Synthesis, quantitative structure-activity relationship and biological evaluation of 1,3,4-oxadiazole derivatives possessing diphenylamine moiety as potential anticancer agents. *Chemical and Pharmaceutical Bulletin*, 2013. 61: p. 151-159.

137) Dash, S., Kumar, B.A., Singh, J., Maiti, B.C., Maity, T.K., Synthesis of some novel 3,5-disubstituted 1,3,4-oxadiazole derivatives and anticancer activity on EAC animal model. Med Chem Res, 2011. 20: p. 1206-1213.

138) Savariz FC, Formagio ASN, Barbosa VA, et al. Synthesis, antitumor and antimicrobial activity of novel 1-substituted phenyl-3-(3-alkylamino methyl)-2-thioxo-(1,3,4-oxadiazol-5-yl)-b-carboline derivatives. J Braz Chem Soc. 2010; 21: 288-298.

139) Chen Y, Wang G, Duan N, et al. Synthesis and antitumor activity of fluoroquinolone C3-isostere derivatives: oxadiazole *Mannich* base derivatives in Chinese. Yingyong Huaxue. 2012; 29: 1246-1250.

140) Yadav, N., Kumar, P., Chikara, A., Chopra, M., Development of 1,3,4-oxadiazole- thione based novel anticancer agents: Design, synthesis and in-vitro studies. Biomed Pharmacother, 2017. 95: p. 721–730.

141) Bajaj, S., Roy, P.P., Singh, J., Synthesis, thymidine phosphorylase inhibitory and computational study of novel 1,3,4-oxadiazole-2-thione derivatives as potential anticancer agents. Comput Biol Chem, 2018. 76: p. 151–160.

142) Sun, J., Ren, S.Z., Lu, W.Y., Discovery of a series of 1,3,4-oxadiazole-2(*3H*)-thione derivatives containing piperazine skeleton as potential FAK inhibitors. Bioorg Med Chem, 2017. 25: p. 2593–2600.

143) Juan S, Hui Z, Zhong-Ming Y, Hai-Liang Z. Synthesis, molecular modeling and biological evaluation of 2-aminomethyl-5-(quinolin-2-yl)-1,3,4-oxadiazole-2(*3H*)-thione derivatives as novel anticancer agent. Eur J Med Chem, 2013. 60: p. 23-28.

144) Medzhitov, R., Inflammation 2010: new adventures of an old flame. *Cell,* 2010. 140: p. 771–776.

145) Ferrero-Miliani, L., Nielsen, O., Andersen, P., Girardin, S., Chronic inflammation: importance of NOD2 and NALP3 in interleukin-1β generation. Clin Exp Immunol, 2007. 147: p. 227–235.

146) Nathan, C. and A. Ding, Nonresolving inflammation. Cell, 2010. 140: p. 871–882.

147) Zhou, Y., Hong, Y., Huang, H., Triptolide attenuates inflammatory response in membranous glomerulo-nephritis rat via downregulation of NF-κB signaling pathway. Kidney Blood Press Res, 2016. 41: p. 901–910.

148) Takeuchi, O. And S. Akira, Pattern Recognition receptors and inflammation. Cell, 2010. 140: p. 805–820.

149) Chertov, O., Yang, D., Howard, O., Oppenheim, J.J., Leukocyte granule proteins mobilize innate host defenses and adaptive immune responses. Immunol Rev, 2000. 177: p. 68–78.

150) Jabbour, H.N., Sales, K.J., Catalano, R.D., Norman, J.E., Inflammatory pathways in female reproductive health and disease. Reprod, 2009. 138: p. 903–919.

151) Lawrence, T., The Nuclear Factor NF-κB Pathway in inflammation. *Cold Spring Harbor Perspectives in Biology*, 2009. DOI: 10.1101/cshperspect.a001651.

152) Libby, P., Inflammatory mechanisms: the molecular basis of inflammation and disease. *Nutrition Reviews,* 2007. 65: p. 140-146.

153) Newton, K. and V.M. Dixit, Signaling in innate immunity and inflammation. Cold Spring Harbor Laboratory Press, all rights reserved. 2012. DOI 10.1101/cshperspect .a006049.

154) https://www.msdvetmanual.com/pharmacology/anti-inflammatory-agents/chemical-mediators-of-inflammation

155) Nigam, S. and C.R. Pace-Asciak, Lipoxygenases and their Metabolites: Biological Functions. 2012. 447.

156) Mak, T.W., Saunders, M.E., Jett, B.D., Primer to the Immune Response. Newnes; 2013.

157) Bailey, J.M., Prostaglandins, Leukotrienes, Lipoxins, and PAF: Mechanism of Action. *Molecular Biology and Clinical Applications*, 2013.

158) DuBois RN, Abramson SBL, Crofford RA, et al. Cyclooxygenase in biology and disease, FASEB J, 1998. 12: p. 1063–1073.

159) Kawahara, K., Hohjoh, H., Inazumi, T., Tsuchiya, S., Yukihiko Sugimoto, Y., Prostaglandin E2-induced inflammation: Relevance of prostaglandin E receptors. Biochimica et Biophysica Acta, 2015. 1851: p. 414–421.

160) Wallace, J.L., Prostaglandin biology in inflammatory bowel disease. *Gastroenterology clinics of North America*, 2001. 30(4): p. 971–80 PubMed: 11764538.

161) Ricciotti E. and G.A. FitzGerald, Prostaglandins and inflammation. Arterioscler Thromb Vasc, 2011. 31(5): p. 986–1000.

162) Singh, P., Singh, I.N., Mondal, S.C., Singh, L., Garg, V.K., Platelet-activating factor (PAF)-antagonists of natural origin. Fitoterapia, 2013. 84: p. 180-201.

163) Kolb-Buchofen, V., Kuhhn, A., Suschek, C.V., The role of nitric oxide. Rheumatol, 2006. 45: p. 317–319.

164) Forstermann U, Closs EI, Pollock JS, et al. Nitric oxide isozymes, characterization, purification, molecular cloning, and functions. Hypertension. 1994; 23: p. 112–131.

165) Knowles, R.G. and S. Moncada, Nitric oxide synthases in mammals. Biochem J, 1994. 298: p. 249–258.

166) Cook, H.T., and V. Cattell, Role of nitric oxide in immune-mediated diseases, Clin Sci, 1996. 91: p. 375–384.

167) Hernández-Díaz, S. and L.A. García-Rodríguez, Steroids and risk of upper gastrointestinal complications. Am J Epidemiol, 2001. 153(11): p. 1089–1093.

168) Meek, I.L., Mart, A.F.J., Laar, V.D., Vonkeman, H.E., Non-Steroidal Anti-Inflammatory Drugs: An Overview of Cardiovascular Risks. Pharmaceuticals, 2010. 3: p. 2146-2162.

169) Punchard, N.A., Whelan, C.J., Adcock, I., J Inflammation; 2004.

170) Shan, B., Cai, Y.Z., Sun, M., Corke, H., Antioxidant capacity of 26 spice extracts and characterization of their phenolic constituents. J Agri Food Chem, 2005. 53: p. 7749-7759.

171) Sanchez-Moreno, C., Larrauri, J., Saura-Calixto, F., Antioxidant Activity of Selected Spanish Wines in Corn Oil Emulsions. J Sci Food Agric, 1999. 79: p. 1301-1304.

172) Schich, K.M., *CRC Critical Reviews in Food Science and Nutrition*, 1980. 13: p. 189.

173) Fishwisk M.J. and P.A.T Swoboda, J Sci Food Agric, 1977. 28: p. 387-391.

174) Grob D. The Antiproteolytıc Actıvıty Of Serum: III. Physiological Significance. The Influence of Trypsin and Antiprotease on Bacterial Growth and Sulfonamide Action. 1943. DOI: 10.1085/jgp.26.4.431.

175) Kreamer, B.L., Siegel, F.L., Gourley, G.R., A novel inhibitor of beta-glucuronidase: L-aspartic acid. Pediatric Res, 2001. 50: p. 460-466.

176) https://www.abcam.com/wst-1-assay-reagent-cell-proliferation-ready-to-use-ab155902.html

177) Tan, A.S. and M.V. Berridge, Superoxide produced by activated neutrophils efficiently reduces the tetrazolium salt, WST-1 to produce a soluble formazan: a simple colorimetric assay for measuring respiratory burst activation and for screening anti-inflammatory agents. J Immunol Met, 2000. 238 (1–2): p. 59-68.

178) Brantner, A.H., Quehenberger, F., Chakraborty, A., Polligger, l., Sosa, S., Loggia, R.D., HET-CAM bioassay as in vitro alternative to the croton oil test for investigating steroidal and non-steroidal compounds. ALTEX, 2002. 19(2): p. 51-56.

179) Saima J, Bozhanka M, Rilka T, et al. In vitro anti-inflammatory effect of Carthamus lanatus. L Naturforsch, 2003. 58: p. 830-832.

180) Abreu, P., Matthew, S., Gonzalez, T., Costa, D., Segundo, M.A., Fernandes, E., Antiinflammatory and antioxidant activity of a medicinal tincture from Pedilanthus tithymaloides. Life Sci, 2006. 78: p. 1578-1585.

181) Bose, S. and H. Kim, Evaluation of in vitro anti-inflammatory activities and protective effect of fermented preparations of rhizoma atractylodis macrocephalae on intestinal barrier function against lipopolysaccharide insult. Evid Based Complement Alternat Med, 2013. DOI: 10.1155/2013/363076.

182) Phanse, M.A., Patil, M.J., Abbulu, K., Pravin D. Chaudhari, P.D., Patel, B., In-vivo and in-vitro screening of medicinal plants for their antiinflammatory activity: an overview. J App Pharm Sci, 2012. 2(6): p. 19-33.

183) Lee, D.Y., Anti- inflammatory effects of Asparagus cochinchinensis extract in acute and chronic cutaneous inflammation. Journal of Ethnopharmacology, 2009. 121: p. 28-34.

184) Ilavarasan, R., Mallaika, M., Venkataraman, S., Antiinflammatory and antioxidant activities of Cassia fistula Linn. Bark extracts. Afr J Tradit Complement Altern Med, 2005. 2: p. 70-85.

185) Paschapur, M., Evaluation of anti-inflammatory activity of ethanolic extracts of Borassus falbellifer (L. male flowers inflorescences) in experimental animals. *Journal of Medicinal Plants Research,* 2009. 3: p. 49-54.

186) Badilla, B., Arias, Y., Mora, G.A., Poveda, L.J., Antiinflammatory and antinociceptive activities of Loasa speciosa in rats and mice. Fitoterapia, 2003. 74: p. 45-51.

187) Ghule, B.V., Analgesic and anti inflammatory activities of Lagenaria siceraria stand. Fruit juice extract in rats and mice. *Pharmacognosy Magazine*, 2006. 2: p. 232-236.

188) Manny-Aframian, V., Shafran, A., Zlotogorski, A., Ginsburg, I., Dikstein, S., Measurement of croton oil induced rabbit ear swelling and evaluation of anti-

inflammatory agents with a standard low pressure caliper. Skin Res Technol, 1996. 2(3): p. 142-145.

189) Arunachalam, G., Subramanian, N., Pazhani, G.P., Ravichandran V., Anti inflammatory activity of methanolic extract of Eclipta prostrate L. (Astearaceae). Afr J Pharm Pharmaco, 2009. 3: p. 97-100.

190) Jain, R., Anti- inflammatory action of Abutilon indicum L. sweet leaves by HRBC membrane stabilization. *Research Journal of Pharmay and Technology*, 2009. 2: p. 415-416.

191) Hosseinzadeh, H. and H.M. Younesi, Antinociceptive and antiinflammatory effects of Crocus sativus L. stigma and petal extracts in mice. BMC pharmacology, 2002. 2.

192) Abdullah NH, Kean OB, Pisar M, et al. Bioassay guided isolation of anti-inflammatory principles from Prismatomeris tetrandra Roxb., K. Schum. Asian J Pharm Pharmacol. 2017; 1(4): 5-15.

193) Sevastre, B., Antiinflammatory activity of Peucedanum officinale on rats, *Bulletin USAMV-CN,* 2007. 64: p. 295-298.

194) Pavia, D.L., Lampman, G.M., Kriz, George S., Engel, R.G., Introduction to Organic Laboratory Techniques: A Small-Scale Approach, 1st Ed. Brooks/Cole, Pacific Grove, CA, 1998.

195) Kiemer, A.K. and A.M. Vollmar, Effects of different natriuretic peptides on nitric oxide synthesis in macrophages. 1997. Endocrinology, 138(10): p. 4282-90.

196) Murr, C., Widner, B., Wirleitner, B., Fuchs, D., Neopterin as a marker for immune system activation. Curr Drug Metab, 2002. 3: p. 175–187.

197) Blois, M.S., Antioxidant Determinations by the Use of a Stable Free Radical. *Nature,* 1958. 181: p. 1199-1200.

198) Friesner RA, Murphy RB, Repasky MP, et al. Extra precision Glide: Docking and scoring incorporating a model of hydrophobic enclosure for protein-ligand complexes. J Med Chem. 2006; 49: 6177-6196.

199) Cingolani G, Panella A, Perrone MG, et al. Structural basis for selective inhibition of Cyclooxygenase-1 (COX-1) by diarylisoxazoles mofezolac and 3-(5-chlorofuran-2-yl)-5-methyl-4-phenylisoxazole (P6). Eur J Med Chem. 2017; 138: 661-668.

200) Orlando, B.J. and M.G. Malkowski, Substrate-selective inhibition of cyclooxygenase-2 by fenamic acid derivatives is dependent on peroxide tone. J Biol Chem, 2016. 291(29): p. 15069–15081.

201) Watts, K.S., Dalal, P., Murphy, R.B., Sherman, W., Friesner, R.A., Shelley, J.C., ConfGen: A conformational search method for efficient generation of bioactive conformers. J Chem Inform Modeling, 2010. 50: p. 534-546.

202) Schwab, C.H., Conformations and 3D pharmacophore searching. *Drug Discovery Today: Technologies*, 2010. 7: p. 245-253.

203) Fischer, E. And A. Speier, Darstellung der ester. Ber Dtsch Chem Ges, 1895. 28: p. 3252-3258.

204) Zhang X, Breslav M, Grimm J, et al. A new procedure for preparation of carboxylic acid hydrazides. J Org Chem. 2002; 672(6): 9471-9474.

205) Young, R.W. and K.H. Wood, The cyclization of 3-acyldithiocarbazate esters, Division of Organic Chemistry of the American Chemical Society, 1954. 77: p. 400-403.

206) Dawood, R.S., Synthesis and characterization of 1,3,4-oxadiazoles derived from 9-fluorenone. *Baghdad Science Journal*, 2013. 10(2): p. 499-509.

207) https://pubchem.ncbi.nlm.nih.gov/compound/682050#section=UV-VIS-Spectra

208) https://www2.chemistry.msu.edu/faculty/reusch/virttxtjml/spectrpy/uv-vis/spectrum. htm

209) Uddin MJ, Elleman AV, Ghebreselasie K, et al. Design of fluorine-containing 3,4-diarylfuran-2(*5H)*-ones as selective COX-1 inhibitors. ACS Med Chem Lett. 2014; 5: 1254−1258.

210) Limongelli V, Bonomi M, Marinelli L, et al. Molecular basis of cyclooxygenase enzymes COXs) selective inhibition. PNAS. 2010; 107(12): 5411–5416.

211) Perrone, M.G., Scilimati, A., Simone, L., Vitale, P., Selective COX-1 Inhibition: A Therapeutic Target to be Reconsidered. Curr Med Chem, 2010. 17: p. 3769-3805.

212) Zheng X, Oda H, Takamatsu K, et al. Analgesic agents without gastric damage: Design and synthesis of structurally simple benzenesulfonanilide-type cyclooxygenase-1-selective inhibitors. Bioorg Med Chem. 2007; 15: 1014-1021.

213) Blobaum, A.L. and L.J. Marnett, Structural and Functional Basis of Cyclooxygenase Inhibition. J Med Chem, 2007. 50(17). DOI: 10.1021/jm06 13166.

214) Pacher, P., Beckman, J.S., Liaudet, L., Nitric oxide and peroxynitrite in health and disease. Physiol Rev, 2007. 87: p. 315–424.

215) Terao, J., Dietary flavonoids as antioxidants. *Forum of Nutrition,* 2009. 61: p. 87–94.

216) Sun J, Cao N, Zhang XM, et al. Oxadiazole derivatives containing 1,4-benzodioxan as potential immunosuppressive agents against RAW264.7 cells. Bioorg Med Chem. 2011; 19: 4895–4902.

217) Shaha, S., Arshia, Kazmia, N.S., Diclofenac 1,3,4-oxadiazole derivatives; biology-oriented drug synthesis (BIODS) in search of better non-steroidal, non-acid antiinflammatory agents. Med Chem, 2018. 14: p. 674-687

218) Leong SW, Faudzi SMM, Abas F, et al. Synthesis and SAR study of diarylpentanoid analogues as new anti-inflammatory agents. Molecules. 2014; 19: 16058-16081.

219) Erdal, E.P., Litzinger, E.A., Seo, J., Zhu, Y., Ji, H., Silverman, R.B., Selective neuronal nitric oxide synthase inhibitors. Curr Top Med Chem, 2005. 5: p. 603-624.

220) Levesque, M.C., Ghosh, D.K., Beasley, B.E., CLL cell apoptosis induced by nitric oxide synthase inhibitors: Correlation with lipid solubility and NOS1 dissociation constant. Leuk Res, 2008. 32: p. 1061–1070.

221) Haitao J, Sidhartha T, Jotaro I, et al. Selective neuronal nitric oxide synthase inhibitors and the prevention of cerebral palsy. Ann Neurol. 2009; 65(2): 209–217.

222) https://statistics.laerd.com/statistical-guides/pearson-correlation-coefficient-statistical-guide.php

223) http://statistics-help-forstudents.com/How_do_I_interpret_data_in_SPSS_for_Pearsons_r_and_scatterplots.htm#.XK2yT5gzZPY

224) Colasanti M, Cavalieri E, Persichini T, et al. Bacterial lipopolysaccharide plus interferon-gamma elicit a very fast inhibition of a Ca2+-dependent nitric oxide synthase activity in human astrocytoma cells. J Biol Chem. 1997; 272: 7582-7585.

225) Suzuki, K., Araki, H., Mizoguchi, H., Furukawa, O., Takeuchi, K., Prostaglandin E inhibits indomethacin-induced gastric lesions through EP-1 receptors. Digestion, 2001. 63: p. 92–101.

226) Yokotani, K., Okuma, Y., Osumi, Y., Inhibition of vagally mediated gastric acid secretion by activation of central prostanoid EP3 receptors in urethane-anaesthetized rats. Br J Pharmacol, 1996. 117: p. 653–656.

227) Dao, T.T, Chi, Y.S., Kim, J., Kim, H.P., Kimb, S., Park, H., Synthesis and inhibitory activity against COX-2 catalyzed prostaglandin production of chrysin derivatives. Bioorg Med Chem Lett, 2004. 14: p. 1165–1167.

228) Brenneis, C., Maier, T.J., Schmidt, R., Inhibition of prostaglandin E2 synthesis by SC-560 is independent of cyclooxygenase 1 inhibition. FASEB J, 2006. 20(9): p. 1352-60.

229) Coussens, L.M. and Z. Werb, Inflammation and cancer. Nature, 2002. 42069(17): p. 860–867.

230) Hussain, S.P., Hofseth, L.J., Harris, C.C., Radical causes of cancer. Nat Rev Cancer, 2003. 3(4): p. 276–285.

231) Tandon, V.R., Verma, S., Singh, J., Mahajan, A., Antioxidants and cardiovascular health. J Med Educ Res, 2005. 7(2): p. 115–118.

232) Ravipati AS, Zhang L, Koyyalamudi SR, et al. Antioxidant and anti-inflammatory activities of selected Chinese medicinal plants and their relation with antioxidant content. BMC Complement Altern Med. 2012; 12. DOI: 10.1186/1472-6882-12-173.

233) Harman, C.A., Turman, M.V., Kozak, K.R., Marnett, L.J., Smith, W.L., Garavito, R.M., Structural basis of enantioselective inhibition of cyclooxygenase-1 by S-alpha-substituted indomethacin ethanolamides. J Biol Chem, 2007. 282(38): p. 28096-28105.

7. CURRICULUM VITAE

Personal Informations

Name	Tuğçe	Surname	Ozyazici
Place of Birth	Eminönü-Istanbul	**Date of Birth**	03.09.1990
Nationality	Turkish	**TR ID Number**	27125486960
E-mail	tugceozyazici90@gmail.com	**Phone number**	05073001772

Education

Degree	Department	The name of the Institution Graduated From	Graduation year
Doctorate	Faculty of Pharmacy Pharmaceutical Chemistry	Yeditepe University	2019
Master	Faculty of Pharmacy Pharmaceutical Chemistry	Yeditepe University	2013
University	Faculty of Pharmacy	Yeditepe University	2013

Languages	Grades (#)
English	IELTS: 6.5 YDS:60 YOKDIL:76

All the grades must be listed if there is more than one (KPDS, ÜDS, TOEFL; EELTS vs),

Work Experience (Sort from present to past)

Position	Institute	Duration (Year - Year)
Researching assistant	Yeditepe University	2013-2019

Computer Skills

Program	Level
Microsoft Programs: Word Excel Powerpoint	Good

Scientific works
Articles

I. Ö. Dagliyan, M. Köksal Akkoç, **T. Özyazici**, S. B. Kadioglu Yaman, H. Sipahi, A. Bozkurt, S. S. Bilge. Some Novel Mannich Bases Of 5-(3,4-dichlorophenyl)-1,3,4-oxadiazole-2(3H)-one And Their Anti-inflammatory Activity, Archiv Der Pharmazie, 2016, 350, 9: 1700153

Conference Papers

1. T. ÖZYAZICI, F. SAHIN, M. KÖKSAL AKKOÇ, Design, Synthesis And Biological Activity Study Of Disubstituted 1,3,4-oxadiazole Derivatives, Poster Sunumu, Isops 12th International Symposium on Pharmaceutical Sciences, 26-28 June 2018.

2. E. A. DEDEOGLU, E. KARAÇAYIR, **T. ÖZYAZICI**, H. SIPAHI, M. KÖKSAL AKKOÇ, Design, Synthesis and Antioxidant Activity Study of 1,3,4-oxadiazole-2(3H)-thione, Oral presentation, Emupps 4th Annual Congress 2018, 09-12 May 2018.

3. M. KÖKSAL AKKOÇ, **T. ÖZYAZICI**, E. E. GÜRDAL HAKGÖR, M. YARIM YÜKSEL, E. DEMIRPOLAT, M. B. AYCAN, Hexahydropyrimidine-2,4- diones: Synthesis and Cytotoxic Activity, Oral presentation, ICMPS 2017: 19th International Conference on Medicine and Pharmaceutical Sciences, 25-26 December 2017.

4. T. ÖZYAZICI & M. KÖKSAL AKKOÇ, Synthesis and Anticancer Screening of Novel 3,5-disubstituted-1,3,4-oxadiazole-2(3H)-thiones, Poster presentation, Ilaç Arastırma Ve Gelistirme Uluslararası Çok Disiplinli 2017 Sempozyumu (DRD-2017), 05-07 October 2017.

5. T. ÖZYAZICI, S. B. KADIOGLU YAMAN, H. SIPAHI, M. KÖKSAL AKKOÇ, Yeni 5-(3,4- disübstitüefenil)-1,3,4-oksadiazol-(2h)-on Türevlerinin Sentezi Ve In Vitro Antiinflamatuvar Etkilerinin Degerlendirilmesi, Poster presentation, 1. Ulusal Marmara Eczacılık Kongresi, 03-05 November 2016.

Projects

TUBITAK 3001-PROJECT SCOLARSHIP- Synthesis of New Piperazinylpyrimidine Structures and Their Anticancer Activity Studies (Project code: 215S157) -**Project completed**- SBAG-Saglik Bilimleri Arastirma Destek Grubu, Yeditepe University, February 2016-2018.